OZONE MAXIMA OVER SOUTHERN AFRICA: CHARACTERISTICS AND MECHANISMS

JANE COMBRINK

Submitted in partial fulfillment of the
requirements for the degree of
Doctor of Philosophy
in the
Department of Geographical and Environmental Sciences,
Univeristy of Natal

Durban
December 18, 1995

PREFACE

The work described in this thesis was carried out in the Department of Geographical and Environmental Sciences, University of Natal, Durban, from January 1992 to 1995, under the supervision of Professor Roseanne D. Diab.

This study represents original work by the author and has not been submitted in any form to another University. Where use was made of the work of others, it has been duly acknowledged in the text.

The topic to be examined in this research concerns the relationship between day-to-day weather and ozone maxima (high ozone levels) over southern Africa. This research initiative began with a preliminary investigation into the nature of total column ozone amounts over South Africa, in which, an attempt was made to link variations in total column ozone to changing surface weather conditions. The results of this study were submitted as a Bachelor of Science Honours dissertation in September 1989.

Further investigation into the relationship between total column ozone and changing weather conditions was undertaken and the results submitted as a Master of Science dissertation entitled *"Spatial and temporal variations in total ozone over South Africa"*. The research suggested that there is a good relationship between ozone maxima and the passage of mid-latitude weather systems over South Africa.

This preliminary research has provided a basis from which a more in-depth analysis of the role of the mid-latitude weather systems on ozone maxima could be examined. In addition, the study was extended to include the influence of other circulation patterns which could produce ozone enhancement. The objectives of the research were greatly facilitated by data collected during SAFARI-92. Extensive use has been made of the data collected at the ground-based ozone sounding stations, operative during the campaign, to address the research questions.

During the course of this research, a number of papers have either been published or have been submitted for publication. These include:

Barsby[1], J. and Diab, R.D. (1995).

---

[1] Combrink née Barsby

Combrink, J., Diab, R.D., Sokolic, F. and Brunke, E-G. (1995).

Diab, R.D., Jury, M., Combrink, J. and Sokolic, F. (1996b).

Diab, R.D., Thompson, A., Zunckel, M., Coetzee, G., Combrink, J., Bodeker, G., Fishman, J., Sokolic, F., McNamara, D., Archer, C. and Nganga, D. (1996a).

Others have been presented at local and international conferences. These include:

Barsby, J. and Diab, R.D. (1994).

Diab, R.D., Combrink, J., Sokolic, F. and Zunckel, M. (1993).

Combrink, J., Diab, R.D. and Brunke, E. (1993).

Combrink, J. (1994).

Combrink, J., Diab, R.D., Sokolic, F. and Brunke, E-G. (1994).

Combrink, J., Diab, R.D., Sokolic, F. (1995).

Combrink, J. (1995).

ACKNOWLEDGEMENTS

My thanks go to the following persons and organisations:

Professor Roseanne D. Diab for her unfailing guidance and support throughout the duration of this project.

Dr. Anne Thompson, NASA Goddard Space Flight center, Greenbelt, Maryland, USA, for advice and assistance in conducting the trajectory modelling and for her very helpful comments and guidance.

Donna McNamara, NASA Goddard Space Flight center, Greenbelt, Maryland, USA, for the trajectory modelling.

Frank Sokolic, Department of Geographical and Environmental Sciences, University of Natal, Durban, for his invaluable computing assistance.

Dr. Greg Bodeker from the National Institute of Water and Atmospheric Research (NIWA), New Zealand and Mark Zunckel from the Council for Scientific and Industrial Research, for their support and many stimulating discussions.

Gerrie Coetzee from the South African Weather Bureau for coordinating and managing the much awaited ozonesonde launches to coincide with the cut off low event during SA'ARI-94.

Jenny McDowell and Hem Hurrypursad, Cartography Unit, Department of Geographical and Environmental Sciences, University of Natal, Durban, for preparing many of the diagrams.

Dr. J.J. Taljaard, South African Weather Bureau, Pretoria, for his assistance in selecting cut off low events for case study analysis.

The Department of Oceanography, University of Cape Town and The Department of Geography, University of the Witwatersrand for some of the ECMWF data.

Dr. G. Mather (Cloud Quest, Nelspruit, South Africa) for assistance in computerising θ_e calculations.

Dr. Fedor Brioukhan who visited the University of Natal, Durban, in 1993, for his assistance in modelling potential vorticity.

Duncan Waldie, South African Weather Bureau, for the Meteosat images.

The South African Weather Bureau for ozonesonde, radiosonde and ECMWF data.

NASA Langley Research Center, USA, for the Brazzaville ozonesonde data.

Andrew and my family and friends who have provided a great deal of support and encouragement throughout my studies.

The staff of the Departments of Environmental Health and Community Nursing at the Natal Technikon, for their support during the past four months.

Dr. P. McPeters and Dr. A. Krueger (NASA/GSFC); members of the TOMS Nimbus Experiment and ozone processing teams; and the National Space Science Data Center through the World Data Center-A for rockets and satellites, for access to the TOMS ozone data.

A number of institutions and organisations which provided funding, in various forms, for this project. These include: Department of Environment Affairs for SAFARI-92 and SA'ARI; Foundation for Research Development (FRD); Atmospheric Research Group University of Natal, Durban (ARGUND); the University of Natal, Research Fund (URF) and the Staff Development Fund of the Natal Technikon.

ABSTRACT

This thesis aims to clarify the sources of, and mechanisms associated with, the generation of ozone maxima over the southern African region. Inasmuch as, tropospheric ozone concentration is a function of both chemistry and meteorology, this thesis concentrates on the role of atmospheric dynamics. Firstly, a statistical analysis of the relationship between total ozone and meteorological parameters revealed a generally weak negative relationship between total ozone and the height of the 500, 300 and 100 hPa geopotential surfaces. The relationship is best expressed by the passage of a mid-latitude cyclone while anticyclonic conditions exhibited a weak relationship. An examination of the spatial distribution of total ozone and potential vorticity (PV), during the passage of westerly troughs, prompted a more thorough investigation of the exchange of ozone between the stratosphere and troposphere.

The relationship between tropospheric ozone, and low pressure and anticyclonic systems is investigated further using data obtained during the South African Fire-Atmospheric Research Initiative (SAFARI) conducted in 1992. Ozone concentrations, as expressed by ozonesonde data, reveal different characteristic profiles for the two scenarios. Explanations for the differences observed are sought in the observed circulation patterns during the experiment.

Case studies at Okaukuejo (Namibia), Irene (South Africa) and Brazzaville (Congo), which were utilised as ground stations during SAFARI, are presented in an attempt to gain insight into the vertical distribution of ozone over the entire expanse of the study region. The role of convective systems in the generation of short-lived upper tropospheric ozone maxima at tropical latitudes is illustrated while the different vertical ozone signatures, expressed under cyclonic and anticyclonic systems as described earlier, are reconfirmed by the Okaukuejo and Irene data.

An attempt is made to investigate dynamic links between the troposphere and stratosphere and the concomitant exchange of ozone during the passage of westerly trough systems. Particularly deep troughs or cut off low pressure systems are identified as important mechanisms in the generation of upper tropospheric ozone maxima. An examination of the vertical distribution of ozone at Irene during the passage of a COL, using data obtained from the SA'ARI 1994 experiment, suggests concurrence with Danielsen's (1968) model of tropopause folding. The intrusion of high PV and dry stratospheric air,

coupled with downward flow near the tropopause, in the vicinity of the upper tropospheric disturbance, promotes the transport of ozone-rich air to tropospheric altitudes.

The limited availability of data has severely hampered the understanding of tropospheric ozone in southern Africa in the past. This study demonstrates the value of daily vertical ozone data, even for very short periods.

LIST OF FIGURES

3.5 Schematic diagram of ozone-weather relationships: (a) assumed initial, undisturbed, meridional distribution of total ozone amount in cm.; (b) disturbed state; thin solid lines give ozone distribution resulting from horizontal displacement only and represent approximate 200-mb contours; dashed lines are 200-mb isotherms; solid line is intersection of tropopause with 200-mb surface; (c) ozone deviations (cm.10^3) due to vertical displacements; (d) final distribution of total amount in cm., taking account of both horizontal and vertical displacements; and (e) heavy solid lines are high-level contours; thin solid lines are sea-level isobars; surface fronts depicted according to usual conventions; dashed lines are total ozone deviations (cm.10^3). Redrawn from Reed (1950) p. 266).

4.1 Day-to-day correlation, expressed as r^2 values, between (TOMS) total ozone (DU) and heights of the 300 hPa surface (ECMWF) for 1987 and 1988.

4.2 The distribution of TOMS total ozone (DU) over South Africa, June 6-9, 1988. Illustration compiled by Space Physics Research Institute, University of Natal, Durban, from TOMS data supplied by the National Space Science Data Center (NSSDC), USA.

4.3 Surface synoptic charts for 23 and 24 May 1987. Surface pressure expressed as isobars (hPa) over the sea and heights of the 850 hPa surface (gpm) over the land (from Daily Weather Bulletin, SAWB) and 300 hPa synoptic charts for 23 and 24 May 1987, prepared from ECMWF 12 Z data.

4.4 Vertical cross sections of PV (x 10^{-7} $KhPa^{-1}s^{-1}$) through 30°S, over South Africa, for 23 and 24 May 1987. Prepared from ECMWF data.

4.5 Spatial distribution of PV (x 10^{-7} $KhPa^{-1}s^{-1}$) on 340 K isentropic surface for 23 and 24 May 1987 for an area bounded by latitudes 0° to 50°S and longitudes 10°W to 50°E. Prepared from ECMWF data.

4.6 Spatial distribution of TOMS total ozone (DU) for 23 and 24 May 1987 for an area bounded by latitudes 0° to 50°S and longitudes 10°W to 50°E.

4.7 Dominant transport types derived from trajectory models depicting easterly and westerly transport from southern Africa and recirculation within the anticyclonic system. Redrawn from Garstang *et al.* (1996).

4.17 Mean equivalent potential temperature (θ_e) profiles for the composite anticyclonic and westerly trough synoptic types, at Okaukuejo, during the SAFARI period. Data from the SAWB.

4.18 Composite cross section of RH (%), through 20°S, which corresponds closely to the latitude of Okaukuejo, for the westerly trough type circulation. Data from the SAWB.

4.19 Composite spatial representation of RH (%), on 850, 700, 500 and 300 hPa isobaric surfaces at Okaukuejo during the SAFARI period. Prepared from ECMWF data.

4.20 Spatial distribution of PV (x 10^{-7} $KhPa^{-1}s^{-1}$) on 330 K isentropic surface for the composite anticyclonic type during the SAFARI period. Prepared from ECMWF data.

4.21 Surface synoptic charts over southern Africa for 28 September to 6 October 1992. Isobars (hPa) are denoted by light lines. From the Daily Weather Bulletin (SAWB).

4.22 700 hPa synoptic chart over southern Africa for 28 and 29 September 1992. Prepared from ECMWF data.

4.23 700 hPa wind vectors over southern Africa, derived from ECMWF u and v wind components, for 28, 30 September and 1 and 6 October 1992.

4.24 Ozonesonde mixing ratio profiles (ppbv) between 0 and 12 km (asl), at Okaukuejo for 30 September, 3, 5 and 6 October 1992. Data from the SAWB.

4.25 Eight day back trajectories on 314, 316, 318 and 320 K isentropic surfaces, from Okaukuejo, for 6 October to 28 September 1992. Start time was 12 Z. The trajectory originating from the central point of the array is given as a solid line. Start pressure (hPa) is denoted by large type and end pressure by smaller type. Source NASA/GSFC.

4.26 Time-pressure plot of the middle-point eight day back trajectories on 314, 316, 318 and 320 K isentropic surfaces, from Okaukuejo, for the period 6 October to 28 September 1992. Pressure is given as a log scale (hPa) and time is in 24 hour intervals. The start time is denoted by 0 hours and the end time -192 hours. Source NASA/GSFC.

4.37 Eight day back trajectories on 312, 314, 316, 318 and 320 K isentropic surfaces, from Irene, for the period 30 to 22 September 1992. Start time was 12 Z. The trajectory originating front the central point of the array is given as a solid line. Start pressure (hPa) is denoted by large type and end pressure by smaller type. Source NASA/GSFC.

4.38 Time-pressure plot of the middle-point eight day back trajectories on 312, 314, 316, 318 and 320 K isentropic surfaces, from Irene, for the period 30 to 22 September 1992. Pressure is given as a log scale (hPa) and time is in 24 hour intervals. The start time is denoted by 0 hours and the end time -192 hours. Source NASA/GSFC.

4.39 Surface synoptic charts over southern Africa for 14 to 22 October 1992. Isobars (hPa) denoted by light lines. From Daily Weather Bulletin (SAWB).

4.40 700 hPa synoptic charts over southern Africa for 14 to 17 October 1992. Prepared from ECMWF data.

4.41 300 hPa synoptic charts over southern Africa for 14 to 17 October 1992. Prepared from ECMWF data.

4.42 700 hPa wind vectors over southern Africa, derived from ECMWF u and v wind components, for 14 to 17 October 1992.

4.43 Ozonesonde mixing ratio profiles (ppbv) between 0 and 12 km (asl), at Irene during for 14, 15, 17, 18, 21 and 22 October 1992. Data from the SAWB.

4.44 The difference between the ozone mixing ratio (ppbv) profile on 18 October, and the mean profile, at Irene, for the SAFARI period. Data from the SAWB.

4.45 Relative humidity (%) profiles between 0 and 12 km (asl), at Irene, for 14, 15, 17 and 18 October 1992 (Data from the SAWB).

4.46 Eight day back trajectories on 314, 316, 318 and 320 K isentropic surfaces, from Irene, for the period 22 to 14 October 1992. Start time was 12 Z. The trajectory originating from the central point of the array is given as a solid line. Start pressure (hPa) is denoted by large type and end pressure by smaller type. Source NASA/GSFC.

6.11 Spatial distribution of TOMS total ozone (DU) in the area bounded by latitudes 0° to 50°S and longitudes 10°W to 50°E for 26 to 29 September 1987. Prepared from data supplied by NSSDC.

6.12 Spatial distribution of PV (x 10^{-7} $KhPa^{-1}s^{-1}$) on the 340 K isentropic surface, in the area bounded by latitudes 0° to 50°S and longitudes 10°W to 50°E, for 26 to 29 September 1987. Prepared from ECMWF data.

6.13 Vertical cross sections of PV (x 10^{-7} $KhPa^{-1}s^{-1}$), through 30°S, for 26 to 29 September 1987. Prepared from ECMWF data.

6.14 Vertical cross sections of RH (%), through 30°S, for 26 to 29 September 1987. Prepared from ECMWF data. RH ≤ 10% is shaded.

6.15 Vertical cross sections of the v component of the wind (m s^{-1}), through 30°S, for 26 to 29 September 1987. Prepared from ECMWF data.

6.16 Vertical cross sections of ω (Pa s^{-1}), through 30°S, for 26 to 29 September 1987. Prepared from ECMWF data. Arrows indicate upward and downward motion. Regions of upward motion (ω < 0) are shaded.

6.17 Vertical cross sections of temperature (°C), through 30°S, for 26 to 29 September 1987. Prepared from ECMWF data.

6.18 Surface synoptic charts over southern Africa for 27 to 30 May 1994. Surface pressure expressed as isobars (hPa) over the sea and heights of the 850 hPa surface (gpm) over the land. From Daily Weather Bulletin, SAWB.

6.19 Meteosat visual satellite images (12:00 local time) for 27 to 30 May 1994, supplied by SAWB.

6.20 300 hPa synoptic charts for an area bounded by latitudes 0° to 50°S and longitudes 10°W to 50°E for 27 to 30 May 1994. Prepared from ECMWF data.

6.21 700 hPa wind vectors for 26 to 30 May 1994 for the area bounded by latitudes 0° to 50°S and longitudes 10°W to 50°E. Prepared from ECMWF data.

6.22 300 hPa wind vectors for 26 to 30 May 1994 for the area bounded by latitudes 0° to 50°S and longitudes 10°W to 50°E. Prepared from ECMWF data.

6.23 Spatial distribution of TOMS total ozone (DU) for an area bounded by latitudes 0° to 50°S and longitudes 10°W to 50°E for 27 to 30 May 1994. Data supplied by NSSDC.

6.24 Vertical profiles of ozone partial pressure (mPa) at Irene for the period 27 to 30 May 1994. Ozonesonde data supplied by SAWB.

6.25 Time-height cross section of ozone mixing ratio (ppbv) derived from four ozonesonde ascents at Irene for the period 27 to 30 May 1994. Data supplied by SAWB. Values greater than 700 ppbv are excluded.

6.26 Spatial distribution of PV (x 10^{-7} $KhPa^{-1}s^{-1}$) on 340 K isentropic surface for 27 to 30 May 1994 in the region bounded by latitudes 0° to 50°S and longitudes 10°W to 50°E. Derived from ECMWF data.

6.27 Vertical cross sections of PV (x 10^{-7} $KhPa^{-1}s^{-1}$) through 25°S for 26 to 30 May 1994. Derived from ECMWF data.

6.28 RH (%) profiles at Irene for 27 to 30 May 1994. Prepared from radiosonde data supplied by SAWB.

6.29 Vertical cross sections of wind speed (m s^{-1}), through 25°S, for 27 to 30 May 1994. Derived from ECMWF data.

6.30 Vertical cross section of the ω, through Irene (25°S), for 27 to 30 May 1994, derived from ECMWF, 12 Z data. Arrows indicate upward and downward motion. Regions of upward motion ($\omega < 0$) are shaded.

LIST OF TABLES

LIST OF ABBREVIATIONS

Standard chemical abbreviations, used in this document, are not included in this list.

agl	above ground level
asl	above sea level
AVHRR	Advanced Very High Resolution Radiometer
BUV	Backscatter Ultraviolet
CAT	Clear-air turbulence
COL	Cut off low
DU	Dobson Units
ECC	Electrochemical Concentration Cell (rawindsondes)
ECMWF	European Centre for Medium Range Weather Forecasts
GOES	Geostationary Orbiting Environmental Satellite (NASA)
GSFC	Goddard Space Flight Center (NASA)
IGBP	International Geosphere Biosphere Programme
ITCZ	Inter-Tropical Convergence Zone
METEOSAT	Meteorological Satellite
NASA	National Aeronautics and Space Administration
NMC	National Meteorological Center (USA)
NOAA	National Oceanic and Atmospheric Administration
NRC	National Research Council (USA)
NSSDC	National Space Science Data Center (NASA)
PBL	Planetary Boundary Layer
PV	Potential Vorticity
QBO	Quasi-Biennial Oscillation
RH	Relative Humidity
SA'ARI	Southern African Atmosphere Research Initiative
SACCAIM	Special Programme on Southern African Climate Change: Analysis, Interpretation and Modelling
SAFARI	South African Fire-Atmospheric Research Initiative
SAOZ	System for the Analysis of Observations at Zenith

SAWB	South African Weather Bureau
SSW	Sudden Stratospheric Warming
STARE	Southern Tropical Atlantic Regional Experiment
STE	Stratospheric-tropospheric exchange
STEP	Stratosphere-Troposphere Exchange Project
TOGA	Tropical Ocean and Global Atmosphere
TOMS	Total Ozone Mapping Spectrometer
TRACE-A	Transport and Atmospheric Chemistry near the Equator-Atlantic
UV	Ultraviolet radiation
WCRP	World Climate Research Program
ZAB	Zaire Air Boundary

CONTENTS

CHAPTER 1

INTRODUCTION

1.1 BACKGROUND

Changes in global stratospheric ozone and the discovery of the Antarctic ozone hole (Farman and Shanklin, 1985) have focused attention on atmospheric ozone in recent years. Findings have shown that ozone loss is significant over the entire globe and that rapid ozone depletion, of up to 65%, has been observed at Antarctic stations during the spring months (Shanklin, 1994). Further, recent data have shown alarming springtime depletions above the United Kingdom and Europe, even greater than that over South America or New Zealand which are located close to the Antarctic ozone hole (Department of the Environment and the Meteorological Office, 1991). Such observations provide cause for concern and strong support for research into the behaviour of stratospheric ozone. The protective nature of ozone in the stratosphere alone renders this topic worthy of significant attention.

On the other hand, ozone in the troposphere is increasing and although ozone is considered to be a trace gas, it plays a dominant role in determining the thermal structure of the atmosphere (Bojkov, 1995). In addition, ozone has a highly reactive chemical nature in the troposphere and as such, plays a significant role in global tropospheric chemistry. Near the surface it may be considered a pollutant, with many undesirable characteristics, and in the free troposphere it may contribute to global warming through its absorption of longwave terrestrial radiation.

Ozone has indeed become a global issue and has precipitated a great deal of research originating within a variety of disciplines. Much work has concentrated on trends in total column ozone using the historical Total Ozone Mapping Spectrometer (TOMS) satellite data and ground-based data sets from the Dobson spectrophotometer network (Stolarski *et al.*, 1991; among others). The effects of interannual factors on total ozone trends, such as the quasi-biennial oscillation (QBO), have also been considered (UNEP, 1994). Such studies have focused on both large scale, regional, and individual station analysis. Considerably more data are available for the Northern Hemisphere mid- and high altitudes where the majority of the ground-based stations are located (UNEP, 1994).

Seasonal variations in total ozone have been examined extensively. Much of the work concerning seasonal variations in total ozone, in the Southern Hemisphere, has been inspired by the observed seasonal depletion of ozone, in the austral spring, over the Antarctic (for example Diab *et al.*, 1992).

Short term, or day-to-day fluctuations in total ozone have been examined in detail for the Northern Hemisphere. In particular, the relationship between total ozone and daily weather patterns is well documented in the literature (Reed, 1950). Many subsequent studies have developed the understanding of this relationship further (for example, Ohring and Muench, 1960; Orlanski, 1989). Due to the lack of meteorological data and ozone measurements in the Southern Hemisphere, short term ozone characteristics have not been as extensively studied as in the Northern Hemisphere. This is particularly true for the southern African region.

In recent years, greater attention has been focused on increasing global tropospheric ozone levels and the nature and causes of the observed long term, seasonal and daily variations (Logan, 1985; Crutzen, 1988). Traditionally, industrial and urban development has been blamed for the substantial increase in substances which pollute the atmosphere (Urone, 1986). Other less-well understood contributing factors, such as rural fire and biogenic emissions, are now being more carefully considered (for example Swap *et al.*, 1996; Thompson *et al.*, 1996a). In the last four years much attention has been focused on the southern and central African region, and as a result, the transport of, and chemistry of tropospheric ozone and ozone precursors is better understood.

This study is motivated by the scarcity of research concerning ozone and weather relationships in the southern African region. In particular, this thesis aims to contribute to the understanding of the relationship between ozone maxima, or high ozone levels, and day-to-day weather patterns in southern Africa. An attempt is made to answer pertinent questions, through an examination of the circulation patterns and horizontal and vertical transport mechanisms, concerning the origin of tropospheric ozone maxima.

It is recognised that at any one time and place, tropospheric ozone concentration is a function of both chemistry and meteorology. This thesis concentrates on the role of atmospheric dynamics. However, a review of the factors which influence ozone concentrations, including ozone sources and sinks, is provided as a basis for this study.

1.2 OBJECTIVES

Tropospheric ozone concentrations fluctuate over the southern African sub-continent from day-to-day. It is hypothesised that there are two main sources, or a combination of both, which will explain the evolution of tropospheric ozone maxima over southern Africa:

1) The literature (Dobson *et al.*, 1929; Reed, 1950; Danielsen, 1968; Reiter, 1975; Danielsen and Mohnen, 1977; Wakamatsu *et al.*, 1989) suggests that the day-to-day changes observed may be explained by the dynamics of the atmosphere. For example, through a mid-latitude influence whereby large amounts of ozone or ozone maxima would be explained by phenomena such as stratospheric injection occurring in association with the passage of deep low pressure systems and/or tropopause folding. Secondly, through the accumulation of pollutants as a result of stable anticyclonic systems and thirdly, the generation of ozone maxima through tropical convective systems. This hypothesis will be rigorously tested.

2) The chemistry of the atmosphere plays a major role in the evolution of elevated ozone amounts. The southern African region is particularly interesting in this regard. Substantial biomass burning, in the northern and central parts of southern Africa, along with natural (emissions and atmospheric processes) and anthropogenic (urban and industrial emissions) influences provide substantial sources of ozone and ozone precursor gases. Although ozone chemistry is not the focus of this thesis, the inter-related nature of ozone sources and atmospheric processes is acknowledged.

1.2.1 Key questions to be addressed

The key questions to be addressed in this thesis are summarised below. Answers to these questions will be sought in the relevant literature, and by way of analysis of meteorological and ozone data collected for the southern African region.

* What are the dynamic factors causing day-to-day fluctuations in ozone amounts over southern Africa?
* What are the circulation patterns which give rise to elevated tropospheric ozone levels over southern Africa?
* What is the nature of tropospheric ozone maxima at different locations in southern Africa?

* Does stratospheric-tropospheric exchange (STE) contribute to ozone maxima over southern Africa?
* What are the circulation patterns which give rise to STE?
* What is the nature of the vertical and horizontal distribution of ozone during atmospheric conditions which are likely to cause STE?

The objectives of this thesis are:

1. To illustrate a thorough understanding of the way in which day-to-day weather patterns influence ozone levels by providing examples in the form of a statistical analysis and composite and individual case studies.

2. To demonstrate the different weather related mechanisms operating in the spatially diverse region of southern Africa by presenting comparisons of site specific data.

3. To examine the relationship between the passage of deep mid-latitude westerly troughs, particularly cut off low pressure systems, and ozone distribution over southern Africa in detail.

4. To investigate the role of STE in the evolution of ozone maxima through the use of individual and composite case studies.

1.3 THE SCOPE OF THIS STUDY

A detailed description of the methodology applied in the thesis, and the data sets and derived meteorological variables utilised is given in Chapter 2. This is followed by a review of the literature concerning sources of, and mechanisms which cause variations in ozone, in Chapter 3. Chapter 4 provides a detailed examination of the relationship between day-to-day weather patterns and ozone levels over southern Africa. The Chapter begins with a statistical analysis of the relationship between synoptic weather, as expressed by the heights of the 500, 300 and 100 hPa geopotential surfaces, and total ozone. The relationship is investigated for nine stations and for the area bounded by longitudes 10°W and 50°E and latitudes 0°S and 50°S. The findings of this study prompted further investigations into the relationship between ozone distribution and anticyclonic and westerly trough circulation, using data collected during SAFARI-92. Composite and individual case studies at Okaukuejo (Namibia) and Irene (South Africa) are presented in this regard. In addition,

the role of tropical circulation in ozone distribution is investigated at Brazzaville in the Congo.

The role of the ozone-rich reservoir, located in the stratosphere, in the production of tropospheric ozone maxima is examined next. Chapter 5 provides an overview of the literature concerning the development of stratospheric-tropospheric exchange (STE) theory and its role in the vertical transport of ozone into the stratosphere is emphasized. Models of STE and ozone transport and their relationship to the passage of deep westerly troughs is reviewed. In particular, the relationship between cut off low (COL) pressure systems and total ozone is described for the northern hemisphere. Previous analyses have considered the variation of total ozone during the passage of COL systems (Vaughan and Price, 1991). This, and similar studies are confined to the northern hemisphere and rely on the strong correlation between potential vorticity (PV), a dynamic tracer of stratospheric air, and stratospheric ozone to identify STE and the concomitant intrusion of stratospheric ozone into the troposphere (example Price and Vaughan, 1993).

Examinations of the vertical distribution of ozone produced by tropopause folding in COL events have been conducted through the use of transport models to simulate intrusion (for example Ebel *et al.*, 1991) and with the aid of chemical tracers (Bamber *et al.*, 1984; and others). Attempts have been made to link COL events, tropopause folding and upper tropospheric ozone enhancement (Bamber *et al.*, 1984).

Chapter 6 is concerned with STE, via tropopause folding, in the evolution of ozone maxima over southern Africa. The relationship is well illustrated during COL events, which are examples of particularly deep westerly troughs. Both composite and individual case studies are presented in order to gain an understanding of the mechanisms associated with the observed upper tropospheric ozone maxima.

Conclusions drawn from the thesis are presented in Chapter 7.

CHAPTER 2

DATA AND METHODOLOGY

This study involves statistical analysis and the use of both composite and individual case study analysis. Two broad data sets are used. These include meteorological data and ozone measurements. Details are provided below.

2.1 METEOROLOGICAL DATA

2.1.1 European Centre for Medium-Range Weather Forecasts (ECMWF) data

Daily gridded upper air data were obtained from the European Centre for Medium-Range Weather Forecasts (ECMWF) in England. ECMWF has created and maintains an archive of analysed atmospheric data in support of projects associated with the World Climate Research Program (WCRP). This forms part of the ECMWF's role as a Tropical Ocean and Global Atmosphere (TOGA) Atmospheric Data Centre (ECMWF, 1994).

A portion of the data used was obtained from the University of the Witwatersrand through the auspices of the Special Programme on Southern African Climate Change: Analysis, Interpretation and Modelling (SACCAIM), which falls under the South African International Geosphere Biosphere Programme (IGBP), while the remaining data were obtained directly from the European Centre.

Data in this study have been extracted from the ECMWF/TOGA Basic Level III Consolidated data set. ECMWF produces routine global analyses for 00, 06, 12 and 18 Z each day (ECMWF, 1994). The un-initialised upper air data set comprises values for the following parameters: geopotential height [gpm], temperature [K x 10], the zonal wind [u-component in ms^{-1}], meridional wind [v-component in ms^{-1}], and vertical motion [ω- Pa s^{-1}] and humidity [percent] at 14 constant pressure levels (1000, 850, 700, 500, 400, 300, 250, 200, 100, 150, 100, 70, 50, 30 and 10 hPa) (ECMWF, 1994). Each parameter at each level is stored as a field of grid point values on a 2,5° by 2,5° rectangular mesh in latitude rows, with each row running from west to east from the 0° meridian.

The ECMWF analysis system undergoes continuous revision and development in order to improve the quality of the data. These improvements are listed in the ECMWF Technical Attachment documents (ECMWF, 1993; 1994) and discussed in the literature, for example Trenberth and Olson (1988) and Illari (1989). However, the Southern Hemisphere data remain less reliable than the Northern Hemisphere data due to the scarcity of observing stations in the region (Fielding, pers. comm., 1995).

ECMWF data, including the geopotential heights for standard pressure surfaces, omega (ω) vertical motion, relative humidity (RH) and temperature are used. RH above 300 hPa provides approximate values in this region of the atmosphere. In addition ECMWF data are used for the derivation of scalar wind speed (from u and v wind components) and potential vorticity (PV). Daily 12 Z analysed data is utilised for:

1. the two year period 1987 to 1988 for the area bounded by longitudes 10°W and 50°E and latitudes 0°S and 50°S with a grid spacing of 2.5° x 2.5°. This area will henceforth be described as the study area.
2. individual stations, including Marion Island (46°55'S;37°45'E), Gough Island (40°20'S;10°W), Cape Town (33°56'S;18°28'E), Port Elizabeth (33°58'S;25°36'E), Durban (29°53'S;31°E), Bloemfontein (29°07'S;26°14'E), Pretoria (25°45'S;28°12'E), Harare (17°43'S;31°05'E) and Nairobi (1°17'S;36°50'E) for the two year period 1987 to 1988. The location of these stations is shown in Figure 2.1.
2. the Southern African Fire-Atmosphere Research Initiative (SAFARI-92) period (September - October 1992). Data were extracted for Okaukuejo (19°11';15°55'E), Irene (25°53'S;28°13'E), near Pretoria, and Brazzaville (4°17'S; 15°15'E). The location of these stations is depicted in Figure 2.1.
3. the mid-season months of January and July for the five year period 1985 to 1990 for the study area.
4. for case study analysis for the periods 26 to 29 September 1987 and for the period 27 to 30 May 1994 for the study area.

2.1.2 Radiosonde data

12 Z radiosonde data were extracted for the SAFARI period for Okaukuejo and Irene and data for the period 26 to 29 May 1994 for Cape Town (33°56'S;18°28'E), Port Elizabeth (33°58'S;25°36'E), and Irene were extracted from the South African Weather Bureau (SAWB) data base.

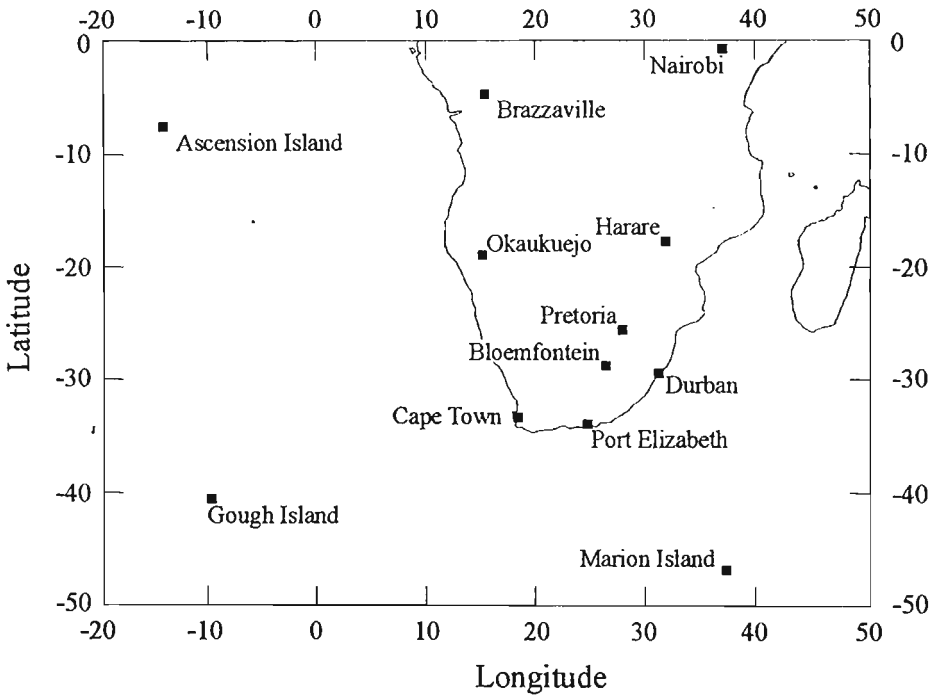

Figure 2.1 The location of the 12 southern African stations. Note, Ascension Island (8°00'S;14°00'W) falls just outside the area (10°W to 50°E and 0°S to 50°S) defined as the study region.

2.1.3 Cloud data

The geostationary European meteorological satellite (Meteosat) provides seven meteorological parameters via the Meteorological Information Extraction Centre at the European Space Operations Centre in Darmstadt, near Frankfurt (Tessier, 1989). The meteorological products include grid-based global cloud coverage data with approximately 200 km resolution (Tessier, 1989). Meteosat visual images for southern Africa at 12:00 local time were obtained from the SAWB for the period 26 to 31 May 1994.

Advanced Very High Resolution Radiometer (AVHRR), on board the National Oceanic and Atmospheric Administration (NOAA) polar satellite, provides daily images of high temperature sources. Details of the AVHRR instruments and data are given in Robinson (1991). In addition, these images provide a source of vegetation and burn scars which facilitate fire count estimation. Other more infrequent satellite data, such as from the Geostationary Orbiting Environmental Satellite (GOES) (3 hour intervals), may miss fires that are not strong enough to burn into the night.

Daily fire count data is derived from the AVHRR imagery and represents the number of very high temperature pixels (Pickering *et al.*, 1994a). The images represent near-infrared radiation for single or multiple orbit/s for approximately 14:00 local time for the south-eastern sector (0°-35°S;13°-23°E) and 13:00 local time for the remaining section (0°-35°S;23°-38°E). Clouds show up as bright white patches representing high reflectance values, while darker areas have lower values (Kendall, pers. comm., 1993). In non-industrial areas, fires are depicted by yellow spots. Blue patches represent areas of uncertainty where appropriate background parameters for determining hot spots were not determined. As a result, these areas represent high brightness/temperatures where fires cannot be identified. Large areas with exposed soil, rock, sand and/or burned vegetation are likely to generate this phenomenon (Kendall, pers. comm., 1993).

National Aeronautics and Space Administration (NASA) supplied images for the period 15 September to 15 October 1992 during SAFARI. These images and the fire count data were used in Chapter 4 for interpretation only and are not shown in this document.

2.2 TOTAL COLUMN OZONE DATA

2.2.1 TOMS, total ozone data

This thesis relies extensively on data supplied by the Total Ozone Mapping Spectrometer (TOMS) experiment. TOMS data were captured by the TOMS instrument on board the United States' Nimbus 7 satellite. The project is an improved version of the Backscatter Ultraviolet (BUV) instrument launched in 1970 (Heath *et al.*, 1975). Total ozone amounts were measured globally on a daily basis throughout the duration of the experiment, 24 October 1978 to 6 May 1993. The experiment has provided a continuous daily series of global total ozone data over the entire sunlit portion of the earth at horizontal resolutions varying between 50 kilometres at nadir and 250 kilometres at extreme off-nadir (Fleig *et al.*, 1986; Bowman, 1988).

The Nimbus 7 satellite follows a noon-midnight near-polar orbital path, maintaining a fixed position with respect to the sun, so that observations at all locations are made near local noon each day (Bowman, 1988). This means that the TOMS instrument views the entire globe at least once a day. During the austral winter, the North Pole faces the sun and consequently no data are received from the South Pole which is in total darkness.

The TOMS instrument on board the Nimbus 7 satellite was accompanied by a number of other instruments including the SBUV or Solar Backscatter Ultraviolet experiment. These two ozone monitoring experiments shared some components and as such, operated in some respects as a single instrument (Bodeker, 1994). The two instruments work on the principle of backscattered ultraviolet radiation illustrated in Figure 2.2. Frederick and Serafino (1985) describe the principle. Solar irradiance ($F\lambda$) is incident on the atmosphere in the wavelength range of interest, 250-340 nanometres. The Solar Backscatter Ultra Violet (SBUV) or BUV instrument intercepts the vertical component ($I\lambda$) of the backscattered radiance in the atmosphere. The quantity that enters the ozone profile derivation is the "backscatter albedo", $I\lambda/F\lambda$, at several discrete wavelengths. Any long term variations in ozone must be manifest in the measured albedos sufficiently in order to be separated from instrument noise and shorter term atmospheric changes.

The TOMS instrument measures integrated ozone amounts through the stratosphere and troposphere as it scans across the flight path of the satellite. The SBUV instrument, on the other hand, has the capability to determine the vertical distribution of ozone in the stratosphere and above (Fishman *et al.*, 1990). The integrated ozone measurements record ozone amounts in a column of air

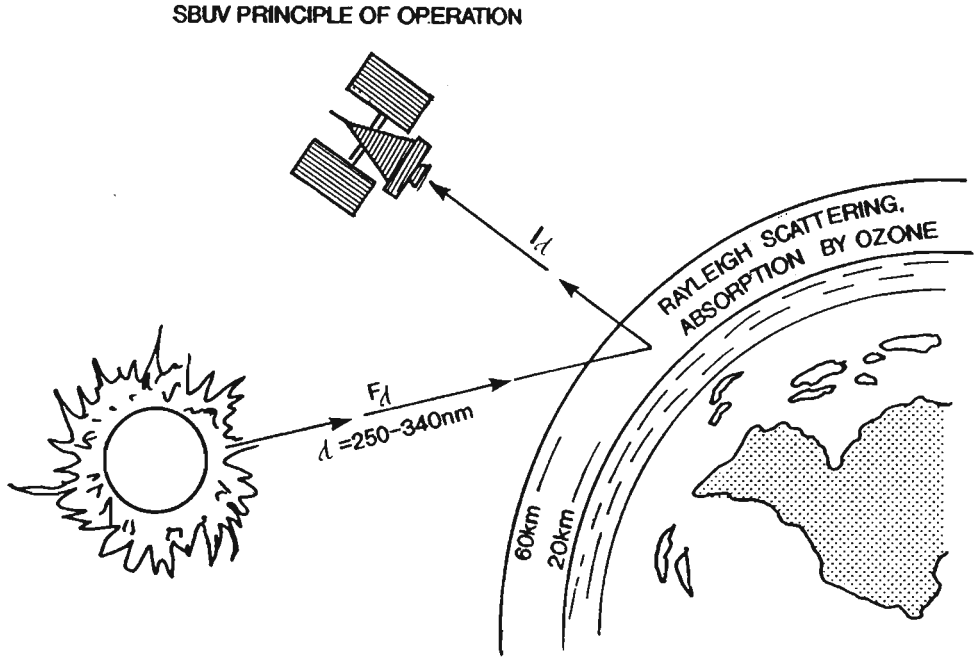

Figure 2.2 Schematic representation of the SBUV observing geometry. The required quantity for an ozone determination is the ratio of the Rayleigh backscattered radiance, Iλ,to the solar irradiance, Fλ, at selected wavelengths over the range 250-340 nm. Redrawn after Frederick and Serafino (1985) p. 905.

above the earth's surface. The units of measurement are Dobson Units (DU), where 1 DU = 2,69 x 10^{16} mol O_3 cm^{-2} (Fishman *et al.*, 1988). Another way of interpreting these measurements is to express them in terms of the thickness the ozone layer would have if all the ozone in the column were brought down to sea level pressure and a standard temperature of 0°C (273.16 K). One Dobson Unit is then equivalent to one-thousandth of a centimetre of ozone or 0.001 cm (Gribbin, 1988; Salby and Garcia, 1990). Total column ozone data will be referred to henceforth simply as total ozone data.

Version 6 TOMS data have been used in this study. This data set has been corrected for inaccuracies created due to the degradation in the reflectivity of the aluminium diffuser plate on the TOMS instrument and the data are precise to within 1.3% (McPeters and Komhyr, 1991). The excellent agreement between the TOMS and Dobson network data also increases the confidence in the data set (Herman *et al.*, 1990; Herman *et al.*, 1991; McPeters and Komhyr, 1991). Factors other than those related to the satellite and its accompanying instruments may also affect the accurate collection of data. Significant attention has been given to the possibility of errors in the TOMS data set produced by the presence of clouds in the atmosphere which mask ozone in the lower layers (Fishman *et al.*, 1990). In particular, the work of Hudson and Kim (1994) shows that TOMS may overestimate ozone values in regions of marine-stratocumulus clouds due to high reflectivity and scattering. An algorithm based on measured reflectivity, a climatological cloud top height and assumed tropospheric ozone column amount is used to correct TOMS total ozone for such cloud effects. Clearly, varying cloud height will produce over or under estimates of column ozone. Attempts are being made to adjust the data to minimise errors (Thompson *et al.*, 1993).

Despite the existence of possible errors in the TOMS data, the TOMS data set is widely used. This is because satellites provide a better global coverage than the ground-based network of Dobson spectrophotometers (Warneck, 1988). One of the major advantages of the TOMS instrument is its ability to provide maps of total ozone over the entire globe on a daily basis (Stolarski *et al.*, 1986). Furthermore, Fishman and Larsen (1987) found that there was virtually no difference in the climatological longitudinal distribution of total ozone at low latitudes when the TOMS data set was screened for cloud by excluding measurements whenever clouds were present.

The TOMS data are made available in the form of digital daily data with a resolution of 1° latitude by 1.25° longitude by the National Space Science Data Center (NSSDC) located at the Goddard Space Flight Center, Maryland, USA. The raw data are accessed by direct electronic link between the Space Physics Research Institute at the University of Natal in Durban, South Africa and NSSDC.

The TOMS data are used to construct spatial plots and time-cross sections at individual stations. The data utilised include:

1. gridded data, with a grid spacing of 5° latitude x 5° longitude (not specified from here onwards) for the study area defined above, and data for individual stations including Marion Island, Gough Island, Cape Town, Port Elizabeth, Durban, Bloemfontein, Pretoria, Harare and Nairobi for the two year period, 1987 to 1988. The locations of the stations and the study area are shown in Figure 2.1.
2. gridded data and data for individual stations including Okaukuejo, Irene and Brazzaville for the SAFARI period.
3. gridded data for the mid-season months of January and July for the five year period 1985 to 1990 for the study area.
4. gridded data for the period 26 to 29 September 1987 for the study area.

2.2.2 Meteor 3 total ozone data

The Nimbus 7 satellite ceased to operate in May 1993. As a result, total ozone data for the period 27 to 30 May 1994 were obtained from the TOMS instrument on board the Meteor-3 satellite which was launched on August 15, 1991 from Plesetsk, Russia (Herman *et al.*, 1994). The satellite was launched into a 1200 km high orbit with an inclination angle of 82.5°. Unlike the near sun-synchronous Nimbus 7 satellite with a orbit precession of 22.5 hours, data capture by the Meteor 3 is more complex because of the nature of its orbit. The Meteor 3 orbit drifts with respect to the sun's angle with a period of 212 days, precessing at a rate of 1.3° per day toward the sunrise terminator (Herman *et al.*, 1994). The most significant difference between the two satellites is their precession period. Because Nimbus 7 was sun-synchronous, its equator crossing time was always approximately noon. It drifted from local noon at the time of launch to 10:45 in 1993 (Bodeker, 1994). This means that Nimbus 7 viewed the entire globe each day. Due to the long precession time of the Meteor 3 orbit, the equator crossing time varies between noon (the sun is overhead and the solar zenith angle = 0°) to the day-night terminator (the solar zenith angle = 90°) thus providing complete global measurements of ozone except when the orbit is near the day-night terminator. Under these conditions, the TOMS instrument may not be able to view one of the hemispheres for a period of up to 3 weeks. This differs from the Nimbus-7/TOMS ozone data which are inaccessible only during the polar winter. Details of the technical differences between the two satellites and their associated discrepancies are given in Bodeker (1994).

The TOMS instrument on board the Meteor satellite is nearly identical to the Nimbus 7/TOMS with the most significant difference being the modification in

the diffuser plate assembly (Herman *et al.*, 1994). This change improves the instrument's in-flight self calibration capability and makes it possible to utilise the "real-time" product.

The Meteor 3/TOMS ozone data are given in a 1° latitude by 1.25° longitude grid for each day of the year. The data are obtained by the Space Physics Research Institute at the University of Natal in Durban, from the NSSDC.

Nimbus 7 and Meteor 3/TOMS data compare very well and comparisons with ground-based instruments reveal close absolute values and day-to-day variations. Concurrent plots of Nimbus 7 and Meteor/3 data have shown similar morphology over the Southern hemisphere with low values over the lower latitudes and increasing values in the mid-latitudes and slightly lower values near the South Pole (Bodeker, 1994). Further details of the Meteor 3/TOMS characteristics and a comparison between the Meteor 3/TOMS and Nimbus 7 TOMS ozone data are given in Herman *et al.* (1994).

The Meteor 3/TOMS data are thoroughly reviewed by the Goddard Ozone Processing Team over an extended period of time prior to archiving (Herman, 1995), so that instrument errors, data processing errors and calibration errors are minimised. The data have been utilised in several studies (Bojkov and Fioletov, 1995; Gleason *et al.*, 1993) in the absence of Nimbus 7 data. Small discrepancies between the Nimbus/TOMS and Meteor 3 data are not critical in this study. In this study, the Meteor 3 data that have been utilised have not been subject to these extensive checks. However, since the data are used to illustrate the downward transport of ozone into the troposphere in a case study, absolute values are not critical. Meteor 3/TOMS data were extracted for Irene (Pretoria) for the period 27 to 30 May 1994.

2.3 VERTICAL OZONE DATA

2.3.1 ECC ozonesondes

The SAWB established a permanent ozonesonde station at Irene where ozonesondes were launched once a week between June 1990 and October 1993. Irene is situated at 25°52'S and 28°13'E, approximately 20 km south of Pretoria (Fig. 2.1). The project was terminated due to the high costs involved (Coetzee, pers. comm., 1993). Data from these routine ascents have been utilised in this study, as well as data from ozonesonde launches at Okaukuejo in the Etosha National Park, Namibia, Ascension Island (8°00'S;14°00'W) and Brazzaville, in

Congo, during the SAFARI-92 experiment. A sounding log of dates during SAFARI and maximum heights to which sondes reached, at each location, is given in Diab *et al.* (1996a). In addition, a series of ozonesondes were launched at Irene for case study analysis between 27 May 1994 and 30 May 1994 as part of Southern African Atmosphere Research Initiative (SA'ARI-94).

In each case the instruments used were Science Pump Type 5A electrochemical concentration cell (ECC) sondes, which were interfaced with Vaisala RS 80-15NE radiosondes. Standard ground receiving equipment based on the Vaisala PP12a Universal Formatter and QuickBASIC software applications were used to provide profiles of pressure (hPa), temperature (°C), humidity (%), and ozone partial pressure (mPa) measurements (Coetzee and Archer, n.d.). Ozone partial pressure (mPa) measurements were converted to mixing ratios (ppbv) by means of:

$$x=\left[\frac{\left(\frac{P}{1000}\right)}{(P_a \times 100)}\right] \times 10^9 \qquad (2.1)$$

where

x = Ozone mixing ratio (ppbv)

P_a = Ozone partial pressure (mPa)

P = Pressure (hPa)

Data were recorded at ten second intervals. Ascent times at Okaukuejo and Irene were 7 Z (09:00 local time) and 6 Z (08:00 local time) respectively.

2.3.2 Integrated tropospheric column ozone

The method used to determine the column ozone at selected heights from an ozonesonde sounding is based on the method developed at the NASA Langley Research Center (Bracket, pers. comm., 1995). The personnel at NASA Langley have had several years experience with ECC sondes and have based the calculation on the gas laws and theory dealing with partial pressures. The column amount of ozone is calculated using the air pressure and the ozone partial pressure measured by the ozonesonde as it ascends through the atmosphere. The thickness of the ozone, in a column (DU), is calculated between a particular point of measurement and the preceding point of measurement, the following formula is used:

$$\text{Ozone (DU)} = \frac{(O_3 \text{ Prev} + O_3 \text{ Curr}) \times \log 10(\text{Pres. Prev.}/\text{Pres. Curr})}{1.1} \qquad \textbf{(2.2)}$$

where

O_3 Prev	=	Ozone partial pressure from preceding measurement (nanobars)
O_3 Curr	=	Ozone partial pressure from current measurement (nanobars)
Pres. Curr	=	Air pressure from current measurement (millibars)
Pres. Prev	=	Air pressure from preceding measurement (millibars)

(Source: NASA Langley Research Center, USA)

The column ozone amounts (DU) calculated for each reading are summed to give the total column ozone. The column ozone amount in the troposphere or the integrated tropospheric column ozone, between 0 and 16 km (agl) was calculated from four ozonesondes launched at Irene during the period 27 to 30 May 1994 and from 11 ozonesonde launches at Brazzaville (0 - 16 km) during the SAFARI-92 period.

2.4 DERIVED METEOROLOGICAL VARIABLES

2.4.1 Potential vorticity

Potential vorticity (PV) is defined from Ertel's theorem, for adiabatic flow, as the vorticity of a parcel of air multiplied by its thermal stability as evaluated on constant θ surfaces (Shapiro, 1980). The quantity PV is the isentropic coordinate form of Ertel's potential vorticity and is defined with a minus (positive) sign so that its value is normally positive (negative) in the Northern Hemisphere (Southern Hemisphere) (Holton, 1992). PV is conserved in the atmosphere in adiabatic, frictionless flow and is advected as a passive tracer along isentropic surfaces (Hill and Browning, 1987). PV is derived

exclusively from meteorological parameters and is regarded as a suitable tracer of stratospheric air and stratospheric ozone (Danielsen, 1968; Danielsen *et al.*, 1970; Danielsen and Hipskind, 1980). PV analysis provides a means of analysing three dimensional motions of the air on surfaces corresponding quite closely to surfaces of equal potential temperature (θ) or isentropic surfaces. θ is thus used as the vertical coordinate.

$$PV = (\zeta + 2\,\Omega \sin\varphi)\frac{\partial\theta}{\partial p} \qquad (2.3)$$

where

$$\zeta = \frac{1}{a\cos\varphi}\left[\frac{\partial v}{\partial\lambda} - \frac{\partial(u\cos\varphi)}{\partial\varphi}\right] \qquad (2.4)$$

where

ζ	=	the vertical component of the relative vorticity vector
θ	=	potential temperature (K)
u	=	meridional wind component (ms^{-1})
v	=	zonal wind component (ms^{-1})
a	=	earth's radius (6.371×10^6 m)
Ω	=	angular speed of rotation of the earth (7.292×10^{-5} rad s^{-1})
λ	=	longitude
φ	=	latitude
PV	=	potential vorticity ($\times 10^{-7}$ $KhPa^{-1}s^{-1}$)
p	=	pressure (hPa)

Using the methods outlined by Haagenson and Shapiro (1979) and Randel (1992), PV was calculated for selected θ surfaces. Units are K hPa^{-1} s^{-1}.

The first step involved calculating θ for each grid point on each isobaric surface. Secondly, the isentropic surfaces which lay between selected isobaric surfaces were determined. This was achieved by scanning all the grid points for the lowest (highest) isobaric surface and determining the highest (lowest) θ on that surface. Isentropic surfaces could then be generated between the highest and lowest potential temperatures and parameters interpolated on these isentropic surfaces. The transformation procedure for isentropic coordinates is given in Haagenson and Shapiro (1979). PV for each grid point on the

isentropic surface was calculated using the u and v components of the surrounding grid points.

Daily PV maps for numerous isentropic surfaces in the study area and PV cross sections were constructed for several days extending over the duration of individual case studies. The primary data source was the ECMWF 12 UTC analysed data set.

2.4.2 Ozone mass

Ozone mass was calculated by utilising the method of Bodeker *et al.* (1992) and Bodeker (1994) to calculate the total mass of ozone in an area 5° latitude x 5° longitude over the centre of the composite cut off low case studies described in section 2.6.2. Daily TOMS data are employed to provide an estimate of total mass of ozone in a given area. Manipulating the ideal gas equation $pV = (M/m)RT$, where M is the total mass, m is the molar mass ($3 \times 16 \times 10^{-3}$ kg), R is the universal gas constant, V is volume and T the temperature and by substituting in $\rho = M/V$, the density of ozone at S.T.P. is estimated to be 2.11 kg m^{-3}. It follows then, that if 1 DU = 10^{-5} m of ozone at S.T.P., for a column of ozone of cross-sectional area 1 m^2, the mass per unit area or mass density (MD) is given by MD = 2.11×10^{-5} D kg m^{-2}, where D is the value in Dobson Units. The mass of ozone in TOMS cells can be summed to obtain the total mass of ozone in a given area (Bodeker *et al.*, 1992).

Ozone mass, in a 5° x 5° grid surrounding the COL centres, was calculated for the composite COL case study as described in section 2.6.2.

2.5 BACK TRAJECTORY MODELLING

Isentropic back trajectory analysis was employed to investigate the origin of ozone maxima over southern Africa. The movement of substances such as water vapour, ozone and radioactivity have been widely studied using this method (Danielsen, 1961; 1974).

Isentropic trajectory analysis uses the conservative property of potential temperature (θ) to trace air movement and eliminates the major source of error generated by the isobaric approach by allowing vertical motion (Danielsen, 1961). This approach is applied in this study to examine the role of large scale circulation in the transport of ozone over the southern African subcontinent. Backward trajectories are typically used for the interpretation of chemical measurements (Pickering *et al.*, 1993a).

Isentropic 8-day back trajectories on θ levels [θ = 312 (one case only), 314, 316, 318 and 320 K], which lie between 900 and 500 hPa have been conducted using the isentropic trajectory model developed by Dr Mark Schoeberl of NASA/Goddard Space Flight Center (GSFC). The model was originally designed for use in stratospheric analyses (Schoeberl *et al.*, 1992) and requires gridded fields of temperature, geopotential heights, u and v wind components, and PV. ECMWF gridded data were used in this study.

The trajectory model has been used extensively for both forward and backward trajectory analysis (Schoeberl *et al.*, 1992; Pickering *et al.*, 1993a; Pickering *et al.*, 1994a)

The use and limitations of this model for tropospheric trajectory studies over the South Atlantic is described by Pickering *et al.* (1993). Significant differences were detected between trajectories computed using ECMWF and National Meteorological Center (NMC) gridded data. The differences are greater for back trajectories initiated over the South Atlantic than over the continent of Africa. The analyses are therefore more similar over the land where there are more observations. The use of ECMWF data has been recommended for the Southern Hemisphere (Trenberth and Olson, 1988). The quality of input data for the trajectory model is emphasised by Pickering *et al.* (1993), who recognise the need for additional data collection in the southern African region in order to enhance the quality of output.

The trajectories were started as 7 x 7 arrays of parcels spaced 0.25° apart, centred around two points, Okaukuejo (19°11'S;15°55'E) and Irene (25°53'S;28°13'E). The start time was 12 Z in each case. Gridded fields of meteorological data from the ECMWF data set were used. The meteorological grid spacing was 2,5° x 2,5° so that the array size was less than the grid size (McNamara, pers. comm., 1993). According to McNamara (pers. comm., 1993) this method provides an insight into the divergent or unstable conditions which decrease the confidence in the accuracy of the middle point trajectory and an indication of the model uncertainties due to spatial interpolation.

Cases were selected for trajectory analysis by subjectively examining the surface synoptic charts for anticyclonic and westerly trough weather patterns during the SAFARI period. Okaukuejo and Irene were used as the initial points for these case studies. Two cases were chosen for each location. These include:

			DAY NUMBER
Okaukuejo	:	6 October - 28 September 1992	(280-272)
		15 October - 7 October 1992	(289-281)
Irene	:	30 September - 22 September 1992	(274-266)
		22 October - 14 October 1992	(296-288)

2.6 COMPOSITE ANALYSIS

Composite analysis has been used widely in the field of climatology (Jury, 1993; Levey, 1993). The method reduces cumbersome data in case study analysis to a generalised set of data, thus reducing the number of figures, maps and tables generated. The resulting composites provide a better indication of common features, trends and patterns in variables than the case study approach. Composite constructions do, however, mask extreme data.

2.6.1 Composite anticyclonic and westerly trough profiles

Composite vertical profiles of ozone and meteorological variables were constructed for typical anticyclonic flow and a westerly trough during the SAFARI period. Stratification of the weather types was based on the classification defined by Garstang *et al.* (1996). The composite anticyclonic ozone profile was computed from ozonesonde ascents on 15, 27 September and 5, 6, 10, 14 and 15 October 1992. The composite westerly trough ozone profile was computed from ascents on 21, 23 September and 11, 13 October 1992. Corresponding composite RH profiles were also computed.

2.6.2 Composite cut off low pressure systems

A specific synoptic feature, the cut off low or COL was selected for case study analysis. Details are provided in Chapters 4 and 6. Six individual COL case studies have been examined by using composite analysis.

18 COL cases which occurred over South Africa or originated in the surrounding ocean and moved over the continent were selected by examining 200 and 300 hPa upper air synoptic charts. The upper air charts were supplied by the SAWB, for January and July 1985 to 1990. By examining the upper air (300 and 200 hPa) and surface synoptic charts and TOMS and PV distributions, 6 case studies were selected for composite analysis. These include:

case 1. 10-01-1985 to 14-01-1985
case 2. 21-07-1986 to 25-07-1986
case 3. 19-07-1987 to 23-07-1987
case 4. 25-09-1987 to 29-09-1987
case 5. 13-07-1989 to 17-07-1989
case 6. 09-01-1990 to 13-01-1990

The remaining 12 cases were excluded on the basis that they were either too short lived (2 days or less) and dissipated prematurely or did not extend sufficiently far over the continent.

Since the COL systems generally lasted between 3-5 days, a time period of 5 days was deemed suitable for the examination of the dynamical effects on ozone. The following time frame (Levey, 1993) was utilised: two days preceding the deepest expression of the COL was labelled day -2, the day of the deepest expression, day 0 and two days following the event, day +2. This will provide an overall picture of the changes observed in ozone before, during and after a deep COL event. Data were excluded on days when either troughs or COLs did not exist (indicated by a blank space in Table 2.1). Data used to compile the composites are summarised in Table 2.1.

Table 2.1 Composite time frame.

CASE	DAY 0	VARIABLE (day)				
		day_{-2}	day_{-1}	day_0	day_{+1}	day_{+2}
1	19850112	*	*	*	*	*
2	19860723		*	*	*	
3	19870719			*	*	*
4	19870927		*	*	*	
5	19890713			*	*	*
6	19900110			*	*	*
	COMPOSITE	$\frac{\Sigma(n_{-2})}{1}$	$\frac{\Sigma(n_{-1})}{3}$	$\frac{\Sigma(n_0)}{6}$	$\frac{\Sigma(n_{+1})}{6}$	$\frac{\Sigma(n_{+2})}{4}$
* denotes data used, n denotes day number						

Vertical cross sections taken as a slice through the atmosphere through the centre of each COL system and spatial distributions, for the study area (defined earlier), of PV, TOMS, ozone mass, RH, scalar wind speed and ω were produced by normalising the COL systems with respect to their centre points

estimated from the 300 hPa upper air chart. Vertical cross sections represent variations in atmospheric parameters through 15° latitude on either side of the COL centre.

*****

The methodology applied and the data used in this thesis have been described in this chapter. The following chapter provides an account of ozone distribution and variation as a background to this study.

CHAPTER 3

OZONE DISTRIBUTION AND VARIATION

3.1 INTRODUCTION

The amount of ozone in the atmosphere may be expressed in terms of total column ozone, stratospheric or tropospheric ozone. The tropospheric component is frequently divided further into expressions of surface and free tropospheric ozone, which describe ozone levels measured near the surface and ozone concentrations found above the planetary boundary layer (PBL) between approximately 4 and 10 km (Fishman, 1991) respectively. Surface ozone measurements are made using ground-based instruments while free tropospheric ozone concentrations are determined from airborne instruments mounted on baloons and aircraft.

The aim of this chapter is to provide an overview of the global distribution of ozone and the trends that have been noted. In particular, pertinent characteristics of ozone concentrations in the southern hemisphere will be highlighted. This will provide a base from which short-lived ozone maxima can be studied over southern Africa.

3.2 CLIMATOLOGY OF OZONE

Ozone is produced in the stratosphere by a series of photochemical reactions which are summarised below.

$$O_2 + h\nu \rightarrow O + O \qquad (3.1)$$

$$O + O_2 + M \rightarrow O_3 + M \qquad (3.2)$$

$$O_3 + h\nu \rightarrow O_2 + O \qquad (3.3)$$

$$O + O_3 \rightarrow O_2 + O_2 \qquad (3.4)$$

Where hv denotes a photon of energy and M an inert third body which in the atmosphere is supplied by either nitrogen or oxygen (Warneck, 1988).

Ozone distribution, in the absence of atmospheric motion, is primarily determined by the chemical processes which create and destroy it. It would be expected then, that ozone would be most abundant in equatorial regions where the photodissociation of molecular oxygen is most efficient (Salby and Garcia, 1990). However, this is not true, since at extratropical latitudes, ozone molecules are present at lower altitudes and higher air densities. Along with the mean meridional circulation of the stratosphere, this promotes gradual sinking at middle and high latitudes (Salby and Callaghan, 1993). Figure 3.1 shows the downward slope of the tropopause toward the poles and the associated ozone number densities.

3.2.1 Total column ozone

Total column ozone measurements are commonly used to represent atmospheric ozone. Total column ozone is a measure of the integrated amount of ozone in a column extending above the earth's surface through the atmosphere and expressed in DU (details are given in Chapter 2). At low latitudes, the tropospheric component contributes approximately 5 to 20% (Levine, 1990; Fishman *et al.*, 1988; Ramanathan, *et al.*, 1987). In the middle and higher latitudes, total ozone measurements are largely representative of stratospheric and upper tropospheric ozone which amounts to about 90% between approximately 15 and 55 km. At these latitudes the tropospheric contribution to column amounts is considered to be less significant.

Total ozone displays both a temporal and spatial variation throughout the atmosphere and is illustrated for both hemispheres in Figure 3.2. Minimum total ozone occurs in a belt near the geographic equator and a marked gradient exists between 20 to 25° and 50 to 55° latitude (IES, 1977). A typical amount of total ozone found in the atmosphere at middle latitudes is approximately 300 D.U., although values of between 225 and 500 D.U. are not uncommon at higher latitudes (Fishman *et al.*, 1992). The highest values in the Southern Hemisphere are believed to occur to the south of the Indian Ocean, Australia and New Zealand, but north of the Antarctic shoreline (IES, 1977) and extremely low total ozone levels, as low as 125 D.U., have been observed over the South Pole in conjunction with the ozone hole (Stolarski, 1988).

Little variation in total ozone during the year is evident at low latitudes (Fig. 3.2). However, a strong seasonal cycle is observed at middle and high latitudes. Total ozone minima, in the Northern Hemisphere, occur during the summer months, while maxima are evident during late winter and spring

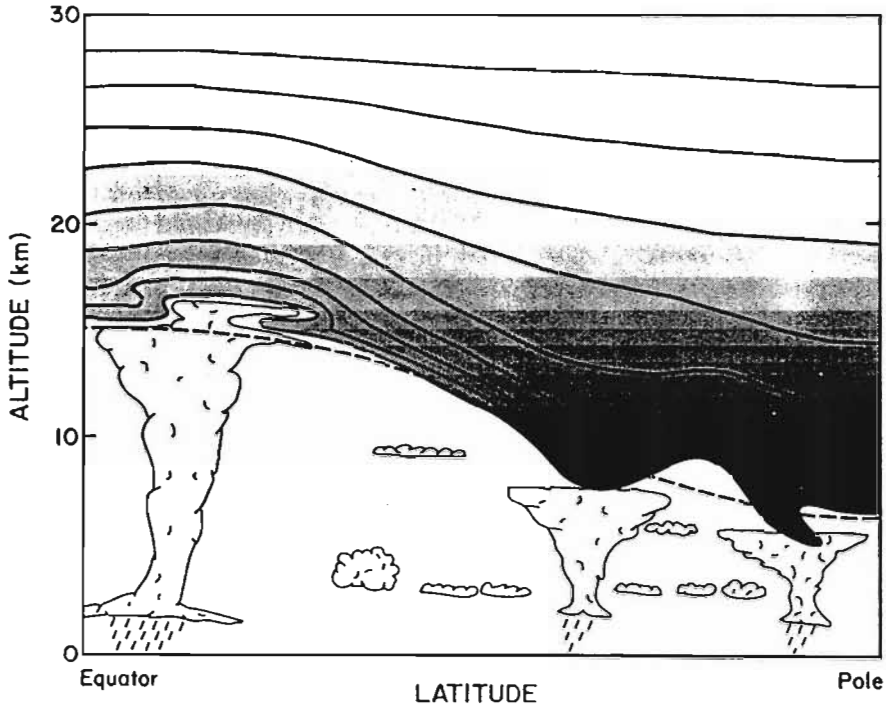

Figure 3.1 Schematic cross section of the troposphere and the lower stratosphere. The ozone number density (stippled) increases sharply above the tropopause, the mean position of which is indicated by a solid dashed curve, and then decreases due to exponentially falling air density. Disturbances in the atmospheric circulation periodically deflect the tropopause and adjacent isentropic surfaces (solid). Ozone-rich air descends along these surfaces and is compressed causing an increase in ozone number density. Reproduced from Salby and Callaghan (1993) p. 2716.

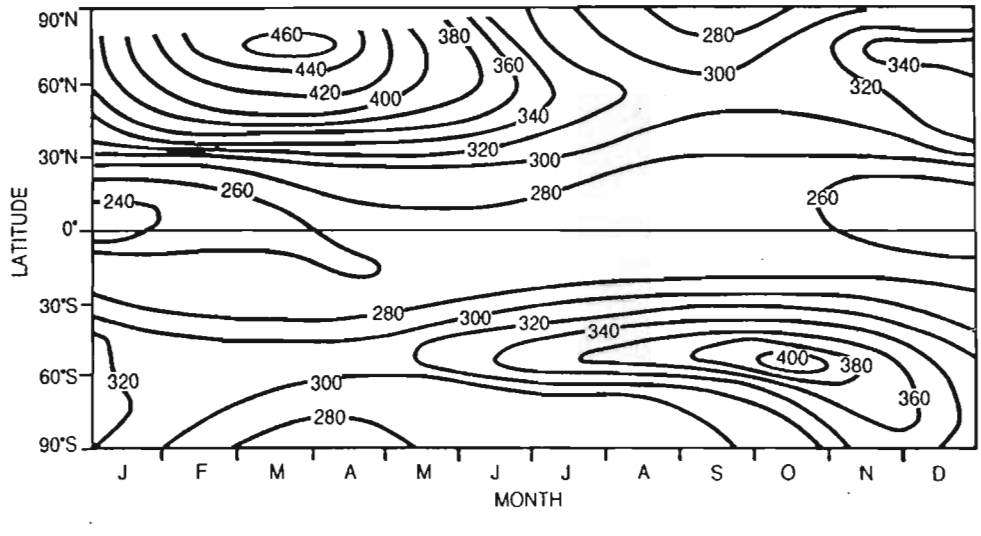

Figure 3.2 Seasonal variation in total ozone. The average column abundance of ozone (DU) is shown as a function of latitude and season. Reproduced from Salby and Garcia (1990) p. 40.

(~ 400 DU) at middle and high latitudes, as the result of the poleward transport out of the tropical source region. At southern hemisphere mid-latitudes highest levels have been recorded in the spring, whilst lowest values occur in the summer months (Diab *et al.*, 1992).

In addition to seasonal variations, there is a global decline in total ozone which is illustrated in Figure 3.3. Changes in ozone concentration also occur over shorter time scales (IES, 1977; Salby and Garcia, 1990). Such variations result from both natural factors, such as variations in meteorology and in biogenic emissions, and those produced by anthropogenic activities, such as industrial and vehicle emissions.

3.2.2 Tropospheric ozone

Tropospheric ozone comprises free tropospheric ozone and surface ozone each having its own unique characteristics. Ozone is transported into the troposphere, from the ozone-rich stratosphere and is produced *in situ* by photochemical reactions driven by naturally occurring and anthropogenically produced chemical species.

Ozone is produced and destroyed in the troposphere by chemical reactions involving free radicals. The process involves the oxidation of CO, CH_4, and hydrocarbons in the presence of nitrogen oxides to form ozone. The destruction process involves reactions of ozone with HO_x radicals and loss through deposition (Chameides and Walker, 1973; Crutzen, 1973; NRC, 1991). The chemical species involved are found in abundance in the polluted urban environments, where industrial and motor vehicle pollution are abundant (NO_x, CO and hydrocarbons) (Chameides and Walker, 1973; Crutzen *et al.*, 1985), and would be expected to be greatest in the northern hemisphere where industry and commerce are concentrated. Another comparable source of ozone is biomass burning (Fishman, 1988). Biomass burning, in particular in tropical Africa and South America, has been shown to contribute significantly to the atmospheric load of trace gases (Lobart and Warnatz, 1993). A diagrammatic representation of the interacting physical and chemical processes which determine the amount of ozone present at a certain time and place in the earth's atmosphere is shown in Figure 3.4.

The long life-time of ozone in the free troposphere enables it to be transported long distances away from its source region, thus affecting areas considerable distances downwind. This type of long-range transport has been shown to be an important factor in the occurrence of seasonal elevated ozone amounts over southern Africa (for example, Garstang *et al.*, 1996). Elevated ozone levels have also been recorded at rural sites where local ozone

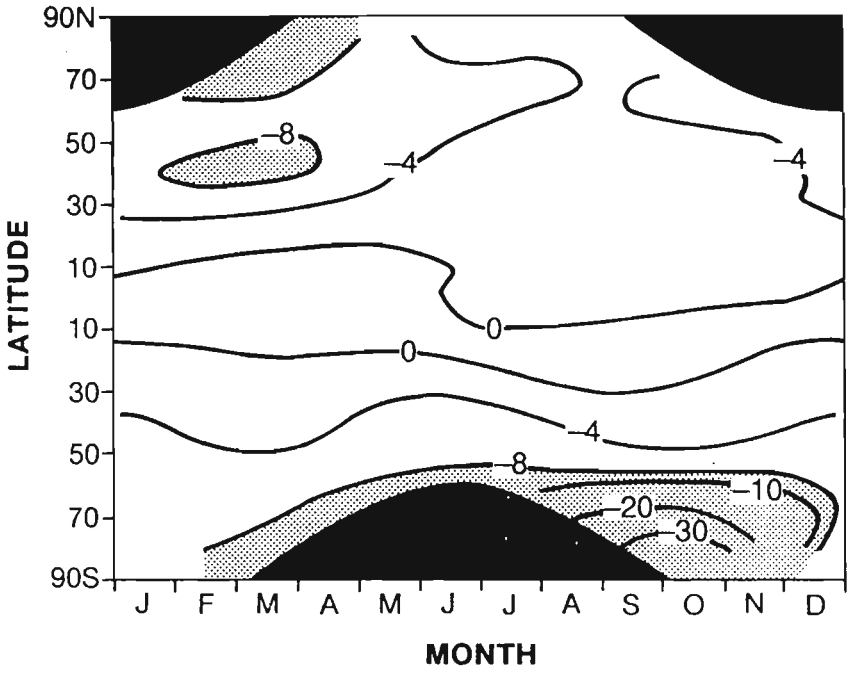

Figure 3.3 Trends in total ozone shown as % change per decade, deduced from the Total Ozone Mapping Spectrometer (TOMS) data according to latitude and season. Reproduced from Stolarski *et al.* (1991). The lightly shaded areas have rates of loss exceeding 8% per decade. The heavily shaded areas show the Arctic and the Antarctic polar nights, when no data is captured. A northern midlatitude peak is evident, in winter and early spring, with a downward trend of more than 8% per decade.

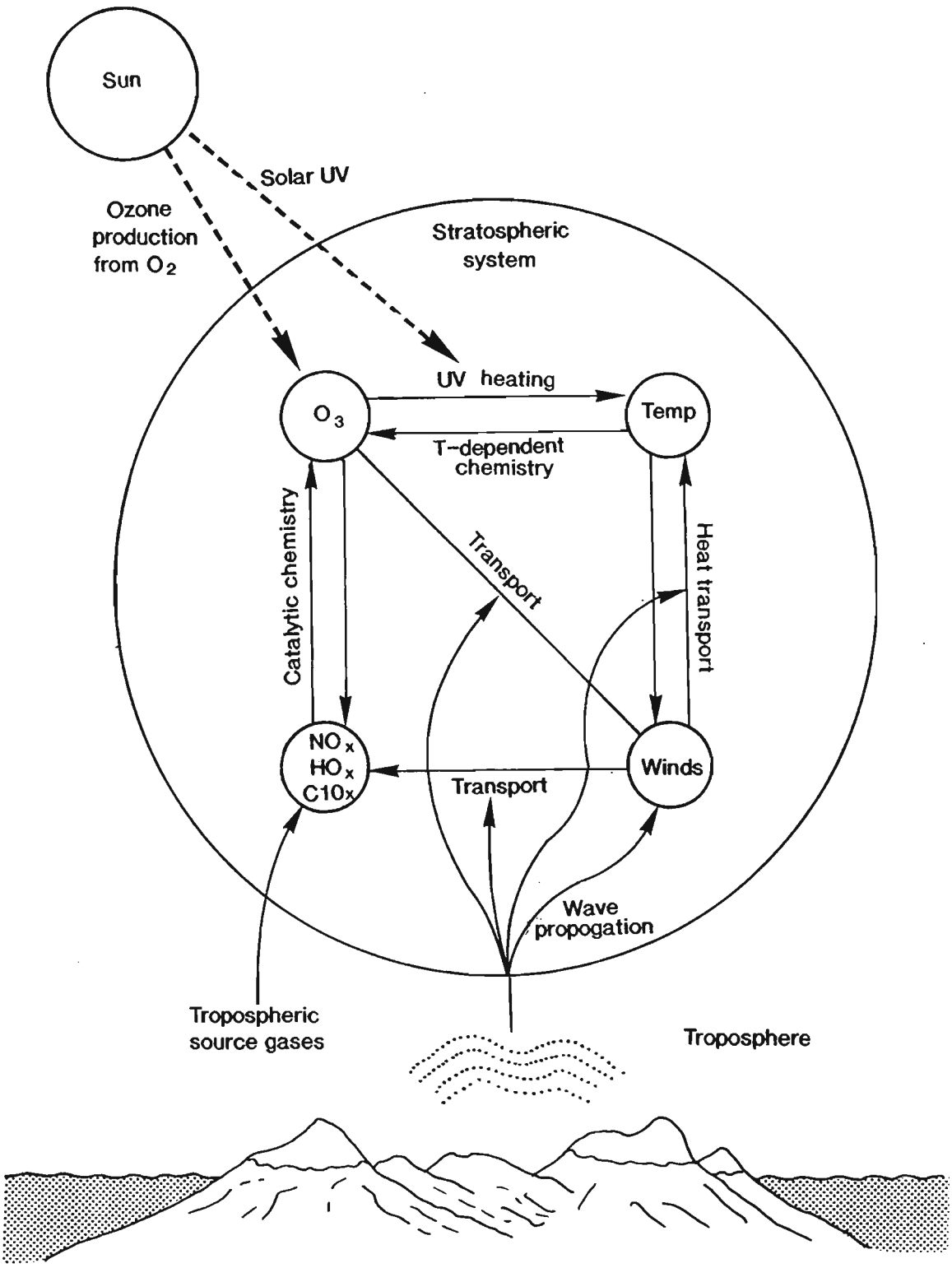

Figure 3.4 Diagrammatic representation of the interacting physical and chemical processes which determine the amount of ozone present at a certain time and place in the earth's atmosphere. Redrawn from Rycroft (1990) p. 4.

precursor sources are absent (Guicherit, 1988).

The redistribution of lower tropospheric air has been shown to enhance ozone production through dilution of the reactive species such as NO (Liu *et al.*, 1980; Fehsenfeld *et al.*, 1988; Pickering *et al.*, 1993b; Pickering *et al.*, 1990). Chatfield and Delany (1990) have described two scenarios which illustrate the significance of dilution in increasing the efficiency of ozone production. The "cook-then-mix" scenario describes the common situation whereby pollution is trapped within the inversion and experiences deposition at the surface. Convection and vertical distribution occurs after a few days. On the other hand, the "mix-then-cook" situation refers to convection occurring during a pollution event and which provides the dilution required for active ozone production. Tropospheric ozone production can be enhanced in this way by up to 50% (Pickering *et al.*, 1990) when ozone precursors (for example, NO, CO and NMHCs) are transported from the boundary layer to the free troposphere.

The significance of the vertical transport of trace gases in convective systems to free tropospheric ozone levels on a regional scale (Pickering *et al.*, 1992b) has been highlighted in investigations seeking explanations for seasonal tropospheric maxima. Recent observations from Brazil (Kirchhoff *et al.*, 1989) and Africa (Fishman and Larsen, 1987; Fishman *et al.*, 1990; 1991; Cros *et al.*, 1991; Fishman, 1994; Thompson *et al.*, 1996c) suggest that elevated ozone concentrations may result from photochemical production associated with biomass burning rather than as a result of the combustion of fossil fuels in urban environments. Episodic convective events would transport insoluble chemical species into the free troposphere away from fires in much the same way as discussed above for pollutants produced in urban areas.

The distribution of ozone with latitude in the middle troposphere is very different from that in the upper troposphere to lower stratosphere region. The middle troposphere reflects similar seasonal patterns to those observed at the surface in the Northern Hemisphere, while the seasonal pattern in the upper troposphere resembles that for ozone in the lower stratosphere (Logan, 1985). Highest mid-tropospheric values are found at northern hemisphere mid-latitudes, between 30° and 50° latitude. This maximum is present in all seasons at 700 hPa, but occurs only in spring and summer at the 500 hPa level. Mid-latitude seasonal cycles show smaller amplitudes in the middle troposphere of the southern hemisphere, and concentrations are largest in spring in the south in contrast to the broad summer maximum in the north. The high latitudes exhibit significant hemispheric asymmetry in the seasonal cycles of ozone.

Evidence suggests that ozone concentrations in the troposphere have increased

in both hemispheres and in the case of the Northern Hemisphere, by a factor of two or more over the past 100 years (UNEP, 1994). The increasing trend in tropospheric ozone has also been observed in the Southern Hemisphere (Zunckel, 1992; Zunckel *et al.*, 1992), although the relationship is less well established due to a lack of sufficient and reliable data.

Surface ozone concentrations depend heavily on location, local meteorological conditions and photochemistry. Thus, ozone at the surface exhibits diurnal and seasonal cycles with maxima and minima occurring as expressions of photochemical production which is enhanced by high levels of ozone precursors and dry, sunny conditions. This is illustrated in the cycles observed for populated urban, and relatively unpopulated and rural areas at northern and southern hemisphere sites.

Logan (1985) describes a broad summer maximum for the populated sites (Europe and the United States) and a minimum in summer or autumn in remote sites (Tasmania and Canada). Variations in the timing of maxima for northern hemisphere sites are documented in Bojkov (1988). In contrast, a spring maximum has been detected at polluted southern hemisphere sites (Combrink et al,, 1995). Observations at non-urban sites for the northern hemisphere indicate an increase in ozone concentration at the surface (about 1% per year) and even stronger in the lower troposphere, with the latter increasing at a greater rate (Bojkov, 1988). A modelling study by Liu *et al.* (1987) suggests that the winter ozone maximum, at northern hemisphere rural sites, is anthropogenic in origin, especially in the lower troposphere at mid- and high latitudes. Also, that the accumulation of ozone during winter and the long lifetime of ozone, contributes substantially to the observed spring ozone maxima at many remote sites. Spring maxima, in remote locations, have traditionally been explained by the injection of ozone from the stratosphere (Liu *et al.*, 1987). A winter maximum has been observed at the Cape Point background monitoring site in South Africa (Combrink *et al.*, 1995) which is consistent with other remote sites such as Cape Grim in Tasmania (Logan, 1985; Elsworth *et al.*, 1988).

3.3 SOURCES OF VARIATION IN OZONE

3.3.1 Introduction

Ozone number density or column abundance is greatest between 10 and 20 km (Salby and Callaghan, 1993), roughly in the region of the tropopause and lower stratosphere (Fig. 3.1). Variations in ozone within this region will most

likely produce the greatest fluctuations in total column ozone.

Essentially, ozone column abundance is a function of firstly, photochemical production or loss and secondly, of transport. Photochemistry has been briefly discussed in section 3.2.2. Transport processes, in turn, are a function of the dynamics of the atmosphere. Transport processes responsible for variations in total ozone include mean meridional circulation, movement of the tropopause, planetary-scale waves, stratospheric-tropospheric exchange (STE) and convective cloud processes. Each of these processes are discussed in the following sections. STE is dealt with separately, and in more detail, in Chapters 5 and 6.

3.3.2 Mean meridional circulation

The zonal mean transport in the lower stratosphere normally takes the form of a hemispheric two-cell diabatic circulation, with rising motion in the tropics and subsidence near the poles (Tung *et al.*, 1986). It has also been proposed by Reiter (1975) that the Hadley cell circulation of the troposphere, extends far into the stratosphere and that the upward-flowing branch moves significant amounts of tropical tropospheric air into the stratosphere. He argued further, for reasons of continuity (except for the seasonal variations in tropopause height), that the same amounts of stratospheric air would return into the troposphere in the middle and high latitudes. According to Reiter (1975), 38% of the equivalent stratospheric mass enters the stratosphere through the tropical branch of the Hadley cell and returns to the troposphere in the subtropical branch.

The effect of this upward transport of air into the stratosphere which is dominant at low latitudes, is to reduce the column abundance of ozone, since the major source of ozone is in the stratosphere (Danielsen, 1993). Compensating downward air mass transport into the troposphere, at higher latitudes, would have the opposite effect.

Riehl and Malkus (1958) and subsequently Reiter (1975) and Shapiro (1980) have pointed out that the upward flux of mass in the tropical branch of the Hadley cell does not occur as a continuous slow motion. Instead, the updrafts occur in cloud formations such as narrow "hot towers" or "cloud turrets" of localized cumulus convection and larger-scale regional upwelling associated with tropical cyclones (Danielsen, 1993), which penetrate the tropical and extra-tropical tropopause providing a means for the exchange of air and its constituents between the troposphere and stratosphere. The role of clouds in vertical transport is discussed further, later in this section.

3.3.3 Movement of the tropopause

Staley (1962) has pointed out that the seasonal variation in tropopause height will lead to equivalent changes in the mass of air contained in the stratosphere. Accordingly, as the tropopause rises there will be a decrease in stratospheric mass and *vice versa*. Based on the seasonal changes in tropopause height for a few selected North American stations as reported by Staley (1962), and assuming that these changes are representative of the northern hemisphere, Reiter (1975) has inferred stratospheric mass changes for different latitude bands (Table 3.1.).

Table 3.1 Seasonal variation of median tropopause pressures (in millibars) over North America. Reproduced from Reiter (1975), p. 462.

Lat., deg	Winter	Summer	ΔP	Mass change, 10^{17}g
0			+(25)	+ 28.4
5			+(25)	+ 56.7
10			+(25)	+ 56.7
15			+(25)	+ 55.0
20	95	120	+ 25	+ 53.3
25	100	120	+ 20	+ 41.3
30	160	120	- 40	- 78.9
35	200	120	- 80	- 148.8
40	220	120	- 100	- 174.6
45	250	140	- 110	- 177.1
50	250	200	- 50	- 72.6
55	240	210	- 30	- 38.8
60	225	225	0	0
65	230	230	0	0
70	240	240	0	0
				Σ-400.5

Between latitude 30°N and 55°N the stratosphere loses mass from winter to summer. Equatorward of 25°N the stratosphere gains mass and poleward of 55°N,

there are no significant seasonal changes in tropopause height. Consequently, the net decrease in stratospheric mass from winter to summer approximates 400×10^{17} g, which means that in one year seasonal changes in tropopause height accounts for a flux of about 10% of the mass of the stratosphere (Reiter, 1975). According to Reiter (1975), however, this net flux does not occur by a gradual and continuous falling or rising of tropopause levels everywhere around the hemisphere. The fluctuation is rather caused by imbalances in the large-scale quasi-horizontal and vertical motions of the mean meridional circulation and in the large-scale eddy transport, mainly in the region of the jet stream.

The effect of the seasonal changes on ozone levels is significant. As the height of the tropopause decreases, ozone-rich stratospheric air moves downward following the tropopause. Chatfield and Harrison (1977) examined ozone mixing ratios and tropopause heights at northern hemisphere sites which revealed greatest penetration of ozone into the troposphere in spring, which coincides with low tropopause levels.

In the early 1950's, a study concerning day-to-day changes in ozone and the height of the tropopause was conducted over Oxford, London, for the three month period of November 1950 to February 1951 (Normand, 1953). The results revealed a statistically significant, inverse relationship between total column ozone and the height of the tropopause.

More recently, Warneck (1988) has confirmed the correlation between total ozone and the pressure at the tropopause level. He suggests that the height of the tropopause serves as an indicator of cyclonic activity where low pressure systems are associated with lower than average tropopause level and above average total ozone. The increase in total ozone is explained by the convergence and subsidence of air in the mid-stratosphere, forcing ozone-rich air downward into the lower stratosphere. The ozone column density thus increases. The reverse of the process occurs for high-pressure systems. Warneck (1988) reports further that the velocity of the vertical air motions can reach 1 km per day, which is sufficient to change total ozone by 25% within a few days.

3.3.4 Planetary-scale waves

An important source of natural spatial and temporal variability in ozone occurs through transport of ozone by planetary-scale waves. Planetary waves cause variations in ozone levels through meridional and vertical transport. In the southern hemisphere, these waves also play an important role in modifying ozone distribution through their interaction with the Antarctic

vortex (Bodeker, 1994). Of interest here are the roles of the semi-stationary planetary waves (wave numbers 1 to 3) and the transient baroclinic or Rossby waves of smaller scales (wave numbers 4 to 6). The former have been cited as being responsible for the springtime buildup of ozone in the mid-latitudes (Holton, 1979; Wang *et al.*, 1983).

Significant ozone transport occurs during sudden stratospheric warming (SSW) events which are associated with the upward propagation of planetary waves (particularly waves 1 and 2), as a result of excitation in the troposphere by orography and longitudinally varying heat sources (Hunt, 1989), and the poleward transport of heat (Schoeberl and Hartmann, 1991). SSW events have been extensively studied (for example, Farrara and Mechoso, 1986; Newman, 1986), and have been found to cause poleward eddy ozone transport in the middle stratosphere (24 to 38 km) and equatorward transport in the upper (above 38 km) and lower (below 25 km) stratosphere (Wang *et al.*, 1983).

The role of baroclinic waves in transporting ozone was first studied by Dobson *et al.* (1929), who noted that maximum positive deviations of daily ozone values from monthly means occurred to the rear of a surface low pressure system, and maximum negative deviations to the rear of a surface high pressure system. Later, Dobson *et al.* (1946) suggested that the maximum ozone deviation occurred directly over a surface low pressure system rather than to its rear. This apparent discrepancy was later resolved by Reed (1950), who attributed it to the difference between the strong baroclinic structure of a developing low pressure system, in which an upper air trough would be displaced to the west of a surface low, and a mature low pressure system, which was vertically stacked with height.

Reed (1950) was responsible for specifying, in detail, the relationship between total ozone and weather, which he attributed to the effects of either horizontal advection or vertical motion or a combination of both, in association with a baroclinic wave. The mechanism, as applicable to the Northern Hemisphere, is described in Figure 3.5.

The horizontal advection theory is based on the fact that, on average, total ozone increases poleward (Fig. 3.5a). As a consequence, advection of air from the north into a trough would be expected to cause an increase, and advection from the equator, a decrease in ozone amount (Fig. 3.5b).

The effect of vertical displacements are shown in Figure 3.5c. A positive ozone deviation consistent with the temperature field (Fig. 3.5b) is associated with the subsiding motion of the upper level trough and consequently increasing ozone, whereas the ridge is associated with decreasing ozone. The final distribution of ozone shows that the poleward and downward

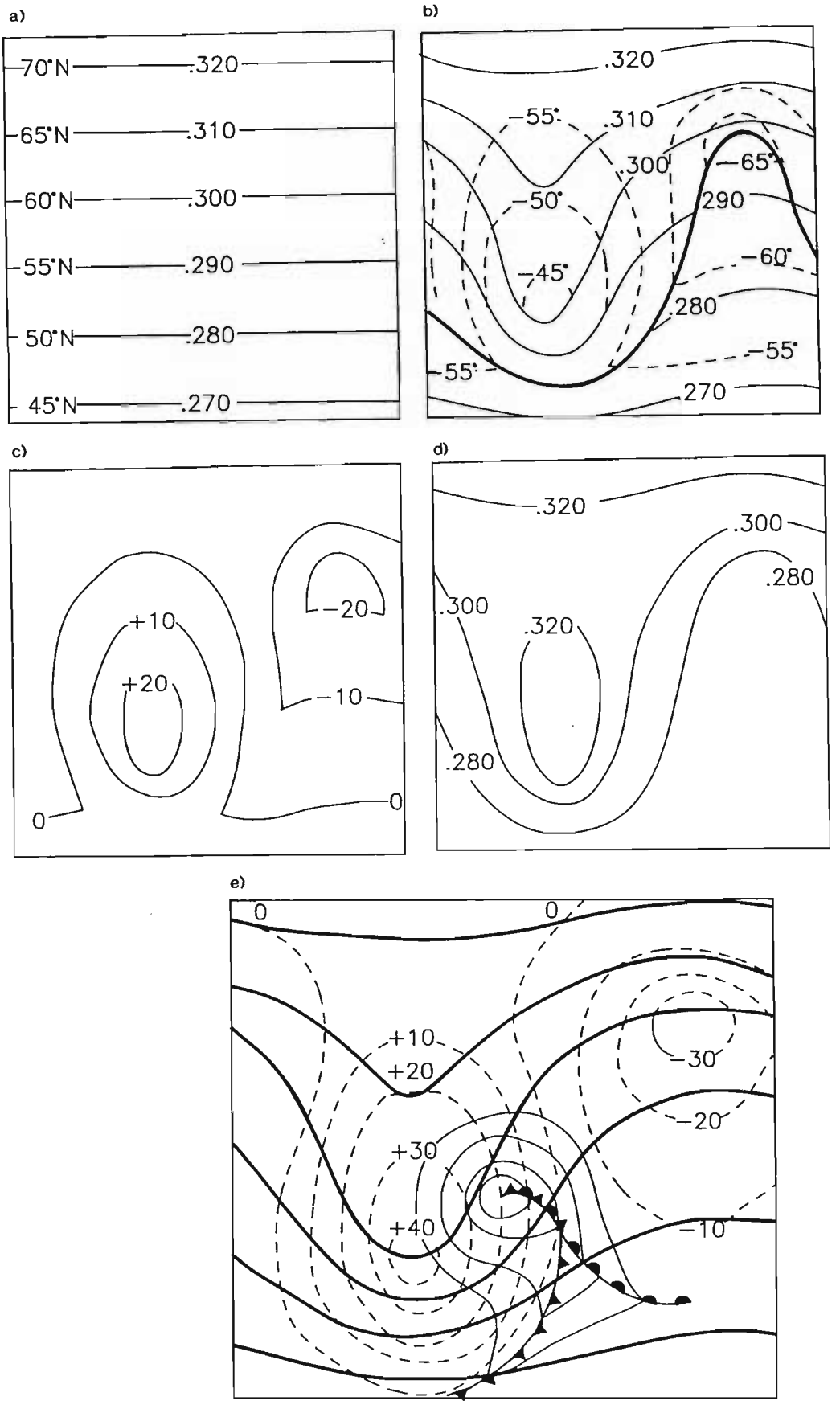

gure 3.5 Schematic diagram of ozone-weather relationships: (a) assumed initial, undisturbed, meridional distribution of total ozone amount in cm.; (b) disturbed state; thin solid lines give ozone distribution resulting from horizontal displacement only and represent approximate 200-mb contours; dashed lines are 200-mb isotherms; solid line is intersection of tropopause with 200-mb surface; (c) ozone deviations ($cm.10^3$) due to vertical displacements; (d) final distribution of total amount in cm., taking account of both horizontal and vertical displacements; and (e) heavy solid lines are high-level contours; thin solid lines are sea-level isobars; surface fronts depicted according to usual conventions; dashed lines are total ozone deviations ($cm.10^3$). Redrawn from Reed (1950) p. 266).

displacement of air into an upper level trough causes high ozone values and the equatorward and upward displacement to an upper level ridge causes low ozone values (Fig. 3.5d). In a baroclinic system, the upper air system is displaced to the rear or west of its surface counterpart, and consequently, high ozone values (positive deviations) are found to the rear of surface low pressure systems and low ozone values (negative deviations) to the rear of surface high pressure systems (Fig. 3.5e).

3.3.5 Role of convection (clouds)

Cumulus convective clouds contribute to the production of ozone maxima through photochemistry and vertical transport. At mid- and higher latitudes convective activity is often associated with cyclonic systems (Preston-Whyte and Tyson, 1988) while deep convective systems form an integral part of the ascending motion of the Hadley cell at tropical latitudes (Riehl and Malkus, 1958). The role of cumulus convection and erosion of the tropopause in association with stratosphere-troposphere exchange (STE) is discussed in Chapter 5.

Much of the literature concerned with STE and the role of cumulus clouds emphasises the irreversible transfer of mass and trace gases from the troposphere to the stratosphere. Conditions favouring such transport are discussed by Newell and Gould-Stewart (1981) who termed the area where air enters the stratosphere from the troposphere a 'stratospheric fountain'. During the Tropical Experiment of the Stratosphere-Troposphere Exchange Project (STEP Tropical) conducted in 1987, the upward transfer of dry air, consistent with low relative humidity of the stratosphere, in cloud systems was investigated (Russel *et al.*, 1993). The effect of this transport on ozone levels was also discussed. Theoretically, the upward transport of tropospheric air into the ozone-rich stratosphere should decrease total column ozone amounts although, mixing across the tropopause, in overshooting cloud turrets, may produce enhanced ozone levels in the upper troposphere (Russel *et al.*, 1993). Downdrafts in cumulus clouds, on the other hand, would contribute to ozone levels at lower altitudes (Stallard *et al.*, 1975).

The transport of lower tropospheric air into the mid- and upper troposphere in cumulus clouds has been extensively studied (Dickerson *et al.*, 1987, Garstang *et al.*, 1988, Connors *et al.*, 1991; Pickering *et al.*, 1990; 1991; 1992a; 1992b; 1993; 1994b). The transport is rapid and is estimated to take a few hours in a thunderstorm (Dickerson *et al.*, 1987). Transport of ozone and ozone precursor gases transported in this way plays a significant role in the production of mid- and free tropospheric ozone maxima. The process is however, complicated by the reactive nature of the chemical substances involved.

Mention of the photochemical processes involved was made in section 3.2.2.

3.3.6 Summary

The entire globe is subject to the redistribution of ozone due to, *inter alia*, the mean meridional circulation, the vertical propagation of waves in the westerlies extending from the troposphere into the lower stratosphere, changes in the level of the tropopause causing diurnal, day-to-day, seasonal and inter-annual variations, redistribution and photochemistry associated with convective cloud systems in both urban and rural environments. These processes operate on different time scales and are more dominant in some parts of the globe than in others. It is expected that a combination of these effects will contribute to ozone maxima observed in the study region.

Chapter 4

ATMOSPHERIC CIRCULATION AND OZONE DISTRIBUTION OVER SOUTHERN AFRICA

4.1 INTRODUCTION

Transport of ozone and ozone precursors plays an important role in the concentration of ozone at any one place and time. It is well known that long range transport of particulates and trace gases occurs in the atmosphere. Ozone in the stratosphere and troposphere is subject to both vertical and horizontal transport initiated by atmospheric processes ranging in scale from the micro to the macro scale. Ozone levels are further controlled by photochemical processes and as a result, photochemical sources and sinks play a significant role in the distribution of ozone.

The objective of this chapter is to investigate the tropospheric transport processes which affect ozone distribution over southern Africa. This task was greatly facilitated by the data collected during the South African Fire-Atmospheric Research Initiative (SAFARI) which took place during September and October 1992, under the umbrella of the Southern Tropical Atlantic Regional Experiment (STARE). This chapter is organised such that first, a general statistical analysis of the relationship between total ozone and synoptic weather systems, as expressed by various meteorological parameters, over southern Africa is presented. Secondly, a more in-depth analysis, focusing on the ozone distributions that characterise anticyclonic circulation and the passage of mid-latitude westerly troughs, was undertaken using data gathered during the SAFARI experiment.

4.2 THE RELATIONSHIP BETWEEN SYNOPTIC WEATHER AND TOTAL OZONE OVER SOUTHERN AFRICA

4.2.1 Introduction

The relationship between ozone and day-to-day weather patterns has been well documented in the literature and has been summarised in Chapter 3. However, most studies have based the explanation for the observed link on the mid-latitude cyclone model. Until recently, very little research had concentrated

on this relationship in tropical and subtropical regions. Since southern Africa is situated astride the subtropics, it provides an ideal location to examine the influences of both mid-latitudes, subtropical and tropical weather disturbances on total ozone.

4.2.2 Statistical analysis of total ozone and meteorological parameters

The relationship between total ozone and meteorological parameters was investigated for an area bounded by longitudes 10°W to 50°E and latitudes 0° to 50°S and for nine individual stations. The stations are Marion Island, Gough Island, Cape Town, Port Elizabeth, Durban, Bloemfontein, Pretoria, Harare, and Nairobi (Fig 2.1).

The meteorological parameters selected to represent the day-to-day change in weather are the heights of the 500, 300 and 100 hPa surfaces. The relationship between daily TOMS total ozone and the heights of these surfaces was examined statistically over the period 1987 to 1988 using simple linear least squares regression and making no allowance for serial autocorrelation in the time series.

The results of the statistical analysis are presented in Table 4.1. The relationships are generally negative but poor, with a maximum of 32% of the variance in total ozone explained by the variations in the height of the 300 hPa surface at Marion Island.

Table 4.1 Relationship between daily TOMS total ozone and the 100, 300, and 500 hPa geopotential heights for nine southern African stations, 1987-1988

Station	Correlation Between TOMS and 100 hPa	r^2 100 hPa	Correlation Between TOMS and 300 hPa	r^2 300 hPa	Correlation Between TOMS and 500 hPa	r^2 500 hPa
Marion Island	-0.32	10.16	-0.57	32.60	-0.52	26.96
Gough Island	-0.26	6.54	-0.49	23.92	-0.41	16.48
Port Elizabeth	-0.22	4.70	-0.39	14.96	-0.32	9.91
Cape Town	-0.26	6.81	-0.46	21.10	-0.39	14.98
Durban	-0.13	1.68	-0.22	5.10	-0.18	3.14
Bloemfontein	-0.15	2.29	-0.28	8.02	-0.21	4.52
Pretoria	-0.12	1.50	-0.18	3.13	-0.12	1.32
Harare	-0.11	1.11	-0.07	0.46	-0.03	0.10
Nairobi	*0.22	4.95	*0.08	0.65	*0.08	0.63

Significant at 95% confidence level; r^2 = percent variance. * Not significant at 95% confidence level. TOMS, total ozone mapping spectrometer

For all stations analysed (except Nairobi and Harare), the relationship is best between total ozone and the 300 hPa surface. There is also evidence of a general deterioration in the relationship with decreasing latitude, and indeed, a reversal in the sign of the correlation coefficient at Nairobi. Some

exceptions to this latitudinal trend occur. For example, Cape Town and Port Elizabeth, situated at approximately the same latitude, show marked differences in their r^2 values. A similar anomaly is noted for Bloemfontein and Durban. The discrepancies are even more marked in the seasonal data presented below.

The data were further analysed over shorter time periods. Widely diverging results were obtained in different seasons and years. The best relationships are observed in spring. For the period October to December 1988, r^2 values for TOMS total ozone and the 300 hPa geopotential height ranged between 72% at Marion Island and 32% at Durban (Table 4.2), consistent with the general comments made above that the relationship is strongest for the more southerly located stations. However, r^2 values for the same period in 1987 are dramatically different (Table 4.3).

Table 4.2 Relationship between daily TOMS total ozone and the 100, 300, and 500 hPa geopotential heights for nine southern African stations, October to December 1988.

Station	Correlation Between TOMS and 100 hPa	r^2 100 hPa	Correlation Between TOMS and 300 hPa	r^2 300 hPa	Correlation Between TOMS and 500 hPa	r^2 500 hPa
Marion Island	-0.81	65.02	-0.85	71.93	-0.81	66.12
Gough Island	-0.79	62.79	-0.78	60.34	-0.66	43.31
Port Elizabeth	-0.59	35.04	-0.66	43.67	-0.56	31.59
Cape Town	-0.62	38.95	-0.73	53.36	-0.61	36.93
Durban	-0.50	25.46	-0.57	32.09	-0.43	18.45
Bloemfontein	-0.50	25.22	-0.65	42.65	-0.55	29.91
Pretoria	-0.47	22.10	-0.65	41.59	-0.44	18.89
Harare	*0.05	0.25	-0.59	34.25	-0.19	3.52
Nairobi	*0.56	30.77	*0.47	22.48	*0.36	13.09

Significant at 95% confidence level; r^2 = percent variance. * Not significant at 95% confidence level. TOMS, total ozone mapping spectrometer

Table 4.3 Relationship between daily TOMS total ozone and the 100, 300, and 500 hPa geopotential heights for nine southern African stations, October to December 1987.

Station	Correlation Between TOMS and 100 hPa	r^2 100 hPa	Correlation Between TOMS and 300 hPa	r^2 300 hPa	Correlation Between TOMS and 500 hPa	r^2 500 hPa
Marion Island	-0.24	5.84	-0.31	9.73	-0.26	6.97
Gough Island	*0.02	0.03	-0.18	3.27	-0.13	1.65
Port Elizabeth	-0.13	1.77	-0.20	4.15	-0.13	1.63
Cape Town	-0.30	9.08	-0.36	12.91	-0.30	8.82
Durban	-0.06	0.32	-0.13	1.56	-0.06	0.42
Bloemfontein	-0.08	0.59	-0.14	2.02	-0.08	0.58
Pretoria	-0.08	0.59	-0.13	1.60	-0.06	0.35
Harare	-0.07	0.46	-0.07	0.54	-0.04	0.18
Nairobi	-0.45	20.63	-0.15	2.11	-0.08	0.68

Significant at 95% confidence level; r^2 = percent variance. * Not signifcant at 95% confidence level.
TOMS, total ozone mapping spectrometer

There is also an indication of a longitudinal component to the dynamical link. For example, Port Elizabeth has lower r^2 values than its latitudinal counterpart, Cape Town. A possible explanation may be that since the relationship is based on the mid-latitudes cyclone model embedded in the westerlies, it is better expressed on the western part of the subcontinent where potential continental influences have had less chance to obscure the relationship.

It can be inferred from these results that there are different dynamics operating in tropical and extra tropical latitudes and, furthermore, that there is a temporal component to the relationship, with varying dynamics in different seasons and years.

There is clearly a very weak link between total ozone and middle to upper tropospheric meteorological parameters (500 and 300 hPa geopotential heights) in the tropics, as represented by data for Nairobi. Here the relationship with stratospheric dynamics (100 hPa geopotential surface) is stronger, consistent with the well-established link between the quasi-biennial oscillation (QBO) and total ozone in the tropics (Angell and Korshover, 1978; Gray and Pyle, 1989). The QBO manifests itself in the equatorial zonal winds as rising or sinking motion at the equator, which in turn amplifies or dampens the Hadley cell circulation. During an easterly phase, the vertical motion (equatorial ascent in the Hadley cell) is increased in the stratosphere, which serves to lower total column ozone amounts, while a westerly phase and weakened equatorial ascent reduces the strength of the upward arm of the Hadley cell producing increased total column ozone (Gray and Pyle, 1989; Oltmans and London, 1982).

The relationship between total ozone and middle to upper tropospheric meteorological parameters is best expressed in the mid-latitudes, suggesting a physical link with the mid-latitude cyclone. It follows that lowering of the mid-tropospheric (300 hPa) pressure surface, as occurs in association with the passage of well-developed mid-latitude troughs is linked with high ozone amounts. Indeed, it is surprising that since 90% of the total column ozone is resident in the stratosphere (Fishman and Larsen, 1987; Fishman et al., 1990), that even 30% of the variance in total ozone is accounted for by upper tropospheric meteorological parameters. It suggests that there is some connection between the stratosphere and the troposphere which underlies the relationship. The most likely explanation is a tropopause break or fold which is accompanied by an injection of stratospheric ozone rich air into the upper troposphere. This is investigated in detail in Chapters 5 and 6.

Clearly, the relationship is a function of the frequency of certain synoptic types which varies with season and even between years. In response to this, the relationship between gridded ozone data and gridded ECMWF geopotential height data (for the 500, 300, and 100 hPa surfaces) over the study area was explored for each day for the period 1987 to 1988. Simple linear least squares regression was used and no allowance for spatial autocorrelation was made.

Relationships as measured by r^2 values between TOMS total ozone and heights of the 300 hPa surface differ markedly on a day-to-day basis. The relationship is generally good, and negative. A seasonal trend is evident, however, with lowest values in the autumn to winter period and highest values in spring and summer (Fig. 4.1). It is contended that the seasonal trend is a reflection of the predominance of certain synoptic situations in some seasons, a point which will be elaborated upon in the following sections.

Although the statistical analysis does not indicate a universally strong relationship between total ozone and synoptic weather parameters, there is little doubt that mid-latitude westerly waves have an influence on ozone concentrations. This is illustrated over a four-day period commencing on 6 June, 1988 (Fig. 4.2), when the west to east movement of an ozone front across South Africa is clearly visible.

Days on which the relationship between total ozone and meteorological parameters was best expressed occurred during the passage of mid-latitude westerly troughs over southern Africa. The relationship between particularly deep troughs, or intense cyclonic systems, which are often associated with tropopause folding and STE, and ozone distribution is investigated in detail in Chapter 6.

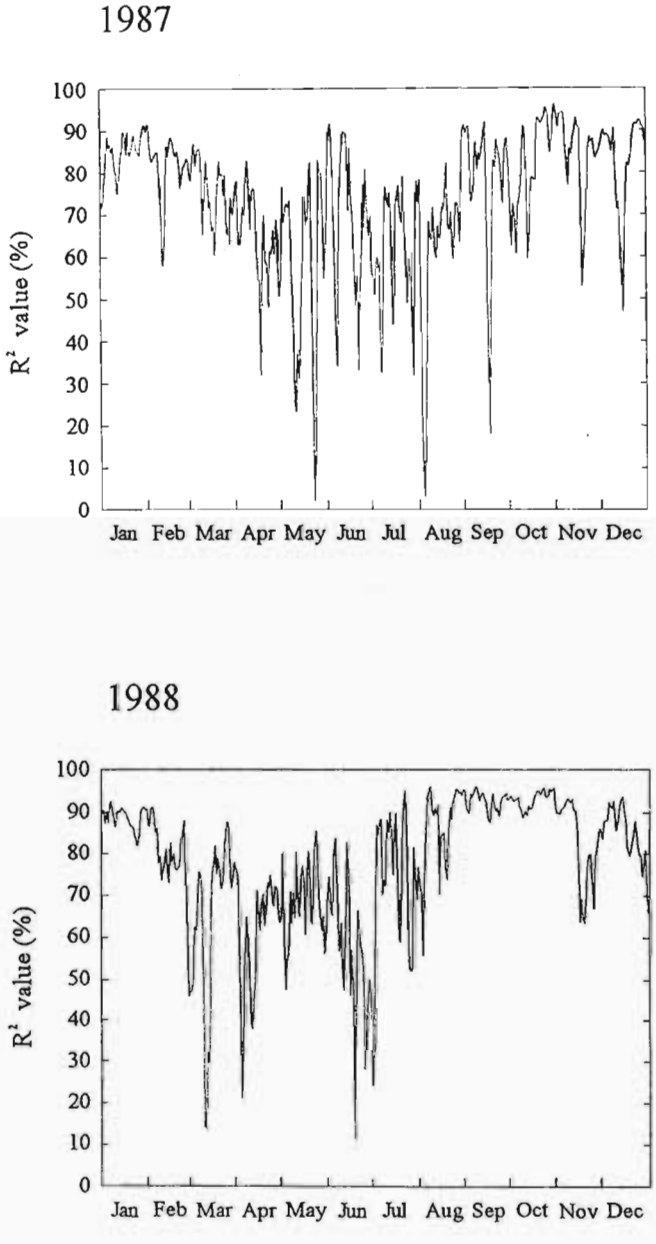

Figure 4.1 Day-to-day correlation, expressed as r^2 values, between (TOMS) total ozone (DU) and heights of the 300 hPa surface (ECMWF) for 1987 and 1988.

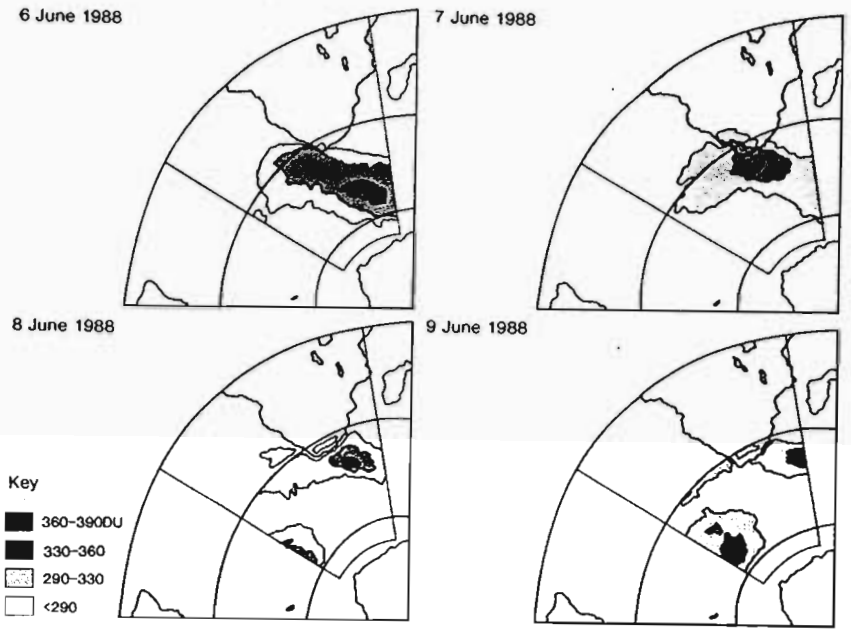

Figure 4.2 The distribution of TOMS total ozone (DU) over South Africa, June 6-9, 1988. Illustration compiled by Space Physics Research Institute, University of Natal, Durban, from TOMS data supplied by the National Space Science Data Center (NSSDC), USA.

Inasmuch as deep low pressure systems strengthen the relationship between total ozone and tropospheric meteorological parameters, it is important to identify those synoptic situations which lead to poor spatial correlation. Circulation patterns on days on which r^2 values were below 20% were examined and were found to be characterized by anticyclonic circulations. The case study of 23 to 24 May, 1987, was selected for detailed investigation.

The lower troposphere was characterized by closed high pressure cells (Fig. 4.3), which were replaced by ridges of high pressure in the upper air (300 hPa). A weak trough is evident to the west of South Africa on 23 May, encroaching over the southwestern parts of the country on 24 May.

PV plots have been used by many authors as indicators of STE. Cross sections of PV through 30°S display evidence of the trough in the dipping of the PV surfaces at approximately 5° and 12°E on 23 and 24 May respectively (Fig. 4.4). However, over most of the continent (10°-30°E) the PV surfaces are aligned horizontally with no evidence of STE. The PV tropopause, taken to be 100 x 10^{-7}K hPa^{-1} s^{-1} (Shapiro, 1978; 1980), is situated consistently between 9 and 11 geopotential kilometres (gpkm).

The lack of any noteworthy dynamical influence is shown also by the spatial distribution of PV on the 340 K isentropic surface (Fig. 4.5), in which there is no evidence of centres of dynamic activity over the continental regions. The TOMS total ozone field is also characterized by a lack of spatial contrast (Fig. 4.6). There is a more-or-less uniform distribution of total ozone, with continental values ranging between 270 and 280 DU.

It is well known that anticyclonic circulations dominate, over southern Africa, in the autumn and winter months (Preston-Whyte and Tyson, 1988) and it follows that they account for the poor relationship observed between total ozone and meteorological parameters in these seasons (see Figure 4.1).

4.2.3 Conclusion

Statistical analysis, using least squares linear regression, revealed a generally poor but negative relationship between total ozone and the heights of the 500, 300, and 100 hPa geopotential surfaces at the nine selected stations.

Circulation patterns on all days on which r^2 values were above and below the arbitrarily selected thresholds of r^2 equivalent to 80 and 20%, respectively, were examined. In the former cases, all occurred in association with the passage of a mid-latitude cyclone. The latter cases were all characterized by

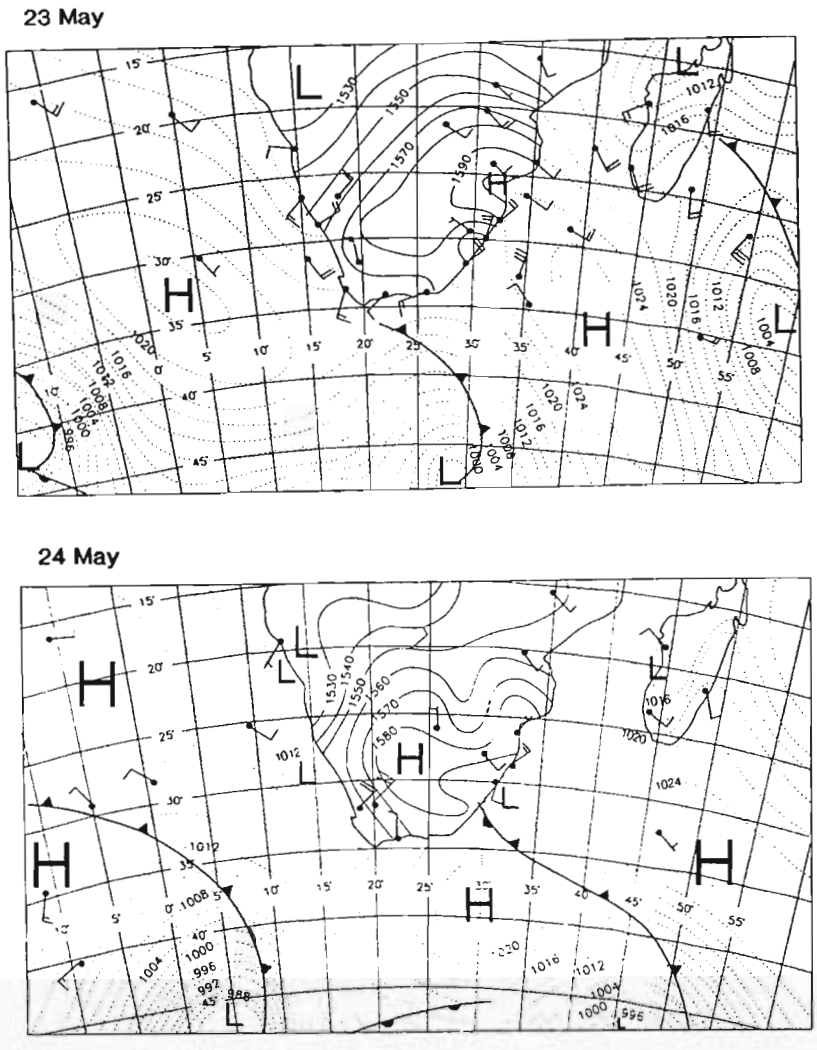

Figure 4.3 Surface synoptic charts for 23 and 24 May 1987. Surface pressure expressed as isobars (hPa) over the sea and heights of the 850 hPa surface (gpm) over the land (from Daily Weather Bulletin, SAWB) and 300 hPa synoptic charts for 23 and 24 May 1987, prepared from ECMWF 12 Z data.

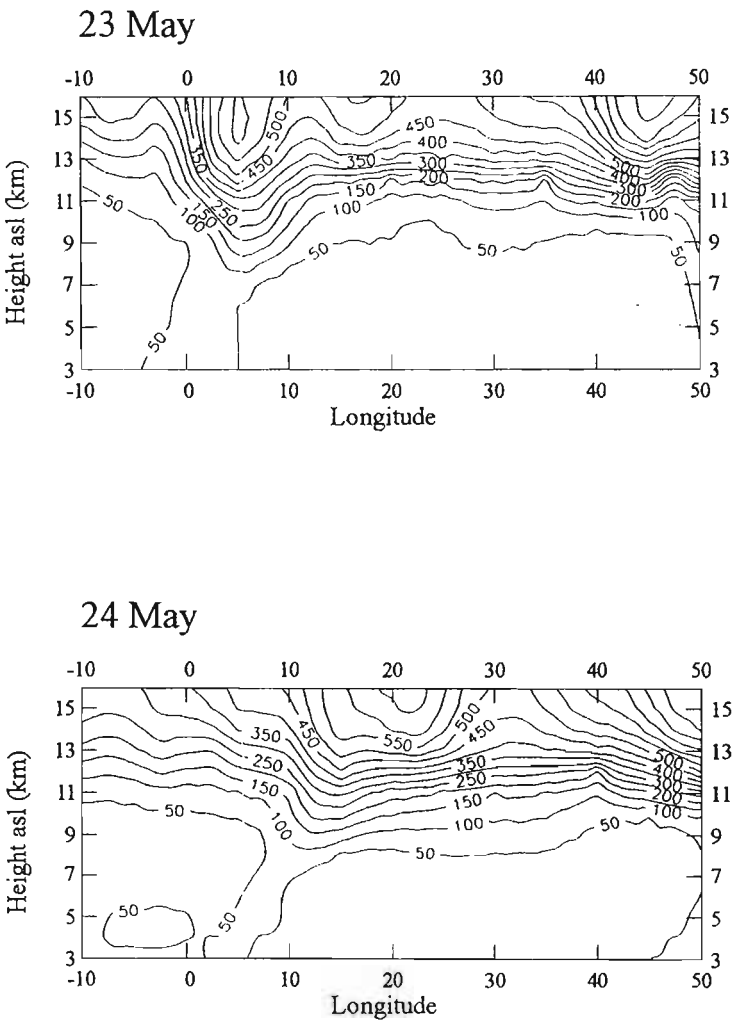

Figure 4.4 Vertical cross sections of PV (x 10^{-7} $KhPa^{-1}s^{-1}$) through 30°S, over South Africa, for 23 and 24 May 1987. Prepared from ECMWF data.

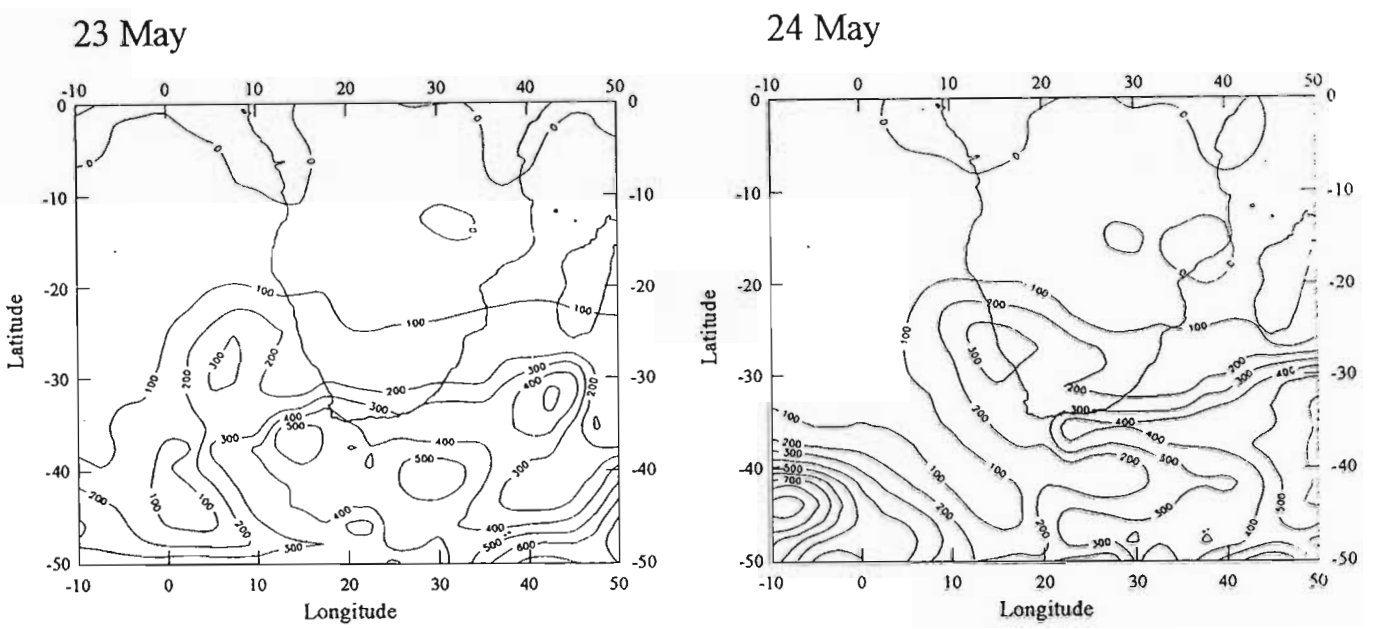

Figure 4.5 Spatial distribution of PV (x 10^{-7} $KhPa^{-1}s^{-1}$) on 340 K isentropic surface for 23 and 24 May 1987 for an area bounded by latitudes 0° to 50°S and longitudes 10°W to 50°E. Prepared from ECMWF data.

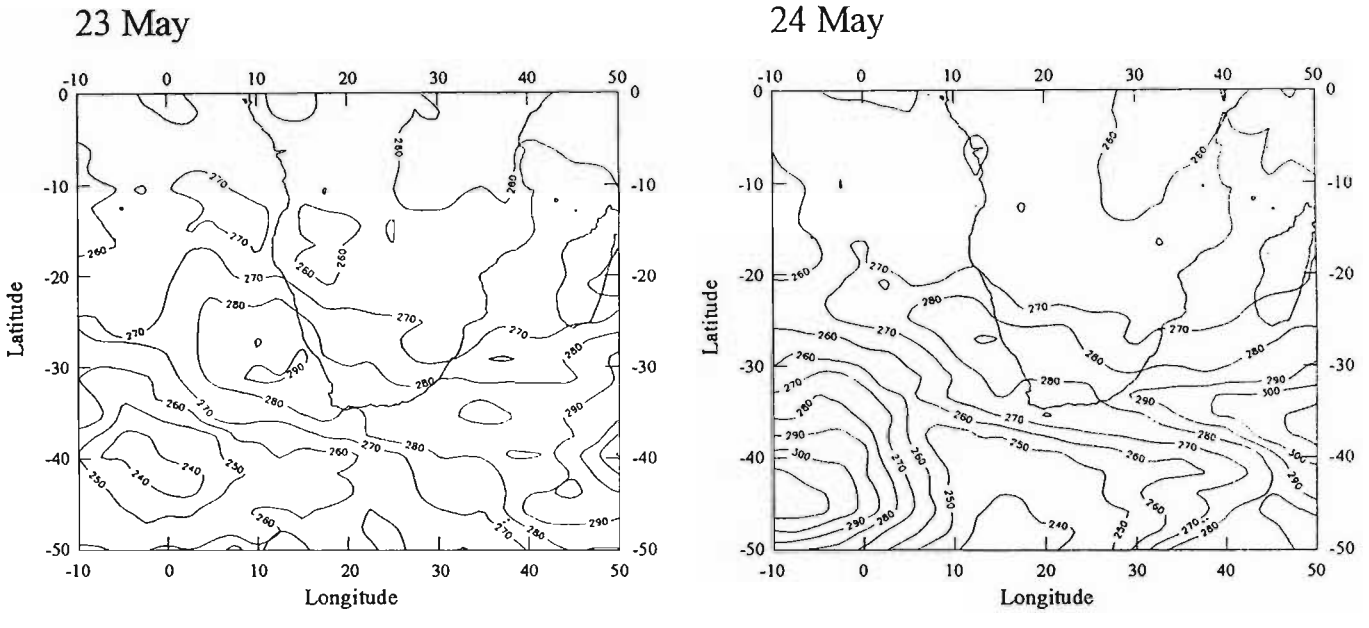

Figure 4.6 Spatial distribution of TOMS total ozone (DU) for 23 and 24 May 1987 for an area bounded by latitudes 0° to 50°S and longitudes 10°W to 50°E.

anticyclonic circulations. A case study was selected to explore the dynamics of a subtropical anticyclone. This revealed no dynamical connection between the stratosphere and troposphere and substantiated the weak statistical relationship found. The relationship between the passage of westerly, mid-latitude troughs is examined further in Chapter 6, where case studies of cut off lows (COLs) are presented in order to investigate STE.

Although the statistical analysis does not indicate a universally strong relationship between total ozone and synoptic weather parameters, there is little doubt that mid-latitude westerly waves play an important role in the generation of enhanced total ozone amounts.

The influence of anticyclonic circulation and the passage of westerly troughs on the vertical distribution of ozone over southern Africa is explored further by examining data collected during the Southern African Fire-Atmosphere Research Initiative (SAFARI) conducted in 1992. The data set comprises both meteorological and ozone data for the southern African region and is described in more detail in the following sections.

4.3 CIRCULATION AND TRANSPORT DURING SAFARI-92

4.3.1 Background to SAFARI-92

The Southern Tropical Atlantic Regional Experiment (STARE) in 1992, was the first intercontinental, international and interdisciplinary experiment designed to investigate fire emissions (Andreae *et al.*, 1993). One of the main aims of the initiative was to investigate biomass burning as a factor in atmospheric chemistry and to examine the nature, and extent of, the transport of the products of fires across the African continent (Lindesay, 1992). An important focus of the initiative was to explore the seasonal enhancement in tropospheric ozone that has been observed over the Tropical Atlantic Ocean (Andreae *et al.*, 1993; Hoell *et al.*, 1991; Fishman *et al.*, 1986; 1990; 1991) and to investigate its relationship with biomass burn products. STARE comprised two major components, of which the SAFARI examined the emissions from fires in southern Africa and The Transport and Atmospheric Chemistry near the Equator-Atlantic (TRACE-A) branch of the STARE campaign investigated the emissions from Brazilian fires.

The programme involved the collection of ground-based, aircraft and satellite measurements. The ground stations included: Brazzaville, Congo; Ascension Island; the temporary station at Okaukuejo, in Etosha National Park, Namibia; and Irene. The location of these stations is shown in Figure 2.1. The three

main objectives of SAFARI were to obtain ground data (vegetation characterisation and fuel loads), meteorological data (both boundary layer and lower and free troposphere using radio- and tethersondes) and trace gas and aerosol emissions which were determined by fire sampling techniques (Lindesay, 1996; Held and Lindesay, 1993).

No planned fires were conducted at Okaukuejo because of the severe drought experienced that year (Jury and Lutjeharms, 1993; Thompson *et al.*, 1996b). However, standard meteorological data (automatic weather station, pilot and tethered balloon ascents), ozone data (TOMS, ozonesonde, SAOZ spectrophotometer), air samples (polycyclic aromatic hydrocarbons) and ultraviolet (UV) data were collected (Diab, 1992). Controlled burning of savanna grasslands was conducted at Kruger National Park during September 1992 (Andreae *et al.*, 1993; Held and Lindesay, 1993). The fires were designed to simulate typical savanna fires. Laboratory studies, aircraft sampling and meteorological (radiosonde, pibal and tethered balloon ascents) and surface ozone observations were conducted. Emission measurements were also made over sugar cane fires in Swaziland and ozone, temperature, humidity and dust aerosol measurements were made at Victoria Falls in Zimbabwe (Andreae *et al.*, 1993). A large number of South African scientists, as well as their international counterparts, were involved in SAFARI. Ground-based data collected at Brazzaville, Okaukuejo, Ascension Island and Irene, and satellite data including TOMS and NOAA/AVHRR fire imagery were used in this study.

4.3.2 Circulation during SAFARI-92

SAFARI took place between August and October 1992. This period encompasses the end of winter, which is characterised by anticyclonic flow, and the onset of spring, during which time, disturbances in the westerly flow such as westerly troughs and cut off low pressure systems, reach a maximum (Preston-Whyte and Tyson, 1988). Westerly disturbances increased in the latter part of SAFARI (Garstang and Macko, 1993). Anticyclonic circulation prevailed over the subcontinent on approximately 55% of all days; westerly wave disturbances occurred for 41% of the time, while easterly wave disturbances occurred on 4% of the days (Garstang *et al.*, 1996).

The main transport patterns identified for the effective transport of aerosols and trace gases are summarised in Figure 4.7. The five basic horizontal transport mechanisms, in the lower (surface to 3 km), and the middle (3 to 6 km) troposphere, have been described (Garstang *et al.*, 1996). These include the direct easterly and westerly transport, and the recirculation of air within the anticyclonic circulation or "continental gyre". Anticyclonic

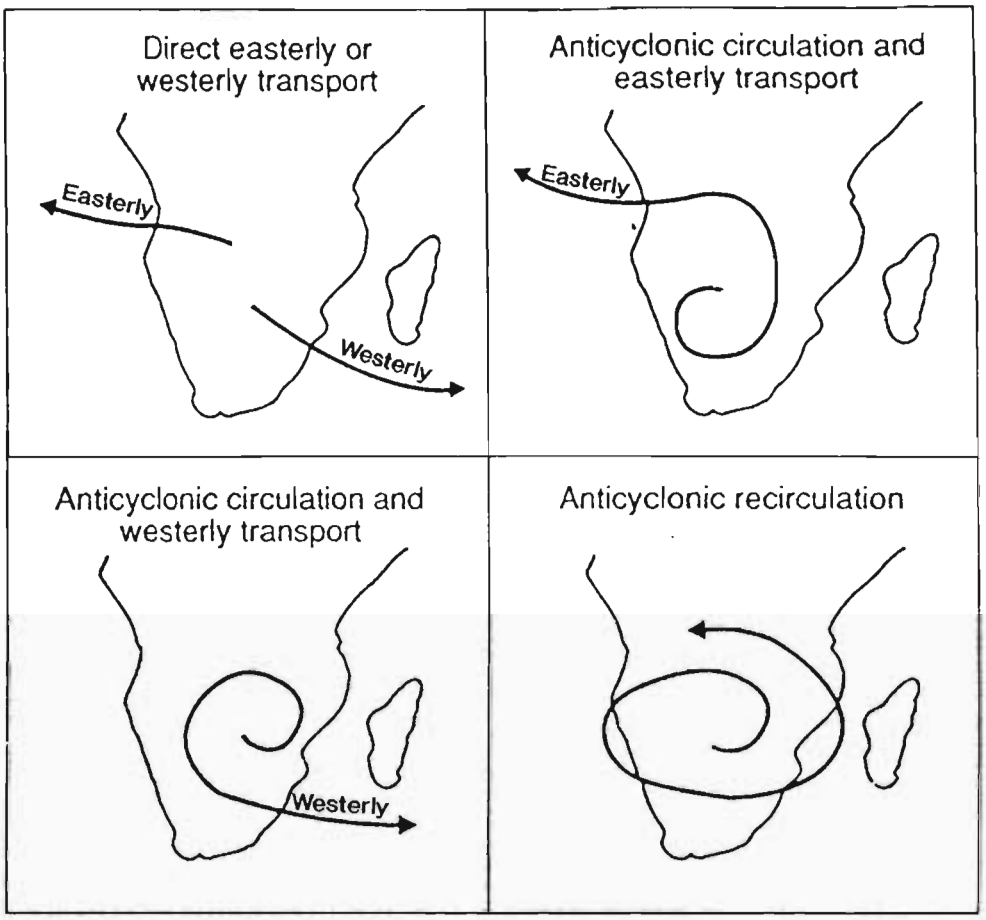

Figure 4.7 Dominant transport types derived from trajectory models depicting easterly and westerly transport from southern Africa and recirculation within the anticyclonic system. Redrawn from Garstang *et al.* (1996).

circulation may be accompanied by transport of air in an easterly direction, from the African continent and over the Indian Ocean (westerly transport), and/or transport which is ejected over the Atlantic Ocean (easterly transport).

Recirculation is a major feature responsible for transport of trace gases over southern Africa (Tyson *et al.*, 1995). Air contaminated by smoke from savanna fires in tropical regions of southern Africa and in Zaire, Zambia, Angola and Tanzania (Andreae *et al.*, 1993) and biogenically emitted substances (Swap *et al.*, 1996), could circulate for up to eight to ten days within the anticyclonic system before being deposited over the continent and surrounding oceans (Garstang and Macko, 1993). Circulation of contaminated air, in the free troposphere, in clear, stable conditions favours the formation of secondary pollutants such as ozone.

Long distance transport may also contribute to ozone levels over southern Africa. Thompson *et al.* (1996a) have shown that convective outflow from Brazil reaches southern Africa and contributes to upper tropospheric ozone at Ascension Island and Brazzaville. Thus, ozone maxima may form as a result of precursor sources which are a long distance away from the continent.

Stable atmospheric conditions with subsidence inversions were observed in association with the anticyclonic system over the continent. This enhanced the ability to trap pollutants from the surface and boundary layers (Garstang *et al.*, 1996). The presence of semi-permanent and spatially-continuous absolutely stable layers observed during the SAFARI period are illustrated in Figure 4.8 (Garstang *et al.*, 1996). The mean characteristics of the absolutely stable layers (when the observed lapse rate was less than the saturated adiabatic lapse rate) are described in Table 4.4.

Table 4.4 Four absolutely stable discontinuities at Pretoria identified on most days during the SAFARI period. From Garstang *et al.* (1996).

	Pressure hPa	Altitude (asl), km	Height above ground, km
1	700	3	1.5
2	550-500	5	3.5
3	350	8	-
4	Tropopause	-	-

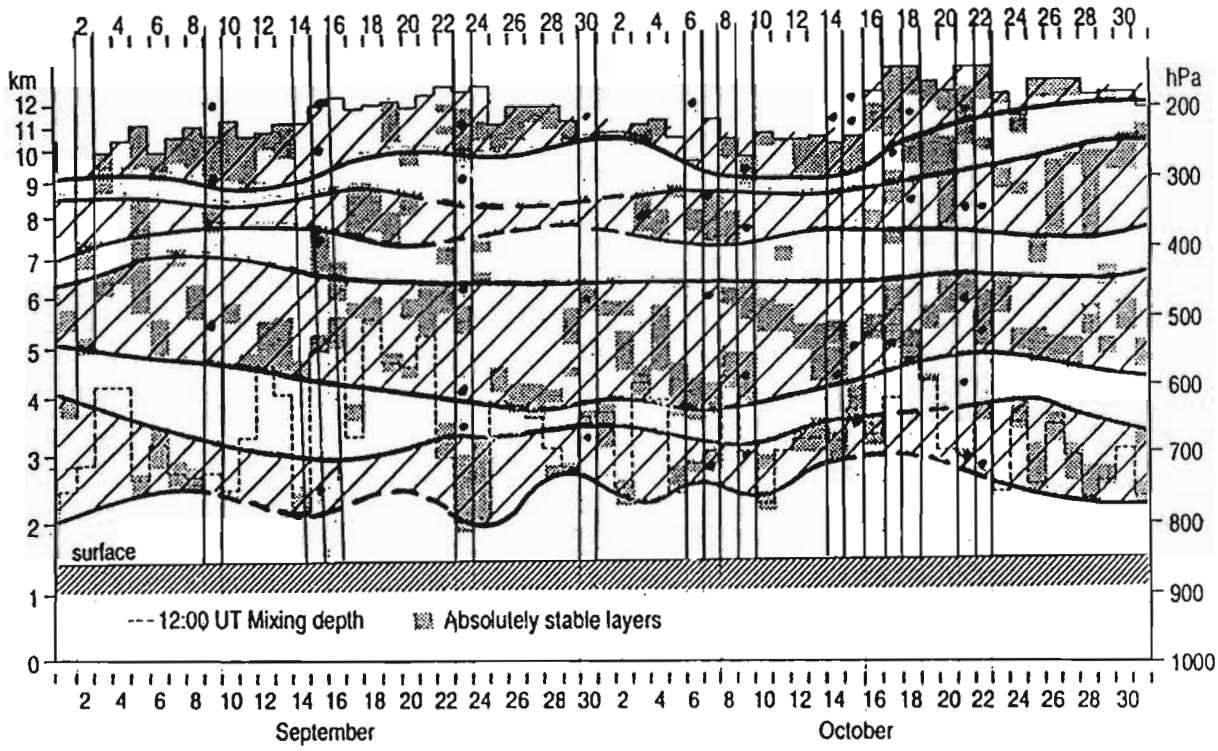

Figure 4.8 Absolutely stable layers (in which the observed lapse rate is < saturated adiabatic lapse rate) at Pretoria during the SAFARI- 92 period. The absolutely stable layers on each day are shaded, the height of the tropopause is indicated by a thin black line. The mixing depth is depicted as thin dashed lines and thick black lines show the four mean stable layers for the SAFARI period. From Garstang *et al.* (1996).

The first discontinuity is associated with the top of the mixing layer and was periodically broken up as a result of the passage of disturbances in the westerlies. This caused the mixing layer to extend beyond the 700 hPa level and disturbed the lower stable layer. The second discontinuity is associated with the main subsidence inversion. The third occurred above the main subsidence produced in the anticyclonic circulation and the fourth absolutely stable layer is associated with the tropopause. The presence of stable layers in the atmosphere causes stratification and traps trace gases and aerosols, preventing transport, mixing and dilution. Vertical transport is limited to those days when synoptic disturbances break down the stable layers (Garstang *et al.*, 1996).

The influence of the vertical layering of the atmosphere through the existence of stable layers was observed in ozone levels over the subcontinent. Tyson *et al.* (1995) identified two layers with a more-or-less continuous stable layer at approximately 6 km, separating them. This corresponds to the mid-level stable layer at 5 km and to a lesser extent, the 3-km stable layer which is periodically eliminated by vertical mixing described by Garstang *et al.* (1996). Tyson *et al.* (1995) suggest that ozone originating at the surface is contained below approximately 6 km and that which is generated above, such as through stratospheric-tropospheric injection, is maintained above this stable layer. Indeed, forward trajectory analysis provides examples of ozone in the troposphere, which having originated in the stratosphere, and which is trapped within the stable layer at approximately 8 km, is transported eastwards at this level and at no stage penetrating the upper stable layer (Tyson *et al.*, 1995).

The absolutely stable layers are both continuous in space and time over the southern African region. According to Garstang *et al.* (1996), the layers increase in altitude towards the equator and ultimately disappear, north of 15°S, in the regions of active convection. The varying elevation of the 3 and 5 km layers is illustrated in Figure 4.9. The height of the mean 3 km absolutely stable layer (< 50 hPa thick) varies from about 1 km in the south and 2,5 to 3 km (asl) in the northern parts. The height of the mean 5 km absolutely stable layer (~ 50 hPa thick) varies in altitude between less than 4 km, in the southeastern parts of the subcontinent, to approximately 5,5 km in the northern parts.

Significant features concerning southern African tropospheric ozone, identified during the SAFARI experiment are summarised in Table 4.5.

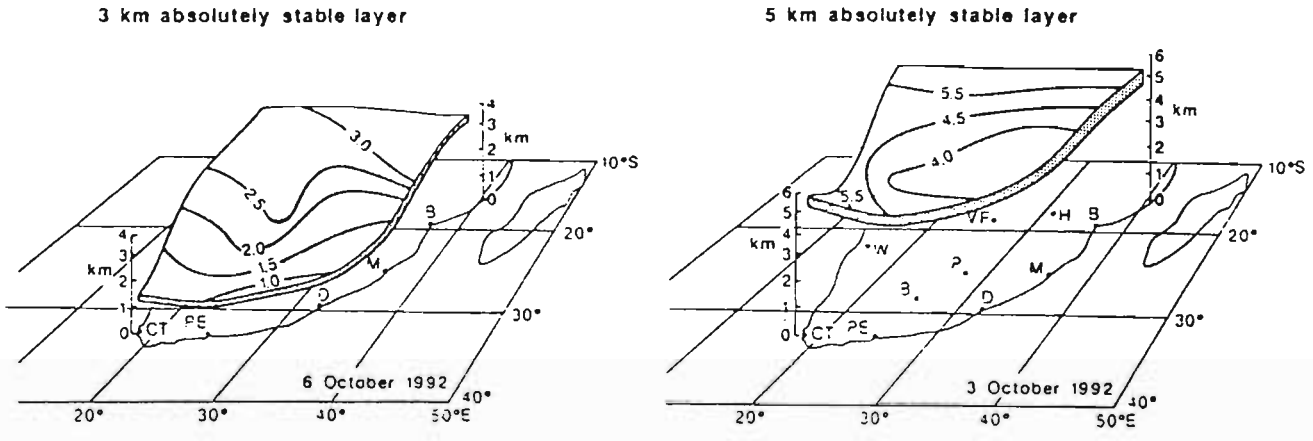

Figure 4.9 Diagrammatic representation of the spatial extent and altitude (asl) of the mean 3 and 5 km absolutely stable layers over southern Africa (6 and 3 October, 1992). Redrawn from Garstang *et al.* (1996).

Table 4.5 Summary of ozone mixing ratios (ppbv) from ozonesondes during SAFARI (September and October) 1992. From Thompson *et al.* (1996c).

Station	Ozone (Mean mixing ratio, ppbv)		
	0-5 km	5-10 km	10-15 km
Brazzaville (4°S)	51	71	86
Ascension Island (8°S)	59	84	81
Okaukuejo (19°S)	57	68	80
Irene (25°S)	49	69	90

Near equatorial sites revealed, on average, higher ozone levels than sites south of 15°S. The TOMS integrated tropospheric ozone average for 0° to 14°S and 12 to 50°E over southern Africa is 40 DU. Nonpolluted values are considered to be equivalent to less than 30 DU (Thompson *et al.*, 1996a). A clear gradient in ozone mixing ratio, from the equatorial region to subtropical latitudes, is evident. High ozone mixing ratios at low latitudes are explained by the close proximity to the region of maximum biomass burning in northern Zambia and Mozambique (Thompson *et al.*, 1996a; Thompson *et al.*, 1996c) which takes place during August to October each year. Ozone pollution from fires is less well observed south of 20°S due to the increased distance from the sources and decrease in injection by transport (Thompson *et al.*, 1996c; Diab *et al.*, 1996a).

In addition, the influence of airflow from Brazil containing biomass burning products has been detected (Thompson *et al.*, 1996c). The influence of local conditions, such as subsidence and the prevalence of a stable atmosphere, may also contribute to high ozone levels.

The effect of transport, associated with westerly troughs and anticyclonic circulation, on ozone levels is explored further in the next section. The meteorological and ozone data collected at Brazzaville, during the SAFARI period, also allowed an investigation into the effects of tropical circulation on ozone levels.

4.3.3 Summary

A brief review of the circulation characteristics and transport of air has been given. Transport models reveal that easterly, westerly and recirculation

type systems occurred over the southern African subcontinent during the SAFARI period. Anticyclonic circulation patterns were dominant, with westerly disturbances increasing in frequency in the latter half of the experiment. Stable anticyclonic conditions facilitated the formation of absolutely stable layers in the atmosphere, thus creating barriers to the vertical transport and dispersal of trace gases.

4.4 SUBTROPICAL AND TROPICAL CIRCULATION AND THE VERTICAL DISTRIBUTION OF OZONE AT OKAUKUEJO, IRENE AND BRAZZAVILLE DURING SAFARI-92

4.4.1 Introduction

Typical transport patterns over the southern African region, have been described in section 4.3. The implication for ozone concentration is that under anticyclonic flow there is considerable recirculation taking place over the subcontinent (Garstang *et al.*, 1996). Marked differences are expected in vertical ozone distribution for the anticyclonic and westerly trough type categories. These are contrasted for two stations, Okaukuejo and Irene, which fall within the sphere of influence of both circulation types. Okaukuejo is located within the tropical-subtropical transition and Irene is situated in the subtropical latitudes.

The influence of anticyclonic and westerly trough circulation conditions is investigated, at Okaukuejo and Irene, through composite analysis and by examining low level flow through isentropic airmass trajectory analysis back in time. Tropical circulation, associated with the Inter-Tropical Convergence Zone (ITCZ) and easterly flow, dominates the region of southern Africa north of the subtropical high pressure belt (Diab *et al.*, 1996b; Taljaard, 1985). The SAFARI ground-based station at Brazzaville provides an opportunity to examine the role of tropical circulation on the horizontal and vertical distribution of ozone.

4.4.2 Okaukuejo

4.4.2.1 Introduction

The influence of transport on ozone levels at Okaukuejo is investigated through the use of composite and case study analysis for the anticyclonic circulation and during the passage of a westerly trough.

4.4.2.2 Composite analysis

Ozone profiles at Okaukuejo were stratified, based on the prevailing circulation type, into either a mid-latitude westerly trough or anticyclonic circulation according to the classification of Garstang *et al.* (1996). Circulation characteristics typical of anticyclonic circulation over southern Africa are shown in Figure 4.10 for 14 September 1992. Anticyclonic circulation dominates throughout the troposphere with a closed cell at the surface and at 500 hPa and a ridge of high pressure at 300 hPa. In contrast, with the passage of a westerly trough, on 21 September 1992 (Fig. 4.11), the high pressure circulation over the land is weakened and a surface cold front and upper air trough are situated over the western part of the subcontinent. The encroachment of the Atlantic high pressure system gives rise to westerly winds throughout the troposphere.

A composite anticyclonic ozone profile comprising ascents on 15, 27 September and 5, 6, 10, 14, 15 October 1992 and a composite westerly trough, ozone profile from ascents on 21, 23 September and 11, 13 October 1992 at Okaukuejo were computed (Fig. 4.12). The composite anticyclonic profile resembles the mean (Diab *et al.*, 1996a), reflecting the dominance of anticyclonic circulation during the SAFARI period (Garstang *et al.*, 1996; Jury *et al.*, 1996). Generally, ozone mixing ratios range between 60 and 80 ppbv. An elevated enriched layer is observed between approximately 9 and 12 km. In this layer, ozone mixing ratios exceed 100 ppbv on individual days compared with 80 ppbv in the mean. Considerable vertical stratification is evident by the standard deviation values (Fig. 4.12). In individual profiles, narrow bands (approximately 100 m deep) of high ozone are separated by bands where concentrations may be 40 ppbv lower. Vertical layering of this nature is indicative of stable atmospheric conditions. Ozone mixing ratios are about 10 ppbv greater than the mean in the middle troposphere (6-8 km) and slightly lower than the mean in the 2 to 6 km layer. These differences are clearly shown in Figure 4.13, which shows the difference between the composite

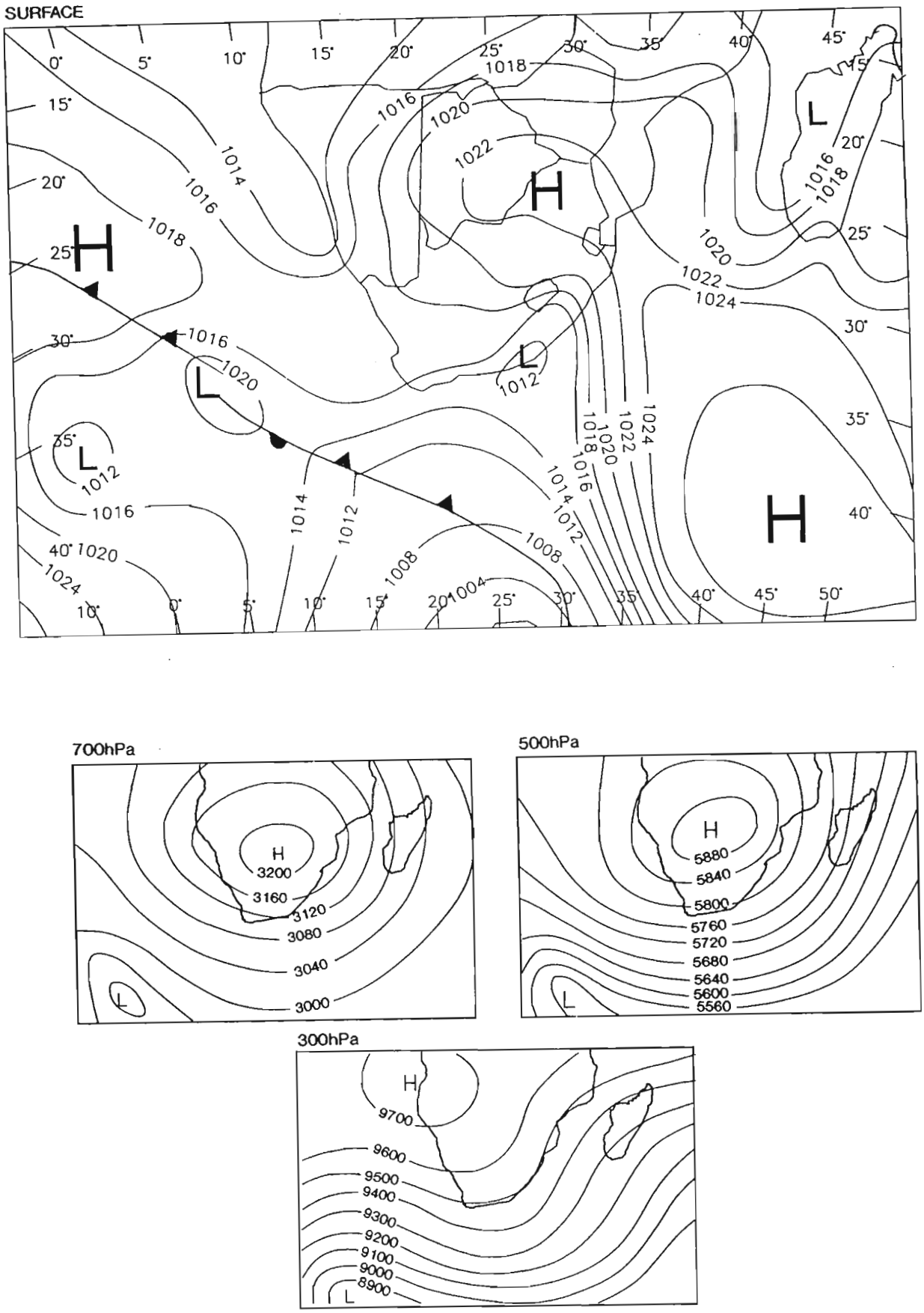

Figure 4.10 Surface synoptic chart (Daily Weather Bulletin, SAWB), 700, 500 and 300 hPa isobaric surfaces (ECMWF) indicating the circulation patterns, for 14 September 1992, which are characteristic of an anticyclonic flow regime at Okaukuejo.

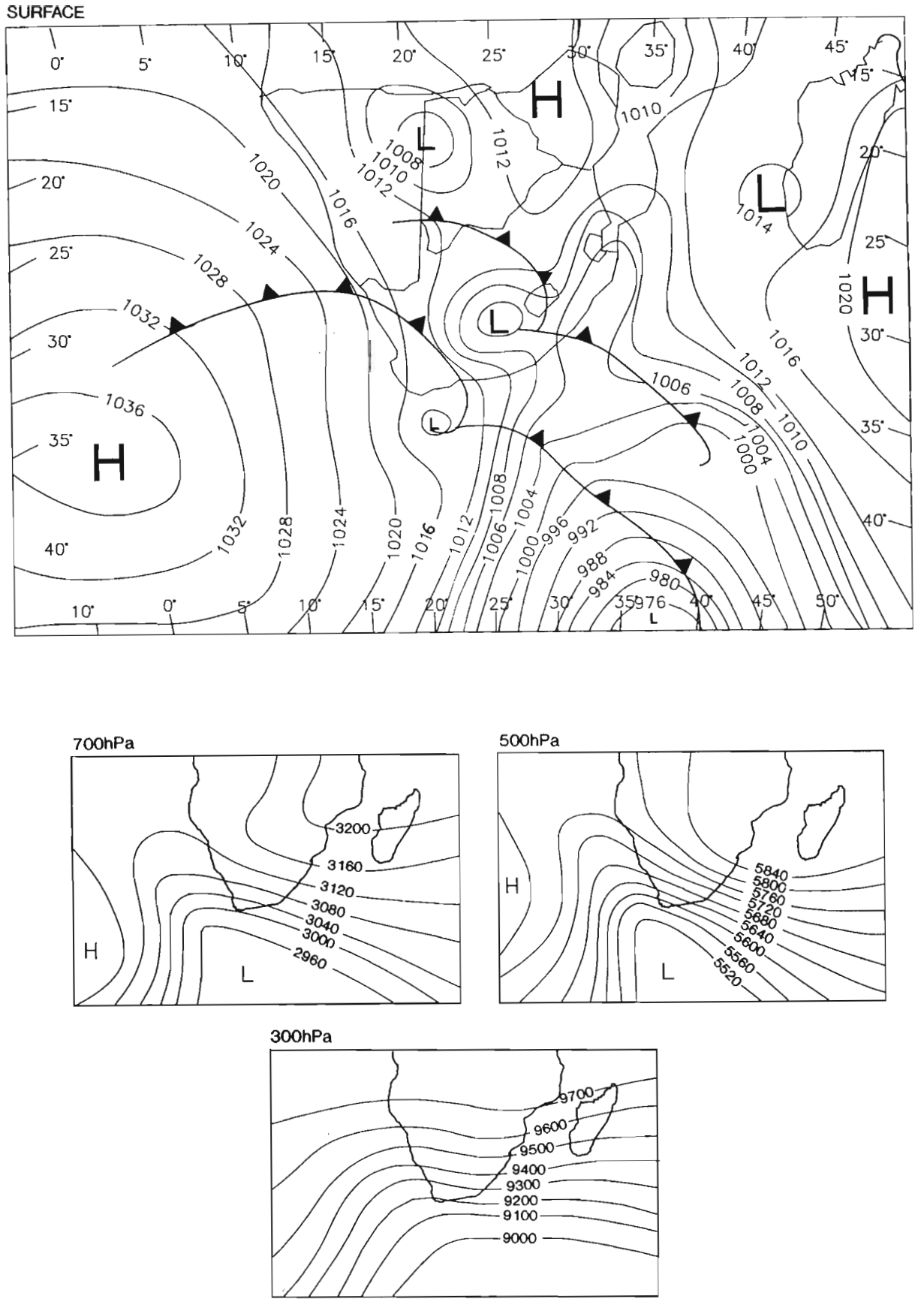

Figure 4.11 Surface synoptic chart (Daily Weather Bulletin, SAWB), 700, 500 and 300 hPa isobaric surfaces (ECMWF) indicating the circulation patterns, for 21 September 1992, which are characteristic of an upper westerly flow regime at Okaukuejo.

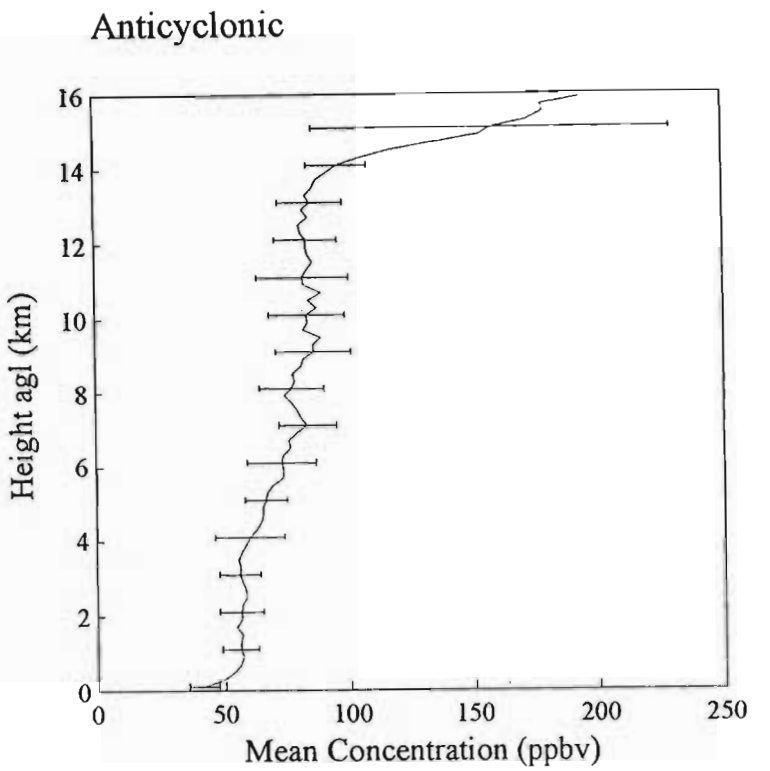

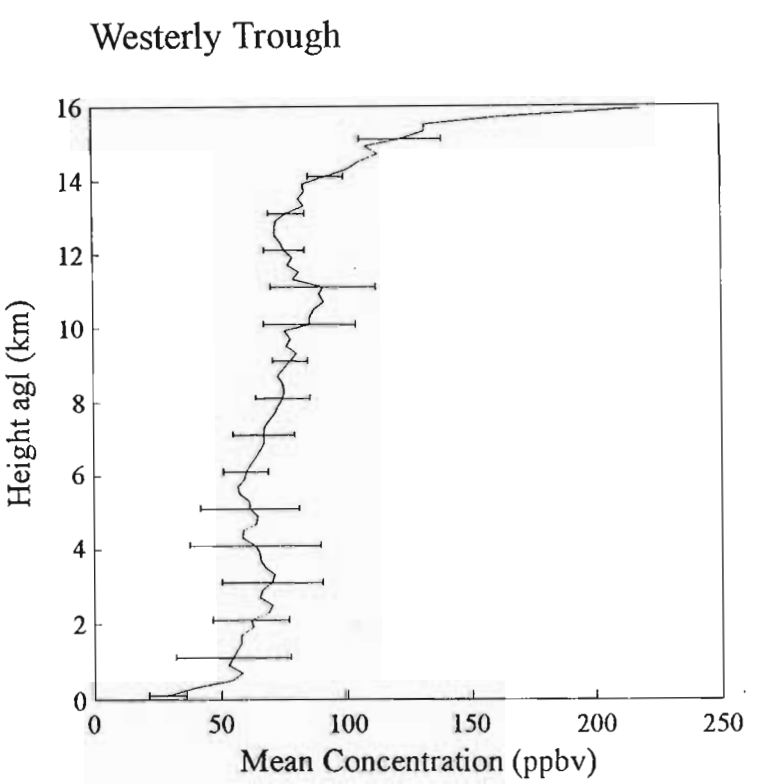

Figure 4.12 Mean ozone mixing ratio profiles (ppbv) and standard deviations estimated for 200 m slices and shown at 1 km intervals for composite anticyclonic and westerly trough synoptic types at Okaukuejo during the SAFARI period.

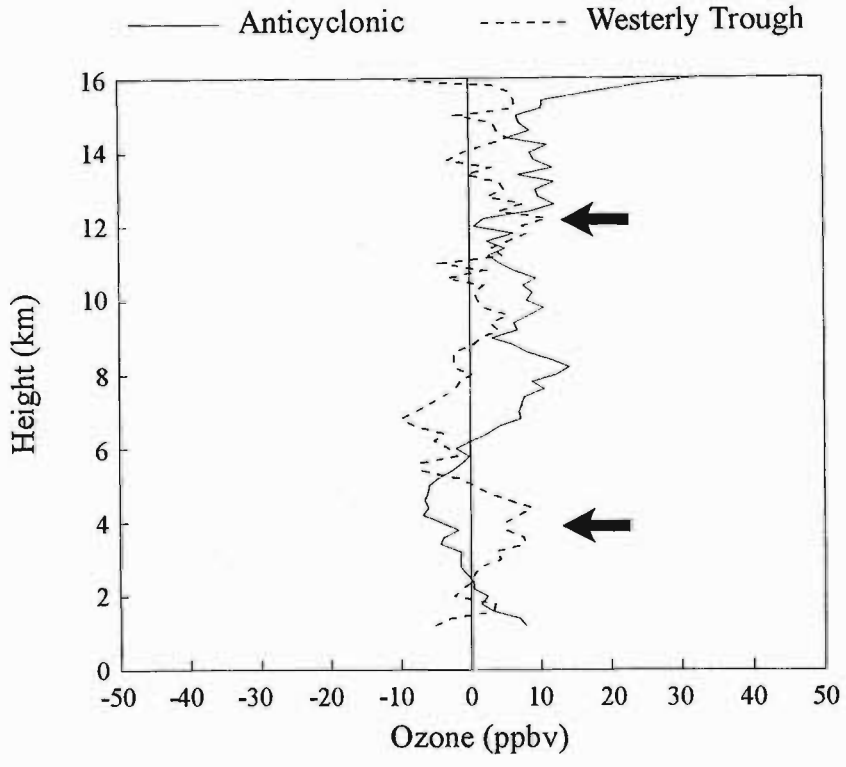

Figure 4.13 Difference between the mean ozonesonde profile (ppbv) and the mean westerly trough and anticyclonic profiles, at Okaukuejo, during the SAFARI period. Arrows indicate the lower and elevated enriched layers for the westerly trough type.

westerly trough, and anticyclonic profiles and the mean ozonesonde profile, for the SAFARI period, at Okaukuejo.

A notable difference between the composite westerly and anticyclonic ozone profiles, is the mid-tropospheric layer (~ 5-8 km) in which ozone mixing ratios, for the westerly trough, are approximately 10 ppbv lower than the rest of the troposphere (Fig. 4.12). Ozone mixing ratios may be reduced to 30 to 40 ppbv on individual days within this layer. This relatively 'clean' layer gives rise to a double ozone maximum in the troposphere, an elevated layer of high ozone (9-13 km) and a broad lower tropospheric maximum (40-70 ppbv) below, and is clearly evident in Figure 4.13. A similar elevated enhanced layer is also described by Thompson *et al.* (1996a). The upper ozone-enriched layer persists despite the change in synoptic flow. This is most likely explained by the existence of the semi-permanent stable layer, at approximately 6 km, described by Tyson *et al.* (1995) which remains intact during the passage of troughs and suppresses vertical mixing. The lower tropospheric maximum of the composite westerly trough, between the surface and 4 km, exhibits large standard deviation values (Fig. 4.12) and banded structure in contrast to the well-mixed profile of the anticyclonic case in the lower troposphere.

The ozone minimum reflects the invasion of relatively clean, ozone-poor, maritime airmass from the south. Its manifestation in the mid-troposphere is a function of latitude. Okaukuejo is located at the northern limit of the influence of westerly troughs and consequently the westerly penetration is not experienced below a certain altitude, in this case 4 km (600 hPa) (Fig. 4.14).

Time-height cross sections of ozone and u, v components of the wind and vertical motion (ω) at Okaukuejo are shown in Figure 4.15. The time-height cross sections of zonal and meridional winds are constructed from twice daily radiosonde data and 10 m wind data at Okaukuejo. Vertical motion data are taken from the ECMWF grid point closest to Okaukuejo.

The ozone time-height cross section (Fig. 4.15) is constructed from ozone soundings at irregular intervals conducted during the SAFARI period. Ozone values in the mid- to upper troposphere (> 6 km) are generally above 75 ppbv, with localised areas of enhancement where mixing ratios exceed 100 ppbv. Periods of relatively lower ozone in the lower troposphere coincide with the passage of westerly troughs as noted below.

Zonal winds are consistently westerly between approximately 8 and 16 km and consistently easterly above (not shown here). Greater variability characterises the lower troposphere. Here winds with an easterly component, characteristic of anticyclonic flow, are dominant, occurring on more than two-

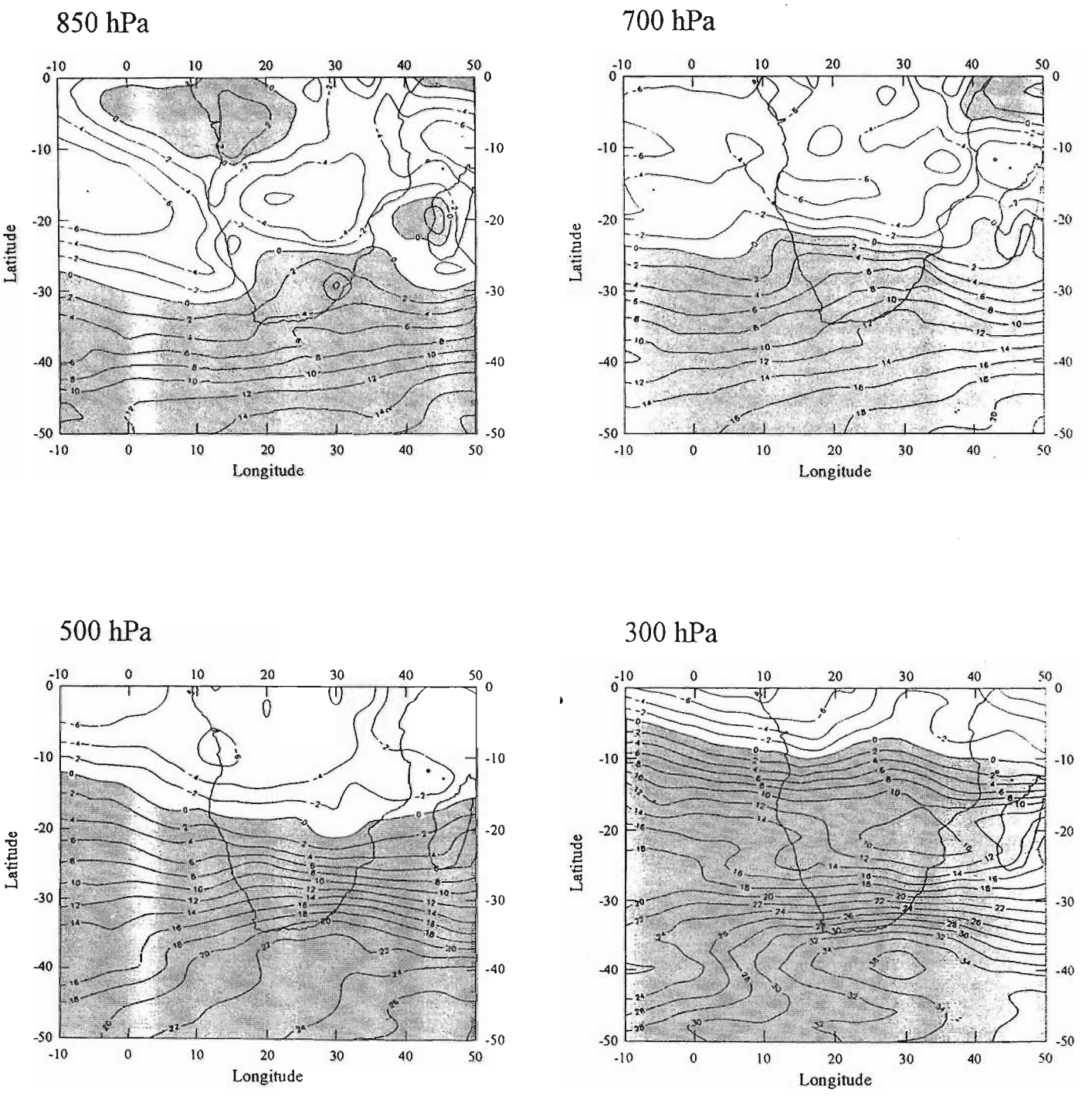

Figure 4.14 Zonal ECMWF winds (ms^{-1}) during the SAFARI period for 850, 700, 500 and 300 hPa surfaces. Westerly winds (positive) are shaded.

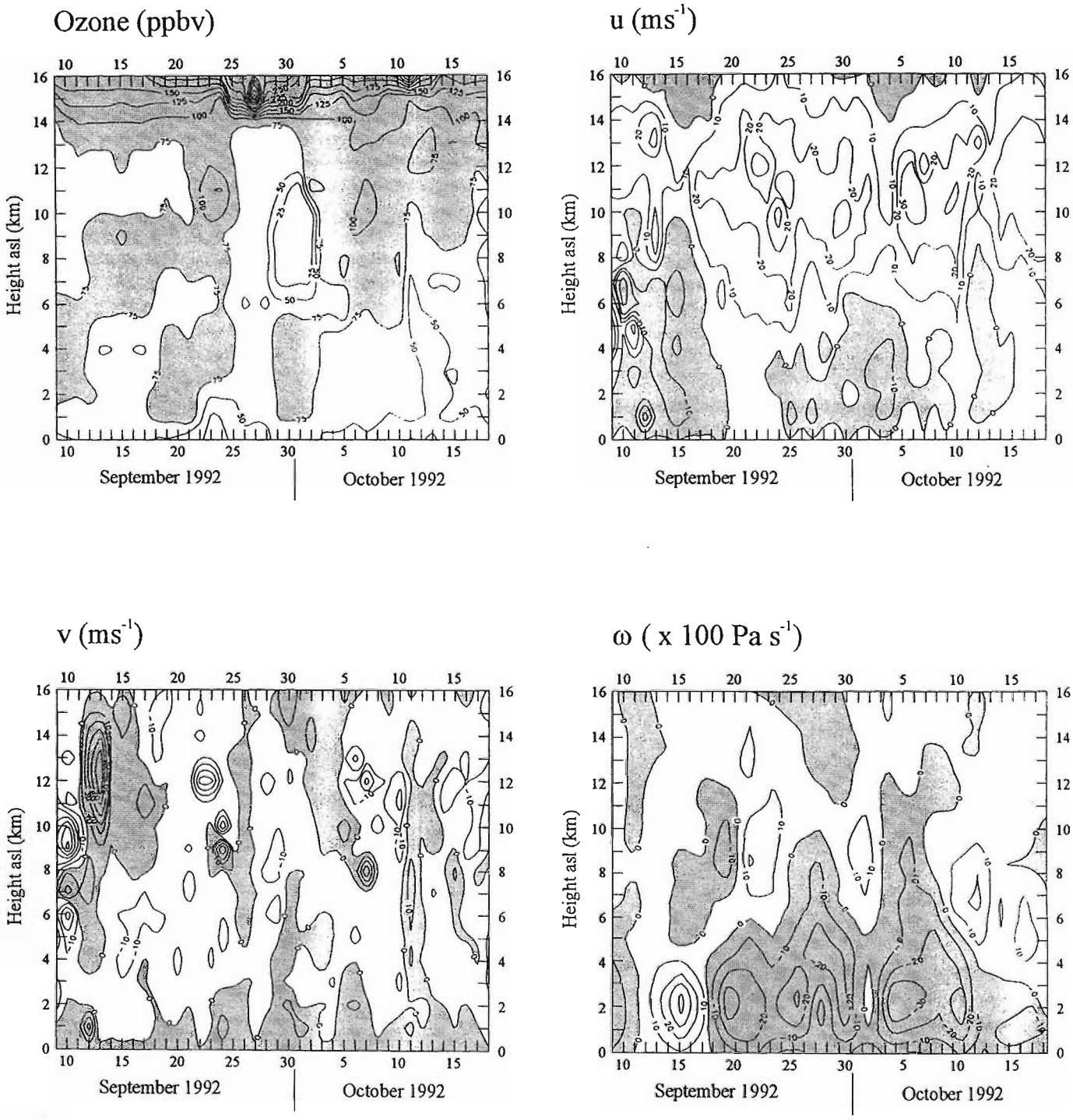

Figure 4.15 Time-height cross sections of ozone (ppbv) from ozonesondes; u and v components of the wind (m s^{-1}) from radiosondes and ω component (x 100 Pa s^{-1}) (ECMWF) at Okaukuejo for the SAFARI period. Areas of easterly ($u < 0$) and southerly ($v > 0$) and upward ($\omega < 0$) are shaded.

thirds of the days. Periods of low level westerly flow are characteristic of westerly troughs which bring ozone-poor maritime air across the continent (Fig. 4.15).

Meridional winds are weak but reveal greater variation. Periods of highest ozone mixing ratios (> 100 ppbv), in the 8 to 12-km layer (also noted in Jury *et al.*, 1996), tend to occur when airflow is northerly having a tropical origin, while mid-tropospheric ozone minima in the 4 to 6 km layer coincide with southerly flow (see also Jury *et al.*, 1996). These relationships are consistent with the characteristics of the composite anticyclonic and westerly trough vertical ozone profiles described above.

The efficient transport of ozone from the PBL to the free troposphere significantly enhances its lifetime. Rapid vertical transport may be effected through deep convective systems, as described in Chapter 3, and the vertical transport time is only a few hours (Garstang *et al.*, 1988; Connors *et al.*, 1991; Pickering *et al.*, 1992a,b). The ECMWF vertical motion field (Fig. 4.15) reveals dominant upward flow in the troposphere extending upwards to approximately 6 km. Upward motion (to approximately 10 km) in the vicinity of Okaukuejo (15°E) is evident in the composite anticyclonic vertical motion field, in the 20°S zone (Fig. 4.16). However, at 20°S, descending motion is dominant throughout much of the troposphere over the continent, marking the southerly limit of the descending limb of the Hadley circulation cell. This provides a stark contrast to the band of strong upward motion, at 10°S and centred at around 20°E, which extends throughout the troposphere between two broader bands of slowly descending air. The same pattern is repeated at 30°S except that the band of upward motion has broadened and weakened.

Low RH over Namibia and particularly at Okaukuejo (generally < 10%), inhibits the formation of convective thunderstorms. However, strong insolation and surface heating with surface temperatures in excess of 30°C and daily mixing depths greater than 3 km above ground level, extending to 4.5 km on some days, allows dry convection to transport air well above the surface. Once ozone reaches this altitude there would be little destruction of ozone by the hydroxyl radical owing to the very dry atmosphere.

Equivalent potential temperature (θ_e) profiles for composite anticyclonic and westerly trough circulation during the SAFARI period are given in Figure 4.17. Marked differences in the stability of the lower atmosphere are observed. The anticyclonic profile displays a pronounced minimum at 3 km indicative of efficient vertical mixing up to this level. The westerly trough composite profile showed much lower values (< 320 K), near the surface, indicative of cooler conditions, and increased steadily to reach a maximum at about 2 km (~ 326 K).

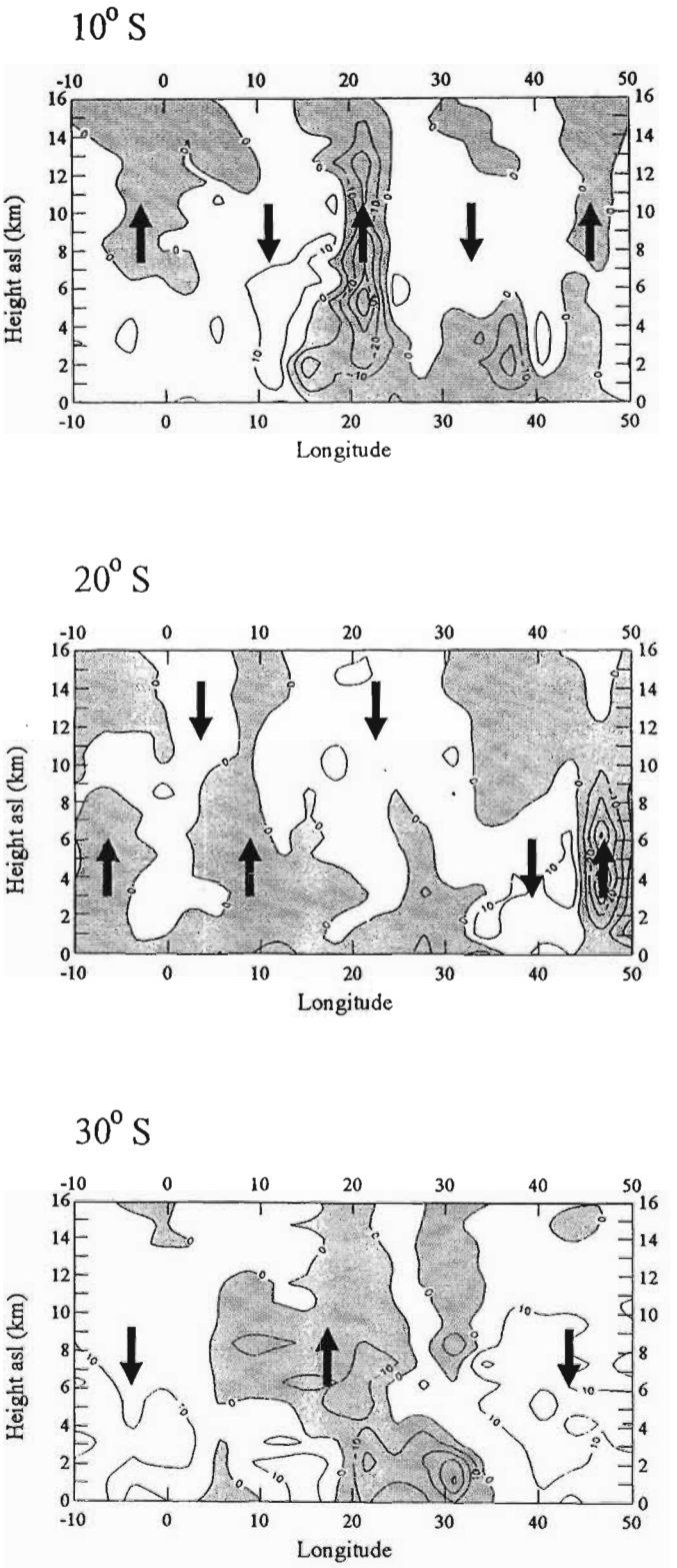

Figure 4.16 Longitude-height cross section of the vertical motion field (x 100 Pa s^{-1}) for the composite anticyclonic type during the SAFARI period along 10°S, 20°S and 30°S. Regions of upward (ω < 0) are shaded. Prepared from ECMWF data.

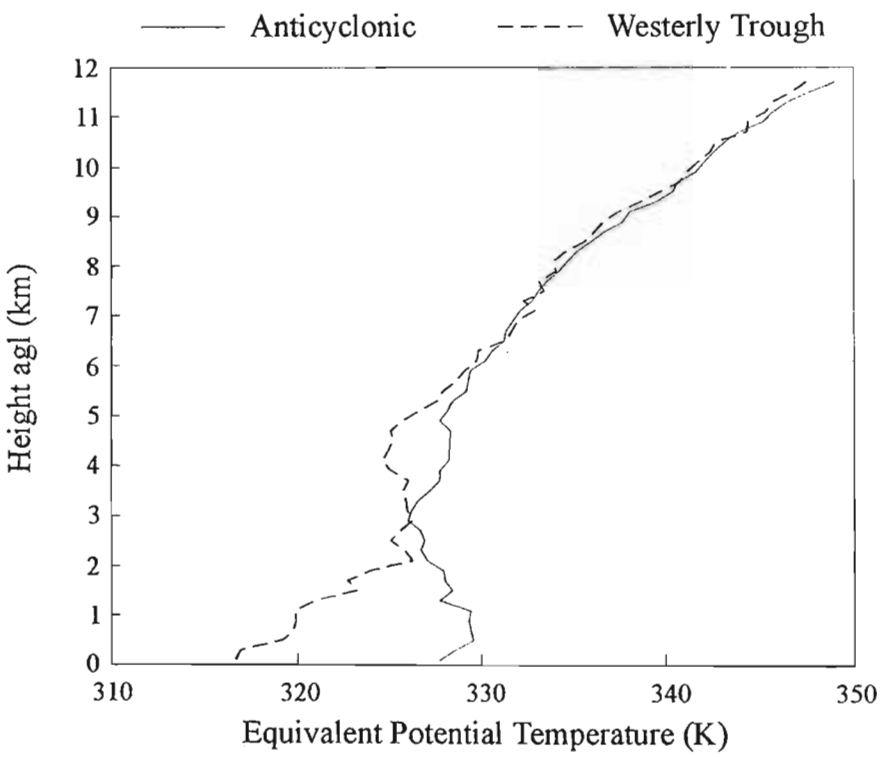

Figure 4.17 Mean equivalent potential temperature (θ_e) profiles for the composite anticyclonic and westerly trough synoptic types during the SAFARI period. Data from the SAWB.

The possibility that the mid-tropospheric minimum was due to localised depletion caused, for example, by changes in water vapour content was also considered. However, it was reasoned that any major increase in water vapour content in this arid region would result from a change in airmass. The effect on ozone concentrations was therefore likely to be experienced regionally rather than locally. A composite cross section of RH, through 20°S which corresponds closely to the latitude of Okaukuejo, for the westerly trough type circulation is given in Figure 4.18. RH values near the surface and in the upper air, above Okaukuejo, are approximately 30%. However, more moist air (RH ~ 40-50%) is prominent between approximately 4 and 8 km. The key to the origin of the moist air is found in a composite spatial representation of RH, on 850, 700, 500 and 300 hPa isobaric surfaces at Okaukuejo (Fig. 4.19). Relatively dry air (RH ~ 30%) is prevalent in the vicinity of Okaukuejo near the surface (850 hPa) and in the upper troposphere (300 hPa). A shallow layer of more moist air (RH ~ 40-50%) is evident at mid-tropospheric levels, particularly at 500 hPa, on the west coast. The advection of a cleaner airmass from the ocean within the westerly trough, and which may be coupled with the moist air located on the west coast, provides a likely explanation for the observed mid-tropospheric ozone minimum.

The spatial extent of the elevated enriched tropospheric ozone layer (~9-12 km) is uncertain. However, there is no evidence of its existence at Irene during the SAFARI period (Diab *et al.*, 1996a). This is most likely a function of latitude and extent of the eddy disturbances in the westerlies. A spatial plot of potential vorticity (PV) on the 330 K isentropic surface, which coincides roughly with the height of the enriched elevated ozone layer (5600-11700 gpm), for the composite anticyclonic case is given in Figure 4.20. The northernmost extent of the relatively high PV values at approximately 20°S is indicative of the northern threshold of the influence of westerly disturbances. Equatorwards of 20°S, stable atmospheric conditions facilitate the build up of an elevated enriched ozone layer.

Clearly, the enhanced ozone in the 8 to 12 km layer at Okaukuejo does not originate from a local ground level source where ozone mixing ratios are much lower. Trajectory analysis in the middle (~7.5 km) and upper (~12.5 km) troposphere indicates the dominant source airflow to be from the Atlantic and as far back as South America (Thompson *et al.*, 1996a). Recirculation of air in the easterlies, and chemical ageing and recirculation of contaminated air from biomass burning over the African continent as described by Garstang *et al.* (1996) and from biogenic emissions (Swap *et al.*, 1996) may also contribute to ozone accumulation at this level.

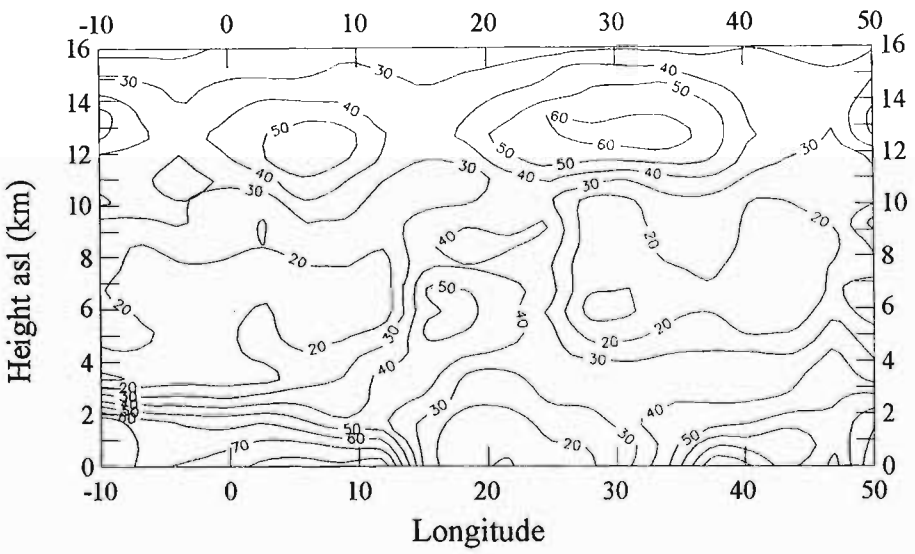

Figure 4.18 Composite cross section of RH (%), through 20°S, which corresponds closely to the latitude of Okaukuejo, for the westerly trough type circulation. Prepared from ECMWF data.

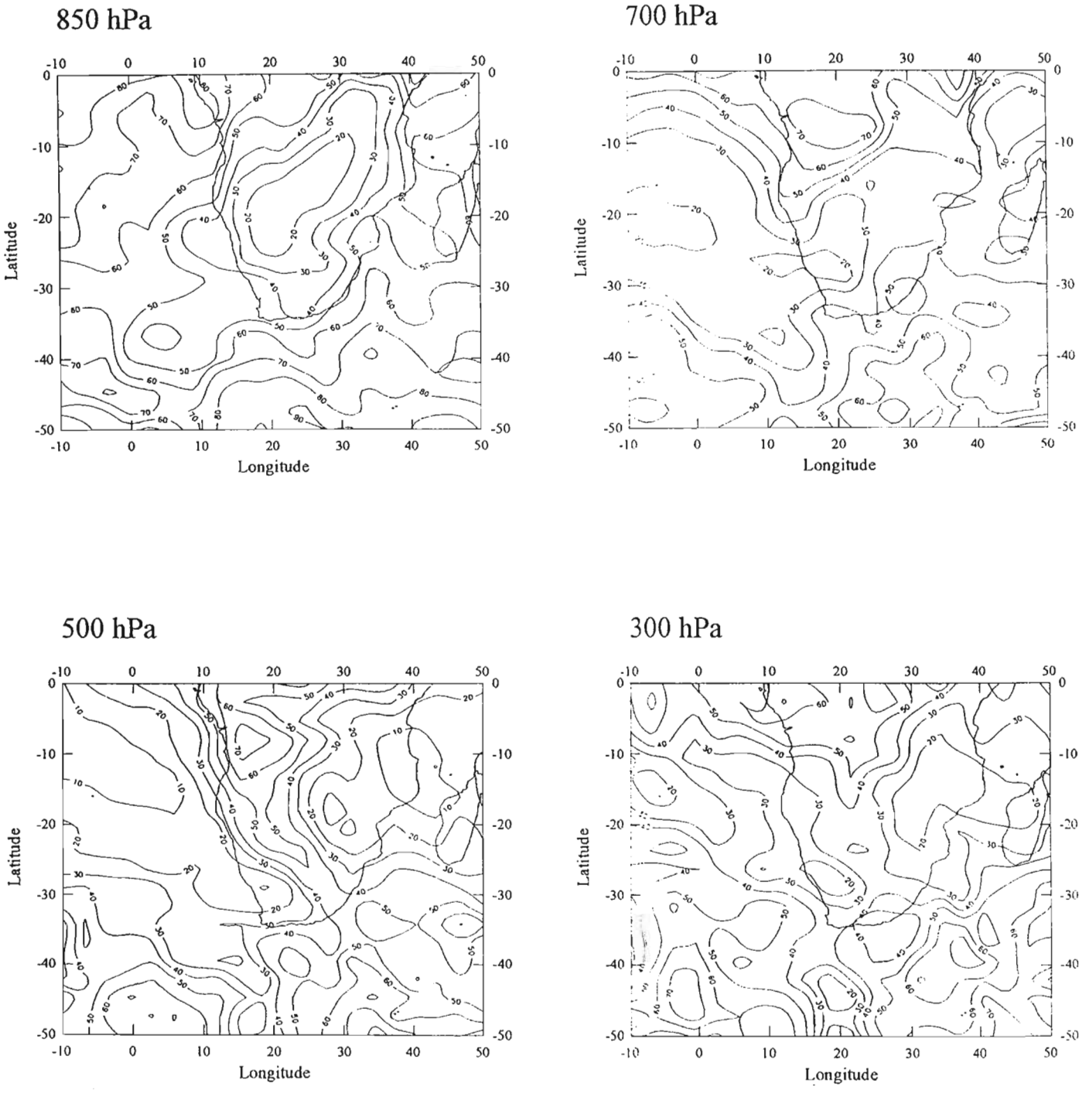

Figure 4.19 Composite spatial representation of RH (%), on 850, 700, 500 and 300 hPa isobaric surfaces at Okaukuejo during the SAFARI period. Prepared from ECMWF data.

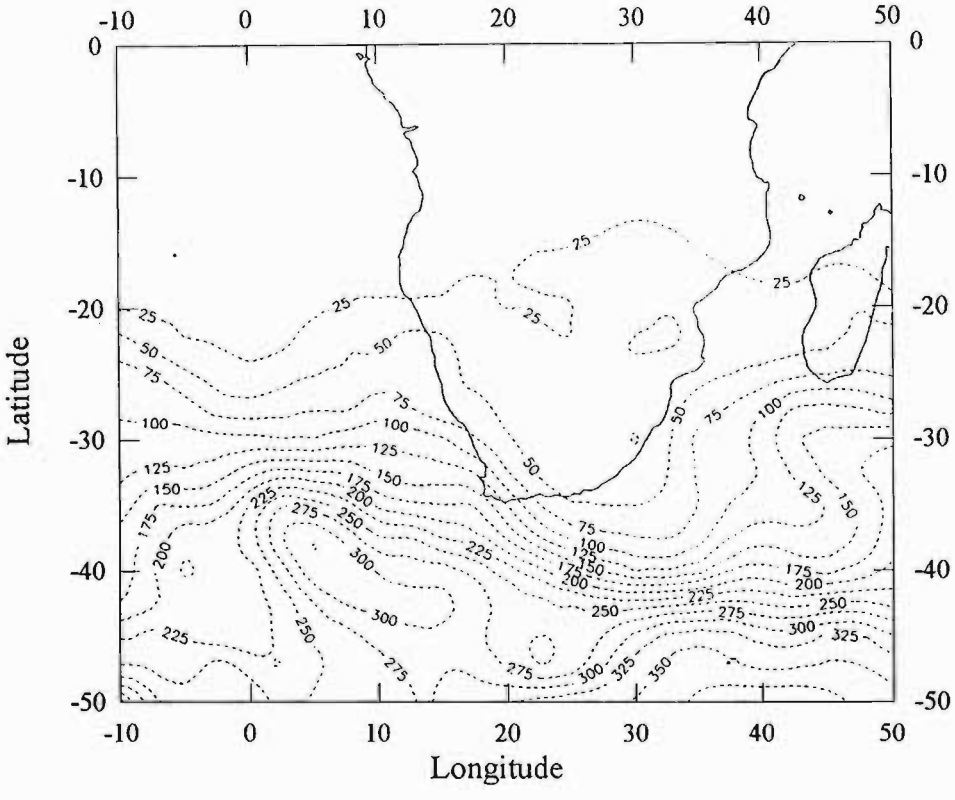

Figure 4.20 Spatial distribution of PV (x 10^{-7} $KhPa^{-1}s^{-1}$) on 330 K isentropic surface for the composite anticyclonic type during the SAFARI period. Prepared from ECMWF data.

4.4.2.3 Summary

Ozone profiles at Okaukuejo, stratified into anticyclonic and westerly trough circulation types, reveal different vertical ozone distribution patterns during the SAFARI period. An elevated enhanced layer of ozone (9-12 km) is present throughout regardless of the circulation type. Under the anticyclonic flow regime, tropospheric ozone reveals a steady increase from a surface maximum to the upper tropospheric maximum (9-12 km) and reflects the recirculation and chemical ageing of trace gases over the subcontinent. Northerly winds, of tropical origin, associated with anticyclonic flow accompany the upper level ozone maximum. The passage of westerly troughs over southern Africa is associated with southerly flow which originates over the Atlantic Ocean. This causes the flow of relatively clean, moist air towards Okaukuejo which is manifest in a mid-tropospheric (5-8 km) ozone minimum.

It has been shown by composite analysis that circulation plays a significant role in determining the vertical distribution of ozone at Okaukuejo. Since composite analysis provides a general representation only, and may mask extreme conditions, case studies of anticyclonic and westerly trough circulation conditions will be presented next.

4.4.3 Case studies

4.4.3.1 Introduction

The influence of anticyclonic and westerly trough circulation on the vertical distribution of ozone is examined for Okaukuejo and Irene. Case studies were selected by examining the prevailing weather conditions as depicted in surface synoptic charts and in plots heights of ECMWF 700 and 300 hPa isobaric surfaces. An analysis of meteorological data, ozone profiles, for the region 0 to 12 km, and eight day back trajectories, for θ levels 312 (one case only), 314, 316, 318 and 320 K which lie between 900 and 500 hPa (~ 0-5 km), is presented. The anticyclonic case study is presented first in each case.

4.4.3.2 Okaukuejo

Surface synoptic charts for the period 28 September to 6 October 1992 show anticyclonic flow over the southern African subcontinent and a surface tropical easterly wave which was confined to the west coast and western interior except on 5 October when it extended south to 30°S (Fig. 4.21). The 700 hPa synoptic charts reveal the confinement of the westerlies to the region

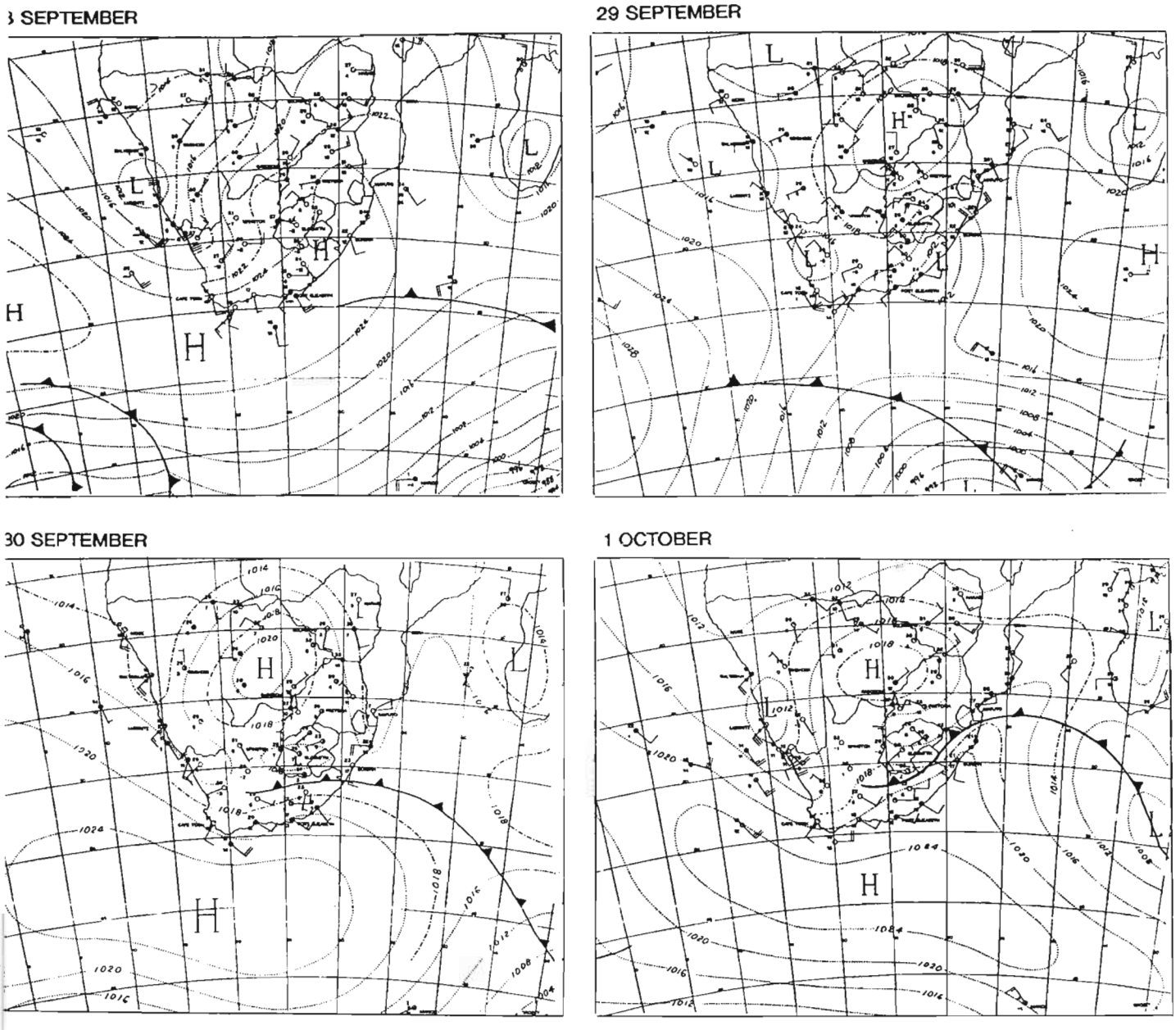

Figure 4.21 Surface synoptic charts over southern Africa for 28 September to 6 October 1992. Isobars (hPa) are denoted by light lines. From the Daily Weather Bulletin (SAWB).

2 OCTOBER

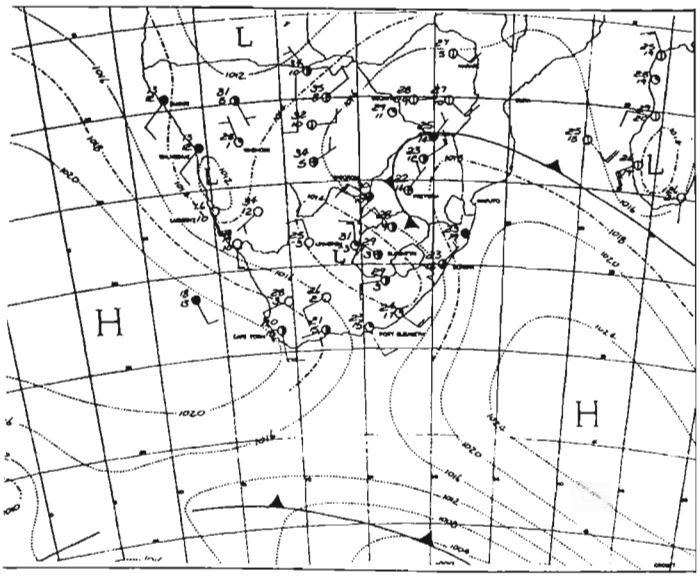

3 OCTOBER

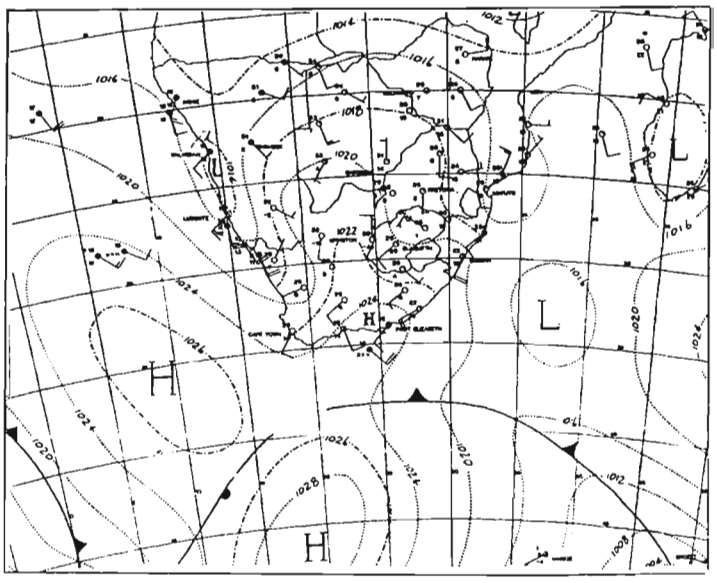

4 OCTOBER

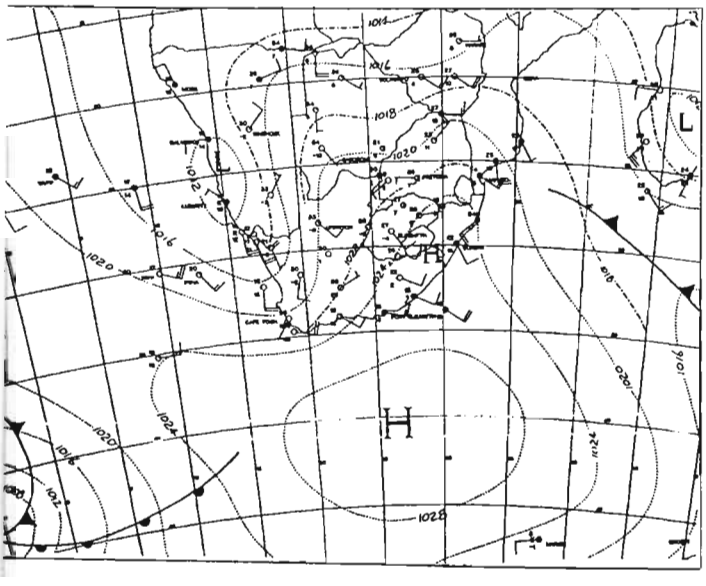

5 OCTOBER

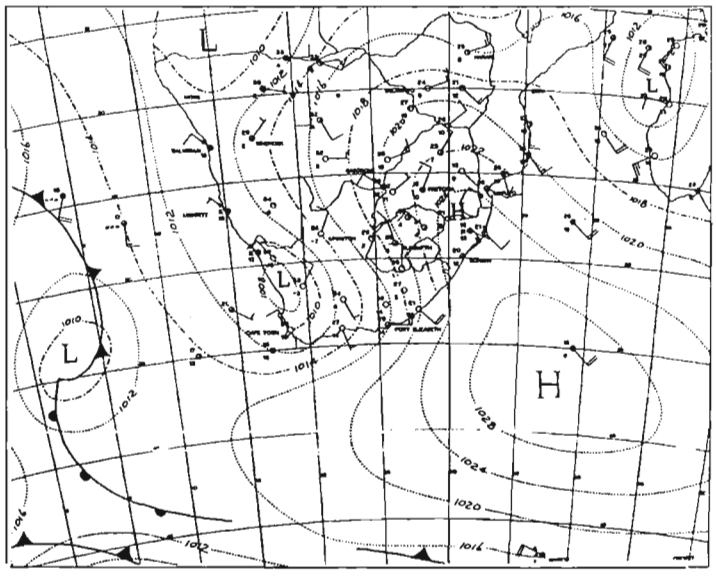

6 OCTOBER

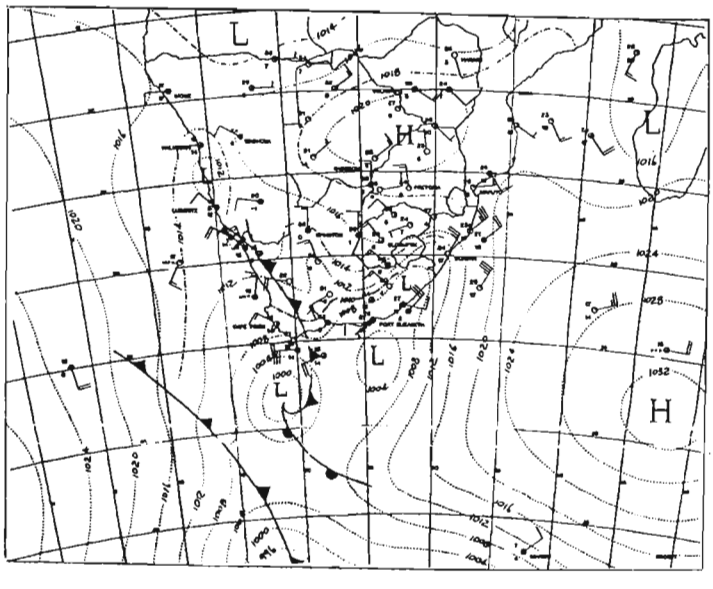

south of the continent, and by inference, that anticyclonic flow persists to the north of the westerly zone. An example of the 700 hPa circulation on 28 and 29 September 1992 is given in Figure 4.22. The dominant anticyclonic circulation is reflected in the light (< 20 m s^{-1}) easterly winds, evident in the vicinity of Okaukuejo, during this analysis period (Fig. 4.23).

In terms of ozone, it is expected that the observed stable conditions would contribute to enhanced ozone levels and that the vertical ozone distribution at Okaukuejo would resemble that of the mean for the SAFARI period, as discussed in section 4.4.2.2.

Vertical ozone profiles, between the surface and 12 km, obtained from irregular ozonesonde launches at Okaukuejo, during the period 28 September and 6 October are given in Figure 4.24. The observed steady increase in ozone mixing ratio from the surface to approximately 9 km on 5 and 6 October resembles the mean anticyclonic profile at Okaukuejo (Diab *et al.*, 1996a). Ozone values in the 9 to 12 km region exceed the mean (> 80 ppbv) on both days. On 30 September, a similar steady increase from the surface to approximately 5 km is noted, but which greatly exceeds the mean. Values above 5 km are not reliable due to the failure of the ozone pump at this level (Sokolic, pers. comm., 1995). Ozone levels are much reduced throughout the troposphere on 3 October and represent about half the concentration present in subsequent profiles.

The origin of the airmass, in the mid- and lower troposphere, at Okaukuejo was examined by conducting eight day back trajectory analysis beginning on 6 October 1992, at Okaukuejo. Figure 4.25 shows back trajectories from Okaukuejo along the 314, 316, 318 and 320 K isentropic surfaces which vary between the surface and approximately 500 hPa (~ 5 km). Clear anticyclonic air flow originating at a point located within the large anticyclonic circulation over the subcontinent is observed. Typical continental anticyclonic flow is evident on the 314, 316 and 318 K surfaces while a tighter anticyclonic spiral originating north-northwest of Okaukuejo is depicted by the 320 K isentropic back trajectory.

Further, the altitude of the middle-point back trajectory, which represents the path of the air parcel originating at the central point of the 7 x 7 array surrounding Okaukuejo, is shown in Figure 4.26. The start time of the back trajectory sequence, at Okaukuejo, is indicated by zero (hours) on 6 October 1992 and is terminated at -192 hours on 28 September 1992. In general, there is little variation in the altitude of the isentropic surfaces and the constant height of the back trajectories confirms the stable nature of the atmosphere during this period. Between 4 and 6 October, the heights of the 314

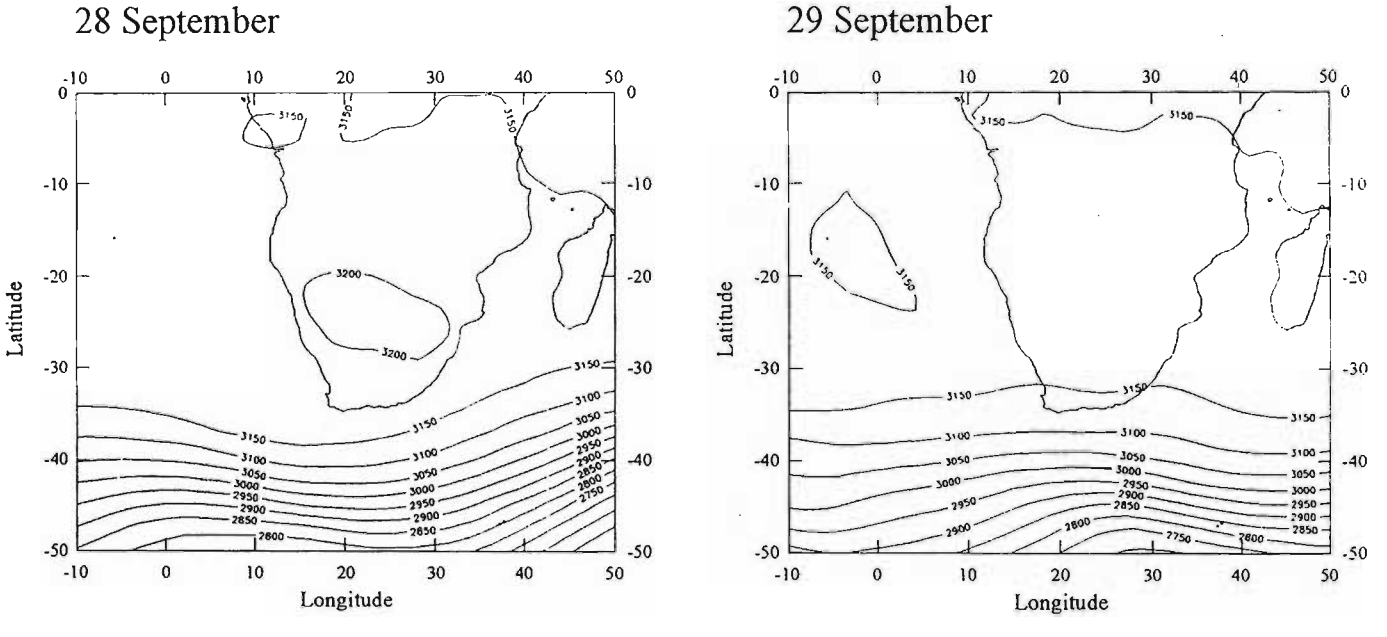

Figure 4.22 700 hPa synoptic chart over southern Africa for 28 and 29 September 1992. Prepared from ECMWF data.

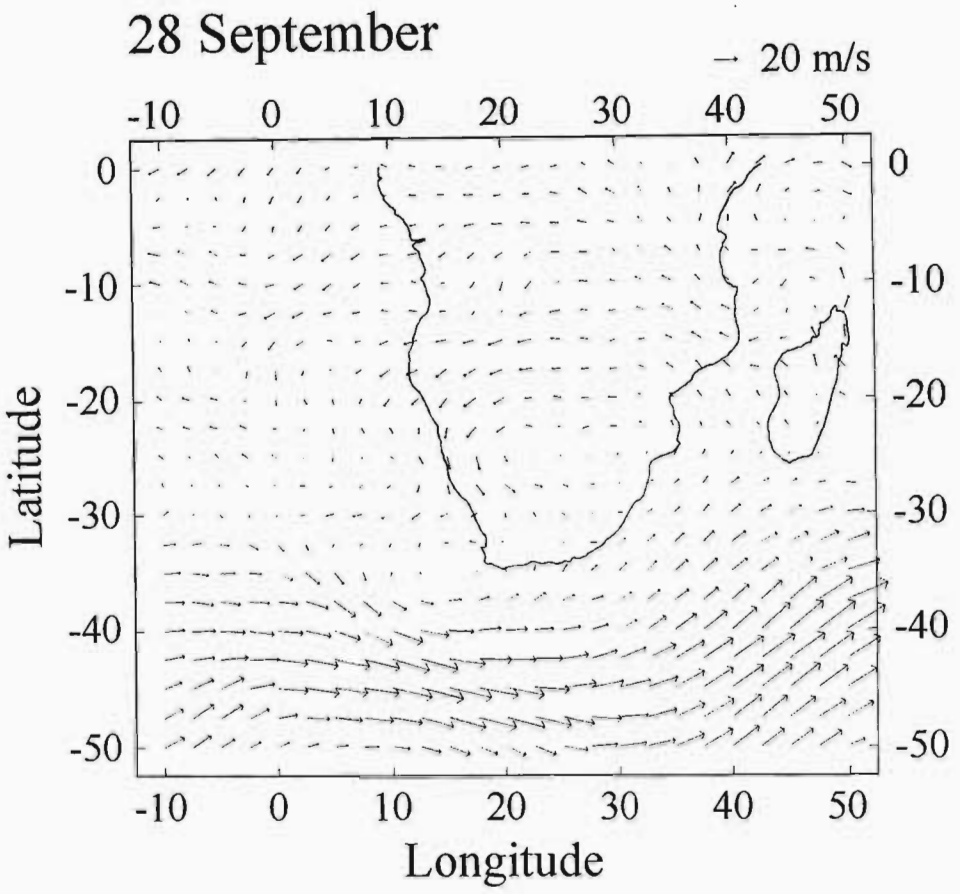

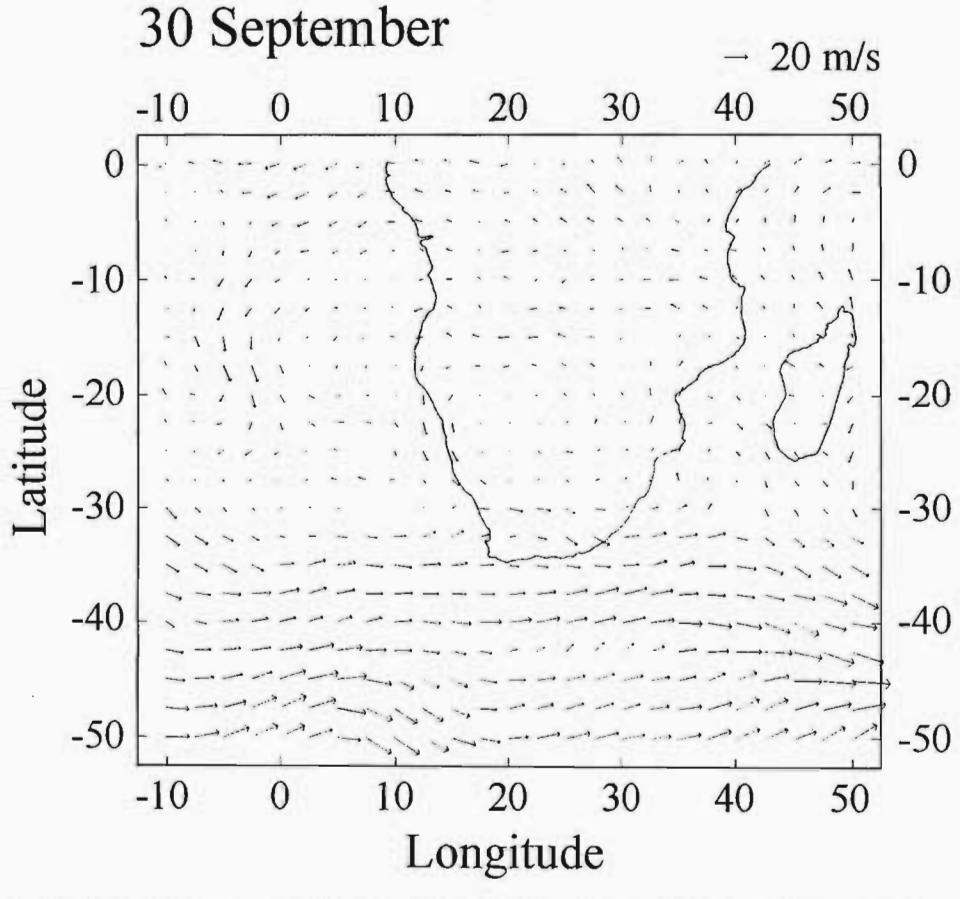

Figure 4.23 700 hPa wind vectors over southern Africa, derived from ECMWF u and v wind components, for 28, 30 September and 1 and 6 October 1992.

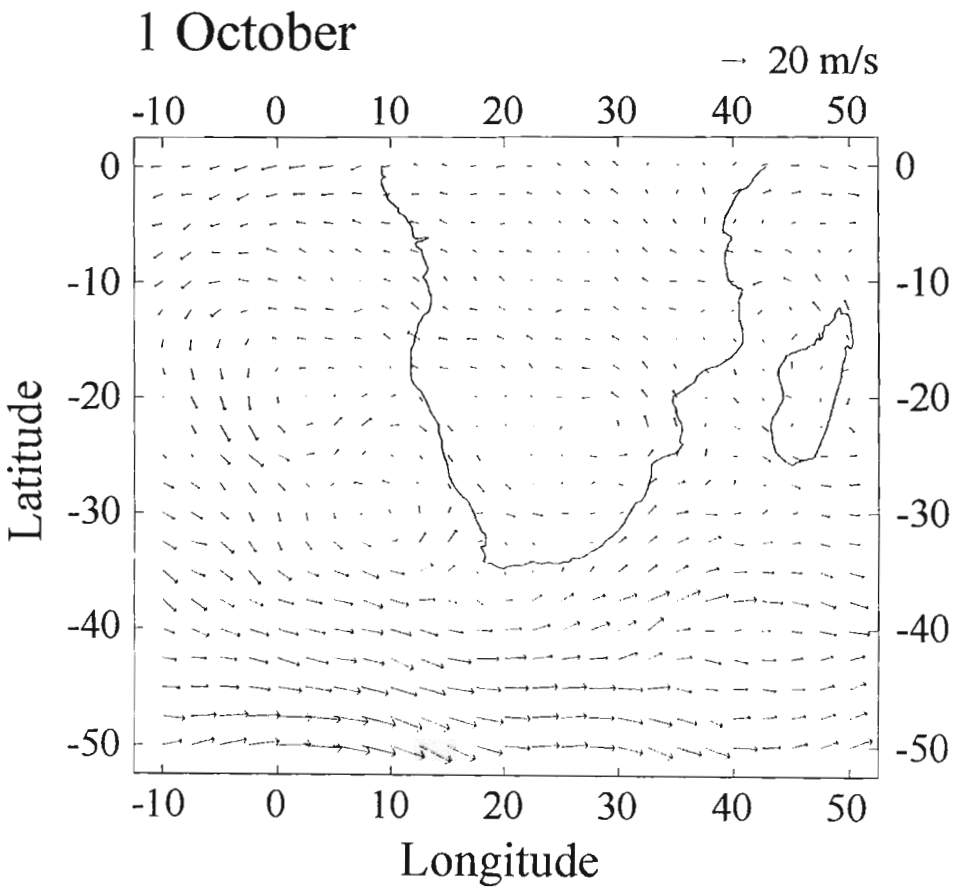
1 October
20 m/s
-10
0
10
20
30
40
50
0
-10
-20
-30
-40
-50
Latitude
Longitude

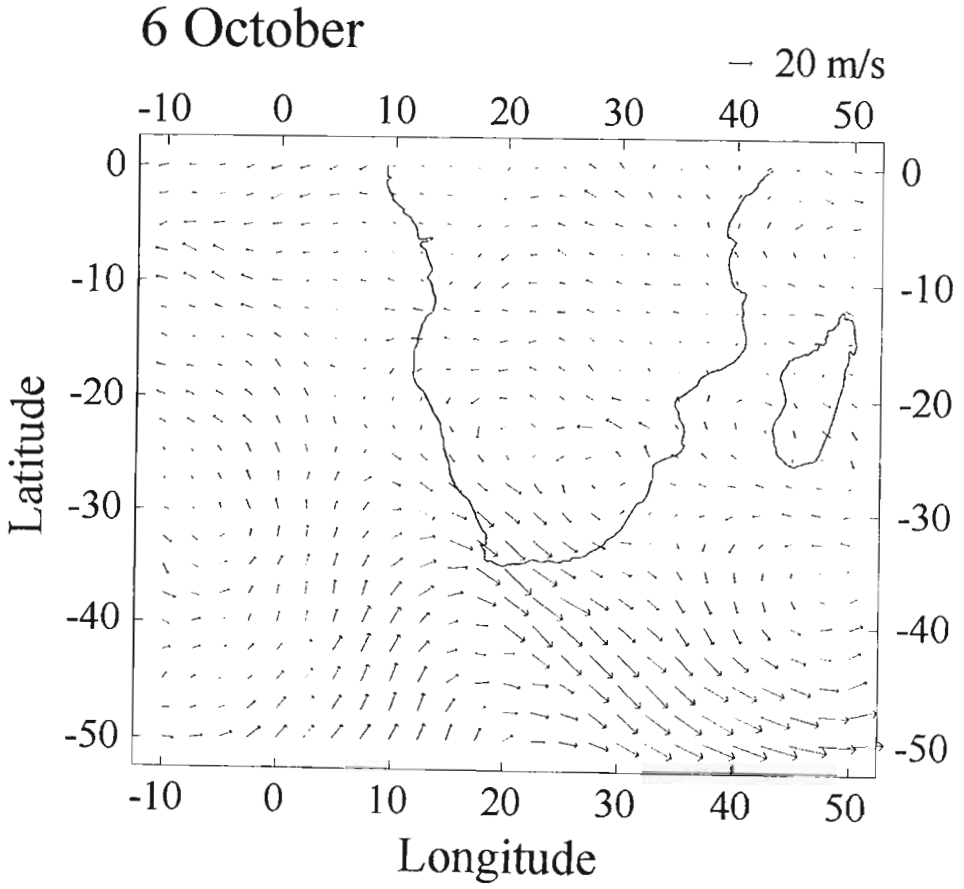
6 October
20 m/s
-10
0
10
20
30
40
50
0
-10
-20
-30
-40
-50
Latitude
Longitude

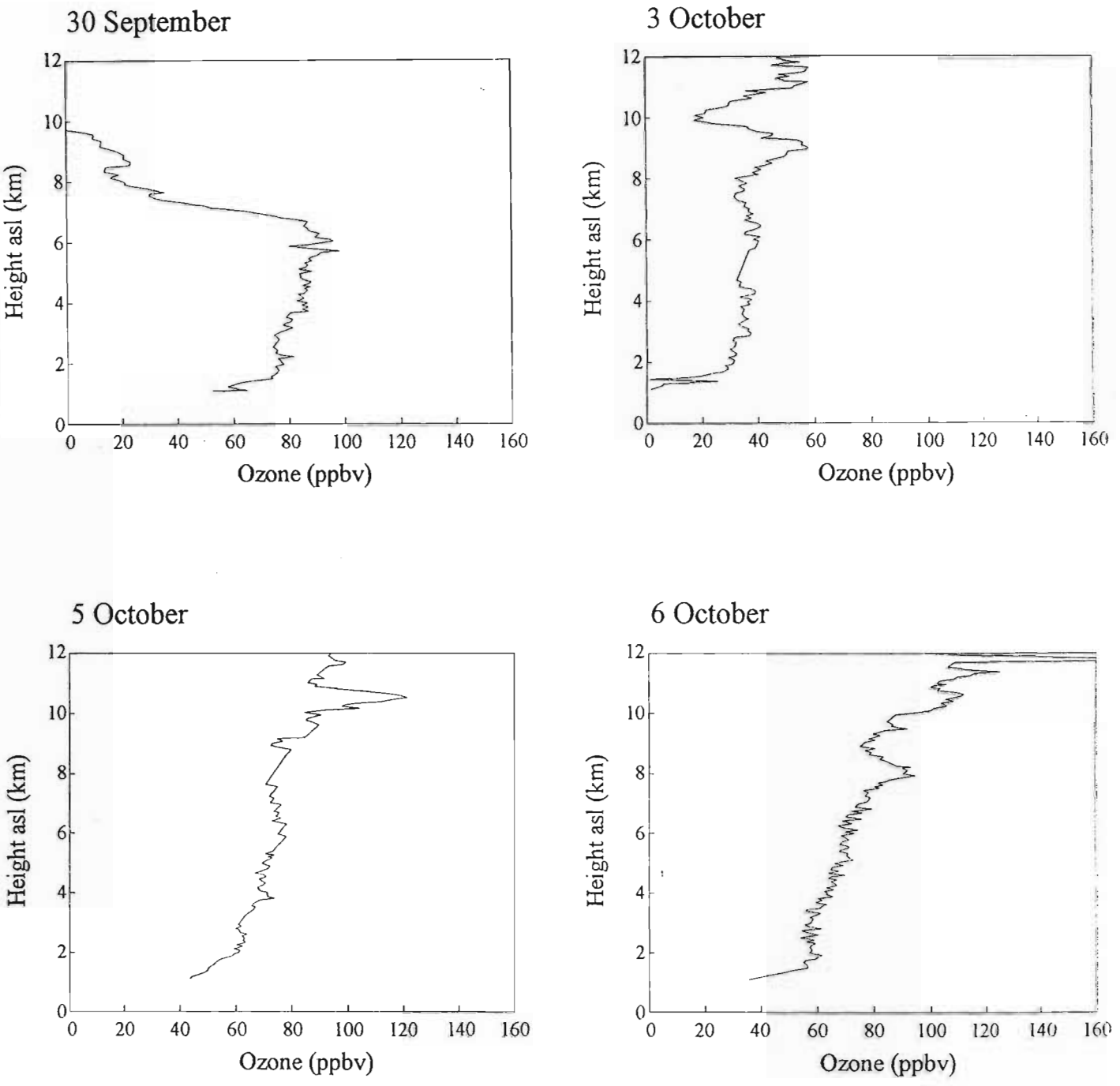

Figure 4.24 Ozonesonde mixing ratio profiles (ppbv) between 0 and 12 km (asl), at Okaukuejo for 30 September, 3, 5 and 6 October 1992. Data from the SAWB.

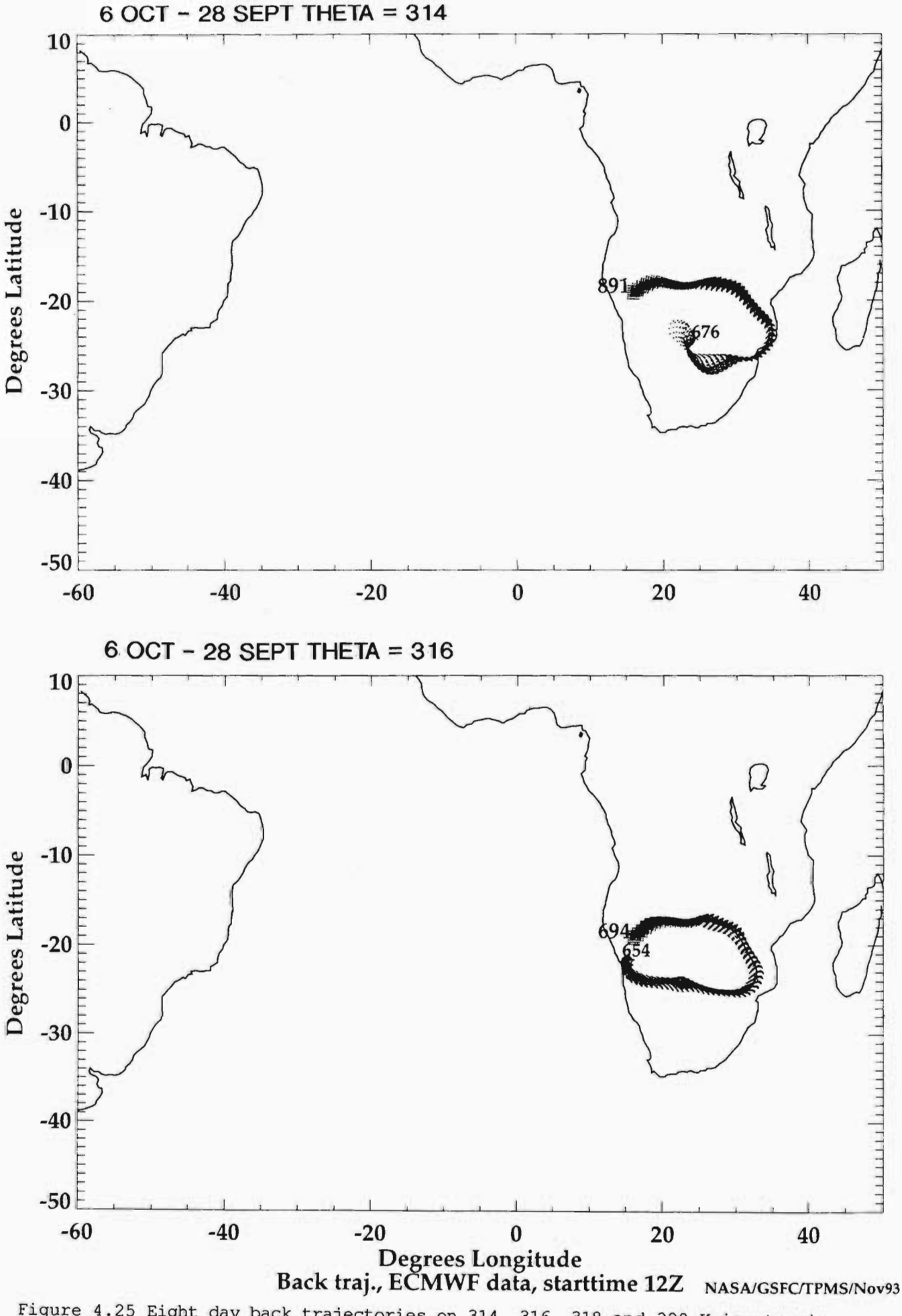

Figure 4.25 Eight day back trajectories on 314, 316, 318 and 320 K isentropic surfaces, from Okaukuejo, for 6 October to 28 September 1992. Start time was 12 Z. The trajectory originating from the central point of the array is given as a solid line. Start pressure (hPa) is denoted by large type and end pressure by smaller type. Source NASA/GSFC.

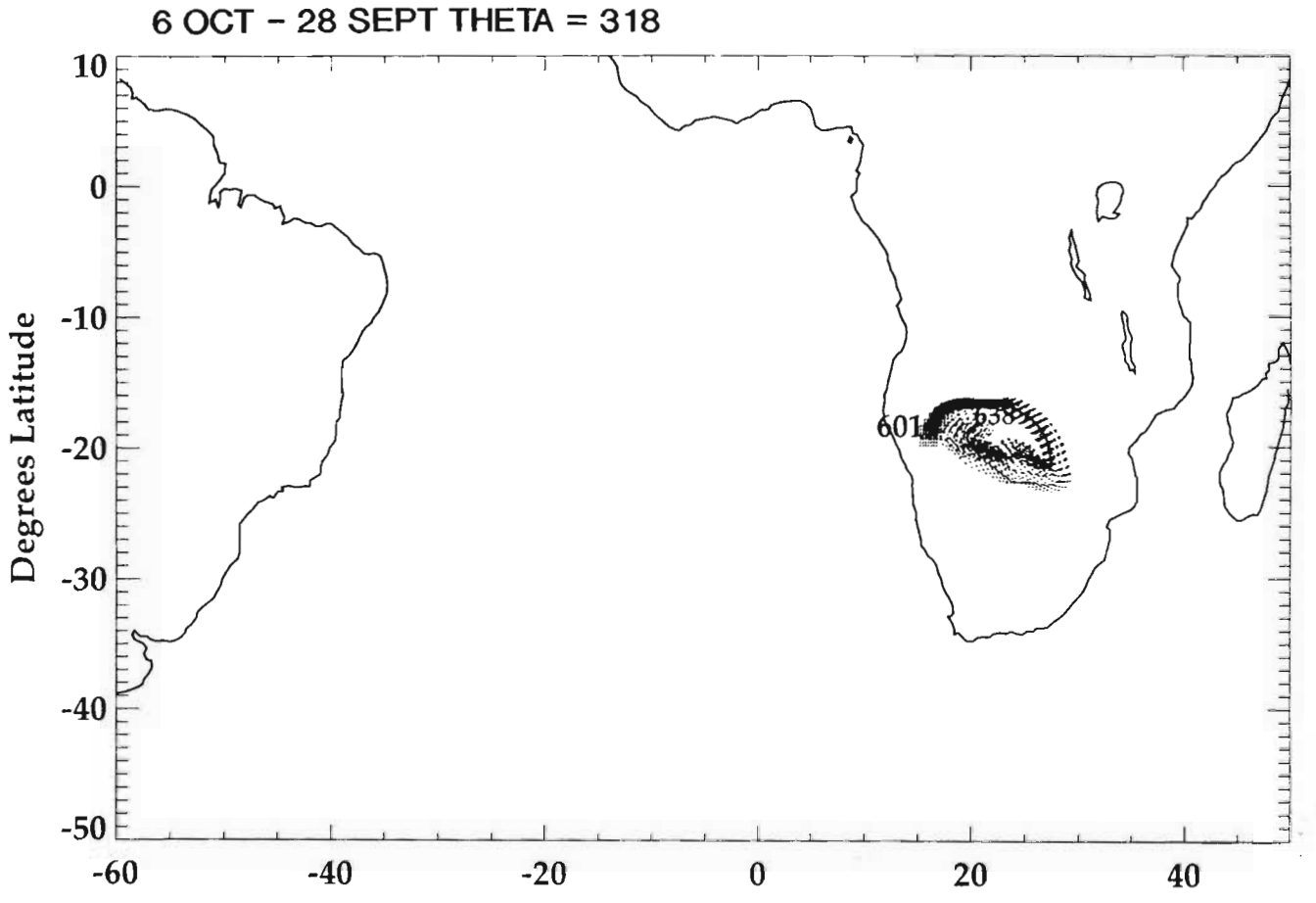

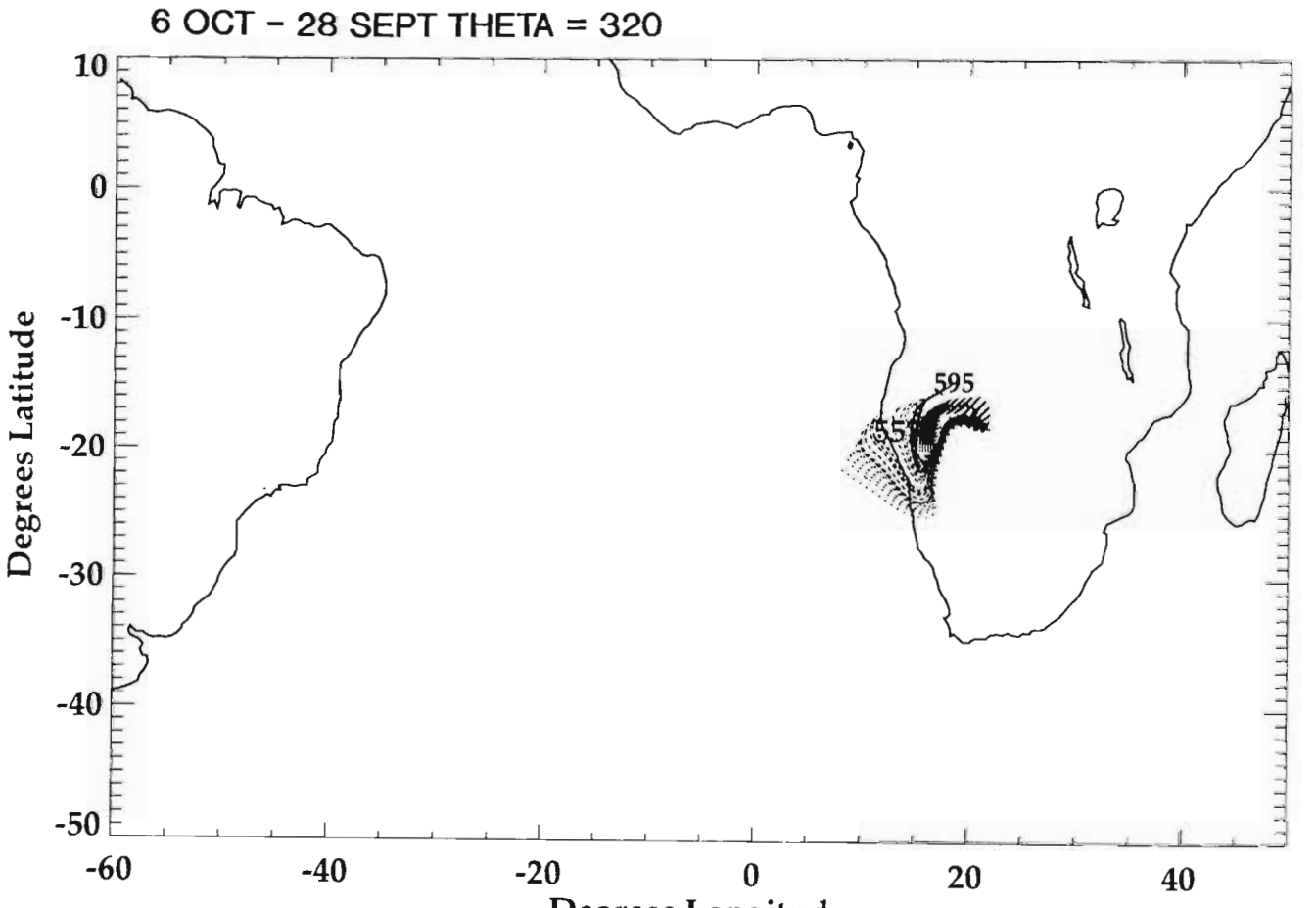

Back traj., ECMWF data, starttime 12Z NASA/GSFC/TPMS/Nov93

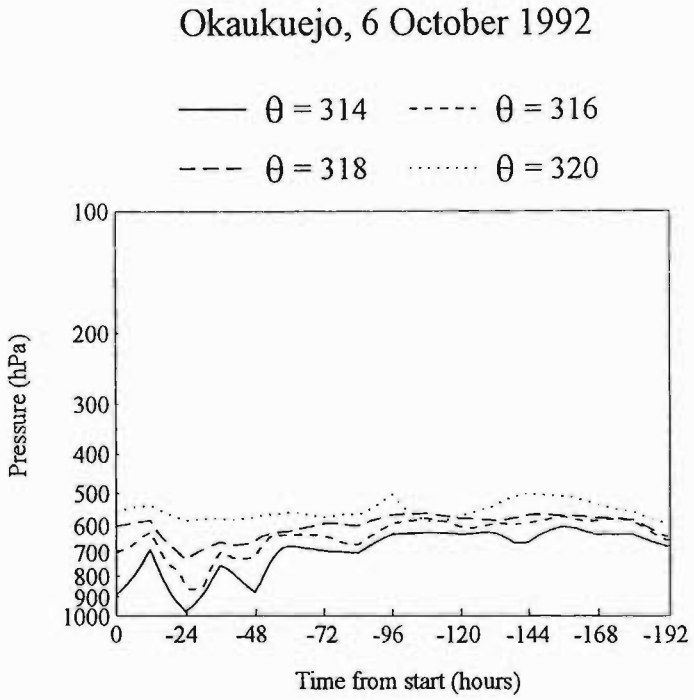

Figure 4.26 Time-pressure plot of the middle-point eight day back trajectories on 314, 316, 318 and 320 K isentropic surfaces, from Okaukuejo, for the period 6 October to 28 September 1992. Pressure is given as a log scale (hPa) and time is in 24 hour intervals. The start time is denoted by 0 hours and the end time -192 hours. Source NASA/GSFC.

and 316 K isentropic surfaces fluctuate between the surface and approximately 3 km, indicative of mixing within the shallow layer.

It is clear that the airmass at Okaukuejo originates within the large-scale anticyclonic gyre, which transports air within stable layers, such as the one observed between 3 and 5 km, as shown by the back trajectories (Fig. 4.26). It has been shown that ozone levels accumulate within such stable layers, during transport (Thompson *et al.*, 1996a), and as a result will contribute to the observed lower and mid-tropospheric ozone maxima at Okaukuejo.

Factors including the abundance of ozone and ozone precursors, from biogenic emissions (Swap *et al.*, 1996) and biomass burning in central Africa at this time of the year (Thompson *et al.*, 1996c; Andreae, 1991), and efficient ozone formation in the atmosphere, particularly in the lowest layers (0-4 km) and in the middle troposphere (8-12 km) (Thompson, *et al.*, 1996a; Zenker *et al.*, 1995) also support the observed ozone maxima at Okaukuejo.

******

In order to examine the relationship between the passage of a westerly trough and vertical ozone distribution at Okaukuejo further, the period 7 to 15 October 1992 was selected for analysis (Fig. 4.27). A westerly trough passed over Namibia and South Africa during the period 10 to 12 October 1992. Thereafter, anticyclonic circulation accompanied by an easterly trough over the western parts of the subcontinent, prevailed. The westerly wave disturbance is reflected in the 700 hPa synoptic charts between 9 and 12 October (Fig. 4.28). The extension of the westerly trough is confined south of 20°S. The presence of the trough is reflected in the strong westerly flow in the southern parts of the subcontinent shown in the 700 hPa windfield (Fig. 4.29). Light (< 20 ms^{-1}) easterly winds prevail over the land, north of the westerly disturbance.

Ozone mixing ratios at Okaukuejo, between the surface and 12 km, prepared from the five ozonesonde launches during this period, are shown in Figure 4.30. Near-surface ozone values range between 40 and 60 ppbv on all days. A similar mid-tropospheric minimum, as observed in the composite westerly trough ozone profile, is apparent. It serves to separate ozone in the lowest layers from an elevated maximum at approximately 9 km (~ > 60 ppbv). The base of the elevated layer varies between approximately 6 and 10 km. Above this level, ozone increases steadily to 12 km and then decreases to the base of the ozone maximum at 16 km (not shown). The mid-tropospheric minimum varies in vertical extent. On 10 October, the region of relatively clean air occurs between approximately 3 and 6 km (agl). On 11 October the depleted layer is slightly elevated and extends from 5 to 8 km. The mid-tropospheric minimum is most

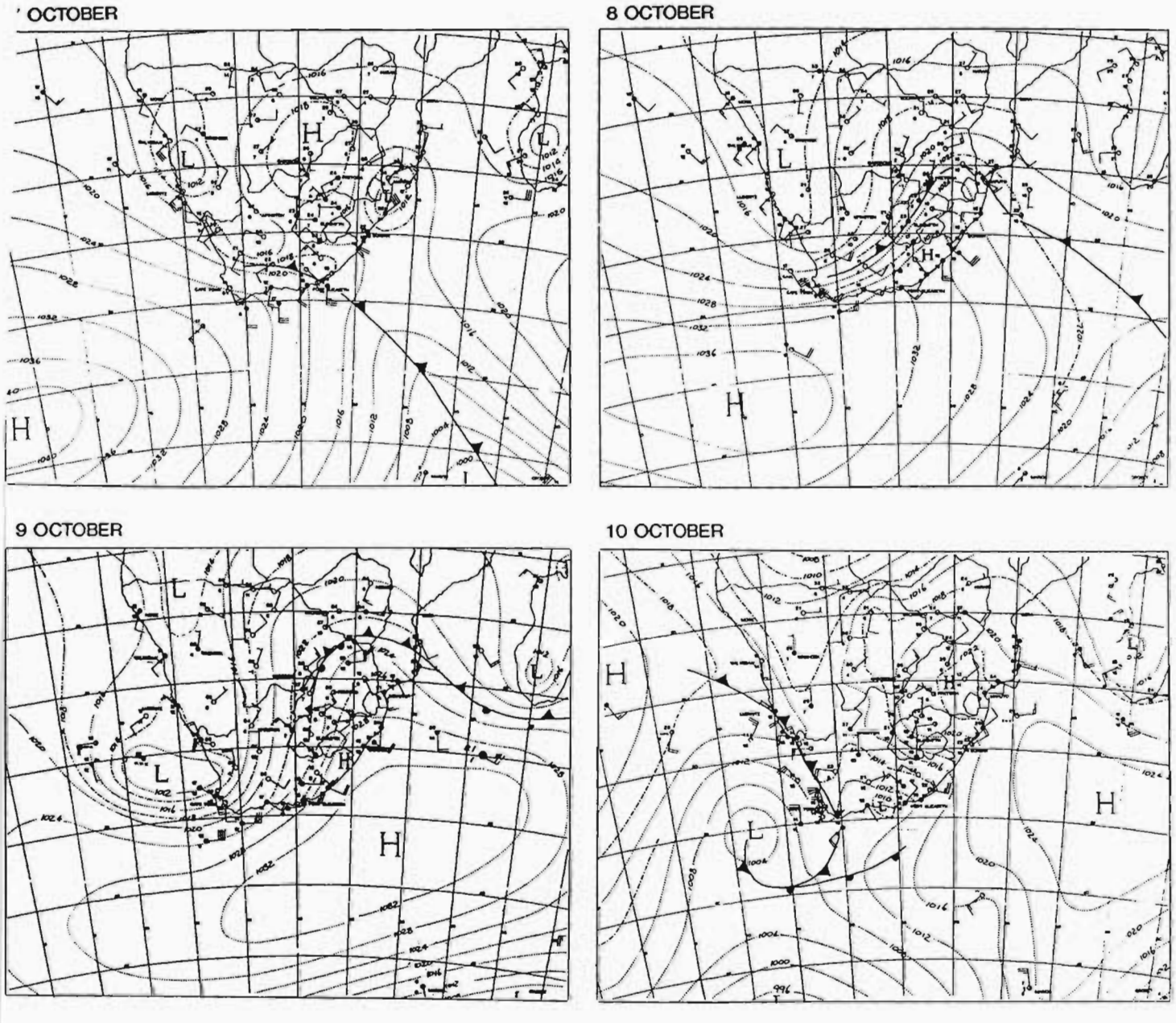

Figure 4.27 Surface synoptic charts over southern Africa for 7 to 15 October 1992. Isobars (hPa) are denoted by light lines. From the Daily Weather Bulletin (SAWB).

OCTOBER

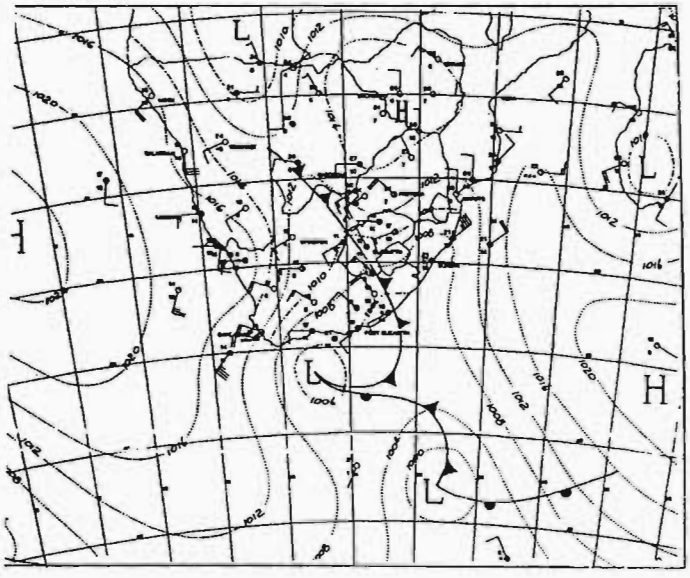

12 OCTOBER

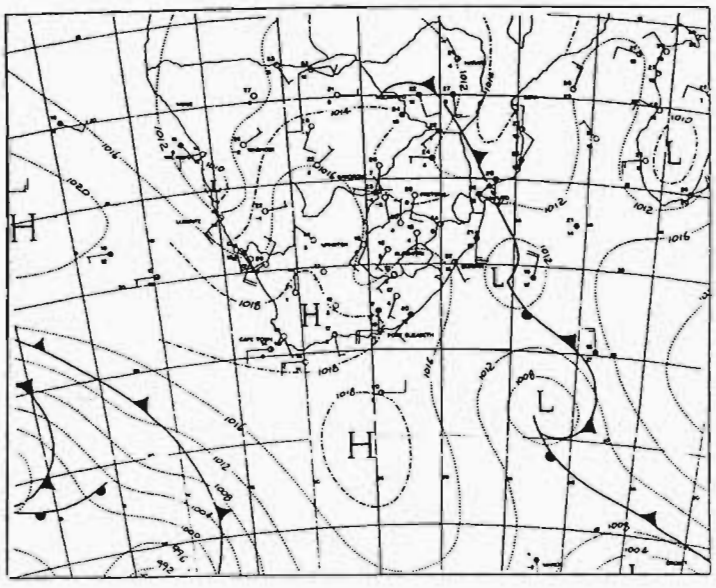

3 OCTOBER

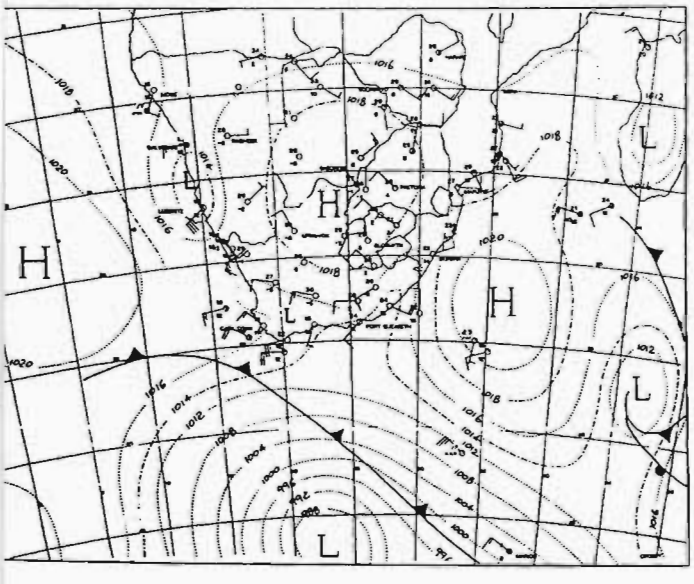

14 OCTOBER

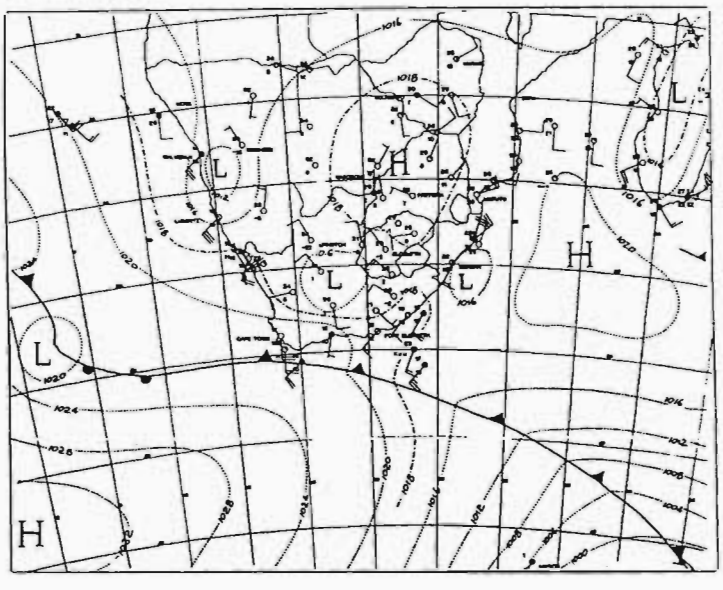

15 OCTOBER

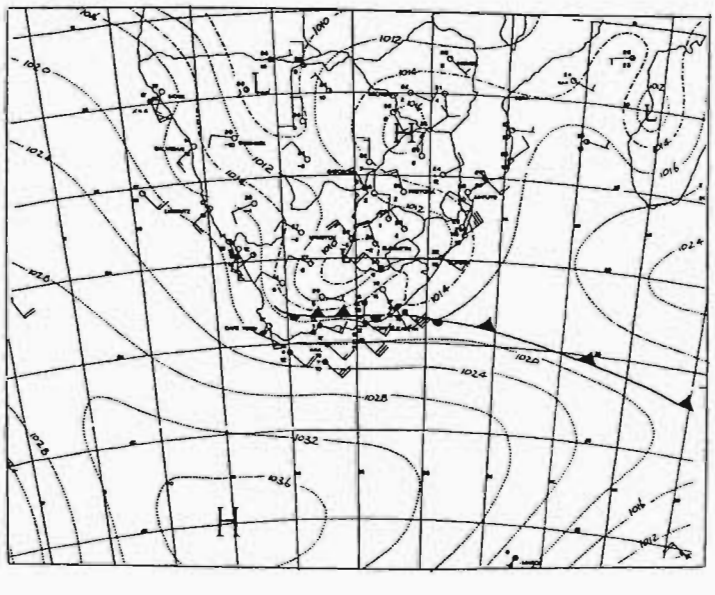

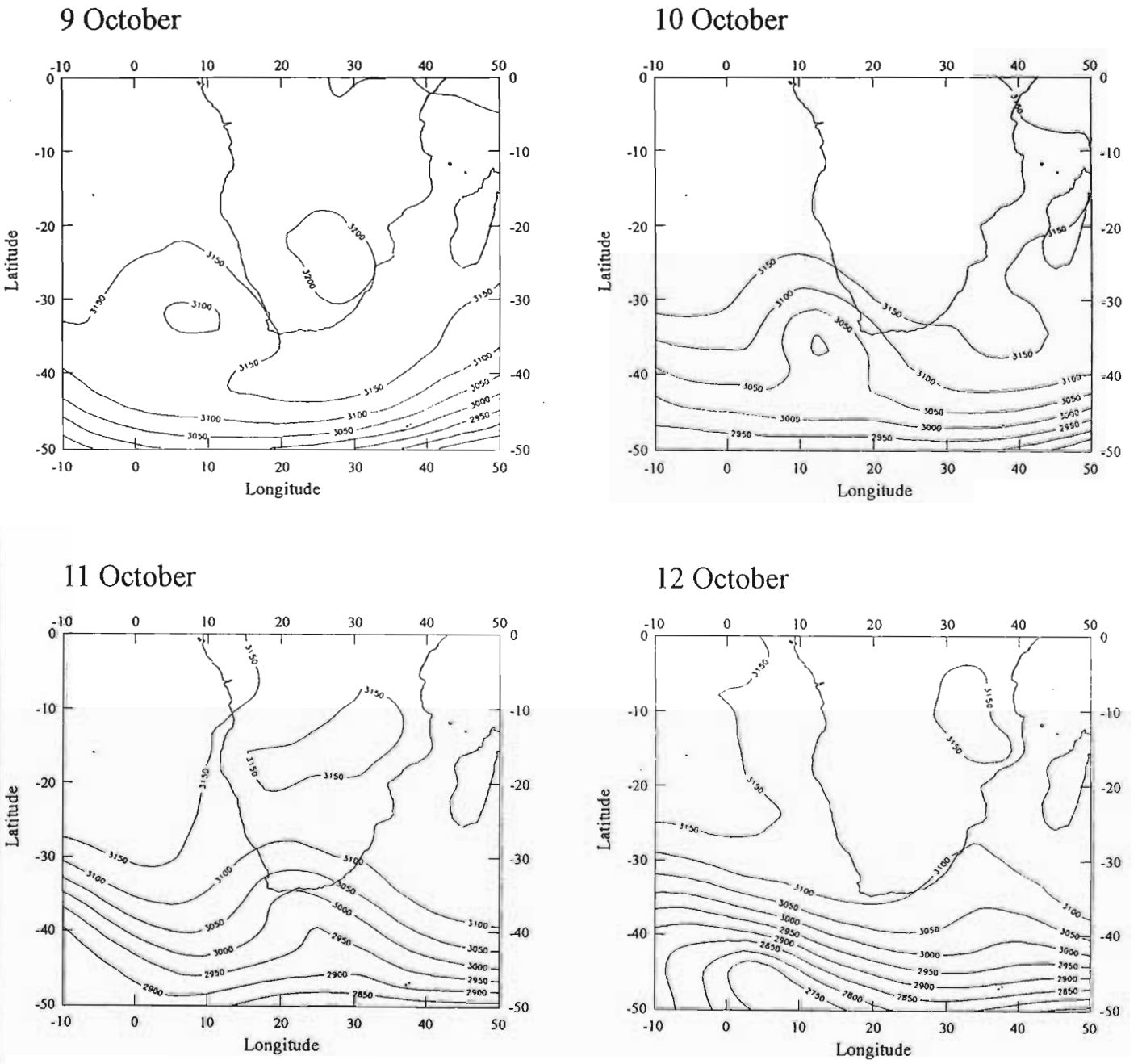

Figure 4.28 700 hPa synoptic charts over southern Africa for 9 to 12 October 1992. Prepared from ECMWF data.

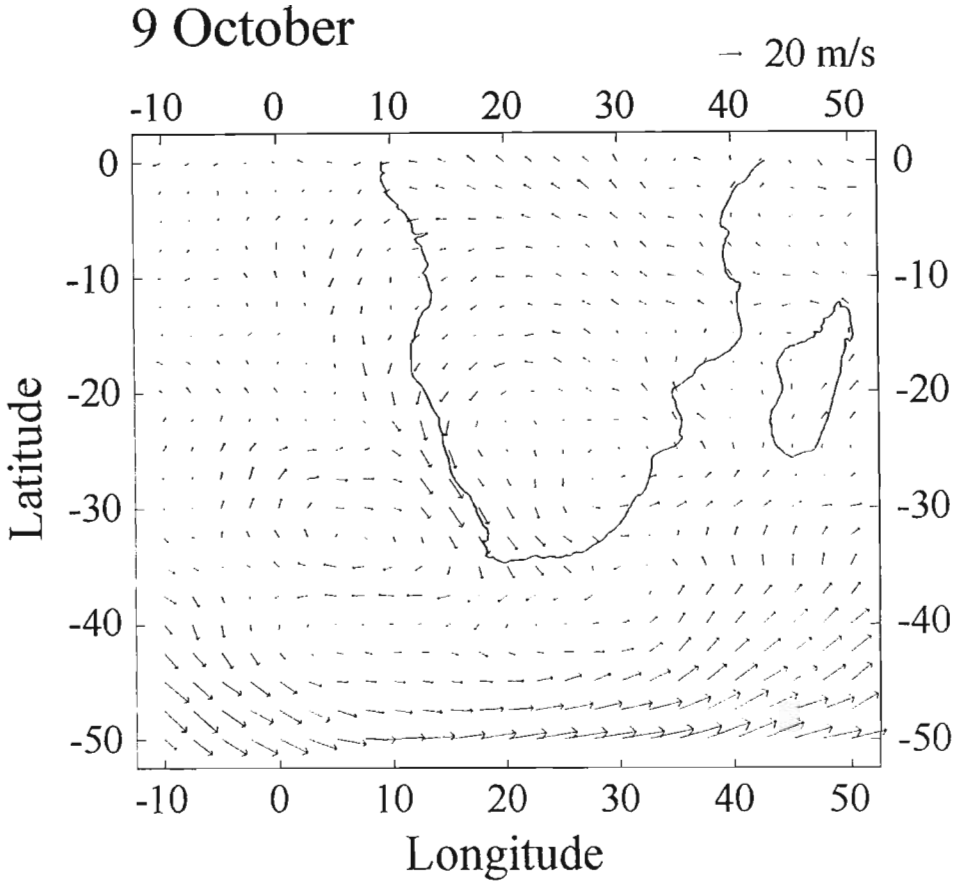

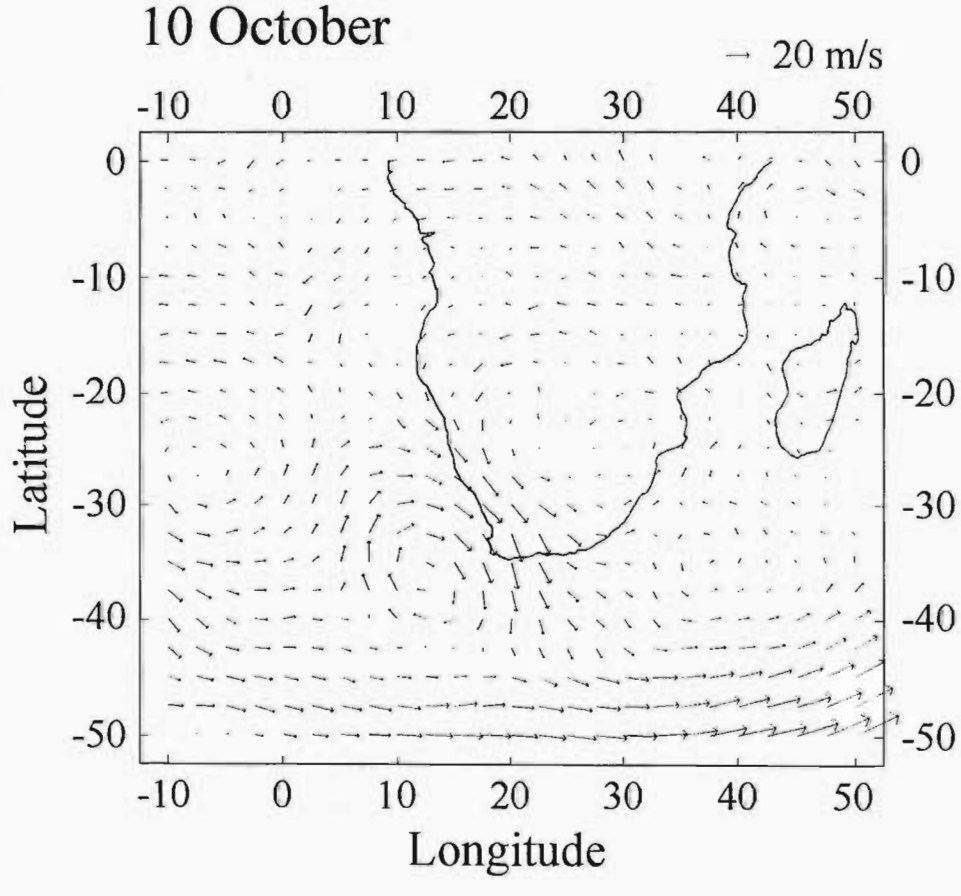

Figure 4.29 700 hPa wind vectors over southern Africa, derived from ECMWF u and v wind components, for 9 to 12 October 1992.

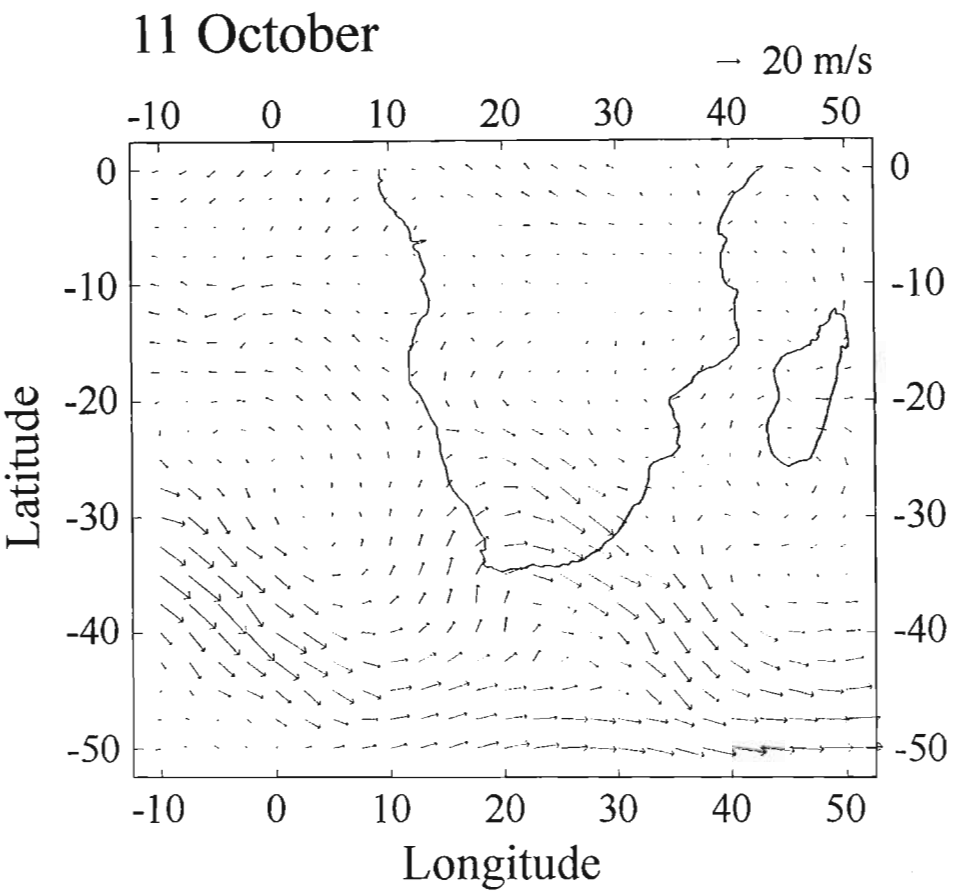
11 October
20 m/s
-10
0
10
20
30
40
50
0
-10
-20
-30
-40
-50
Latitude
Longitude

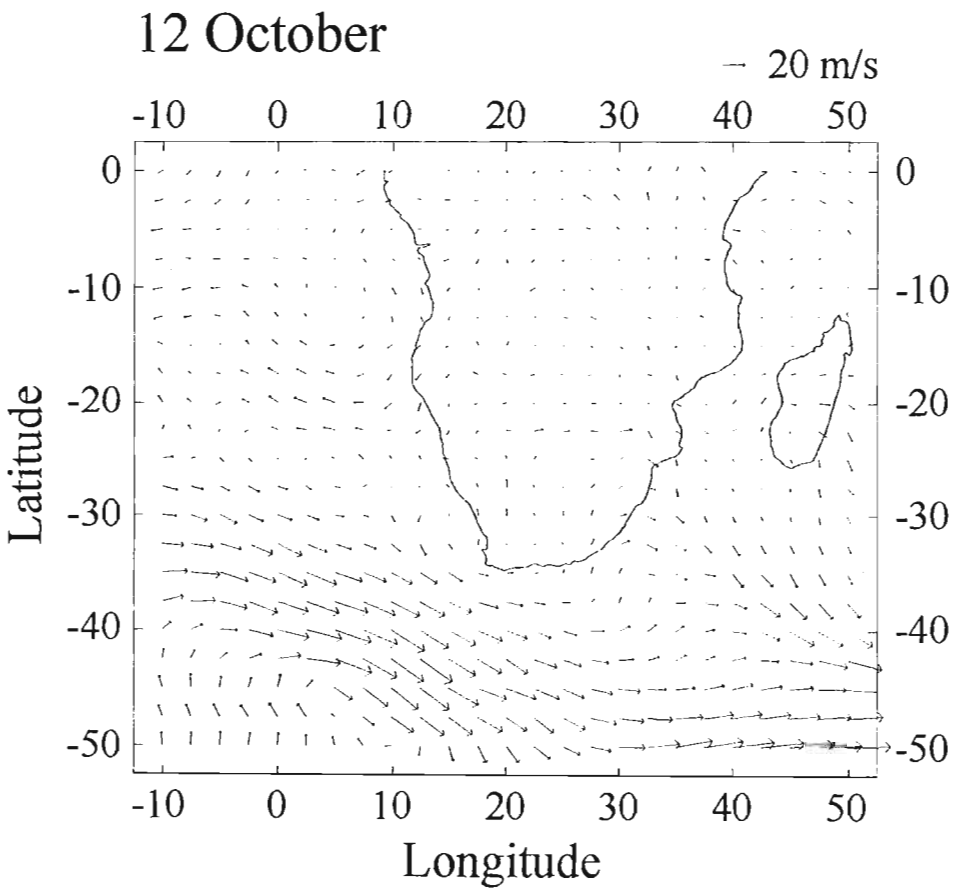
12 October
20 m/s
-10
0
10
20
30
40
50
0
-10
-20
-30
-40
-50
Latitude
Longitude

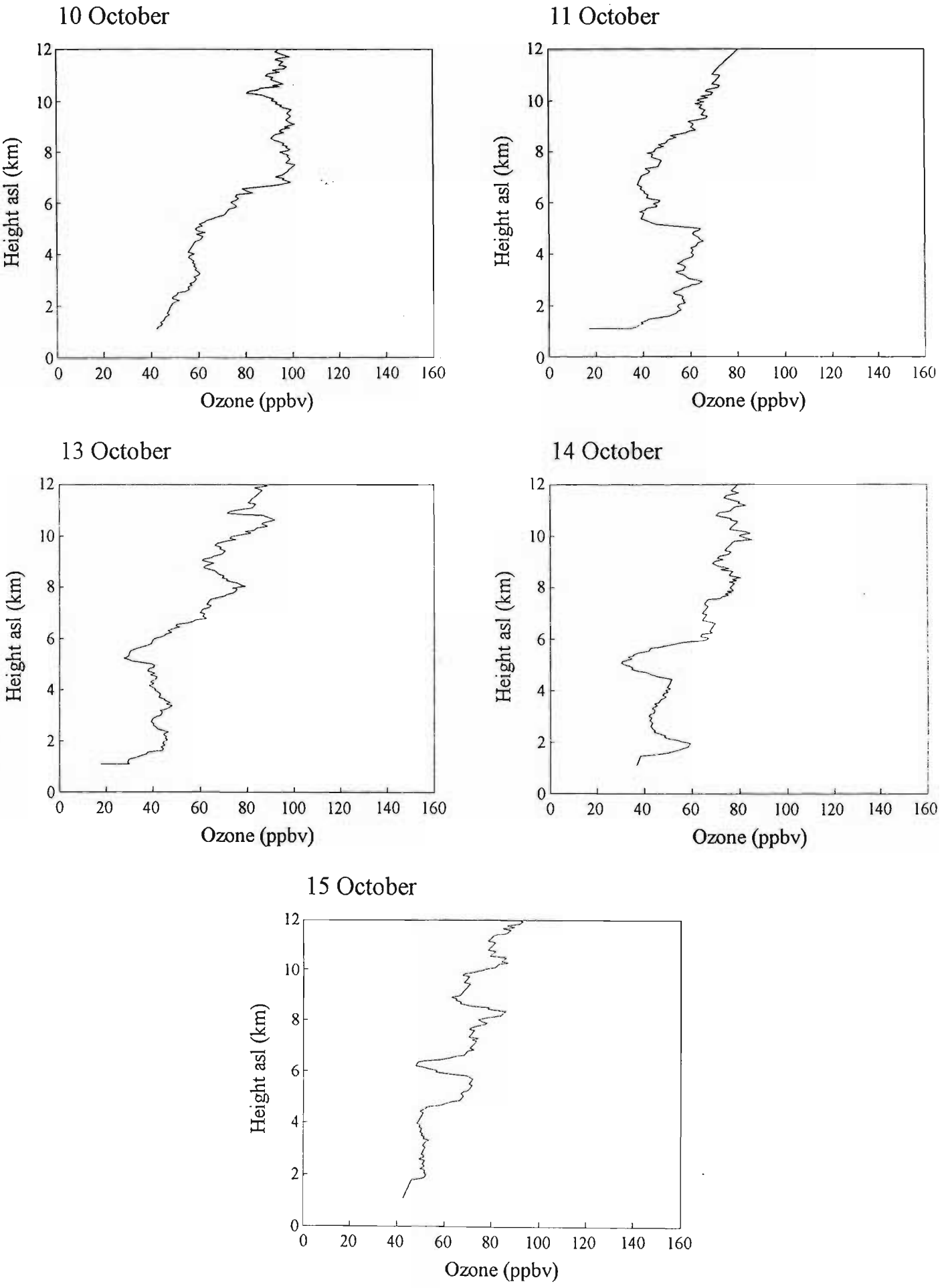

Figure 4.30 Ozonesonde mixing ratio profiles (ppbv) between 0 and 12 km (asl), at Okaukuejo for 10, 11, 13, 14 and 15 October 1992. Data from the SAWB.

pronounced on 11, 13 and 14 October. The enhanced layer is present on all five days and occurs above the persistent absolutely stable layer described by Tyson *et al.* (1995) for the SAFARI period.

The key to the origin of the mid-tropospheric ozone minimum is found in the origin of the airmass at Okaukuejo. Eight day back trajectory analysis from Okaukuejo, between 15 and 7 October (Fig. 4.31), on the 314, 316, 318 and 320 K isentropic surfaces, shows the origin of the airmass in the Atlantic Ocean, as far back as Argentina, South America, at higher levels (316, 318 and 320 K). Some of the trajectories curve inland, in a northerly direction, at the lower levels revealing an origin over the continent. The airmass is caught within the westerly wave, over the ocean, and is transported eastwards around the South Atlantic High pressure system.

Significant variation in altitude of the back trajectories is evident in Figure 4.32. The heights of the isentropic surfaces range from approximately 250 hPa (~ 11 km), on the 320 K isentropic surface, to the surface (θ = 314 K). Airflow descends along all four levels to Okaukuejo. The confinement of the influence of the westerly trough above 600 hPa, is emphasised by the absence of any disturbance below this level after 12 October.

The case study supports the conclusions of the composite westerly trough analysis, at Okaukuejo, for the SAFARI period. The mid-tropospheric minimum is a function of the westerly flow which is manifest as a wedge of relatively clean air.

4.4.3.3 Irene

In order to examine influence of the westerly trough and anticyclonic circulation on the vertical distribution of ozone at Irene, the period 22 to 30 September was selected as a case study. This period was characterised by high pressure circulation over much of southern Africa (Fig. 4.33). An easterly trough was situated over the northwestern part of Namibia (> 20°S). A surface cold front was situated just south of Pretoria on 22 September and which had moved well to the north by 23 September. A second cold front approached the continent from the west on 24 September but which passed south of the country on 26 September and moved off into the Indian Ocean on 27 September. High pressure circulation was dominant over the entire region between 29 and 30 September. The influence of the westerly wave is confined to the southern tip of the subcontinent during this period (Fig. 4.34). Light (< 20 ms^{-1}) low-level (700 hPa) easterly winds associated with anticyclonic circulation dominate the subcontinent during this period (Fig. 4.35) except in the southern parts where stronger westerly flow prevails.

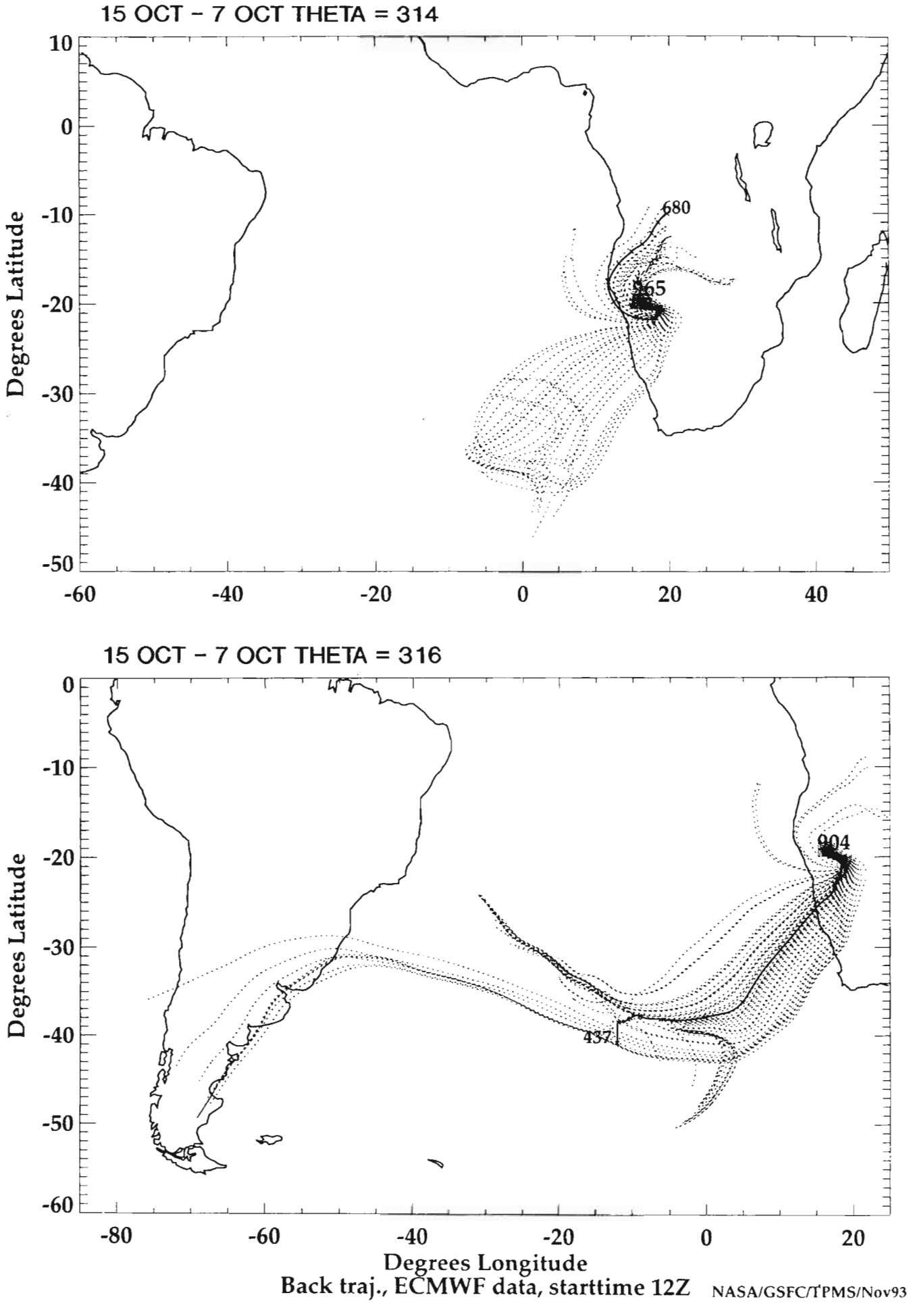

Figure 4.31 Eight day back trajectories on 314, 316, 318 and 320 K isentropic surfaces, from Okaukuejo, for the period 15 to 7 October 1992. Start time was 12 Z. The trajectory originating from the central point of the array is given as a solid line. Start pressure (hPa) is denoted by large type and end pressure by smaller type. Source NASA/GSFC.

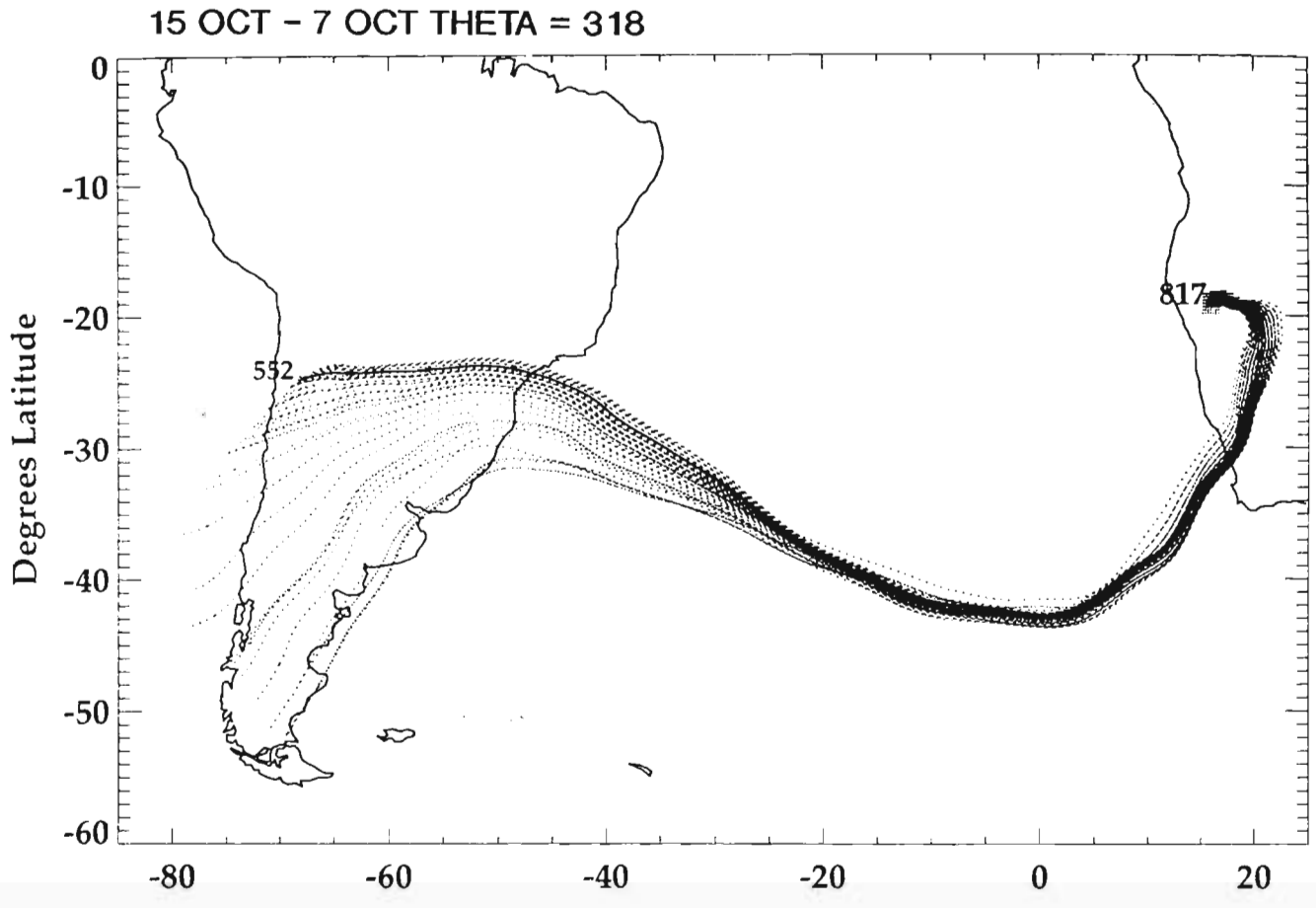

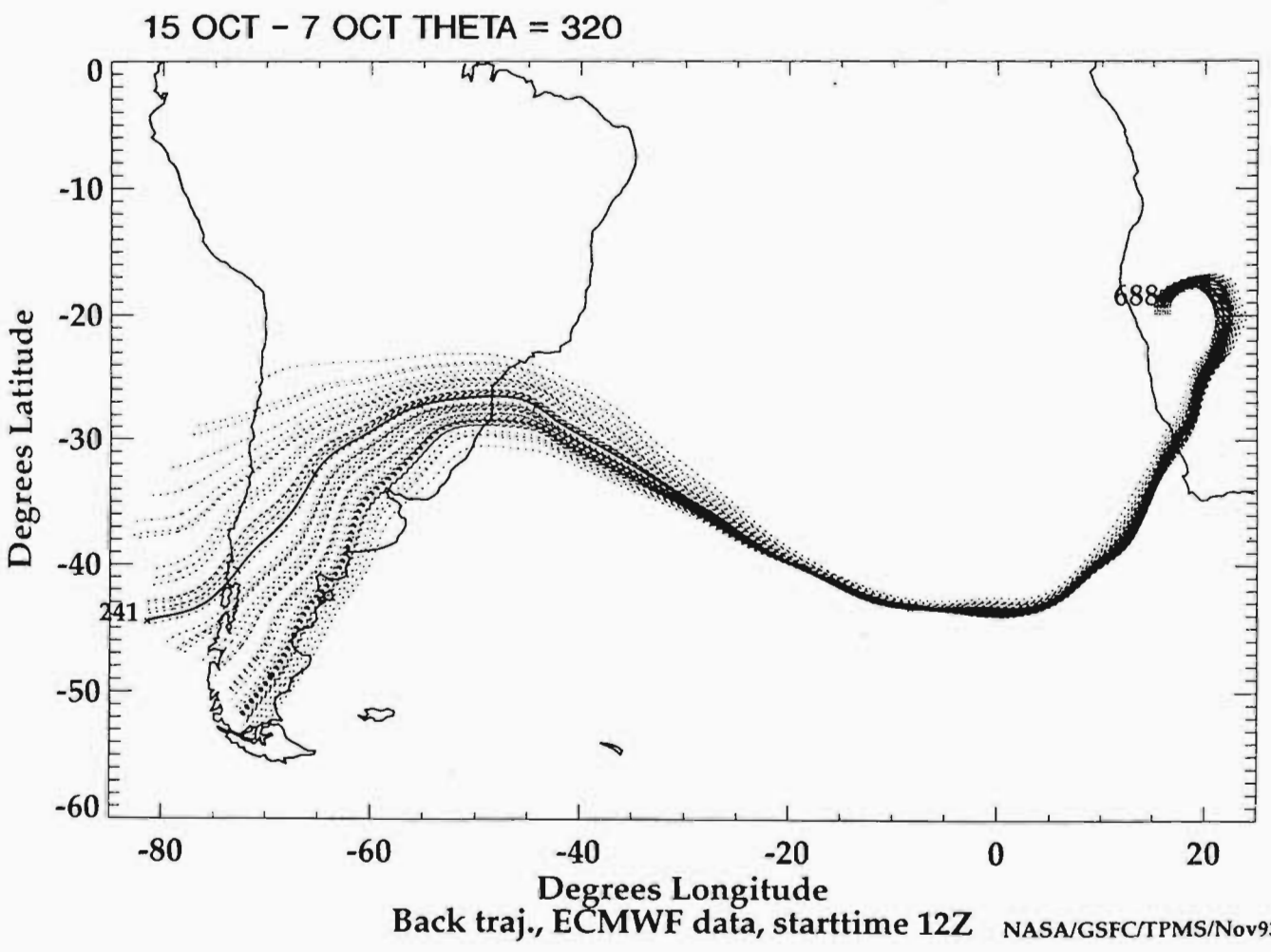

Back traj., ECMWF data, starttime 12Z NASA/GSFC/TPMS/Nov93

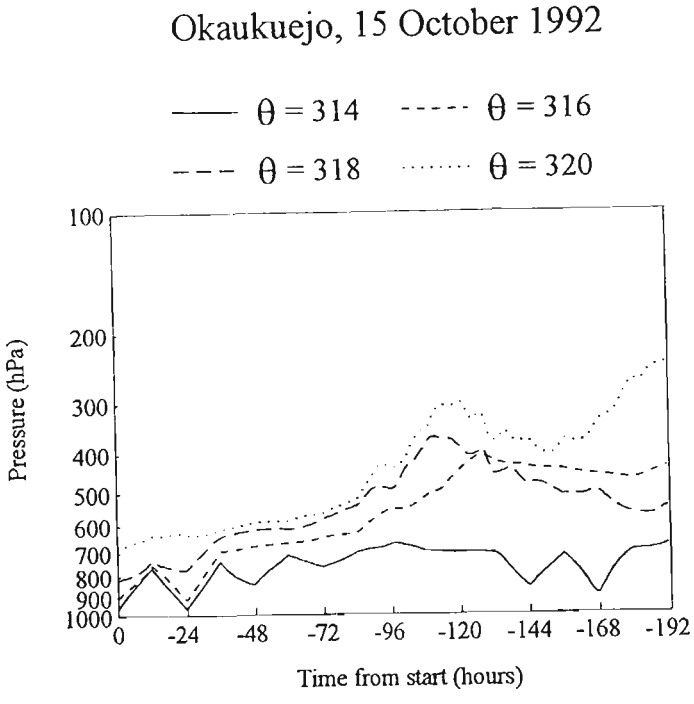

Figure 4.32 Time-pressure plot of the middle-point eight day back trajectories on 314, 316, 318 and 320 K isentropic surfaces, from Okaukuejo, for the period 15 October to 7 October 1992. Pressure is given as a log scale (hPa) and time is in 24 hour intervals. The start time is denoted by 0 hours and the end time -192 hours. Source NASA/GSFC.

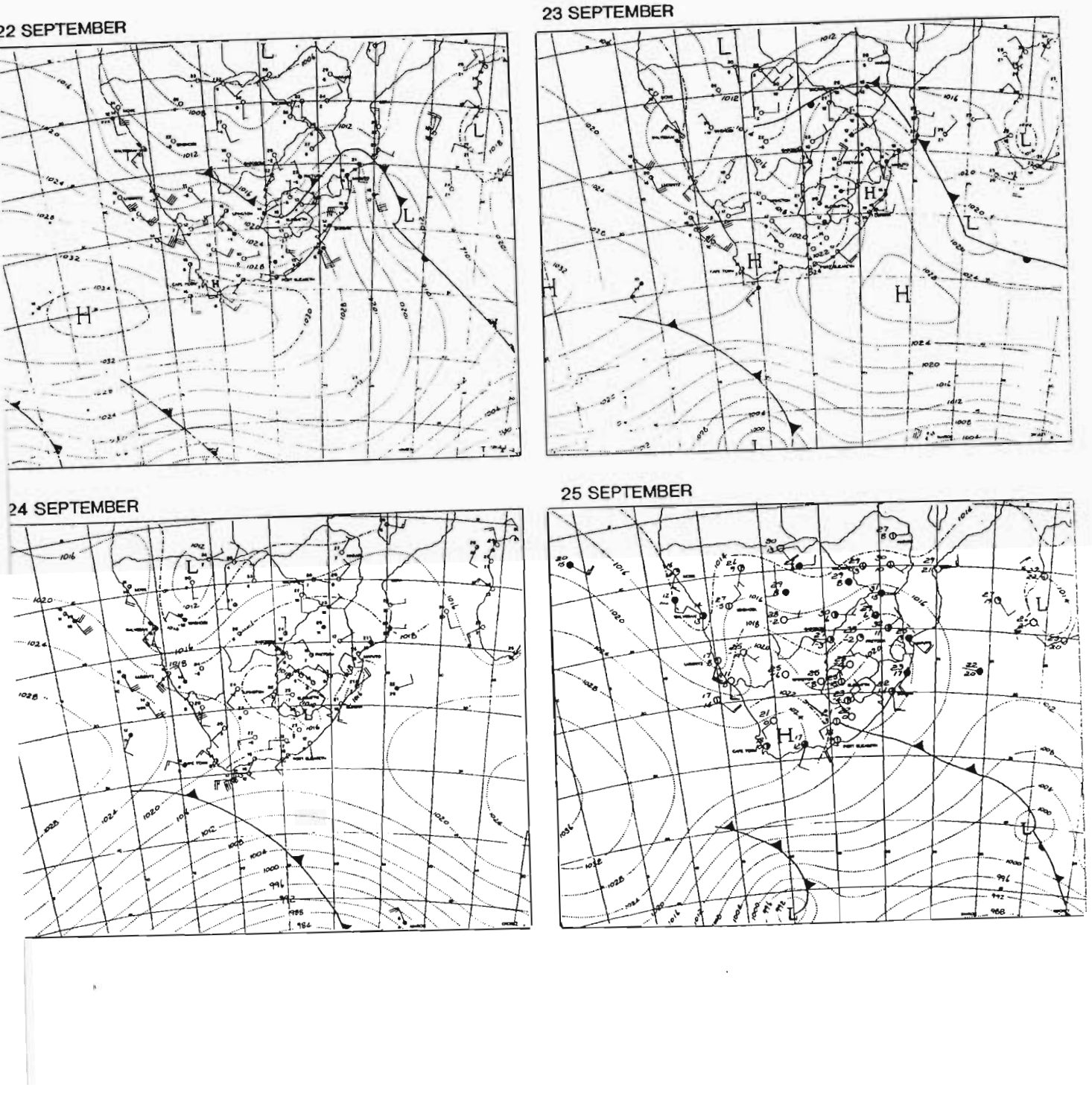

Figure 4.33 Surface synoptic charts over southern Africa for 22 to 30 September 1992. Isobars (hPa) denoted by light lines. From the Daily Weather Bulletin (SAWB).

5 SEPTEMBER

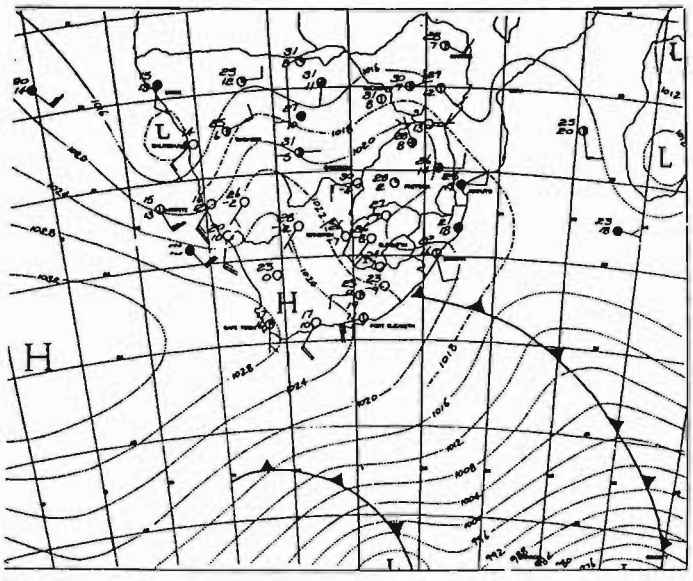

27 SEPTEMBER

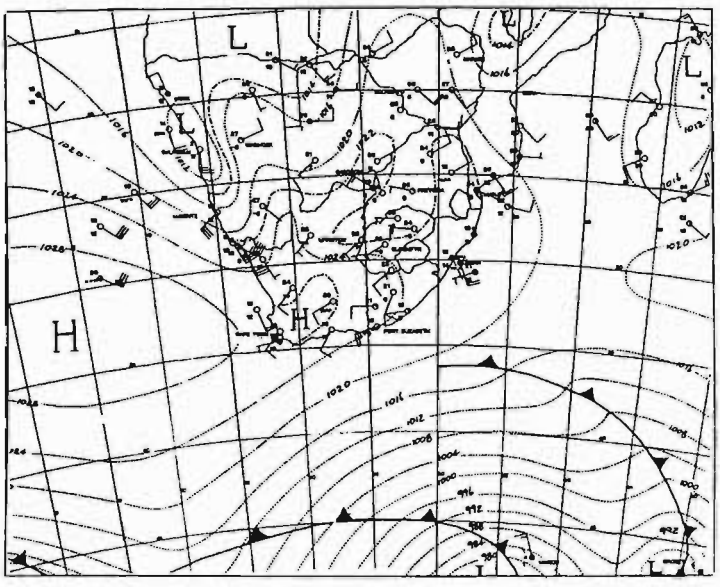

28 SEPTEMBER

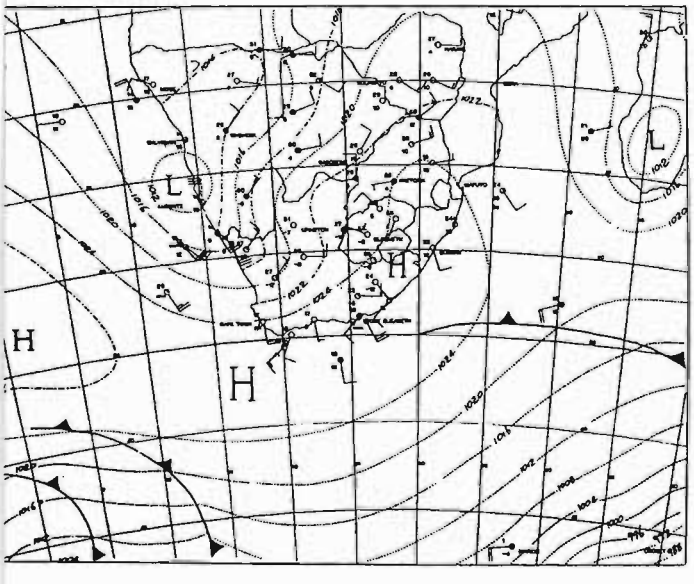

29 SEPTEMBER

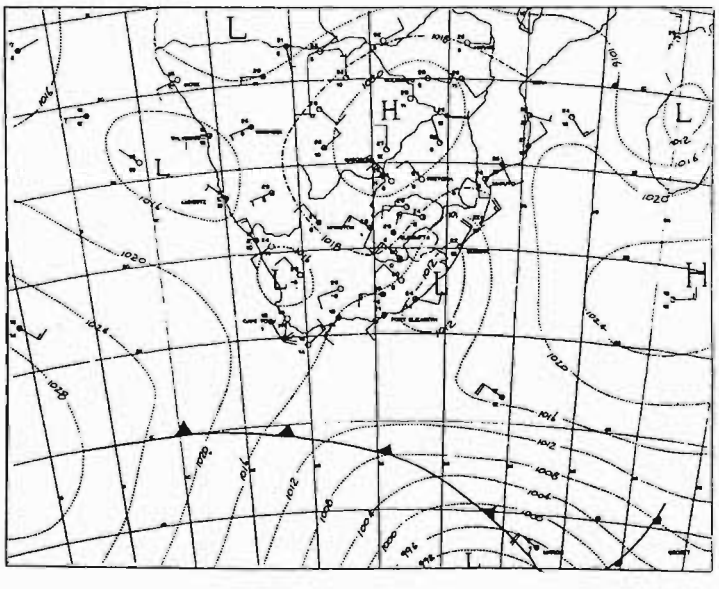

30 SEPTEMBER

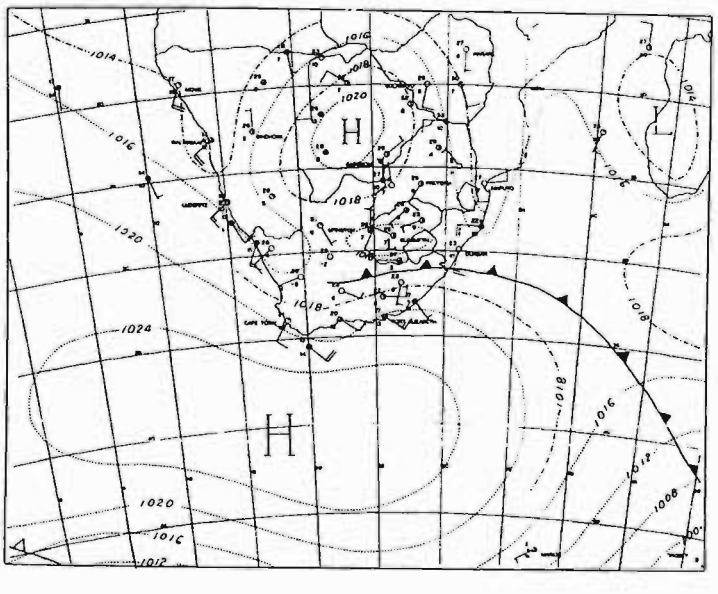

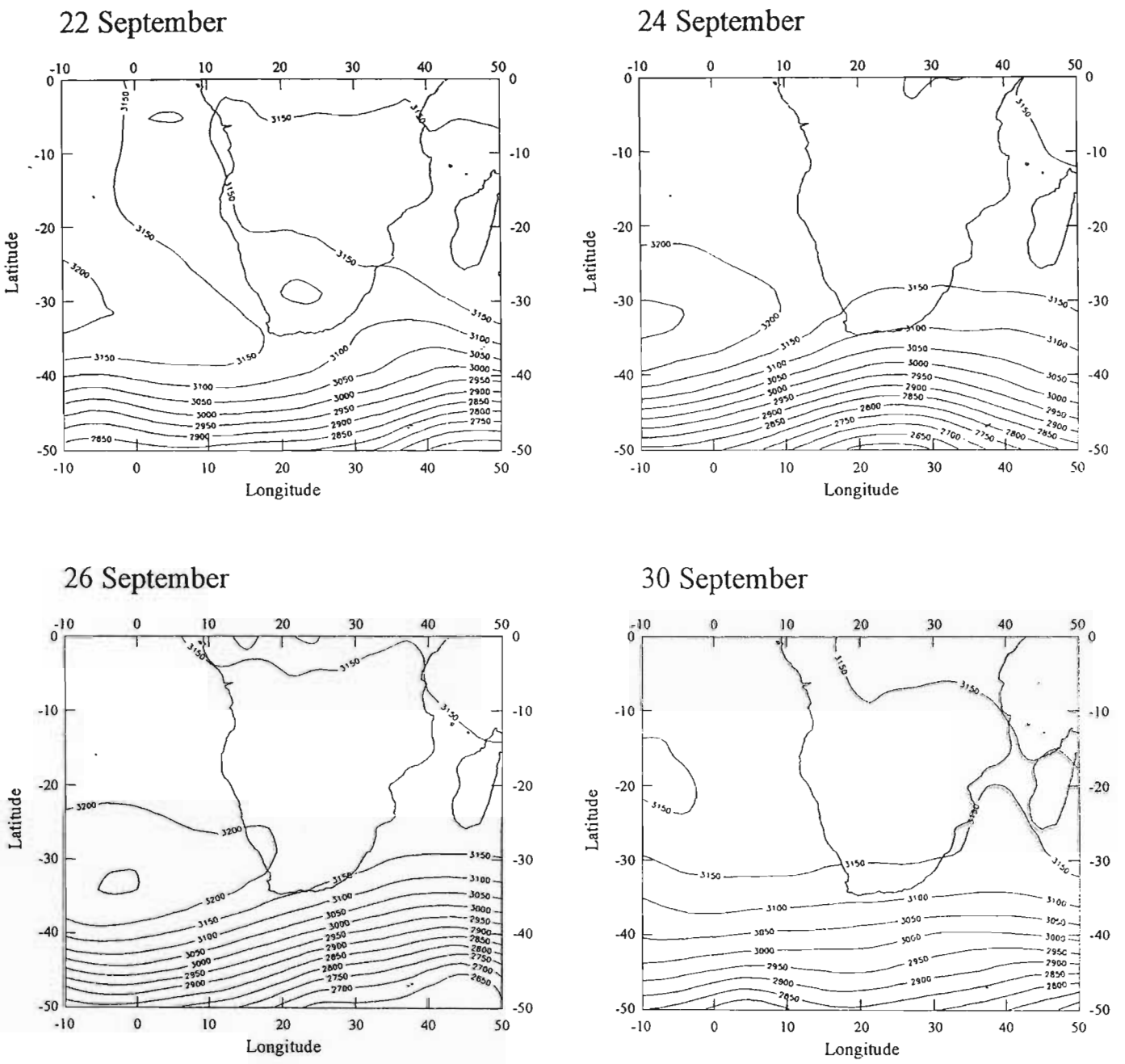

Figure 4.34 700 hPa synoptic charts over southern Africa for 22, 24, 26 and 30 September 1992. Prepared from ECMWF data.

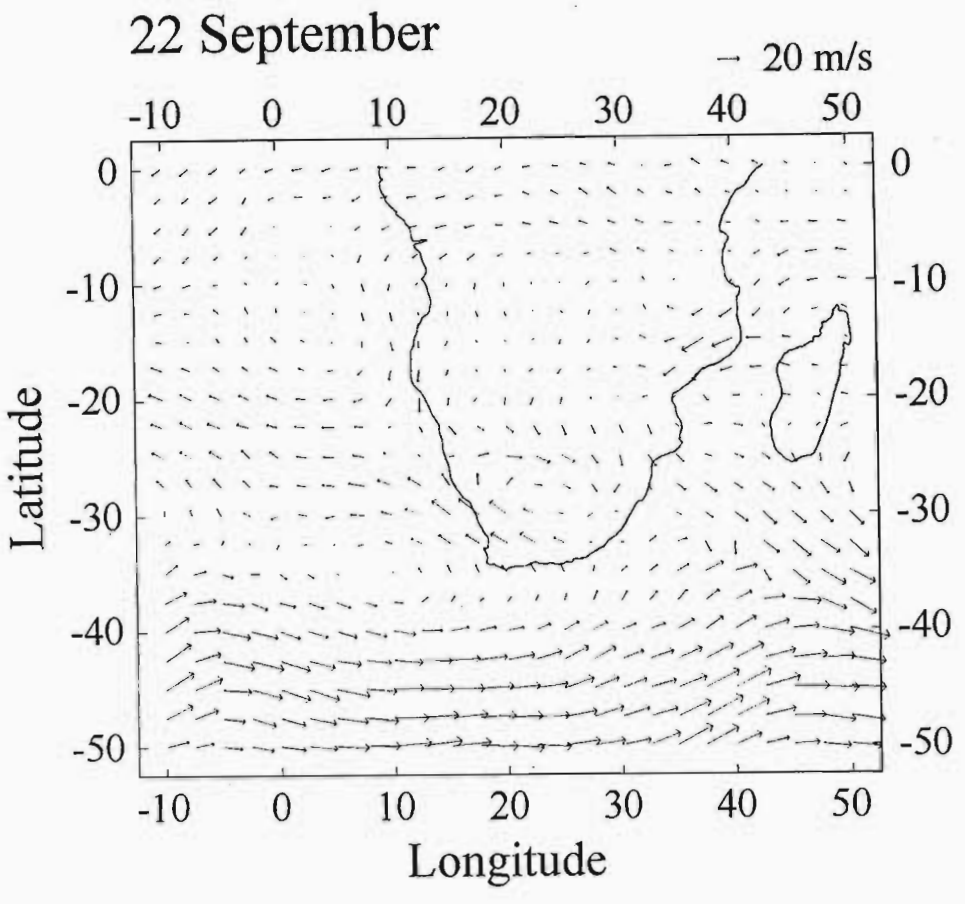

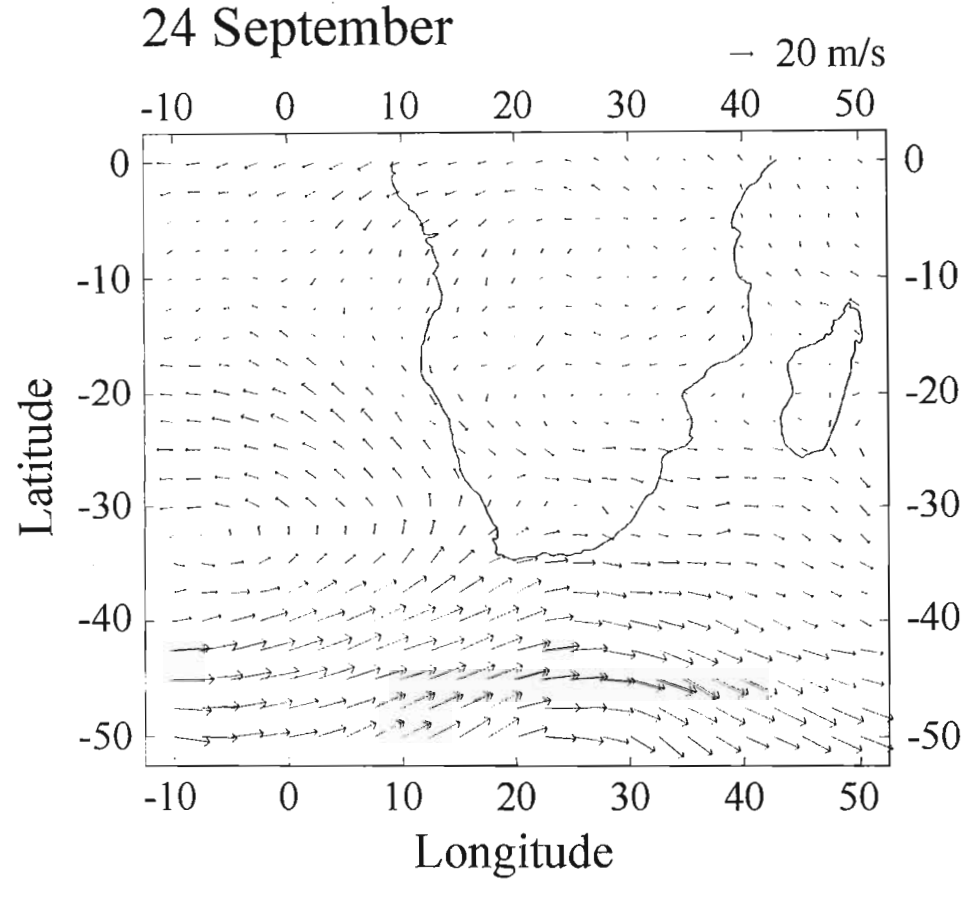

Figure 4.35 700 hPa wind vectors over southern Africa, derived from the ECMWF u and v wind components, for 22, 24, 26 and 30 September 1992.

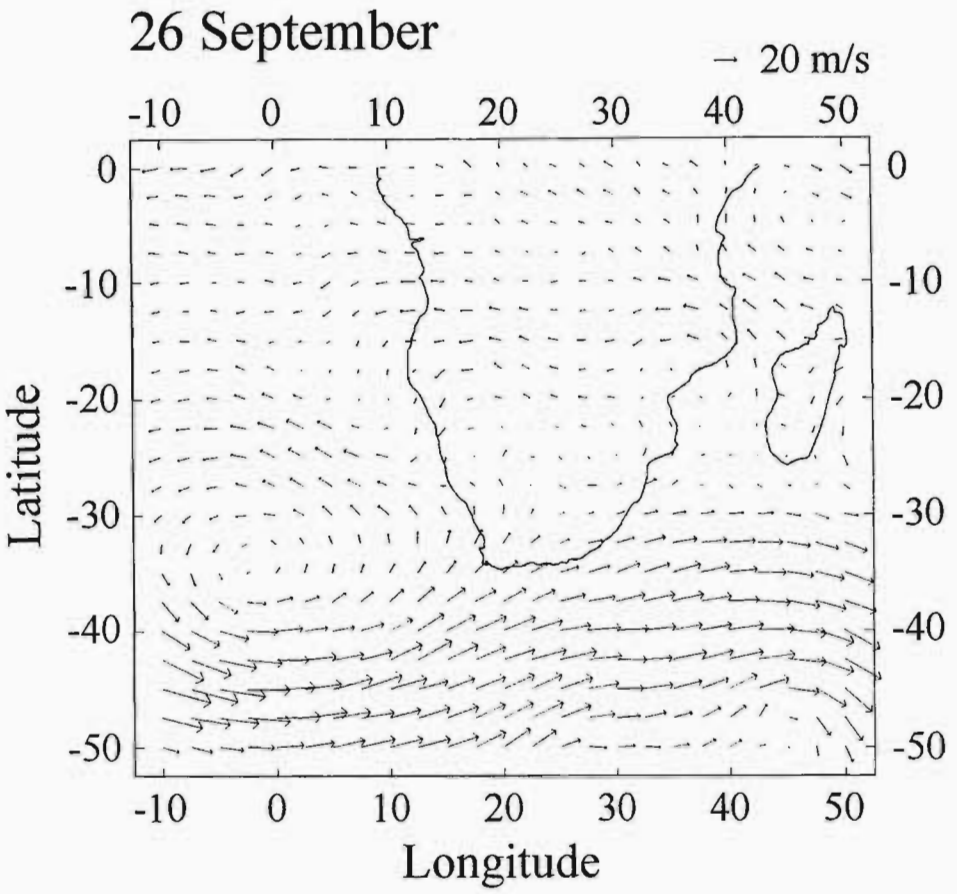
26 September
→ 20 m/s
-10 0 10 20 30 40 50
0 -10 -20 -30 -40 -50
Latitude
Longitude

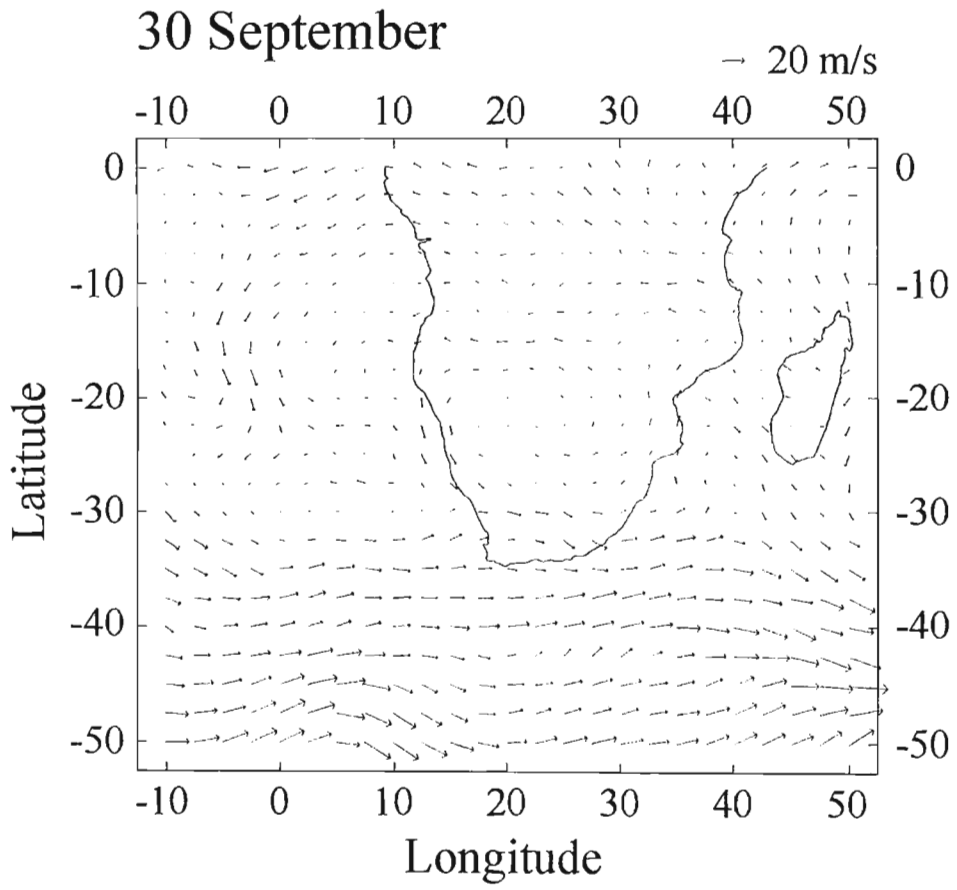
30 September
→ 20 m/s
-10 0 10 20 30 40 50
0 -10 -20 -30 -40 -50
Latitude
Longitude

Only two ozonesonde launches were conducted at Irene during the period 22 to 30 September 1992 (Fig. 4.36). Ozone profiles at Irene for 23 and 30 September reveal two distinct layers in the troposphere. A well-defined low level tropospheric maximum (~ 40 - 60 ppbv) below approximately 6 and 5 km on 23 and 30 September respectively and a second enhanced layer (~ 60 - 80 ppbv) is observed above this layer.

Eight day back trajectories, from 30 September to 22 September 1992, indicate tight anticyclonic circulation, surrounding Irene, at the lower levels (312 and 314 K) with a point of origin to the northwest in the vicinity of northern Namibia (Fig. 4.37). At the higher levels (θ = 316-318) the point of origin, of the middle-point trajectory, extends further back to a point in the Atlantic Ocean to approximately 15°S. Considerable variation about the middle-point trajectory occurs particularly along the 318 K isentropic surface. This is an indication of slight errors in the windfield used in the calculation of the trajectories. Such errors arise from the scarcity of radiosonde data in the Southern Hemisphere, from smoothing the data and lack of terrain effects in the three dimensional model calculations (McNamara, pers. comm., 1993).

Figure 4.38 shows time-pressure plots of the middle-point eight day back trajectories (θ=312, 314, 316, 318, 320 K) to Irene starting on 22 September. The constant height of the back trajectories emphasizes the marked stability in the lower troposphere and two clear stable layers are distinguishable. The first layer occurs between the surface and approximately 3 km within which the two lower back trajectories, along 312 and 314 K isentropic surfaces, are confined. The second layer is depicted by the 316, 318 and 320 K isentropic surfaces which define the stable layer between approximately 3 and 5 km. Similar absolutely stable layers, at Irene, have been described by Garstang *et al.* (1996). See Table 4.4.

The stable nature of the lower troposphere and the tight anticyclonic re-circulation around Irene, indicated by the back trajectories, provides support for the accumulation of ozone. Transport within the anticyclonic gyre alone, as described by Thompson *et al.* (1996a), may enhance ozone levels significantly at Irene. Additional factors, such as the abundance of urban and industrial pollution from Pretoria and from Mpumalanga (formerly the Eastern Transvaal Highveld), which is situated to the west of Irene, support the enhancement. Further, tropospheric ozone is known to reach its peak at Irene in September (Zunckel *et al.*, 1992; Zunckel, 1992).

******

The influence of the passage of a westerly trough on the vertical distribution of ozone at Irene is examined during the period 14 to 22 October 1992. A surface cold front (Fig. 4.39) passed over the country between 14 and 17

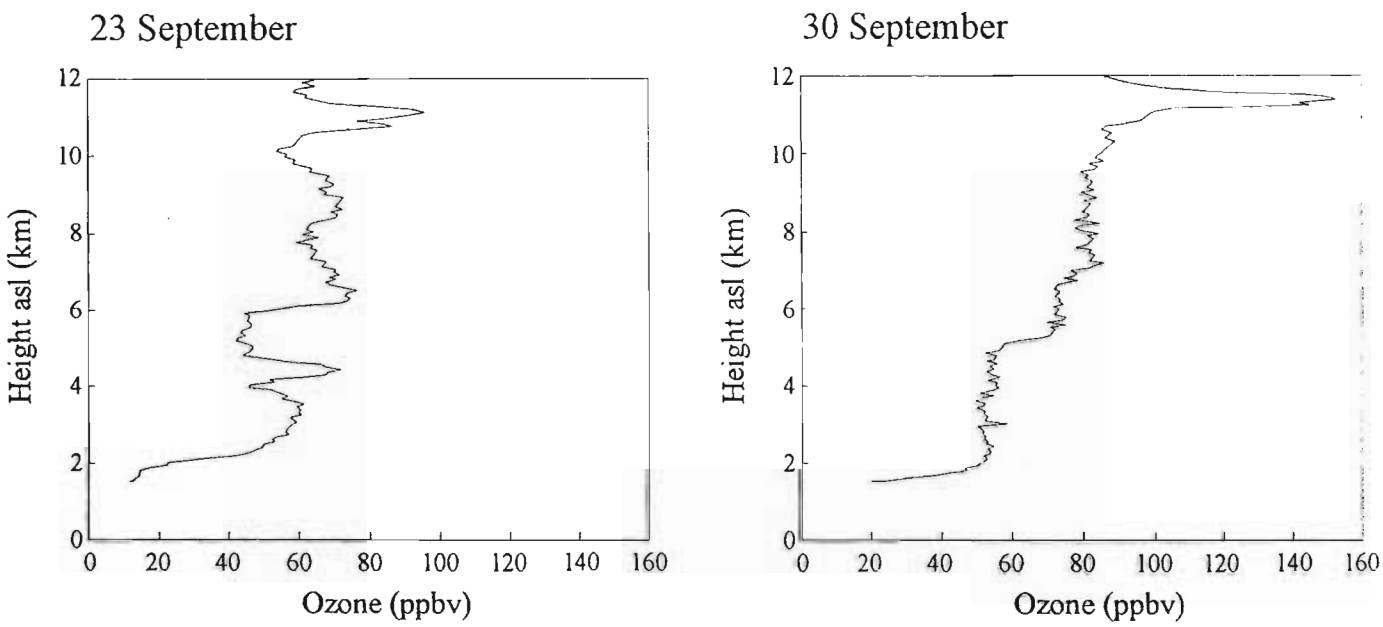

Figure 4.36 Ozonesonde mixing ratio profiles (ppbv) between 0 and 12 km (asl), at Irene for 23 and 30 September 1992 Data from the SAWB.

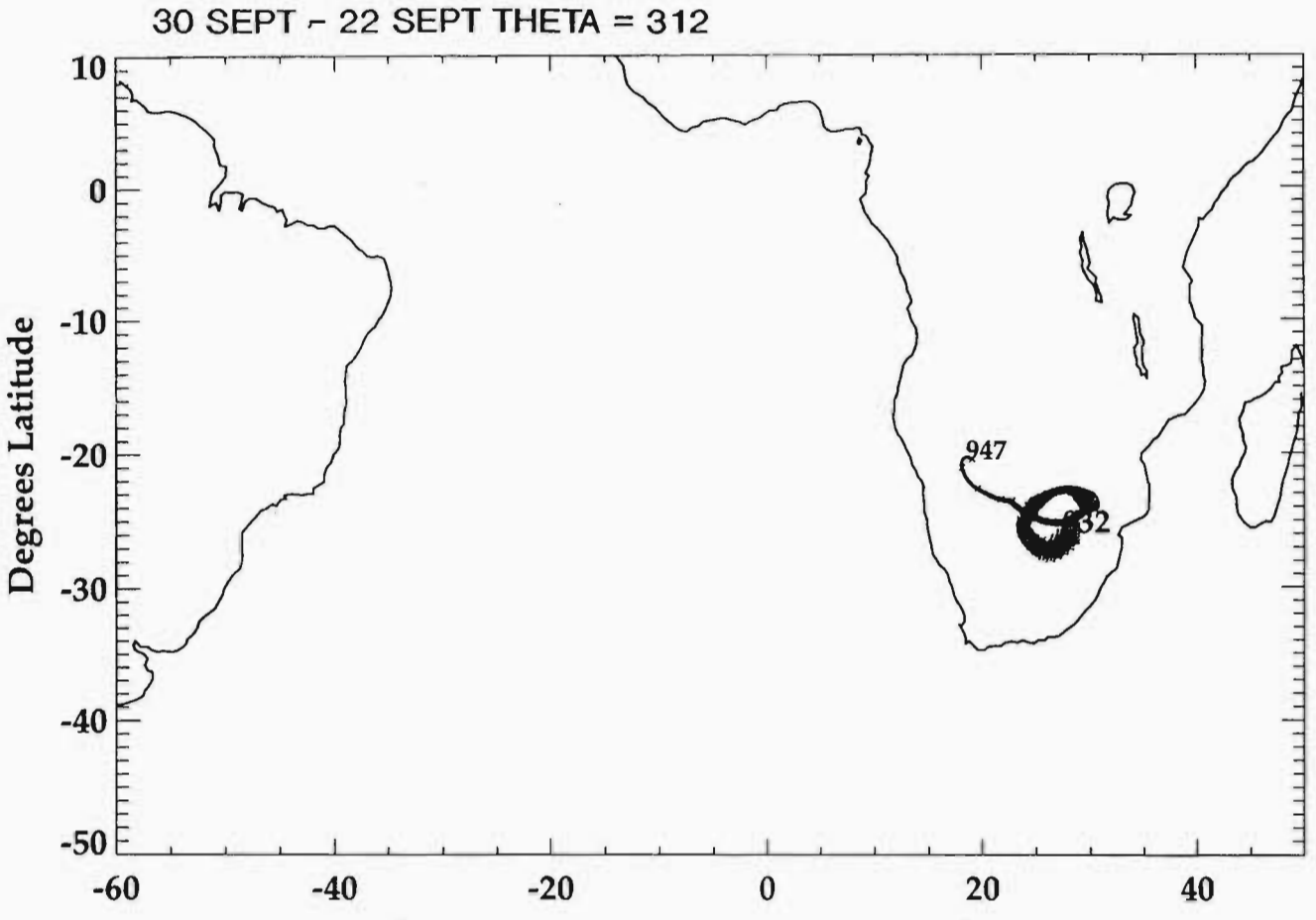

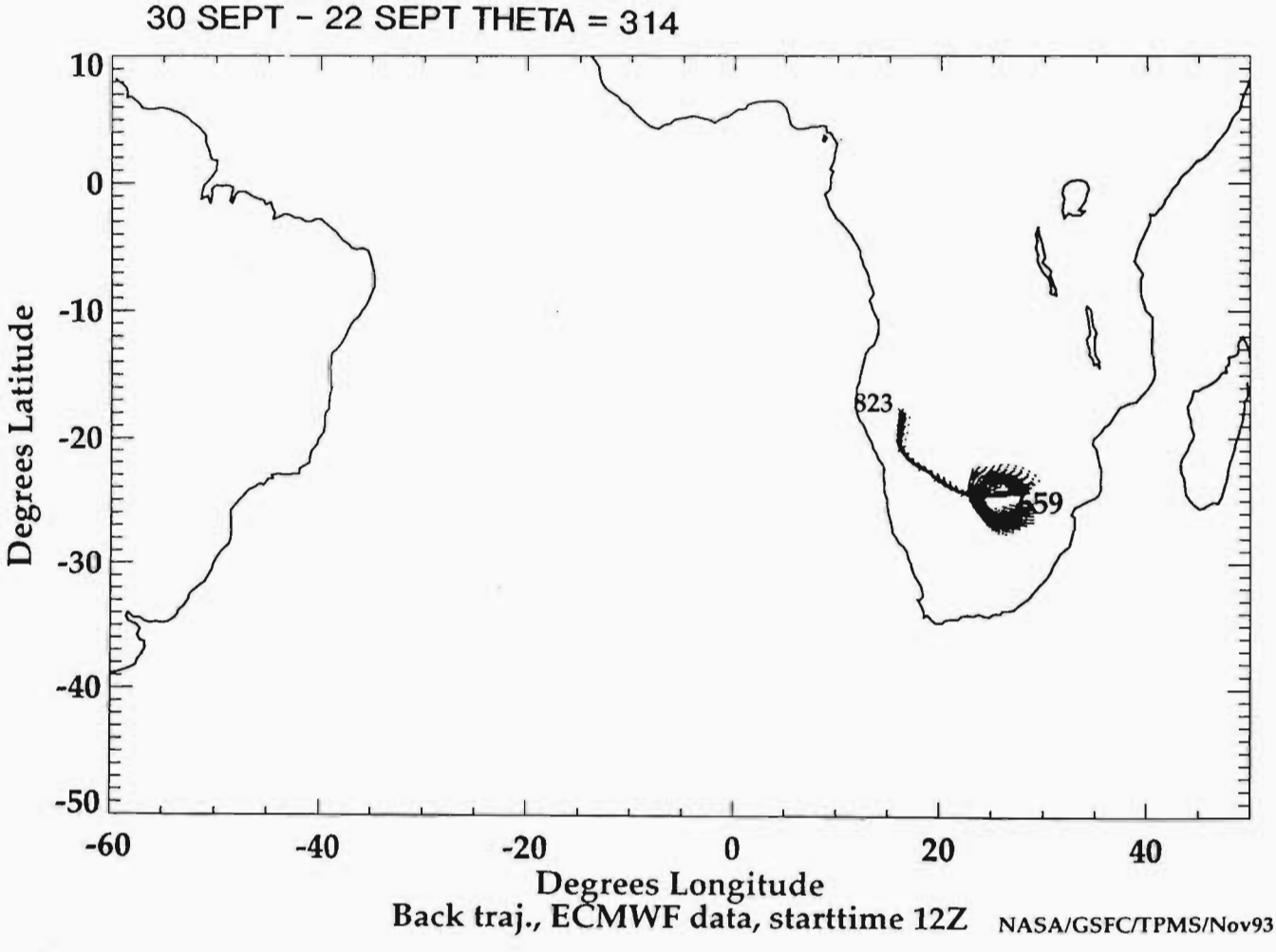

Figure 4.37 Eight day back trajectories on 312, 314, 316, 318 and 320 K isentropic surfaces, from Irene, for the period 30 to 22 September 1992. Start time was 12 Z. The trajectory originating front the central point of the array is given as a solid line. Start pressure (hPa) is denoted by large type and end pressure by smaller type. Source NASA/GSFC.

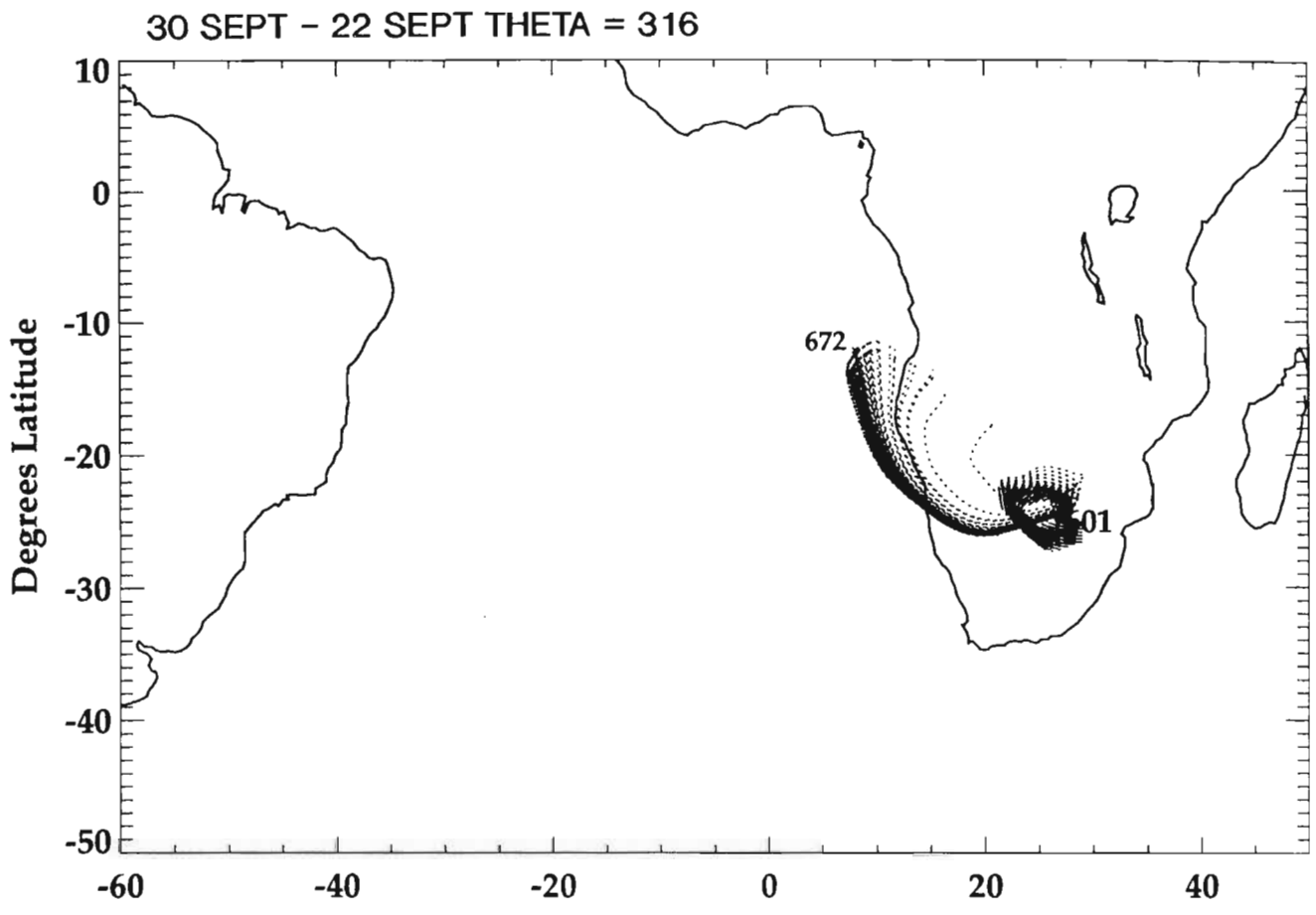

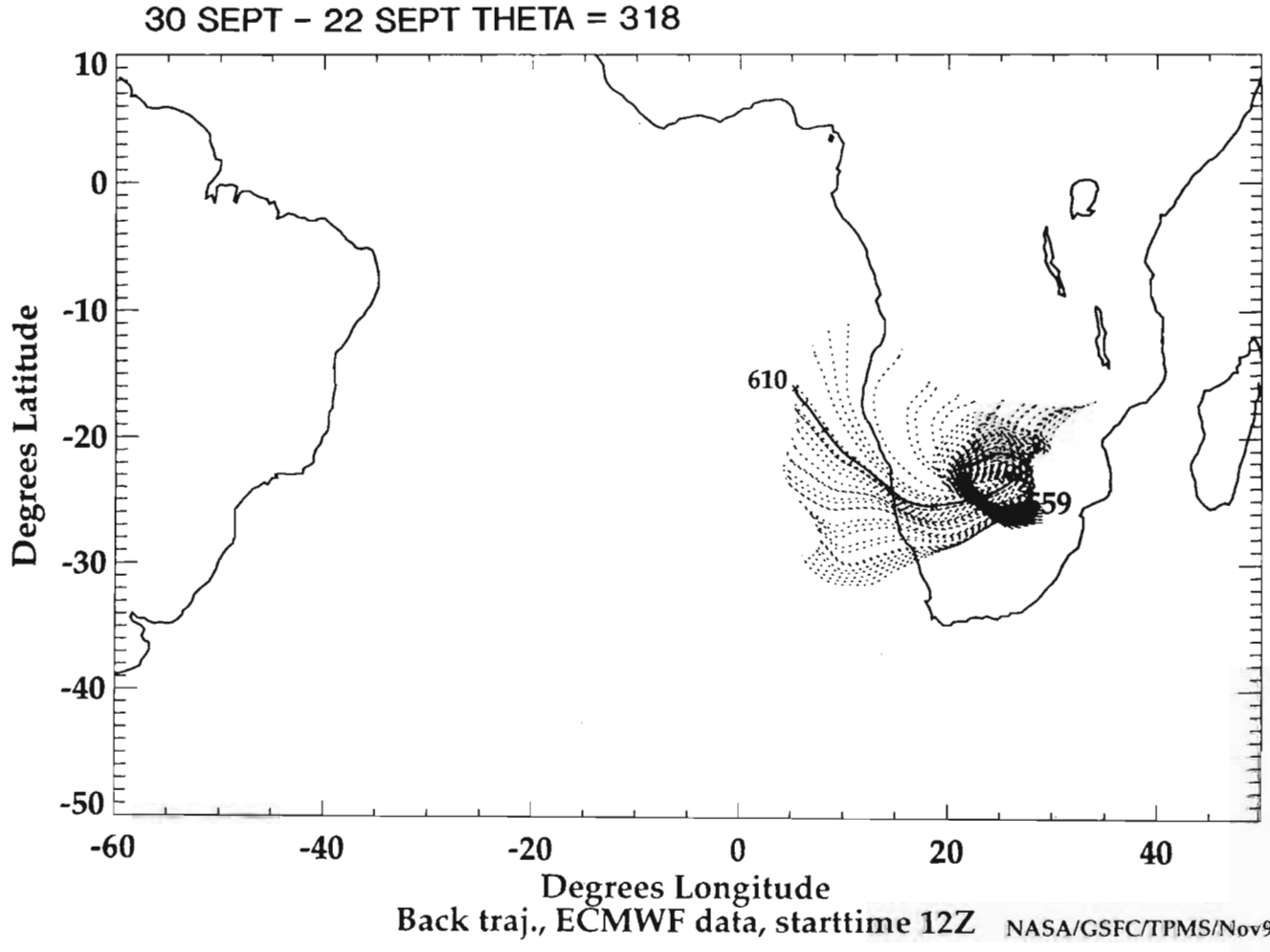

Back traj., ECMWF data, starttime 12Z NASA/GSFC/TPMS/Nov93

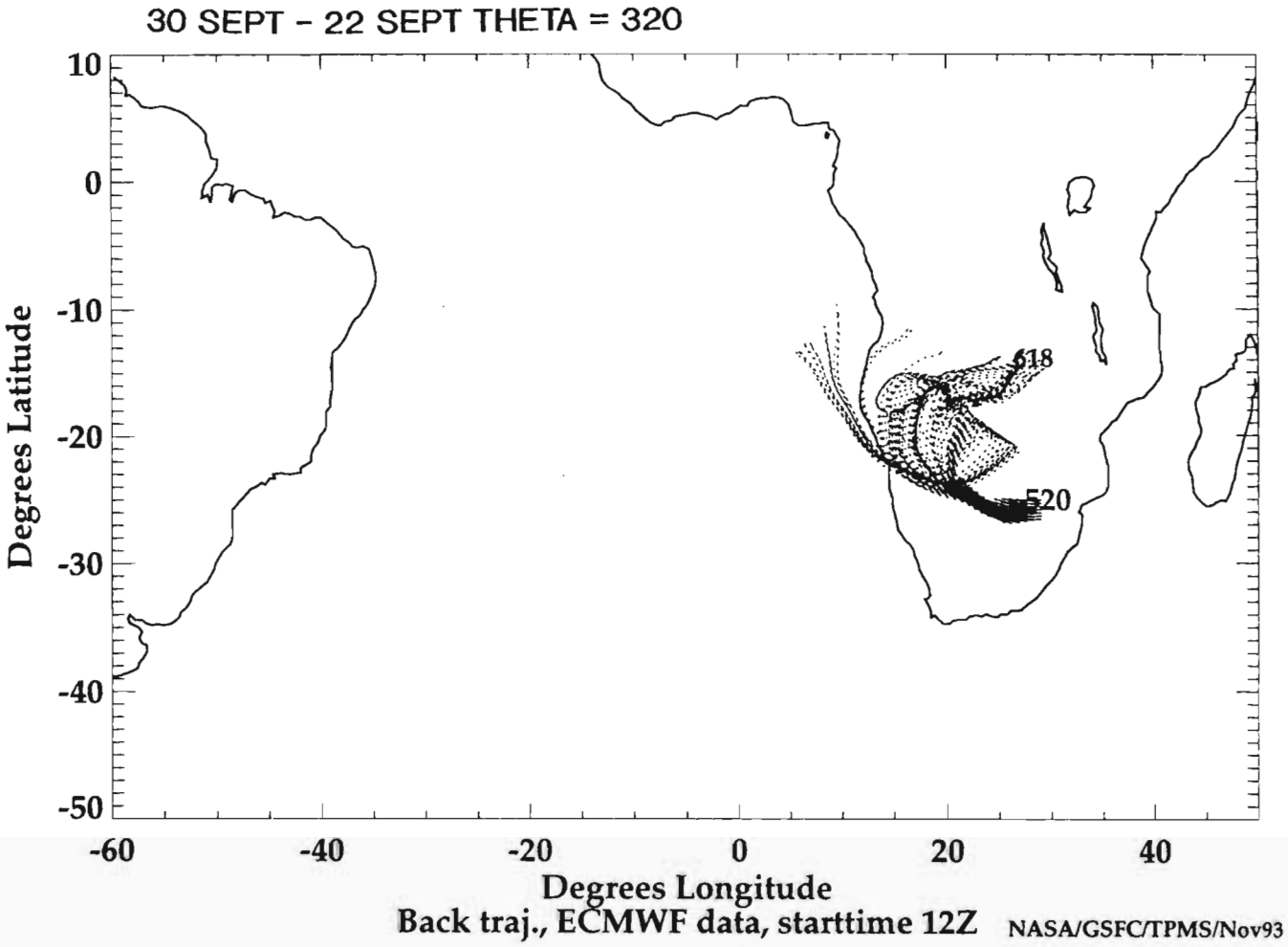
30 SEPT - 22 SEPT THETA = 320
10
0
-10
-20
-30
-40
-50
Degrees Latitude
-60
-40
-20
0
20
40
Degrees Longitude
618
520
Back traj., ECMWF data, starttime 12Z
NASA/GSFC/TPMS/Nov93

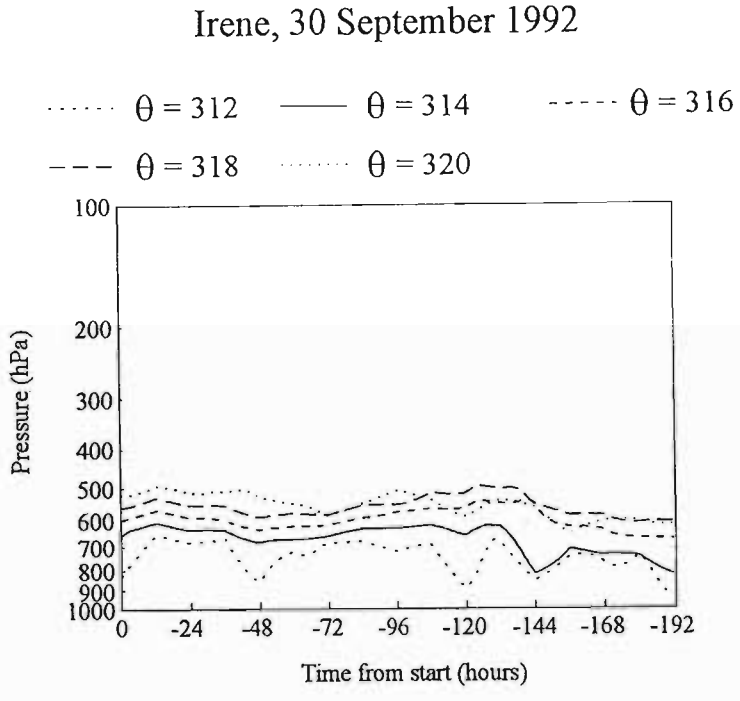

Figure 4.38 Time-pressure plot of the middle-point eight day back trajectories on 312, 314, 316, 318 and 320 K isentropic surfaces, from Irene, for the period 30 to 22 September 1992. Pressure is given as a log scale (hPa) and time is in 24 hour intervals. The start time is denoted by 0 hours and the end time -192 hours. Source NASA/GSFC.

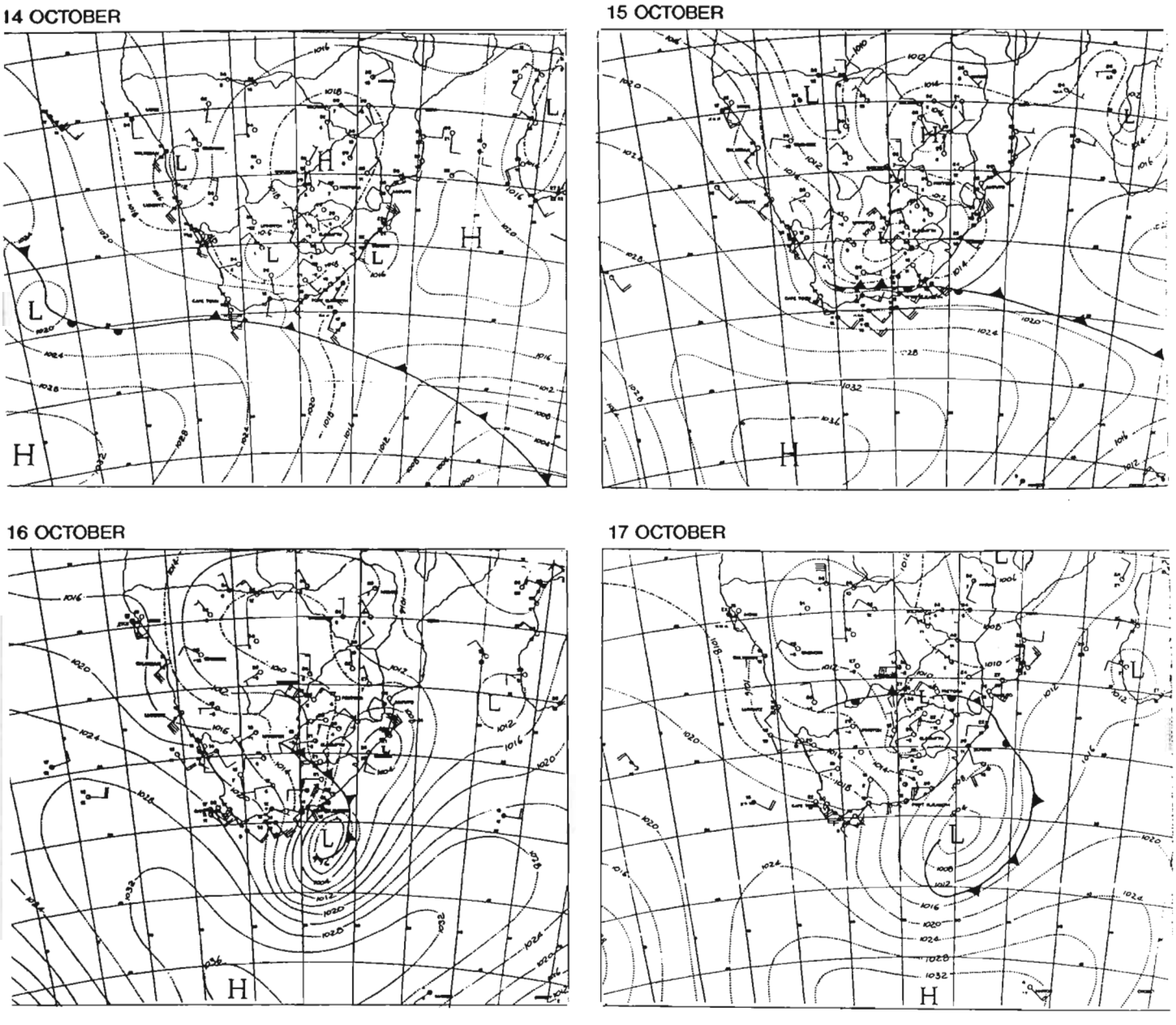

Figure 4.39 Surface synoptic charts over southern Africa for 14 to 22 October 1992. Isobars (hPa) denoted by light lines. From Daily Weather Bulletin (SAWB).

18 OCTOBER

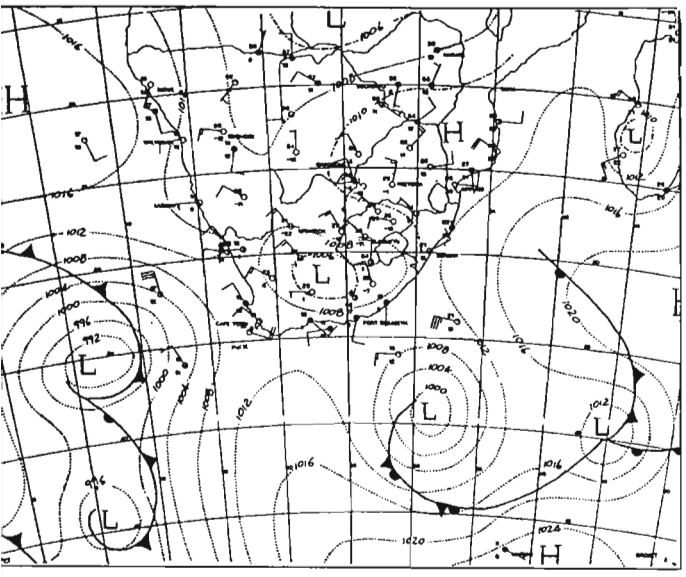

19 OCTOBER

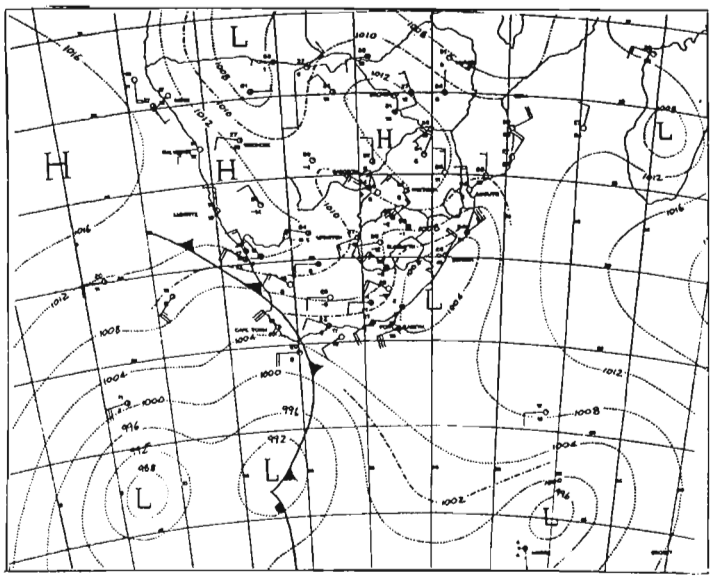

20 OCTOBER

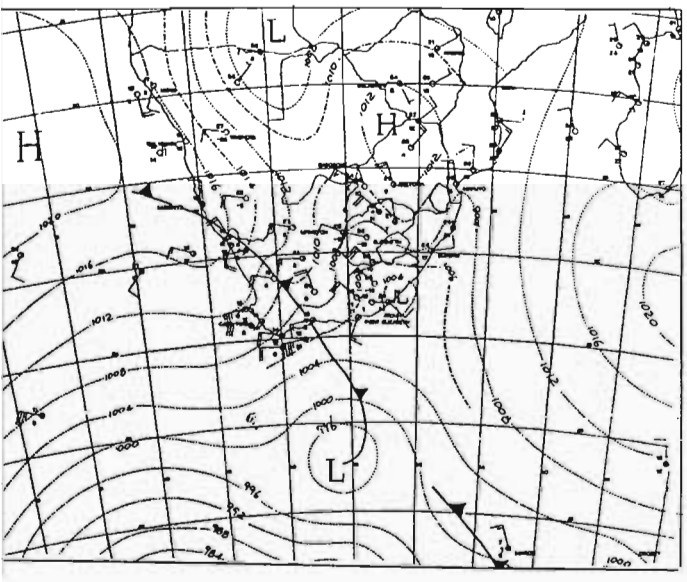

21 OCTOBER

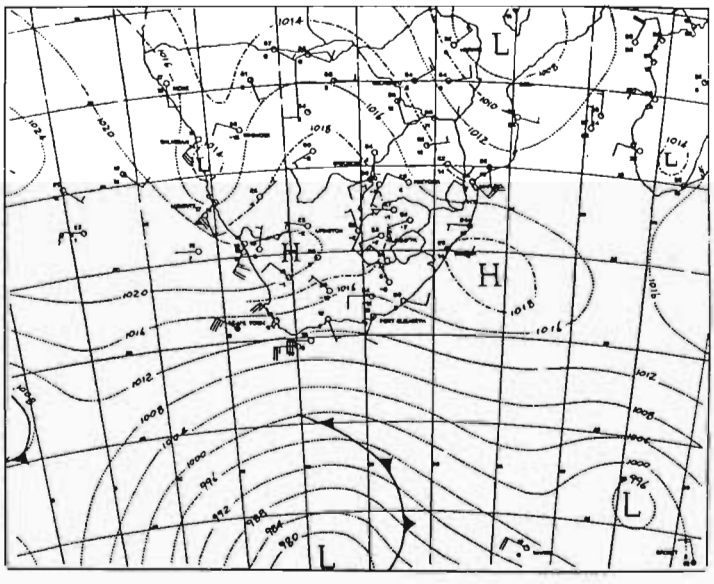

22 OCTOBER

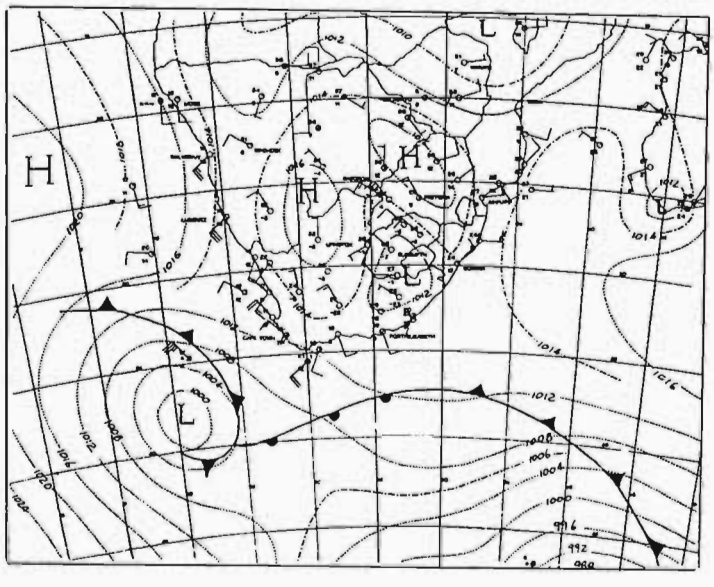

October and moved over Irene on 17 October. Thereafter, high pressure circulation was dominant over the land. The disturbance in the westerly flow is clearly evident in the 700 hPa (Fig. 4.40) and 300 hPa (Fig. 4.41) synoptic charts between 14 and 17 October. The influence of the 700 hPa westerly wave extends to approximately 20°S over the land. Strong westerly flow (Fig. 4.42) is prominent over the southern parts and is also evident at the 300 hPa isobaric level (not shown here). Light (< 20 m s^{-1}) easterly winds prevail north of 25°S during this period.

In terms of ozone, it is expected that the influence of the westerly trough, on the vertical distribution of ozone, would be greater at Irene, due to its more southerly location and close proximity to the region dominated by westerly flow. Six ozonesonde launches were conducted at Irene between 14 and 22 October and are shown in Figure 4.43. On all days, except 18 October, ozone mixing ratio profiles show a general increase from the surface to 12 km (asl). Ozone values range between 40 and 60 ppbv below approximately 9 km and are consistently greater than 60 ppbv between 9 and 12 km. On 18 October, however, ozone mixing ratios are significantly reduced throughout the troposphere, below 9 km. The lower ozone values are clearly evident in Figure 4.44, which depicts the difference between the ozone profile on 18 October and the mean ozone profile (Diab *et al.*, 1996a) for the SAFARI period. The greatest depletion occurs in mid-troposphere (~ 5-9 km (asl)) where ozone is reduced to approximately 30 ppbv within this layer. The sudden drying of the atmosphere indicated by the changes in RH, in the mid- and lower troposphere (~ 3 - 7 km), from 17 to 18 October (Fig. 4.45), suggests a change in the weather conditions. Indeed, the westerly trough passed over Irene on 17 October and had moved off to the east by 18 October.

Figure 4.46 shows eight day back trajectories from Irene, between 14 and 22 October 1992, along the 314, 316, 318 and 320 K isentropic surfaces. The dominance of anticyclonic circulation, in the lower troposphere, is clearly evident by the curved anticyclonic flow exhibited by the trajectories. Figure 4.47 depicts the altitude of the middle-point trajectories along the 314, 316, 318 and 320 K isentropic surfaces. The trajectories are confined between the surface and approximately 5 km and show no evidence of the westerly disturbance.

It is contended that the passage of the westerly trough, accompanied by an increase in atmospheric moisture on 17 October, contributed to the drastic mid-tropospheric ozone depletion observed on that day. The influence of the westerly disturbance was confined below approximately 9 km, and which did not appear to affect the elevated enhanced ozone layer (9 - 12 km (asl)).

14 October

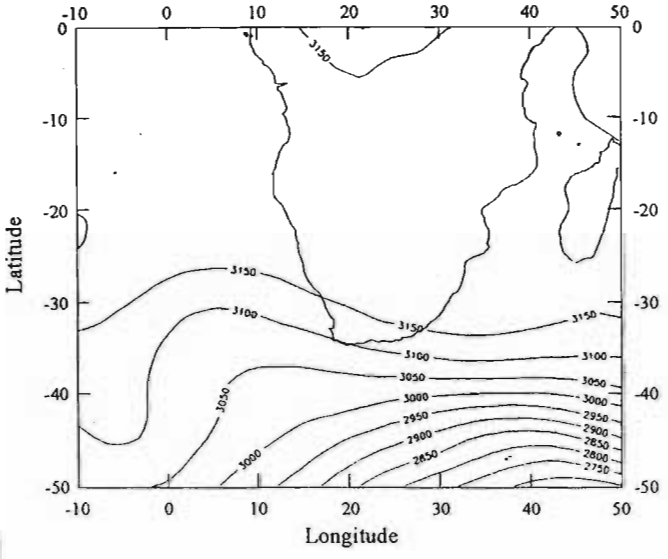

15 October

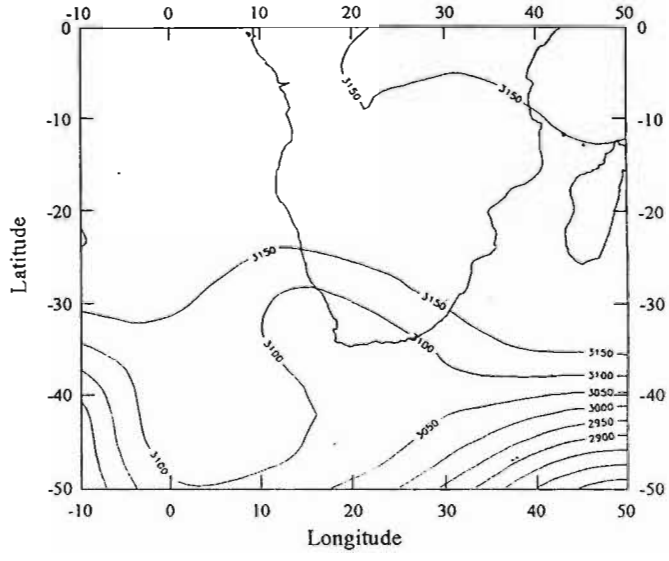

16 October

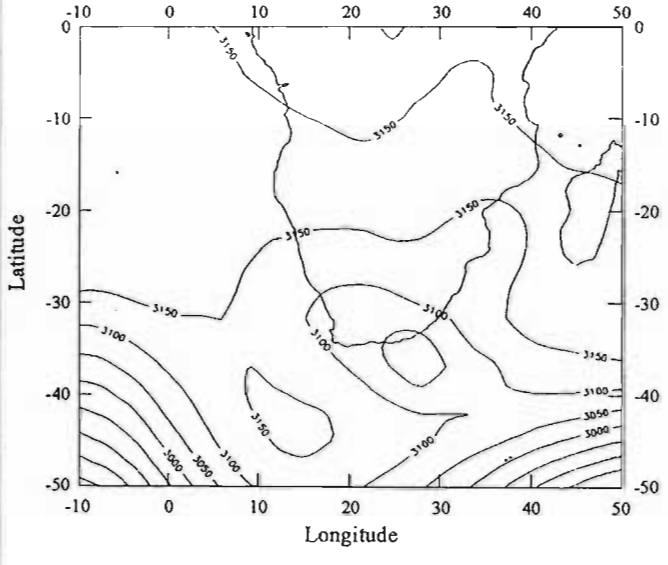

17 October

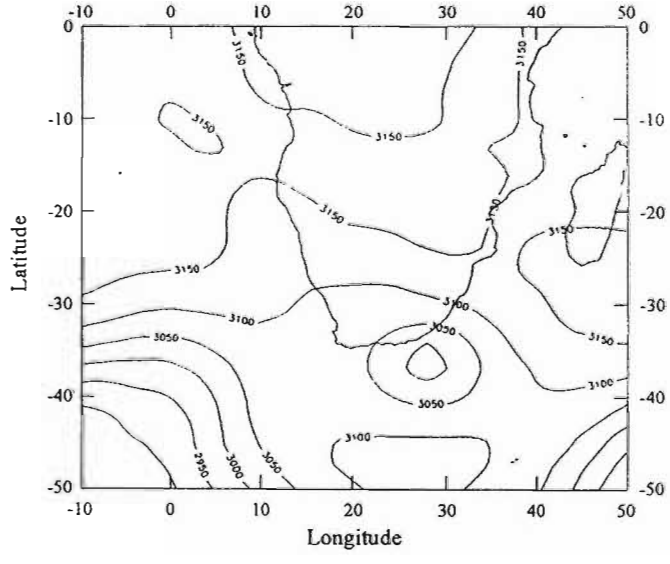

Figure 4.40 700 hPa synoptic charts over southern Africa for 14 to 17 October 1992. Prepared from ECMWF data.

14 October

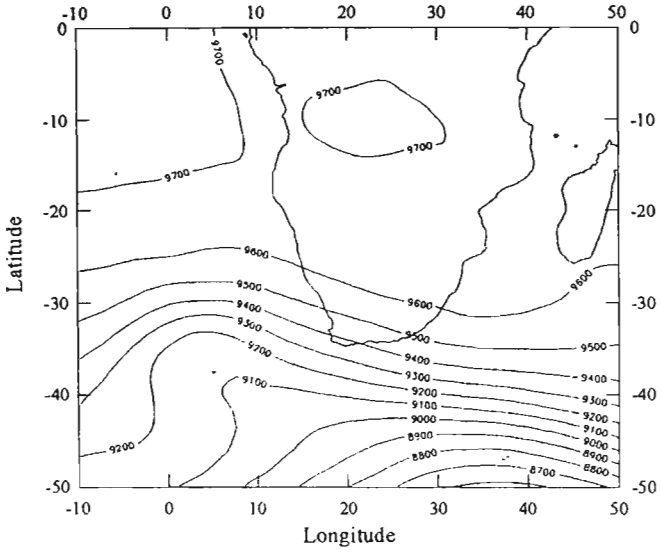

15 October

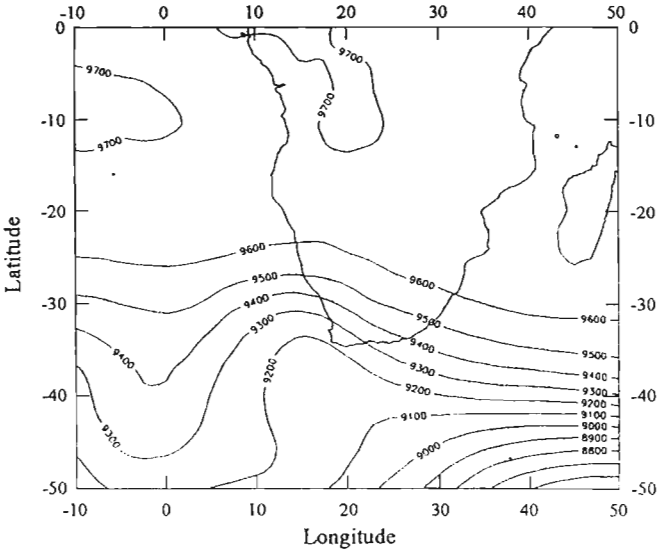

16 October

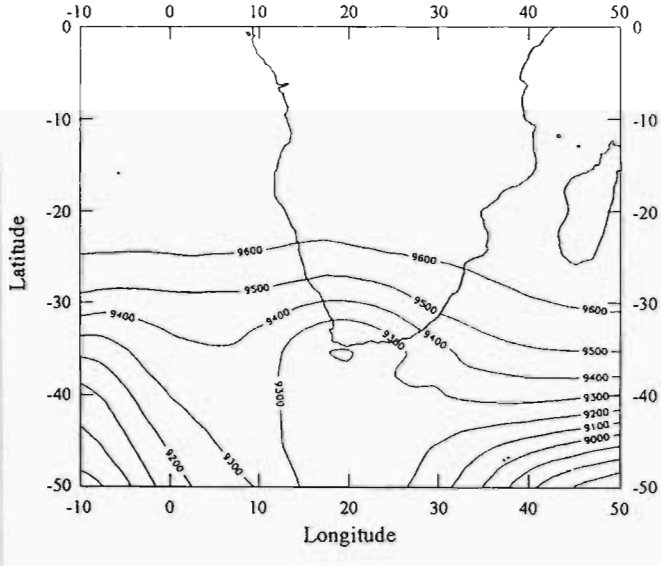

17 October

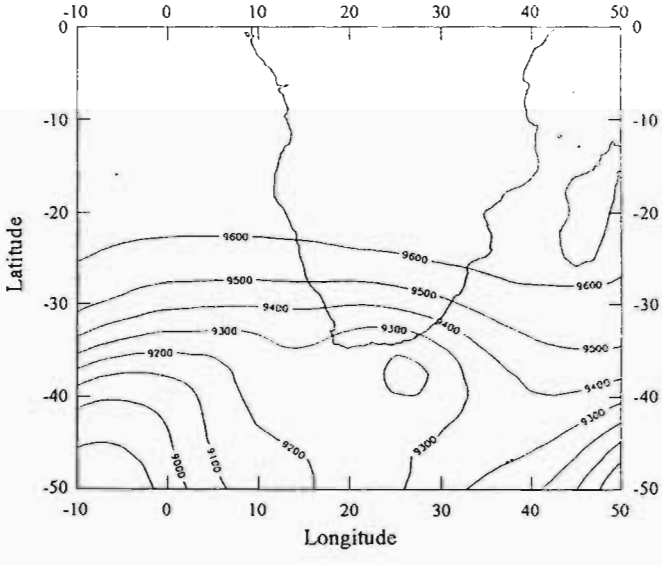

Figure 4.41 300 hPa synoptic charts over southern Africa for 14 to 17 October 1992. Prepared from ECMWF data.

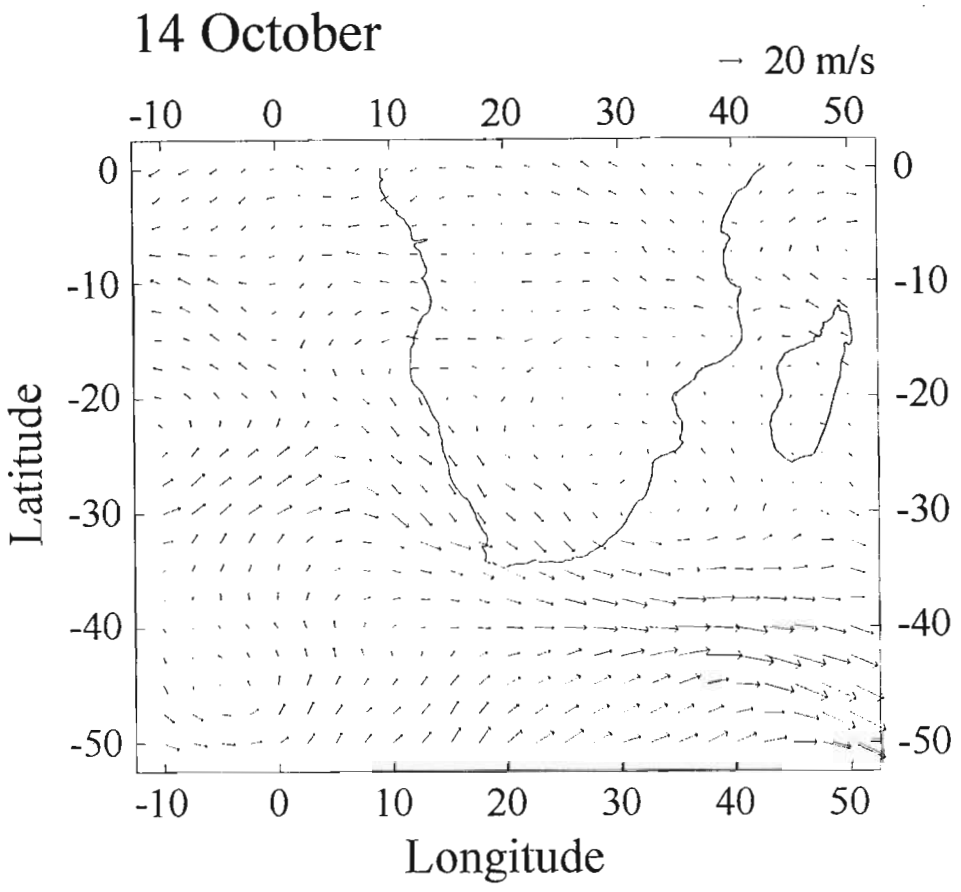

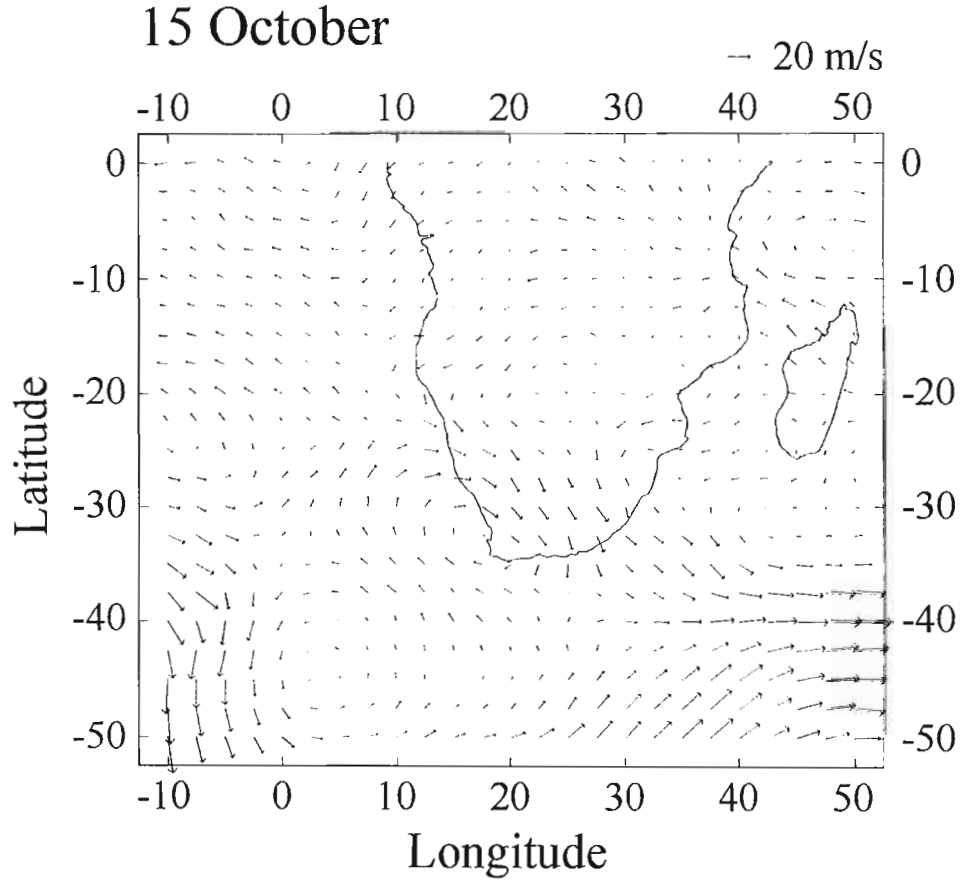

Figure 4.42 700 hPa wind vectors over southern Africa, derived from ECMWF u and v wind components, for 14 to 17 October 1992.

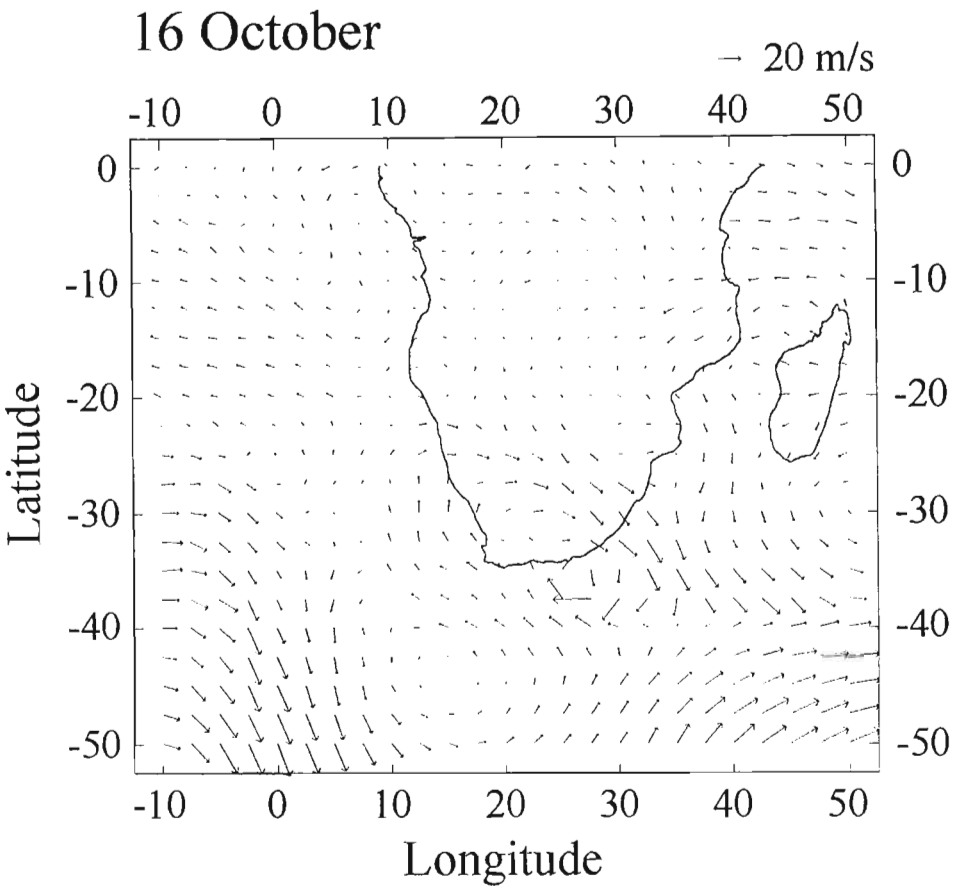
16 October
20 m/s
-10 0 10 20 30 40 50
0 -10 -20 -30 -40 -50
Latitude
Longitude

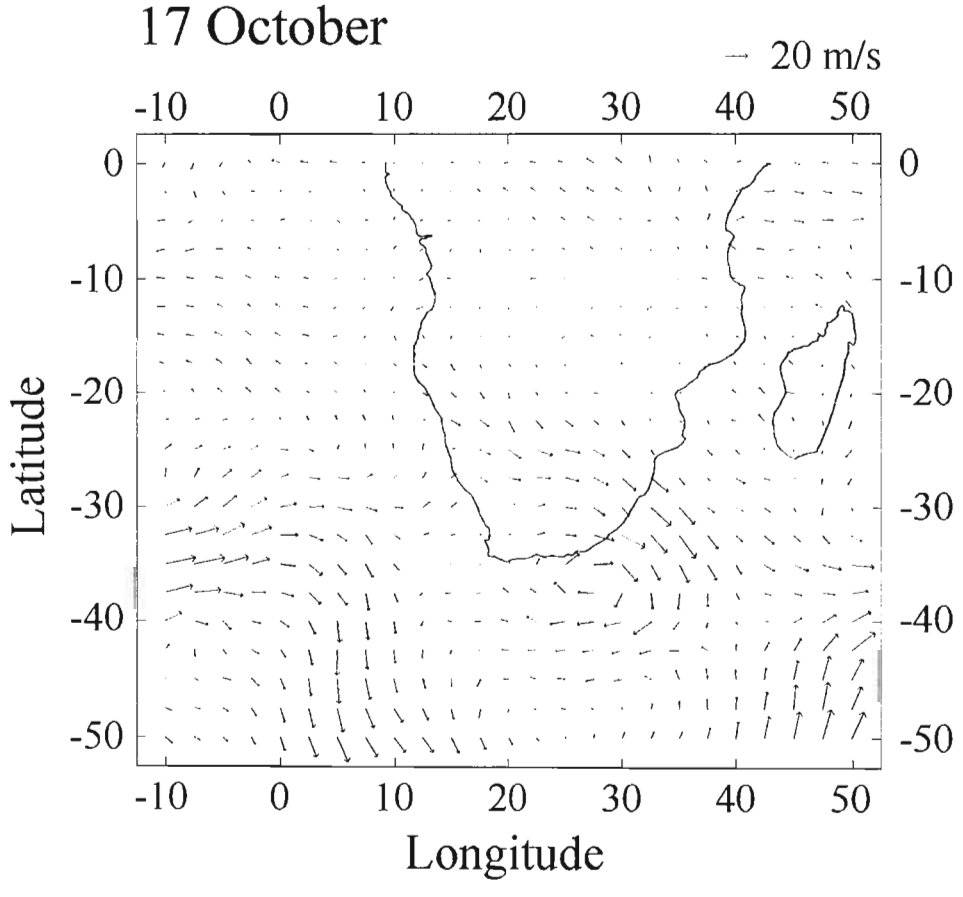
17 October
20 m/s
-10 0 10 20 30 40 50
0 -10 -20 -30 -40 -50
Latitude
Longitude

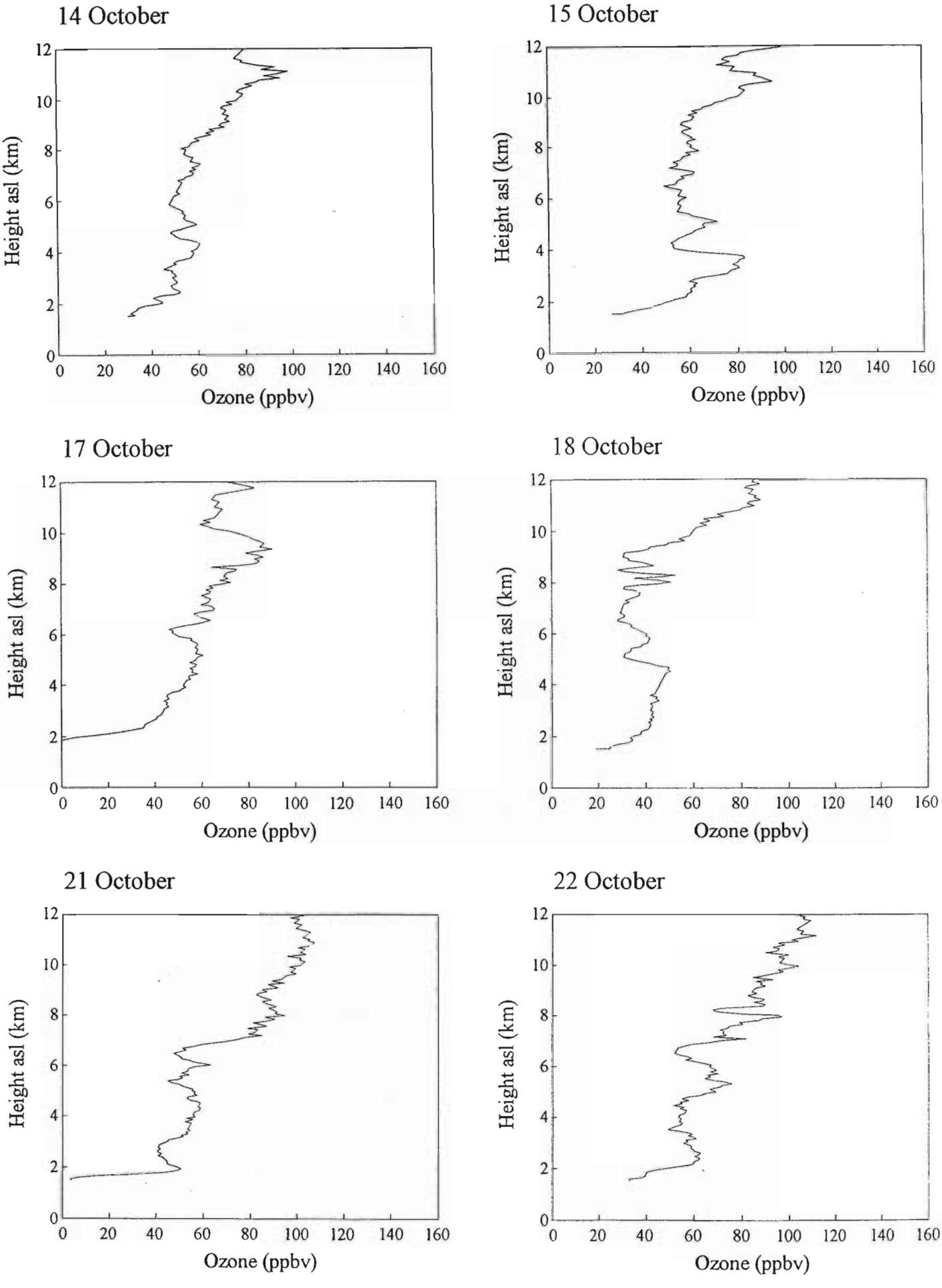

Figure 4.43 Ozonesonde mixing ratio profiles (ppbv) between 0 and 12 km (asl), at Irene during for 14, 15, 17, 18, 21 and 22 October 1992. Data from the SAWB.

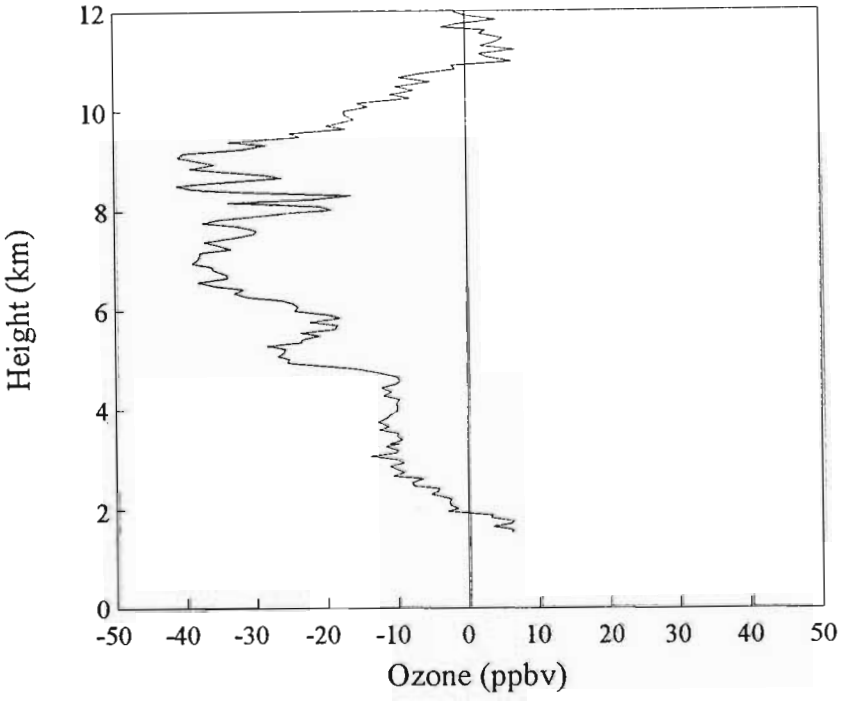

Figure 4.44 The difference between the ozone mixing ratio (ppbv) profile on 18 October, and the mean profile, at Irene, for the SAFARI period. Data from the SAWB.

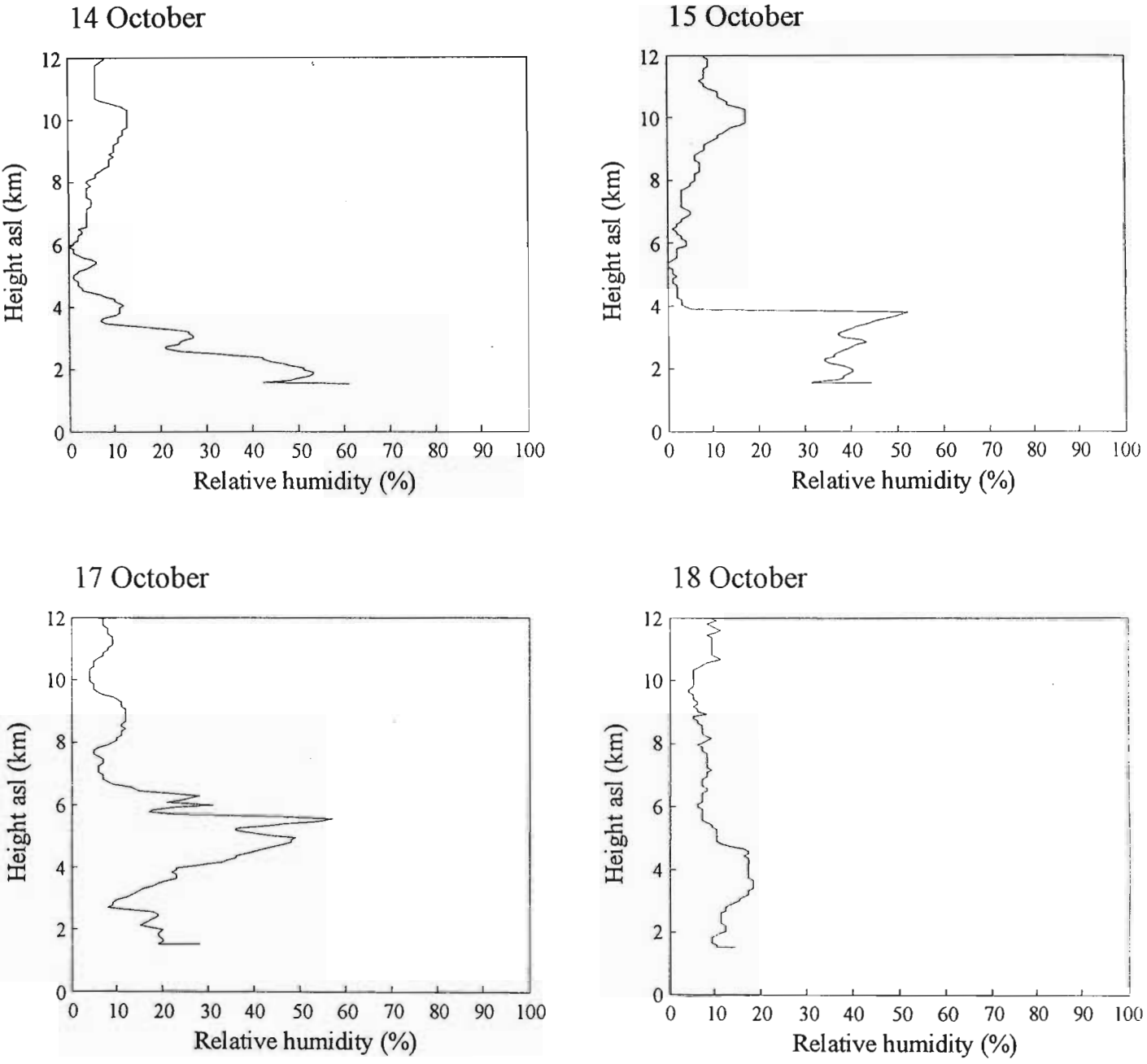

Figure 4.45 Relative humidity (%) profiles between 0 and 12 km (asl), at Irene, for 14, 15, 17 and 18 October 1992 (Data from the SAWB).

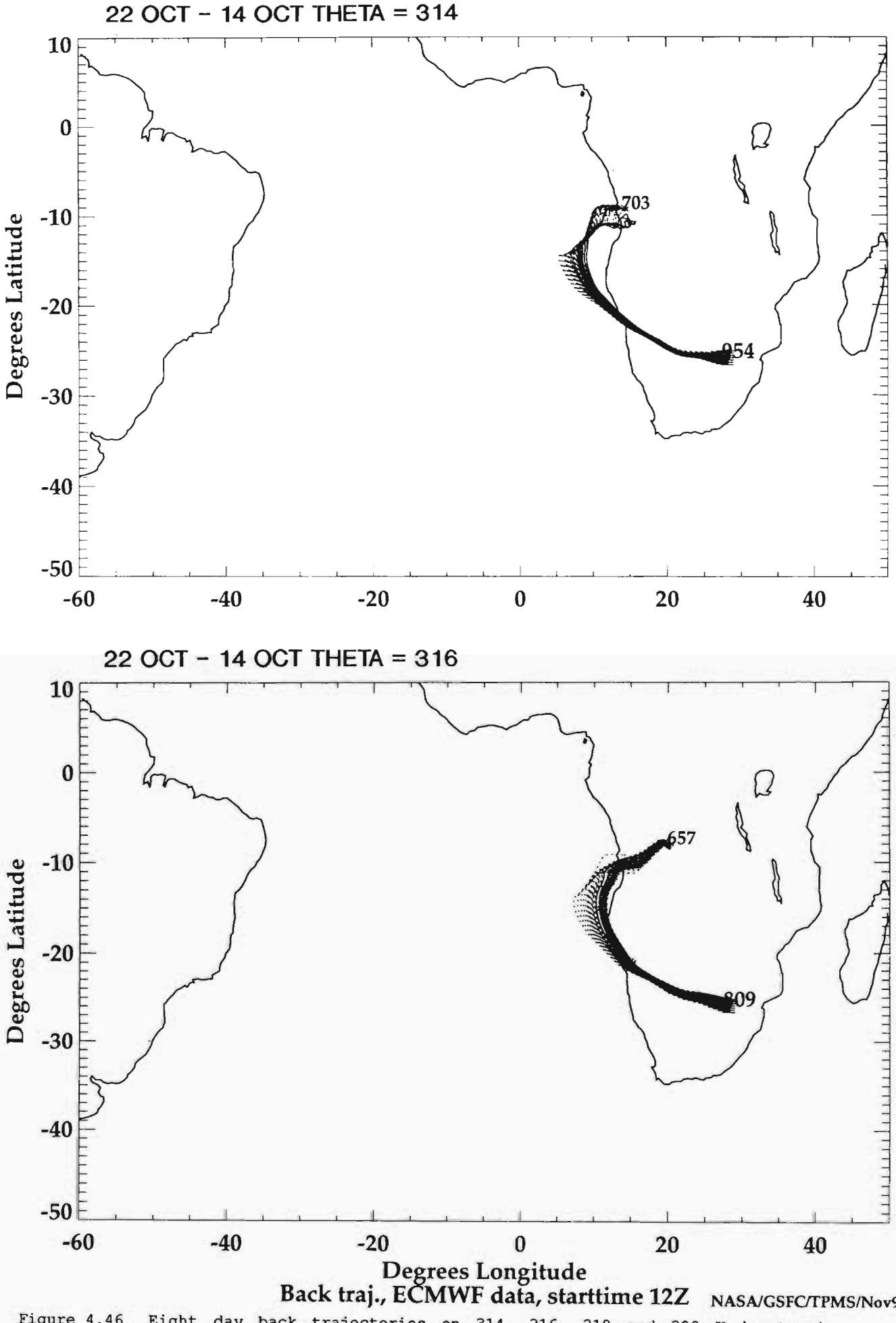

Figure 4.46 Eight day back trajectories on 314, 316, 318 and 320 K isentropic surfaces, from Irene, for the period 22 to 14 October 1992. Start time was 12 Z. The trajectory originating from the central point of the array is given as a solid line. Start pressure (hPa) is denoted by large type and end pressure by smaller type. Source NASA/GSFC.

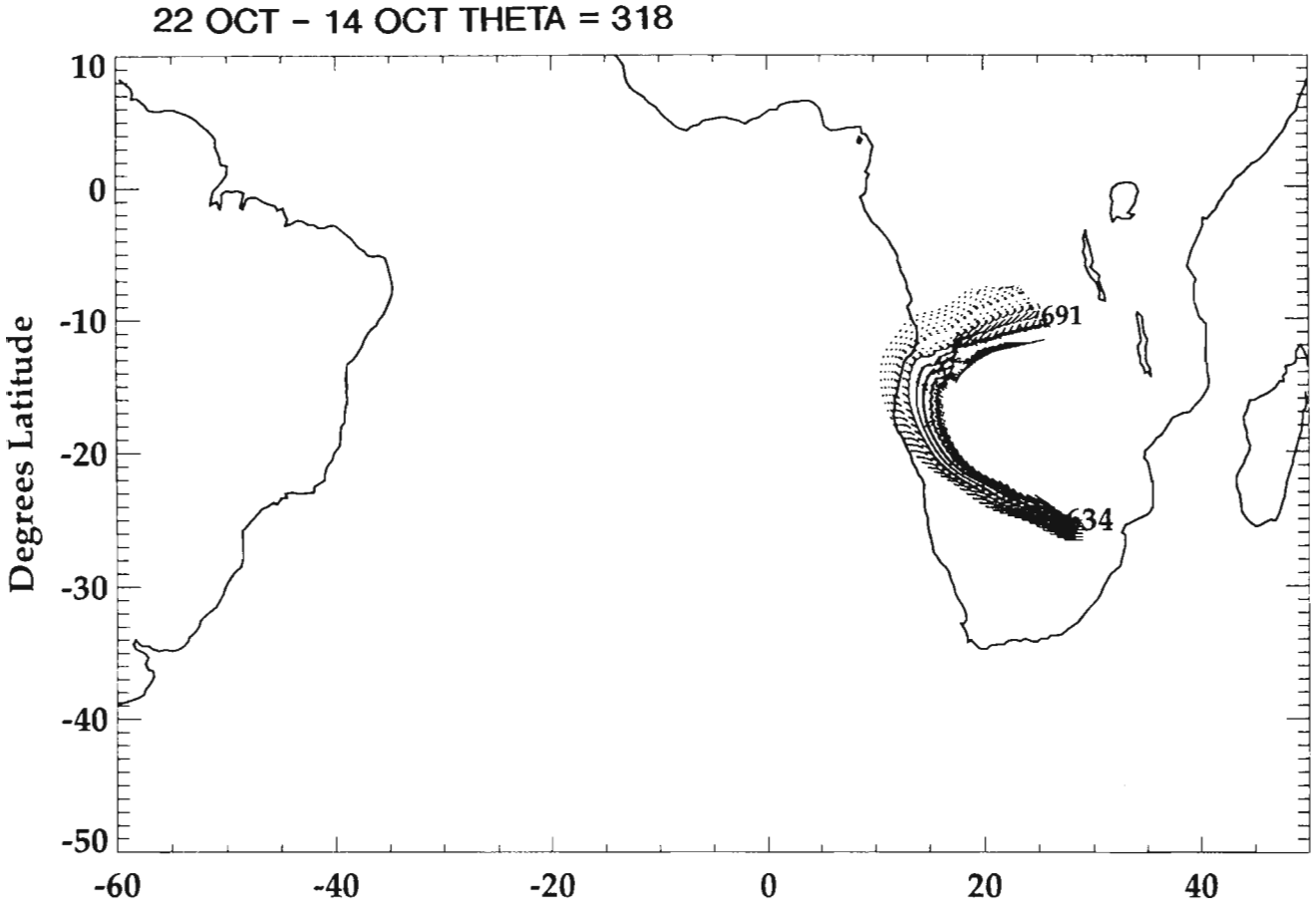
22 OCT - 14 OCT THETA = 318
10
0
-10
-20
-30
-40
-50
Degrees Latitude
691
634
-60
-40
-20
0
20
40

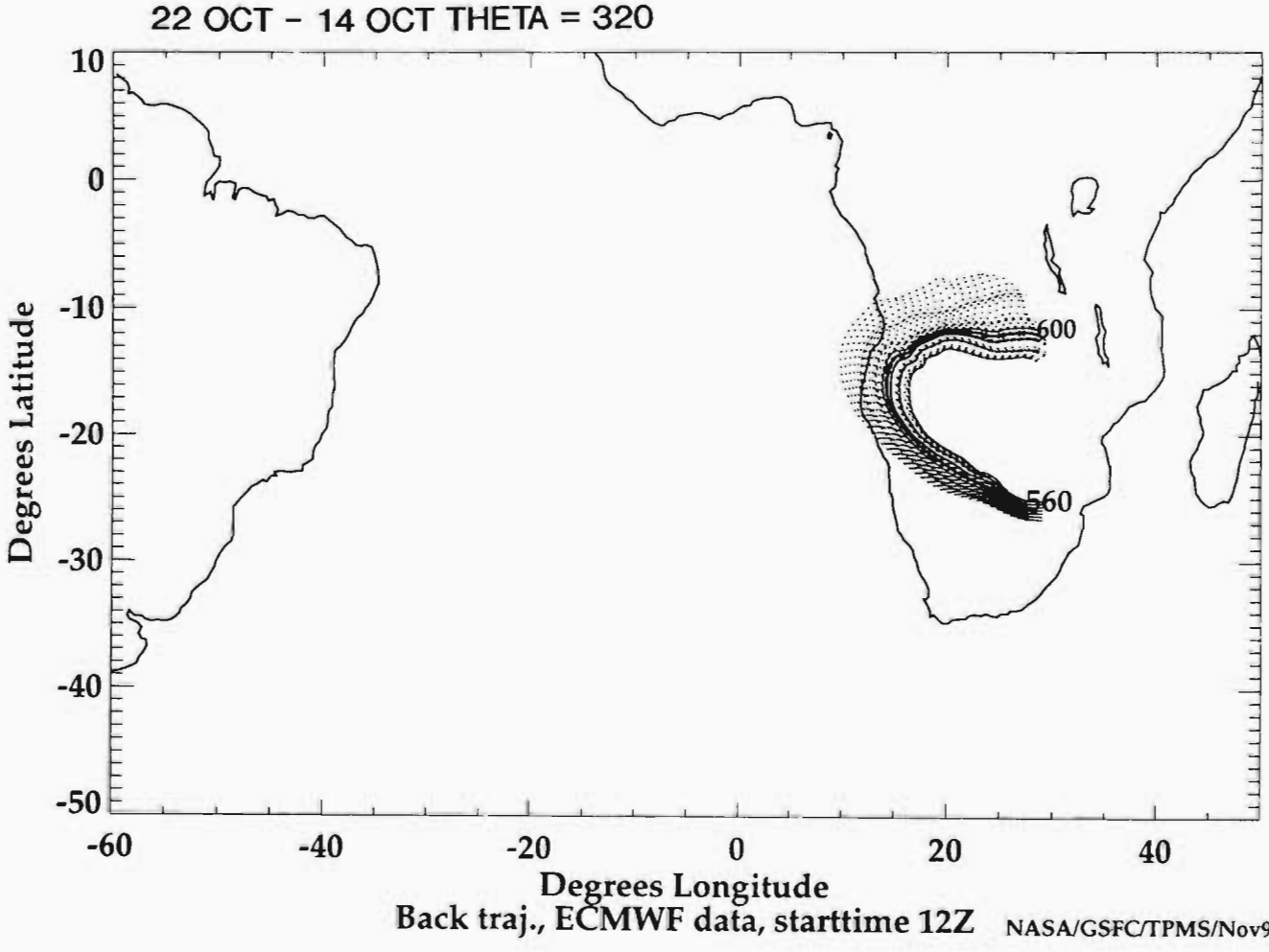
22 OCT - 14 OCT THETA = 320
10
0
-10
-20
-30
-40
-50
Degrees Latitude
600
560
-60
-40
-20
0
20
40
Degrees Longitude
Back traj., ECMWF data, starttime 12Z
NASA/GSFC/TPMS/Nov93

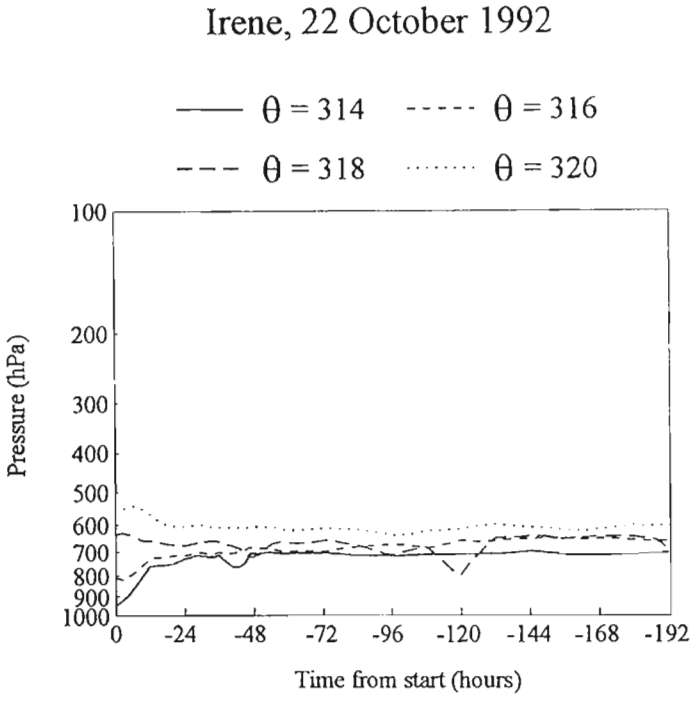

Figure 4.47 Time-pressure plots of the middle-point eight day back trajectories on 314, 316, 318 and 320 K isentropic surfaces, from Irene, for the period 22 to 14 October 1992. Pressure is given as a log scale (hPa) and time is in 24 hour intervals. The start time is denoted by 0 hours and the end time -192 hours. Source NASA/GSFC.

4.4.3.4 Summary

The anticyclonic case study at Okaukuejo, supports the conclusions of the composite analysis. Generally, there is a steady increase in ozone from the surface to approximately 9 km above which is an elevated enhanced layer (> 80 ppbv). At Irene, the ozone profile is similar. The presence of an elevated (> 9 km) enhanced layer (~ 80 ppbv) was confirmed at both stations. It is contended that the observed stable conditions and transport of air within the continental anticyclone coupled with the abundance of ozone and ozone precursors originating from central African fires and urban/industrial emissions, in the vicinity of Irene, support ozone enhancement in the mid- and upper troposphere.

The westerly trough case study, at Okaukuejo, supports the presence of a mid-tropospheric ozone minimum described in the composite analysis. A mid-tropospheric minimum was observed at Irene during the passage of a westerly trough. The elevated enhanced ozone layer was present at both stations, irrespective of the change in synoptic flow.

By way of contrast, the influence of tropical circulation on the vertical distribution of ozone is explored next.

4.4.3.5 Brazzaville

The equatorial location of the ground station at Brazzaville provided an opportunity to study atmospheric dynamics, transport and chemistry in the tropics during the SAFARI period. Brazzaville is situated in the tropical low latitudes, where atmospheric circulation is dominated by the Hadley Cell (Preston-Whyte and Tyson, 1988). Tropospheric circulation is controlled by the position of the ITCZ and the local weather patterns which depend on the thermodynamic structure of the atmosphere (Cros *et al.*, 1987). The ascending limb of the Hadley Cell, coupled with high solar radiation and strong surface heating, encourage the formation of deep convective systems. Intense vertical motion, in convective cells, transports air from the lower layers to the upper troposphere and on occasions into the stratosphere. Circulation over the Congo is dominated by southwesterly flow, originating in the South Atlantic anticyclone, in the lower layers (0-2 km) and easterly flow aloft (Cros *et al.*, 1987). With this background in mind, an analysis of the ozone soundings at Brazzaville during the SAFARI period is presented. In terms of ozone, it is expected that convective activity as described above, will yield enhanced ozone levels in the mid- to upper troposphere in response to rapid vertical transport of ozone and precursors, from the PBL. In addition, as a result of

chemical dilution (Pickering *et al.*, 1992c) and additional NO_x created by lightning (Pickering *et al.*, 1990), further ozone formation reactions are anticipated during convective activity.

A time-height cross section of ozone mixing ratios (ppbv), constructed from ozonesonde profiles at Brazzaville for the SAFARI period, is depicted in Figure 4.48. Ozone levels are constantly below 100 ppbv throughout the troposphere except on 21 September when a region of high ozone occurs in the upper troposphere. The 100 ppbv isoline marks the base of the enhanced layer at approximately 10 km (asl) with a maximum (200 ppbv) occurring at between approximately 12 and 14 km. A similar enhancement, though of smaller magnitude, was observed six days later at Ascension Island (Fig. 4.48) which lies to the west of Brazzaville, suggesting that this is an anomaly associated with easterly winds.

The magnitude of the upper tropospheric enhancement was estimated by subtracting the mean profile for the entire period from the 21 September data. The result is presented in Figure 4.49. It is clear that the ozone enhancement in the upper troposphere (11-13 km) is anomalous for the period. This is shown too, by the integrated tropospheric ozone values calculated from the ozone profiles, which are presented in Figure 4.50. Values peak at approximately 60 DU on 21 September. It is recognised that the increased ozone, in the upper troposphere, on 21 September is a product of one sounding only. However, no peculiarities were recorded regarding the data collected on that day. The anomaly is treated, therefore, as a true upper tropospheric ozone enhancement.

Indeed, TOMS total column ozone values at Brazzaville over this period support the presence of an anomaly. Values increase from 280 DU on 17 September to a maximum of 298 DU on 21 September, and decrease sharply to 288 DU on 22 September.

A time-height cross section of the vertical motion field (ω), at Brazzaville, during the SAFARI period, is given in Figure 4.51. Subsiding motion, with cores that exceed 15 Pa s^{-1}, dominates the mid- and upper troposphere (2-16 km) throughout the period. An exception is the period immediately prior to 21 September. A narrow core of ascending motion, occurs between 17 and 20 September at Brazzaville, and extends upwards to the stratosphere (> 16 km). Upward motion is strongest between the surface and approximately 4 km (-15 Pa s^{-1}) and considerably weaker in the upper troposphere (0 to -5 Pa s^{-1}) on those days. On previous and subsequent days, pockets of upward motion occur near the surface extending upwards to approximately 2 to 3 km (asl). It is expected that the upward motion depicted in Figure 4.51 represents convective activity at Brazzaville, which was particularly well developed between 17 and 20

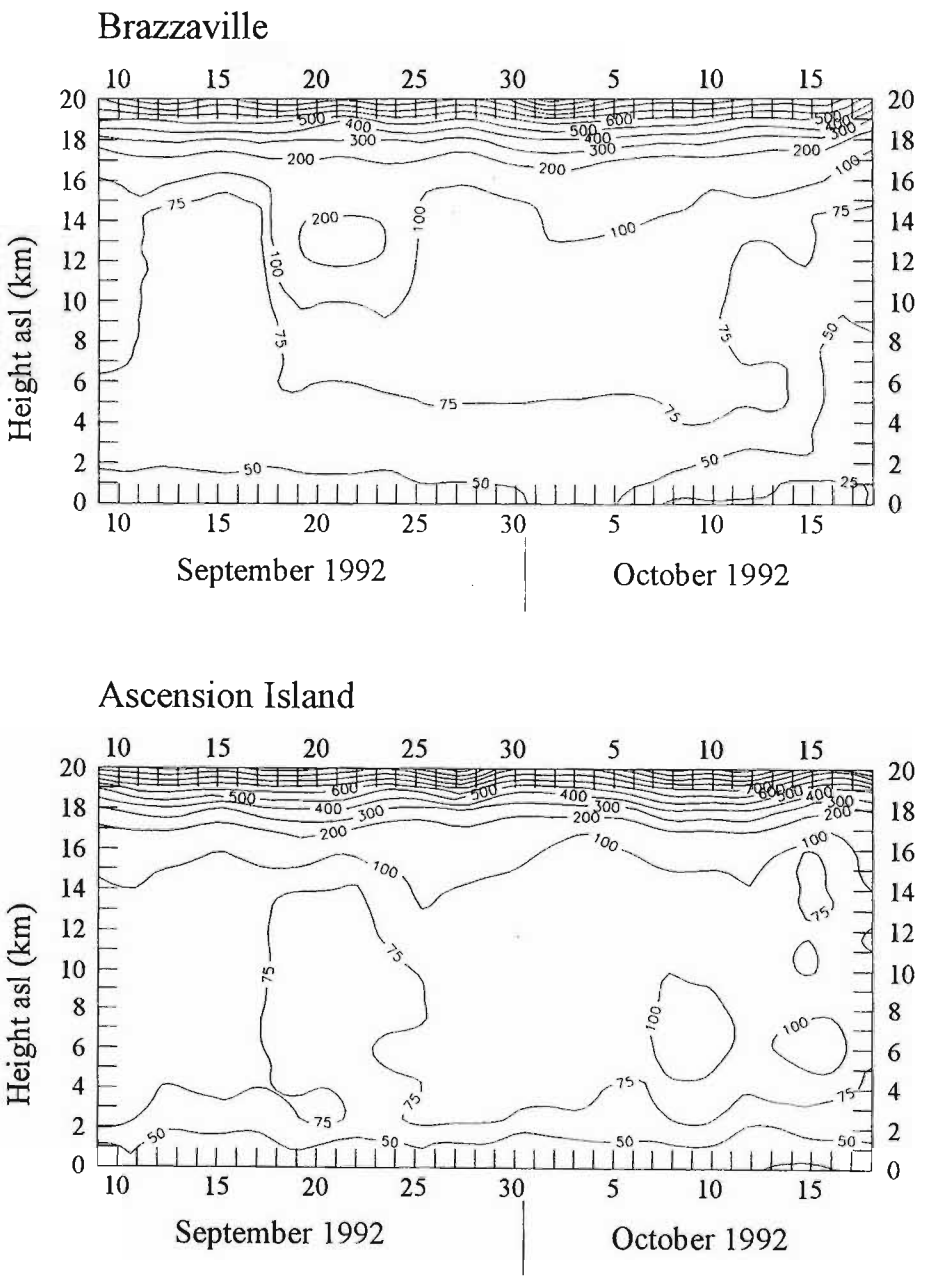

Figure 4.48 Time-height cross section of ozone (ppbv) derived from Brazzaville (5°S) and Ascension Island (6.5°S) ozonesonde data during the SAFARI-92 period. Data from the SAWB. Ascent times for Brazzaville and Ascension Island were approximately 10 Z (12:00 local time) and 9 Z (11:00 local time) respectively. Ozone < 100 ppbv is depicted by 25 ppbv contours.

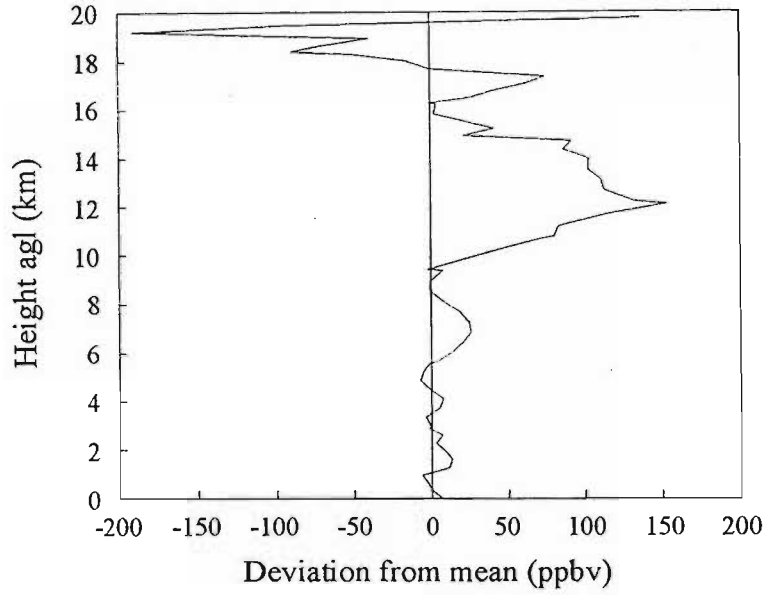

Figure 4.49 Difference between the mean ozonesonde profile (ppbv) during the SAFARI-92 period and the ozone profile for 21 September at Brazzaville.

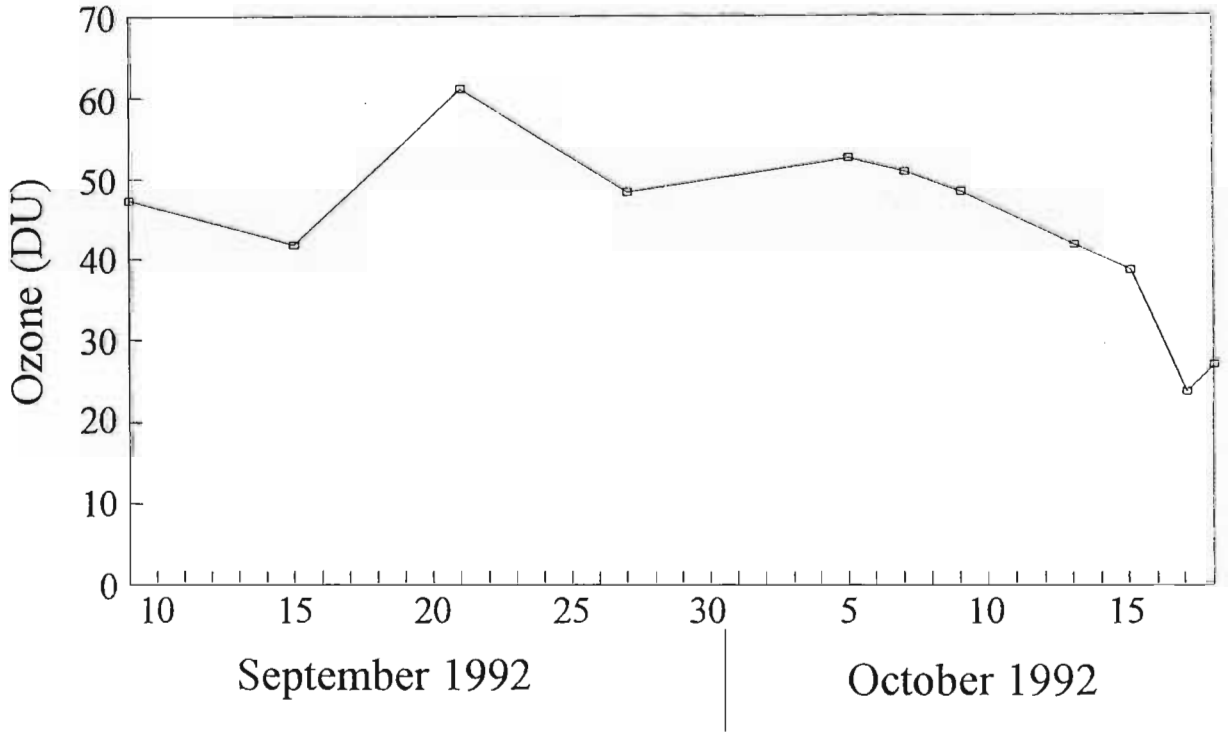

Figure 4.50 Integrated tropospheric ozone (DU), below 16 km, at Brazzaville during the SAFARI period. Prepared from ozonesonde profile data (NASA/Langley).

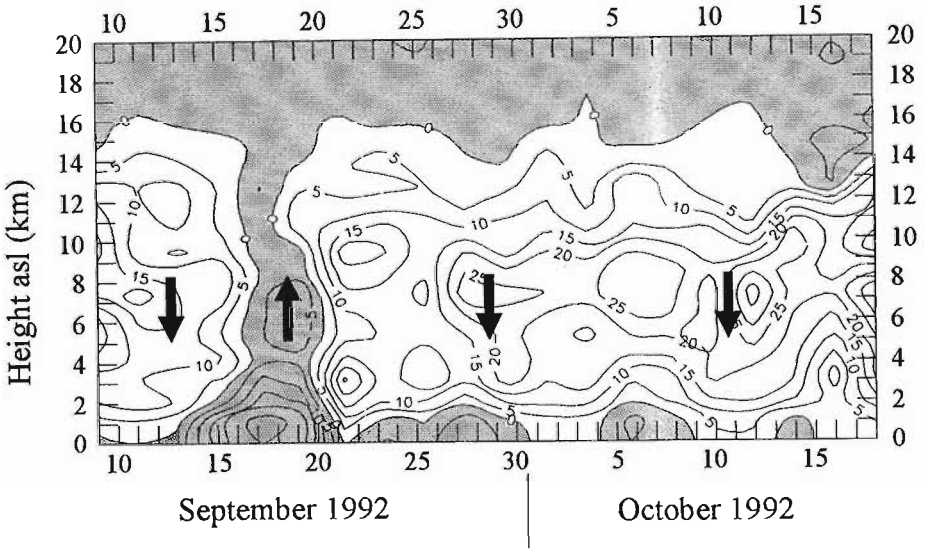

Figure 4.51 Time-height cross section of ω (Pa s^{-1}) at Brazzaville for the SAFARI-92 period. Prepared from ECMWF data. Shading represents upward motion (ω < 0).

September 1992. NOAA/AVHRR cloud images for the period 17 to 22 September, show substantial cloud cover in the vicinity of Brazzaville.

A time-height cross section of RH (%), constructed from ECMWF data, at Brazzaville for the SAFARI period is presented in Figure 4.52. A particularly noticeable feature is the layer of moist air (RH ≥ 70%) (~ 4-6 km (asl) and which persists from the 10 September through to 23 September. The vertical extent of the feature increased from 19 September onwards and was greatest on 21 September when it extended to approximately 10 km (asl). The buildup of moisture accompanied by strong surface heating, characteristic of tropical latitudes, promotes upward transport by convection (Preston-Whyte and Tyson, 1988). On 22 and 23 September, the vertical extent of the moist air was reduced and was absent thereafter. It is therefore contended that there is strong evidence for a convective role in the upper tropospheric ozone enhancement.

The possibility of the transport of ozone and ozone precursors from active fires during this period was considered. Northerly flow, in the vicinity of Brazzaville (Fig, 4.53), in the upper troposphere (300 hPa) on 21 September 1992 may have transported ozone and/or precursors from regions of biomass burning. In addition, the recirculation of air in the easterlies feeding into the South Atlantic westerly wave is particularly prominent in the upper air, on 21 September. The presence of moist air (high RH) and strong and prolonged surface heating, generates conditions favourable for triggering atmospheric instability and convective activity, which is evidenced by the cloud cover and strong upward motion. This provides a mechanism for the vertical transport of ozone near the surface into the upper troposphere. Once in the free troposphere, the lifetime of ozone is considerably lengthened, and may be transported long distances (Pickering *et al.*, 1990). In addition, the accumulation of pollution, as a result of stable conditions, followed by convective venting (a cook-then-mix scenario) and vertical dispersion as described by Chatfield and Delany (1990) may contribute to the observed upper tropospheric ozone enhancement. Lightning, within convective storms, may contribute additional NO_x into the atmosphere, which introduces a further factor in the generation of the upper tropospheric ozone enhancement (Pickering *et al.*, 1990; 1993).

4.4.3.6 Summary

In contrast to the case studies presented for Okaukuejo and Irene, the role of tropical circulation in the vertical distribution of ozone was demonstrated at Brazzaville. It is suggested that a convective event supported by strong upward motion, the presence of extensive cloud cover and moist air in the atmosphere, contributed to the high ozone levels observed in the upper

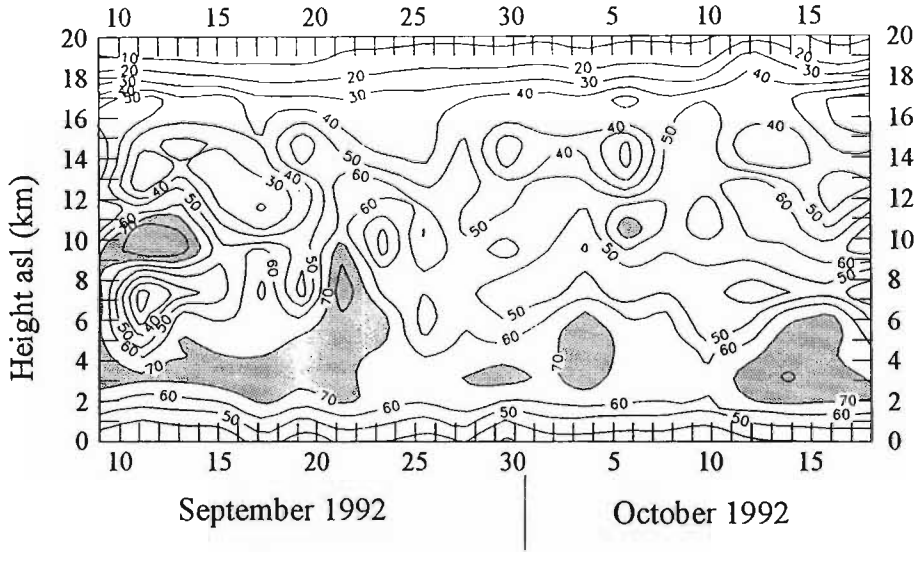

Figure 4.52 Time-height cross section of RH (%) derived from Brazzaville radiosonde data during the SAFARI-92 period. Shading represents RH > 70%.

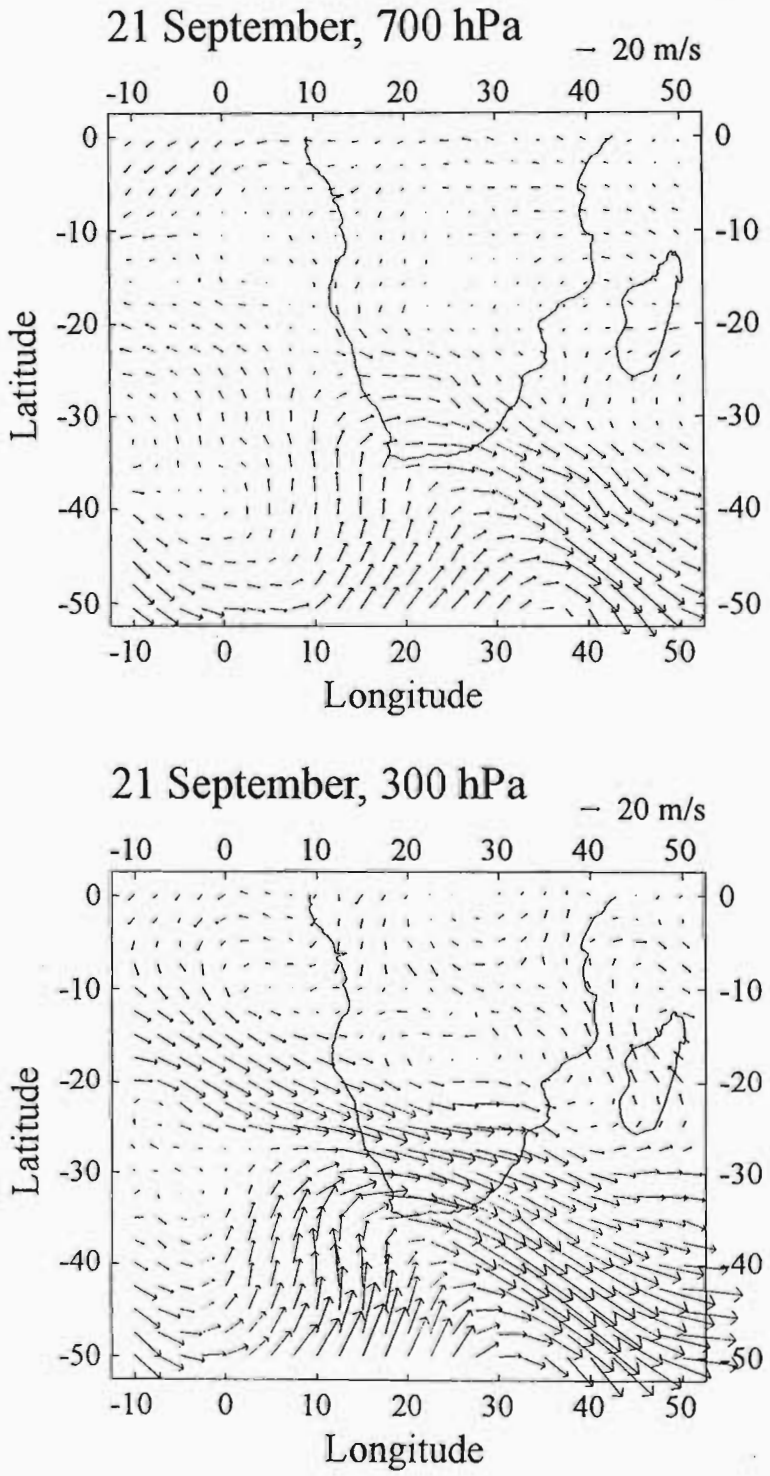

Figure 4.53 700 and 300 hPa wind vectors, over southern Africa, for 21 September 1992. Prepared from ECMWF data.

troposphere, on 21 September, at Brazzaville. The ozone enhancement is supported by TOMS total column ozone values at Brazzaville. Further, convective uplift and subsequent dilution of pollutants, away from the PBL, is known to enhance ozone formation (Chatfield and Delany, 1990; Pickering *et al.*, 1993; among others).

4.5 Summary of main points

It has been shown that there is a generally poor but negative relationship between total ozone and weather parameters as expressed by the heights of the 500, 300 and 100 hPa geopotential surfaces over southern Africa. The relationship was best expressed in association with the passage of a mid-latitude cyclone. A weaker relationship was noted for anticyclonic circulation patterns. A case study of a subtropical anticyclone revealed no dynamical link between the stratosphere and troposphere, as expressed by PV, and substantiated the weak statistical relationship found. On the other hand, it is suggested that the stronger statistical relationship, associated with the passage of a mid-latitude cyclone, is explained by a dynamic link between the stratosphere and troposphere. This relationship is examined in the following Chapters.

The relationship between ozone and anticyclonic circulation and the passage of westerly troughs was examined further at Okaukuejo and Irene. The two synoptic weather types produce distinct vertical ozone signatures. The composite westerly trough and anticyclonic vertical ozone profiles, at Okaukuejo, were corroborated by an examination of case studies. Case studies at Irene and Okaukuejo confirmed the general increase in ozone from the surface to the mid-troposphere and the presence of an elevated enhanced ozone layer under anticyclonic conditions. Further evidence of the presence of a mid-tropospheric ozone minimum, during the passage of a westerly trough over southern Africa, was found. The persistence of the elevated enhanced layer, irrespective of the change in synoptic flow, was highlighted.

The role of tropical circulation in the vertical distribution of ozone was investigated by examining data collected during SAFARI-92 at Brazzaville. A short-lived upper tropospheric ozone maximum was explained by strong upward motion and convective activity on that day. Stable conditions and the accumulation of pollution near the surface, on preceding days, undoubtedly contributed to the observed ozone enhancement.

In order to gain a more thorough understanding of the relationship between the passage of subtropical westerly troughs and ozone distribution, further analysis is presented in the following chapters.

CHAPTER 5

A REVIEW OF MECHANISMS OF STRATOSPHERIC-TROPOSPHERIC EXCHANGE

5.1 INTRODUCTION

The aim of this chapter is to examine the role of STE in the production of ozone maxima over southern Africa. In the tropics, exchange between the troposphere and stratosphere occurs through the medium of cumulus clouds as their large turrets extend upwards into the stratosphere (Russell *et al.*, 1993). In the mid-latitudes, however, STE is dominated largely by frontal scale processes associated with an upper tropospheric jet stream, when baroclinic instability and cyclogenesis cause deformations in the tropopause. Baroclinic waves or smaller scale Rossby waves play a significant role in transporting ozone. These transient waves disturb the circulation of the atmosphere over relatively short durations and produce day-to-day changes in total ozone amounts. The role of these baroclinic transient waves in ozone transport is particularly important in the southernmost parts of southern Africa and in the Ocean to the south.

5.2 TROPOPAUSE FOLDING

Localised wind maxima or jet streams are commonly associated with the formation of frontal zones or zones of enhanced temperature gradients, associated with synoptic scale waves. Frontal zones are also frequently associated with processes, such as tropopause folding, which cause the exchange of air between the stratosphere and troposphere and which produce fluctuations in total column ozone amounts.

5.2.1 Models of tropopause folding

Several models have been proposed to describe the relationship between the tropopause and upper level frontal boundaries, in cases when the deformation of the tropopause produces an intrusion of stratospheric air into the

troposphere. Essentially, the models differ according to the scale of the stratospheric wind shear in the layer of maximum wind ie. whether it is concentrated on the mesoscale or synoptic scale (Shapiro, 1976).

In one of the early models, Berggren (1952) places the upper level front between the polar and subtropical tropopause surfaces and extends the front between the two surfaces into the stratosphere, where its slope is opposite to that in the troposphere (Fig. 5.1). The extension of the front into the upper stratosphere was unsupported by observations and later discontinued in the revised model of Palmén (1958).

In the Palmén model, the cyclonic wind shear is concentrated in the vertical and extended over the 100 km wide frontal zone. The Palmén model altered the Berggren model by extending the front only a short distance into the stratosphere (Figure 5.2).

Later, on the basis of upper air soundings, Reed and Danielsen (1959) proposed the so called 'waterspout' model (Fig 5.3). The essential characteristics of the model are that the polar (northern) tropopause is connected continuously with the lower surface of the polar front, and the higher tropopause surface to the south [subtropical tropopause] curves through the axis of the polar-front jet to become continuous with the upper surface of the polar front. The connected frontal tropopause surfaces form the boundary of sharp discontinuities of PV. The model also provides the means for the transport of stratospheric air into the troposphere (Reed, 1955; Staley, 1960, 1962) and stratospheric-tropospheric exchange of ozone (Danielsen (1968). Whereas Berggren had concentrated the cyclonic shear within the vertically extended 100 km wide frontal zone, Reed and Danielsen distributed this shear uniformly over a distance of hundreds of kilometres. The model presented a satisfactory solution to the problem of connecting frontal boundaries to the tropopause in association with high-level fronts. Subsequent observations confirmed the existence of such a 'waterspout' or folded tropopause (Briggs and Roach, 1963).

One of the characteristic features of tropopause folds, which was originally observed by Reed (1955), is the development of a dry stable layer in the warm air adjacent to the fold. Indeed, it forms as a continuation of the frontal zone beneath the jet stream and slopes downward on the equatorward side of the jet.

Further work concerning the transport of stratospheric air into the troposphere and the link between upper tropospheric fronts and jet streams continued into the 1960's. Danielsen (1968) postulated that the circulation accompanying a tropopause fold consisted of a two-celled circulation

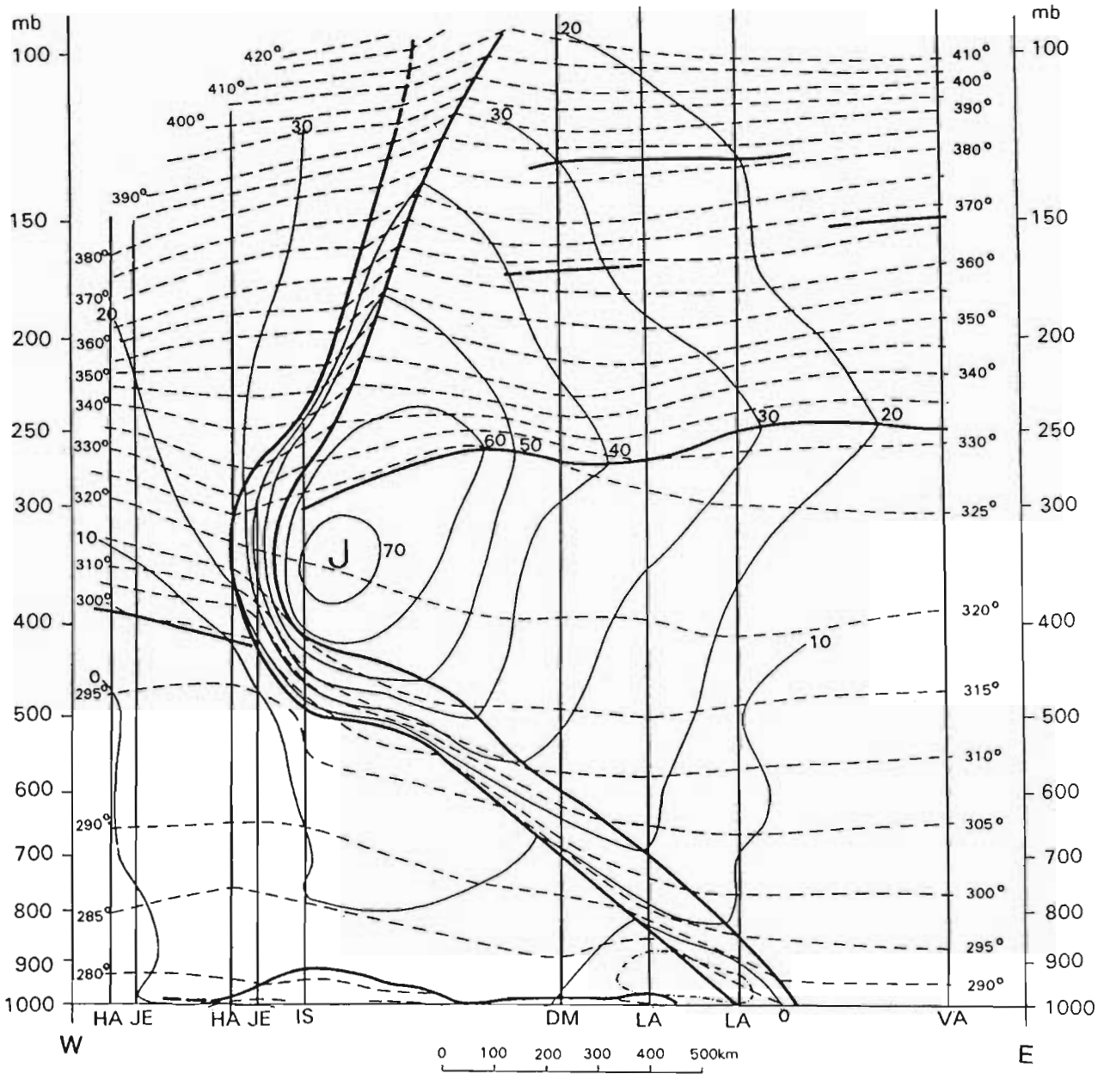

Figure 5.1 Vertical cross section approximately along 54.5°N from Valentia (Ireland) to Hannover (Germany), 9 November 1949, 0300 GCT of potential temperature (K) [thin dashed lines]; wind speed (m s^{-1}) [thin solid lines], and frontal and tropopause discontinuities [heavy solid lines]. Thin vertical lines indicate the location and vertical extent of the wind soundings. Reproduced from Berggren (1952) p. 47.

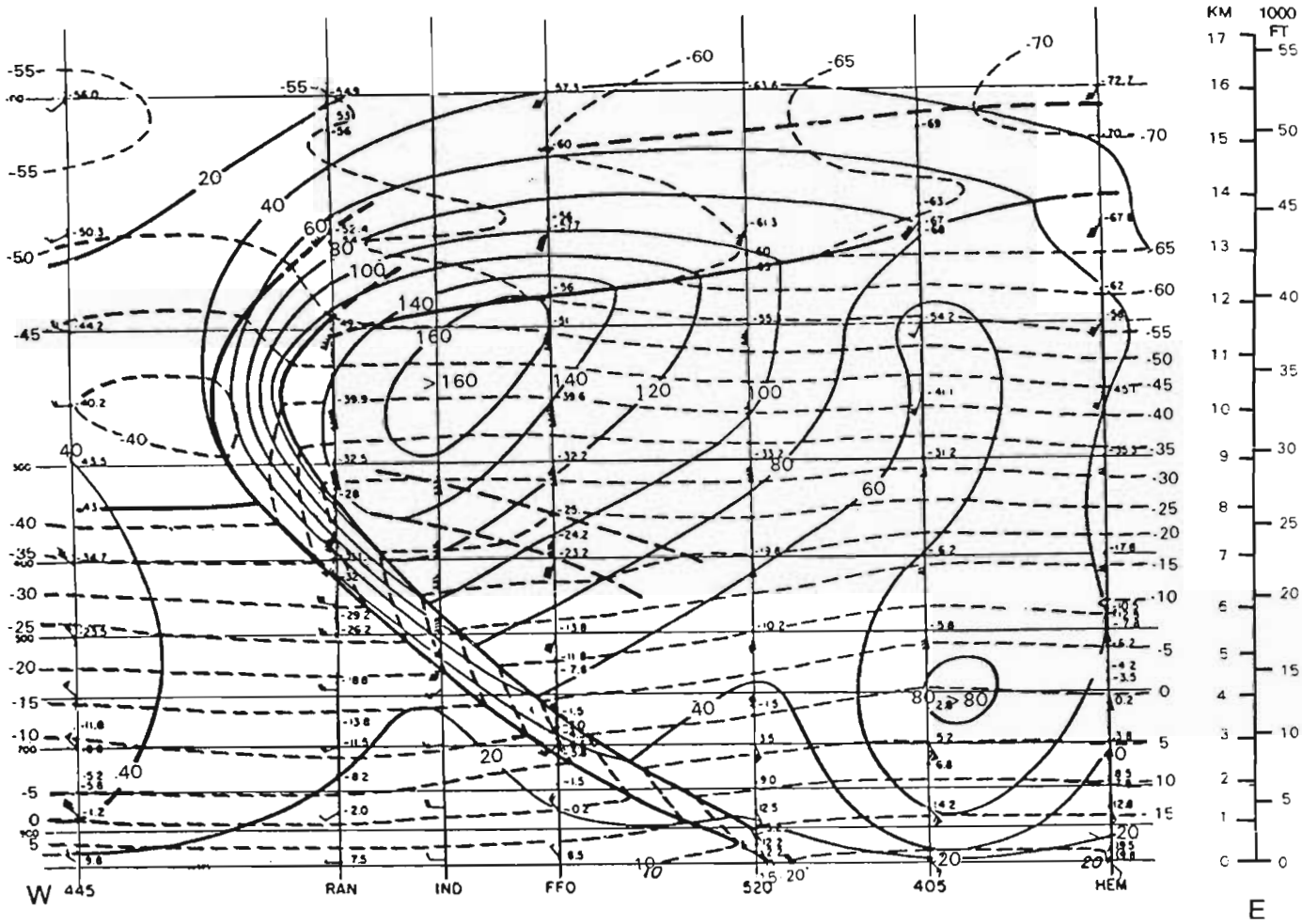

Figure 5.2 Vertical cross section approximately along 40°N through a cold front in the eastern USA, 15 October 1954, 1500 GCT of temperature (°C) [thin dashed lines]; wind speed (kt) [thin solid lines] and frontal and tropopause discontinuities [heavy solid lines]. Reproduced from Palmén (1958) p. 9.

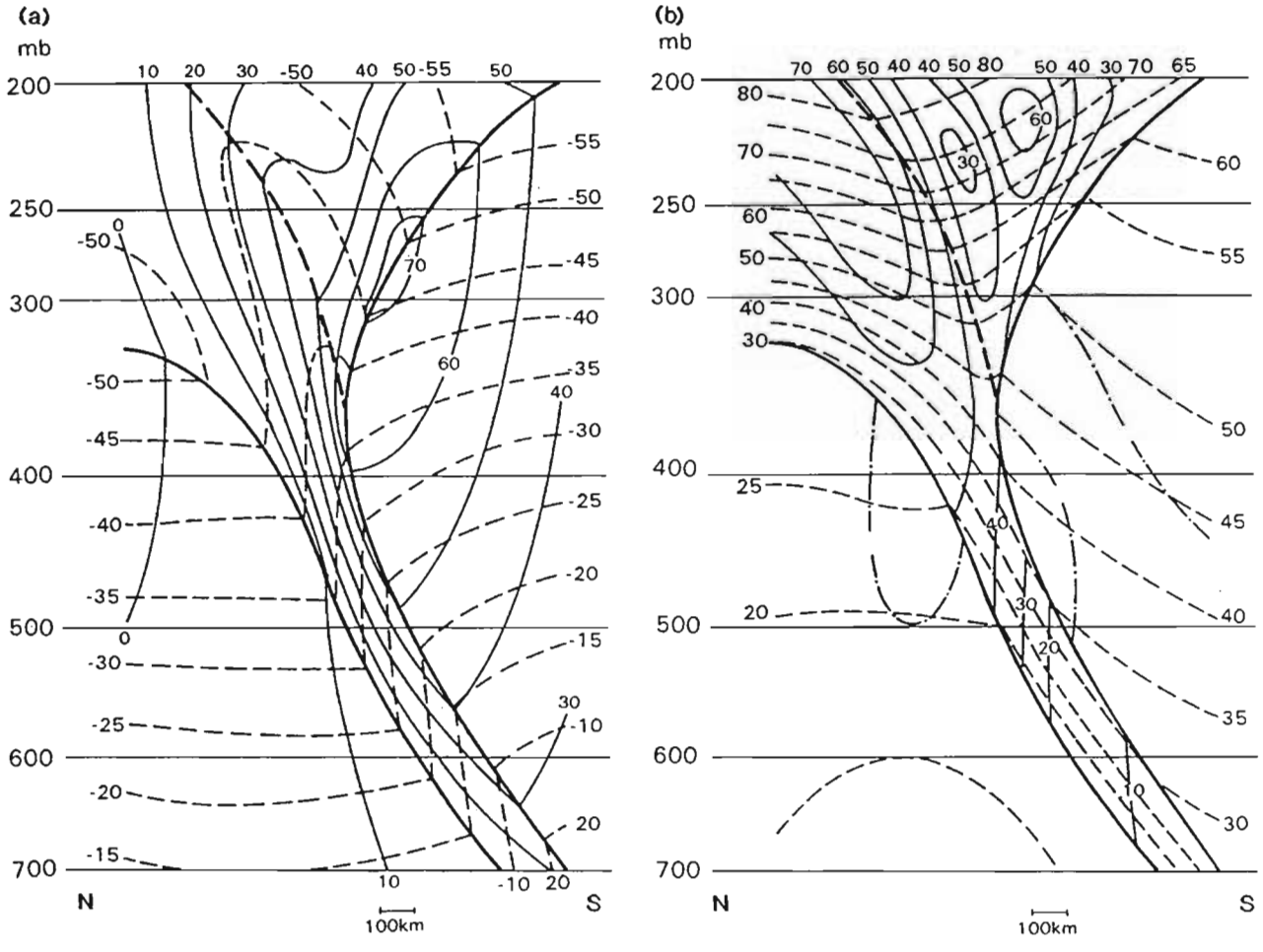

Figure 5.3 (a) Composite cross section of temperature (°C) [dashed lines]; geostrophic wind speed (kt) [thin solid lines]; and frontal and tropopause discontinuities [heavy solid lines]. (b) Composite cross section of PV (10^{-6} $KhPa^{-1}s^{-1}$) [dashed lines] and potential temperature (K) [solid lines]. Reproduced from Reed and Danielsen (1959) p. 11-12.

(Fig. 5.4). Two transverse/vertical circulation cells, one direct and the other indirect, are respectively centred on the warm and cold sides of the tropopause break. The two cell configuration produces a confluence zone in the vertical plane. The folding process is initiated by quasi-geostrophic shear in the baroclinic atmosphere, which is found to the west of a developing trough, and which is subsequently destroyed by convective mixing to the south and east of the vortex (Danielsen, 1968). The isentropic surfaces compress to form a frontal zone, and subsidence, which is a prerequisite for tropopause folding, is maximised on the warm side (equatorward) in the middle and upper troposphere. The warm side of the upper tropospheric front is located directly beneath the jet (Fig. 5.4). STE commonly accompanies intense upper tropospheric frontal development when the jet streak propagates into the upper tropospheric trough in this way (Danielsen, 1968; Singh *et al.*, 1980; Carlson, 1991). Stratospheric air moving along the isentropic surfaces is extruded into the frontal zone, downstream of the ridge in the region of large-scale descent (Carlson, 1991), into the mid- and lower troposphere in response to strong descent at the level of the tropopause.

Shapiro (1981) extended Danielsen's hypothesis. He proposed that cold air advection which would arise as a result of wind shear along the jet was essential for tropopause folding. It was not sufficient to have confluence alone as had earlier been suggested by the work of Hoskins and Bretherton (1972). They had shown that in the presence of pure confluence, the early stages of a tropopause fold could be produced, but that there was an absence of a distinct tropopause fold.

The requirement that shear and cold air advection are necessary to produce the two circulation cells at the correct locations (ie. strongest descent below the jet and in the warm air), so that the upper tropospheric front extends below the mid-troposphere has become known as the Danielsen-Shapiro hypothesis and has been verified by the work done by Keyser and Pecnick (1985), Keyser *et al.* (1986) and others.

5.2.2 Tropopause folding and ozone transport

Danielsen (1968) was the first to propose tropopause folding as a mechanism for transporting ozone-rich air from the stratosphere to the troposphere. This has subsequently been confirmed by a number of other authors (for example, Reiter, 1975; Danielsen and Mohnen, 1977; Shapiro, 1980; Singh *et al.*, 1980; Wakamatsu *et al.*, 1989; Hipskind *et al.*, 1987). Many incidences of tropopause folding are cited in the literature (Briggs and Roach, 1963; Danielsen, 1968; Shapiro, 1978, 1980; Uccellini *et al.*, 1984; Whitaker *et al.*, 1988). These are

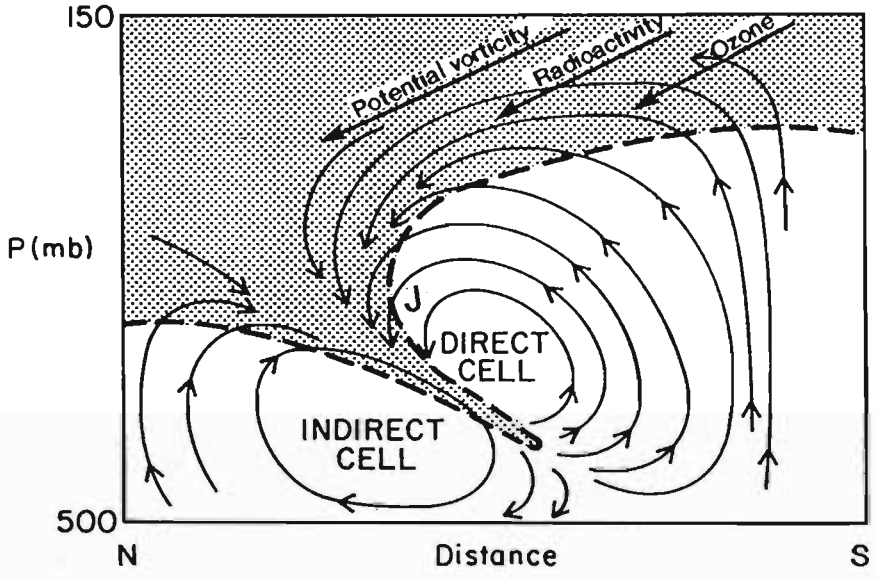

Figure 5.4 Diagrammatic representation of the mean circulation relative to a folded tropopause. J indicates the position of the jet stream. Redrawn from Danielsen (1968) p. 517 and Carlson, 1991, p. 437.

generally described by vertical cross-sections of PV, radioactivity, θ, ozone or wind speed, through the fold (Fig. 5.5).

Values of PV in the stratosphere exceed those below the tropopause by one to two orders of magnitude (Shapiro, 1980). A tropopause fold causes a fold in the PV boundary [taken as the 100 x 10^{-7} $KhPa^{-1}s^{-1}$ isopleth of PV (Shapiro, 1980, 1978; Shapiro *et al.*, 1987)] that separates the high PV region of the stratosphere from the low PV region of the troposphere (Danielsen, 1968). Highest PV values occur near the tropopause just above the polar front jet and on the cyclonic side of the jet stream (Fig. 5.5) (Carlson, 1991).

There is a well established relationship between ozone and PV (Shapiro, 1978; Danielsen and Hipskind, 1980; Shapiro *et al.*, 1982; Browell *et al.*, 1987; Vaughan *et al.*, 1994; among others). Figure 5.5 shows high PV values within the frontal zone moving downward into the troposphere in the region of strong descent of the tropopause fold. Figure 5.6 confirms that high ozone concentrations are commonly found within the tropopause fold where high PV values are located.

A further indicator of stratospheric air movement is found in measurements of radioactive substances. Aircraft measurements of radioactive decay show that high concentrations occur within the folded tropopause (Staley, 1960; 1962; Danielsen, 1968; Danielsen and Mohnen, 1977; among others). Radioactive debris occurs naturally in, and is introduced into the stratosphere through human activity. During the 1950s and 1960s, large amounts of radioactive substances were injected into the stratosphere as a result of nuclear test explosions. The long residence time, of up to several years in the stratosphere and approximately one month in the troposphere (Staley, 1962), make this material an ideal atmospheric tracer. Measurements of PV, ozone and radioactivity in the stratospheric air as it descends into the lower troposphere, within the fold, diminish by a factor of three to ten. This has been explained by turbulent mixing (Shapiro, 1980; Carlson, 1991).

Tropopause folding, and the movement of ozone from the stratosphere into the fold in the troposphere, is not direct evidence of STE. In the absence of diabatic and turbulent mixing processes, that is, under adiabatic flow conditions, PV is conserved and tropopause folding is strictly a reversible process, (Danielsen, 1968; Shapiro, 1980). Stratospheric intrusions may be retracted back into the stratosphere in the ascending flow ahead of the cyclonic disturbances. It is likely that parcels re-entering the stratosphere would acquire some tropospheric properties through mixing and would contribute to transport of these properties into the stratosphere (Shapiro, 1980). It is estimated, however, that the transport from the stratosphere to the troposphere over a 24 hour period is 2.5 times greater than from the

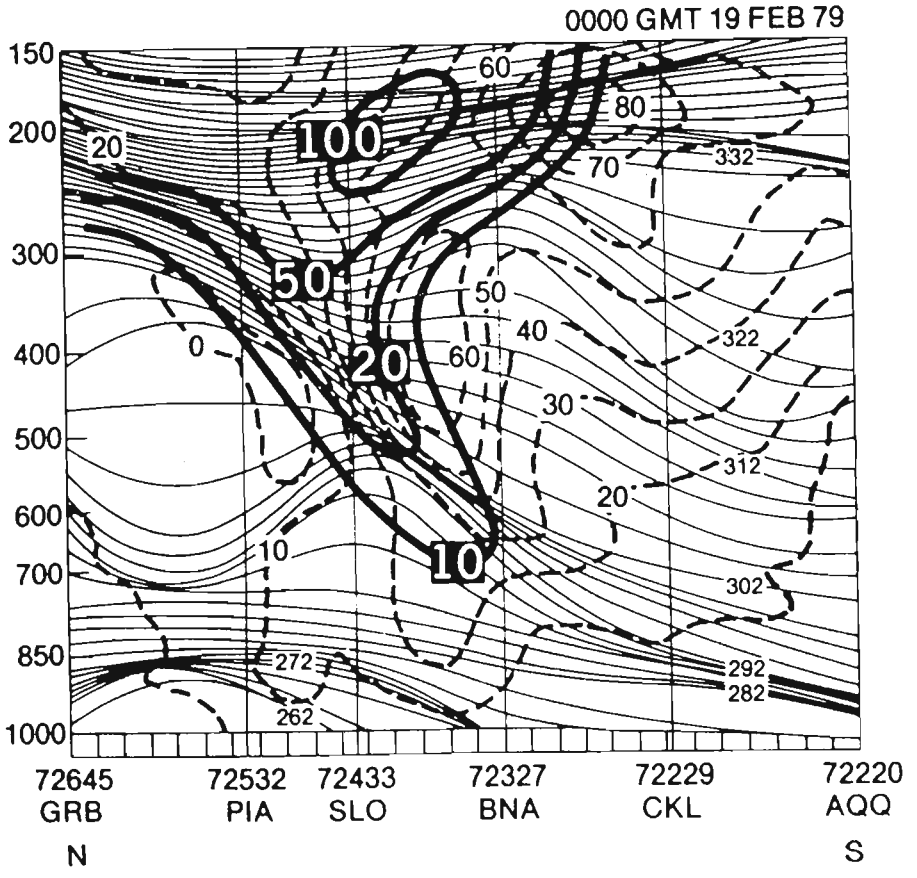

Figure 5.5 Vertical cross section from Green Bay, Wisconsin (GRB) to Apalachicola, Florida (AQQ), USA, 19 February 1979, 0000 GMT, through upper tropospheric trough. Geostrophic wind speed, (m s^{-1}) [broken curves]; potential temperature (K) [thin full curves] and potential vorticity (10^{-6} $KhPa^{-1}s^{-1}$) [heavy full curves], are indicated. Reproduced from Uccellini *et al.* (1985) p. 973.

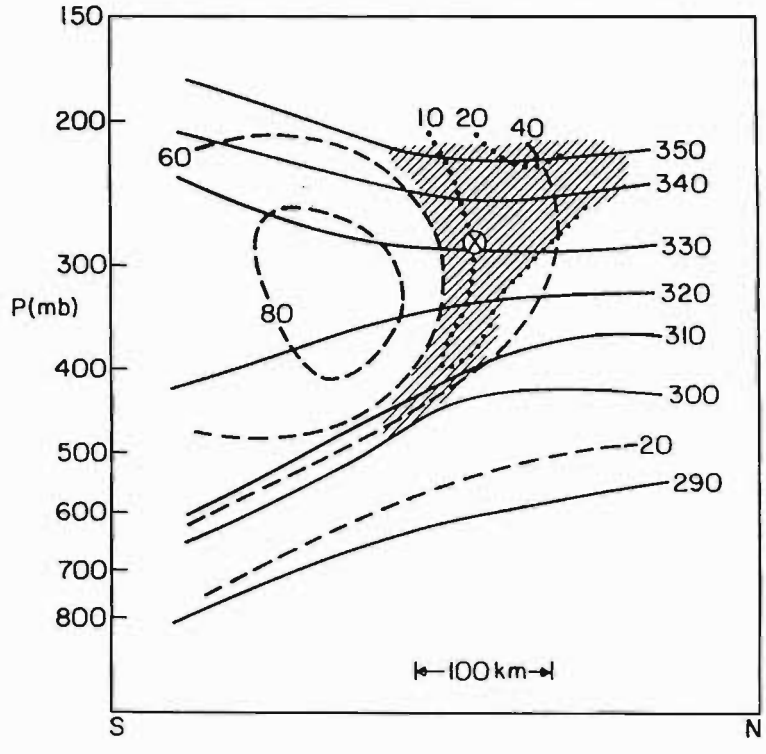

Figure 5.6 Cross section from approximately north (N) to south (S), through a jet streak and tropopause fold. Potential temperature (K) [full curves] and wind speed (m s^{-1}) [broken curves] are shown. Shading indicates the region in which potential vorticity exceeds 90 x 10^{-6} $KhPa^{-1}s^{-1}$. Ozone (pphmv) [dotted curves] is indicated. The circled dot denotes the PV maximum. Based on a figure by Shapiro, 1978, and reproduced from Carlson (1991) p. 428.

troposphere to the stratosphere (Spaete *et al.*, 1994).

The irreversibility of STE is generated by mixing processes within the fold which defies the strict PV conservation. Stratospheric air, within the fold, is subjected to intense mixing which causes flow across isentropic surfaces and the loss of stratospheric properties to the troposphere (Shapiro, 1978; Browell *et al.*, 1987; Holton, 1992). High wind speeds and momentum from the stratosphere generate supergeostrophic flow which facilitates the mixing of stratospheric and tropospheric air (Danielsen, 1968), while air which is cooler and more dense is transported readily across isentropic surfaces within the fold. Turbulent motions produce a downward "downgradient" flux of ozone-rich air which moves ageostrophically from the cyclonic lower stratosphere into the troposphere (Danielsen, 1968; Shapiro, 1980). It is estimated that approximately 50% of ozone entering the fold enters the troposphere (Shapiro, 1980).

The importance of tropopause folding as a mechanism for the exchange of mass between the stratosphere and troposphere is the subject of some dispute. Although most authors agree that between 70% and 80% of the mass of the stratosphere is exchanged with the troposphere annually, Danielsen (1968) attributes all of this exchange to tropopause folding. Reiter (1975), however, assigns 27% to tropopause folding and 60% to the mean meridional circulation. According to Singh *et al* (1980), the reason for the discrepancy lies in the fact that Reiter (1975) only estimates 25% as many tropopause folding events per annum as Danielsen (1968). Furthermore, Danielsen (1968) based his estimates of mass exchange on events of intense cyclogenesis and as such over estimated the number of such events. According to Singh *et al.* (1980), 60-80% of the mass exchange occurs due to tropopause folding and 20-40% due to the mean meridional circulation.

5.3 CUT OFF LOW SYSTEMS

Vertical transport of ozone from the stratosphere to the troposphere occurs in episodic events associated with baroclinic instability and the amplification of large-scale troughs in the upper tropospheric flow and may be expected to be particularly noticeable when tropopause folding occurs. Most vigorous events occur during winter and spring in association with mid-latitude cyclogenesis. Structural changes within the tropopause allows an intrusion of air from the stratosphere to the troposphere. Cut off low systems produce conditions favourable for transfer of air from the stratosphere to the troposphere.

Cut off lows (COLs), otherwise referred to as cold pools, upper cold lows, cold-core cyclones, cold vortices or cold domes (Hill and Browning, 1987) are upper tropospheric cyclones often associated with blocking patterns in the tropospheric flow (Price and Vaughan, 1991). COLs are unstable, baroclinic systems which may slope to the west with increasing altitude and are associated with strong convergence and vertical motion, particularly while deepening (Preston-Whyte and Tyson, 1988).

The formation of COLs and their meteorological properties are well documented in the literature (Palmén, 1949; Sumner, 1953; Hill and Browning, 1987; among others). COLs usually form when an upper air trough extends far enough equatorwards so that a closed cyclonic circulation forms at its tip as a jet streak. Air within the low pressure system usually originates from higher latitudes, is colder than the ambient air and thus the formation of COLs in the mid-latitudes causes displacement of air of polar origin.

Hoskins *et al* (1985) provide a description of COL systems which is based on the distribution of isentropic potential vorticity. COLs are associated with a low tropopause and appear as closed regions of high PV on isentropic surfaces in the upper troposphere and lower stratosphere (Price and Vaughan, 1992; Bell and Bosart, 1993). Once a cyclonic PV region is cut off in this manner, the circulation may penetrate downwards producing a surface cyclone if the surface temperature is not too low (Hoskins *et al.*, 1985). The upper tropospheric cyclone persists as long as the PV anomaly persists but may be re-absorbed into the main polar reservoir or decay *in situ*.

The role of COLs in facilitating the injection of stratospheric air into the troposphere is well known (Bamber *et al.*, 1984; Hoskins, *et al.*, 1985; Price and Vaughan, 1992) and several studies provide evidence for the simultaneous movement of ozone into the upper troposphere at middle to higher latitudes (Vaughan 1988; Vaughan and Price, 1991; Ebel *et al.*, 1991; Haynes, 1993; Price and Vaughan, 1993). Measurements of trace species in COLs also provide evidence of the exchange of air between the stratosphere and troposphere (Bamber *et al.* 1984; Vaughan *et al.*, 1994). Bamber *et al* (1984) found that a substantial depth of air (approximately 2 km) in the upper troposphere of a COL displayed chemical characteristics intermediate between those of the troposphere and stratosphere. These included elevated concentrations of ozone and low values of tropospheric tracers such as CFCs and hydrocarbons.

The occurrence of COLs has been extensively studied for the Northern Hemisphere. Price and Vaughan (1992) conducted a statistical analysis at the 200 hPa level which revealed characteristics of COL systems in the lower stratosphere and upper troposphere region. Three different types of COLs

(Fig. 5.7) were identified, each of which forms from a different jet stream (polar, subtropical and polar vortex). The authors suggest that the polar type (situated at approximately 35°N), which is formed by the equatorward extension of a strong polar jet and as a result tends to form polewards of this jet, is most significant in STE. Cold polar air and large temperature gradients across their boundaries promote conditions favourable for tropopause folding. STE occurs in cut off low systems when mixing takes place across isentropic surfaces and when the tropopause becomes temporarily indistinct (Price and Vaughan, 1994).

Based on tropopause characteristics, Price and Vaughan (1993) recognise three mechanisms for exchange of air between the stratosphere and the troposphere in association with COLS. The first is via convective erosion of the tropopause. COL systems are often associated with deep and extensive convection (Matsumoto *et al.*, 1982; Bamber *et al.*, 1984; Preston-Whyte and Tyson, 1988), generated when cold air masses, forming a COL, are transported equatorward to a region of higher ambient surface temperature and where the solar heating is stronger. Therefore, COLs forming over land in summer or over a warm ocean are most likely to promote deep convection which may lead to an indistinct tropopause and mixing between tropospheric and stratospheric air. The degree of mixing depends also on the extent to which the PV anomaly associated with the tropopause disturbance, destabilises the lower tropospheric air. A layer of air intermediate in character between stratospheric and tropospheric is formed, along with an indistinct tropopause. Figure 5.8 shows a schematic representation of a convective cell penetrating the tropopause, which effectively transfers the tropospheric air into the stratosphere. Upward transport is clearly dominant at low latitudes. Continued convection is likely to cause a re-sharpening of the tropopause at a higher level by further dilution of the mixed layer.

Secondly, turbulence in the vicinity of the jet stream may also play a role in disrupting the tropopause (Briggs and Roach, 1963; Shapiro, 1980; Carlson, 1991; Vaughan and Price, 1993). Figure 5.9 shows that turbulence (associated with relatively low Richardson numbers) is possible near the tropopause fold. Air which eventually forms a COL is transported along the cyclonic side of the jet, within the sloping zones of strong vertical wind shear and horizontal thermal gradient above and below the level of the maximum wind, in the region noted for its clear-air turbulence (CAT) and which may be responsible for mixing across the tropopause (Briggs and Roach, 1963; Shapiro, 1976). Concurrently, the stratospheric properties of the air within the frontal zone are constantly diluted.

The third mechanism is that of tropopause folding as discussed in section 5.2 above. The development of many COL systems accompanies intense upper level

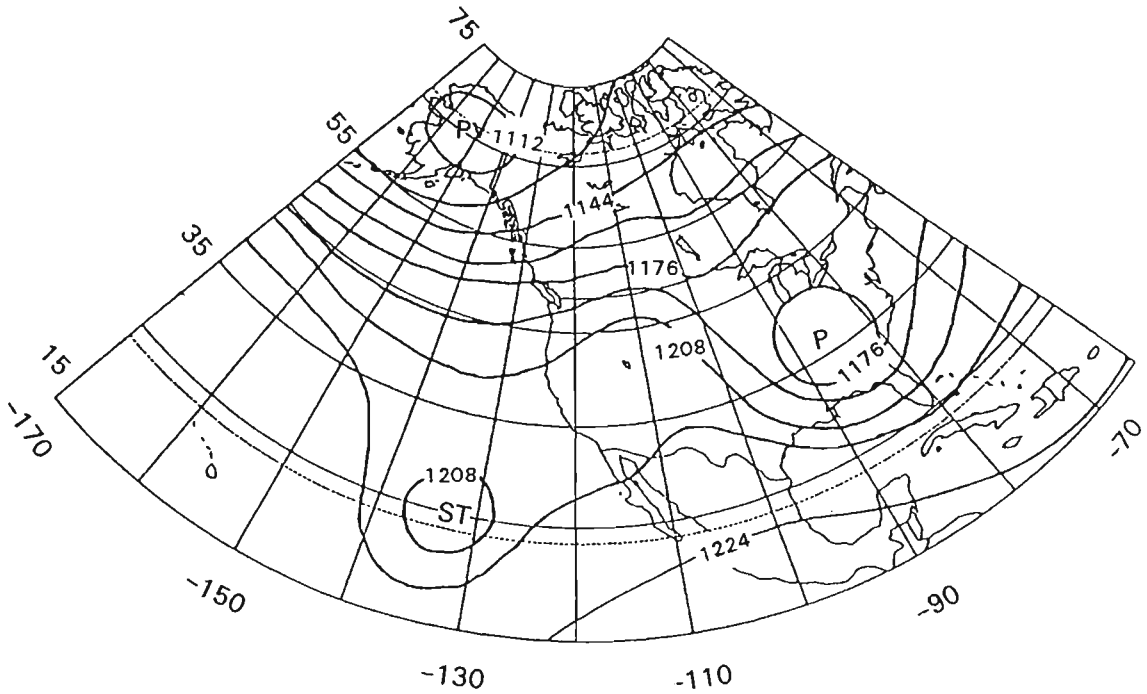

Figure 5.7 Polar (P), subtropical (ST) and polar vortex (PV) COLs and related jet streams on the 200 hPa surface. Redrawn from Price and Vaughan (1992) p. 97.

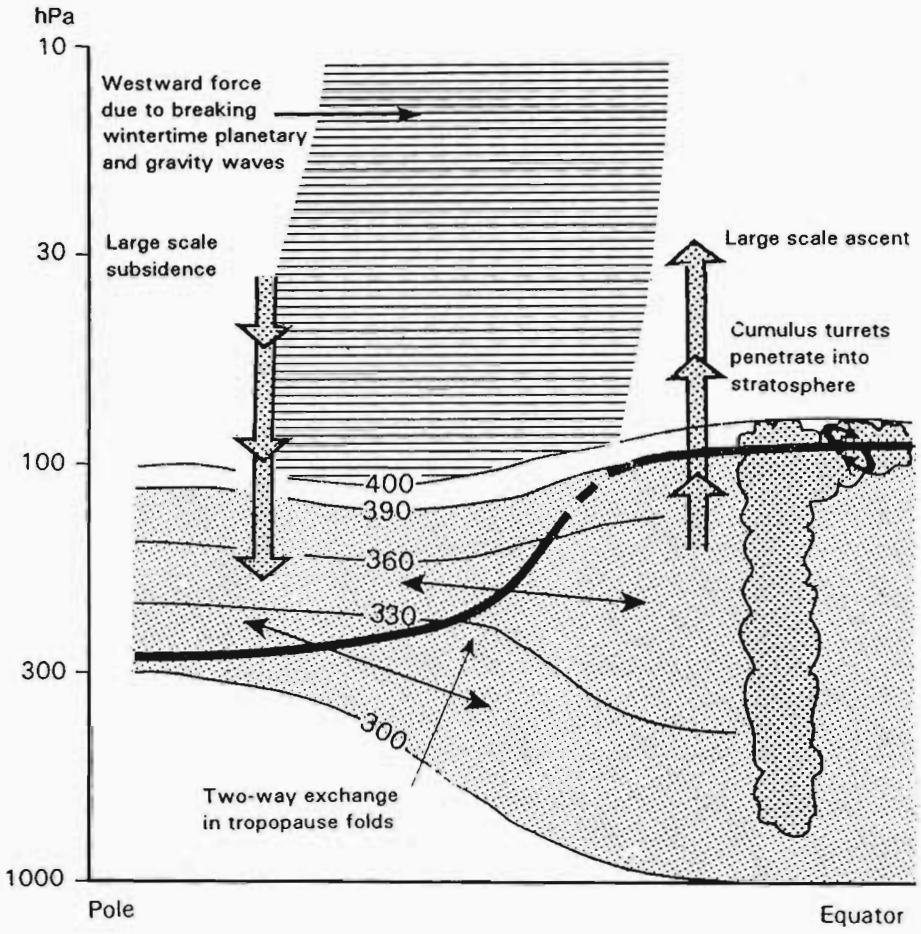

Figure 5.8 Schematic cross section of the troposphere and lower stratosphere showing stratosphere-troposphere exchange mechanisms. Potential temperature (K) [thin full curves] and the tropopause [thick solid and broken curve] are indicated. The light stipple indicates the region where the potential temperature surfaces span the tropopause and, in which the arrows indicate two-way exchange between the stratosphere and troposphere in tropopause folds. Redrawn after Haynes (1993) p. 5.

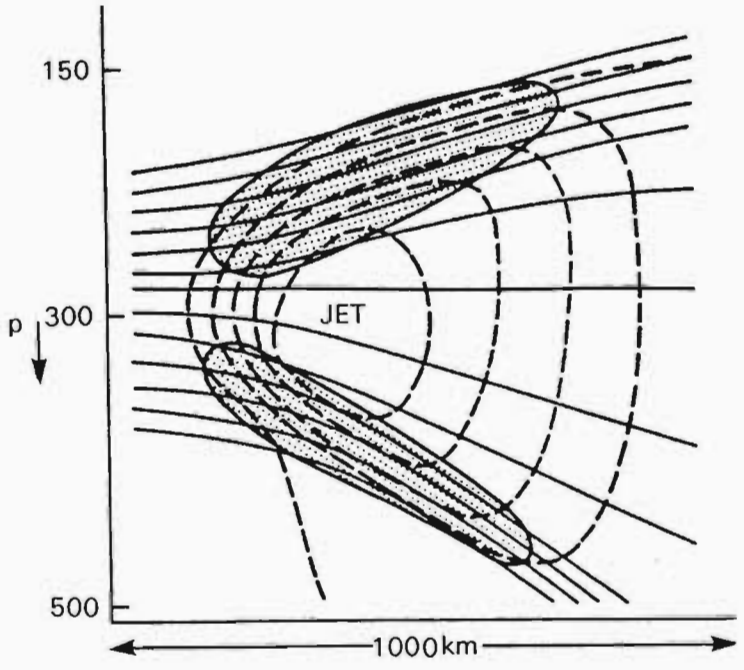

Figure 5.9 Regions of clear air turbulence [stippled] in the vicinity of a jet stream/frontal zone system (north-south cross section). Potential temperature [solid lines]; wind speed [dashed lines] are indicated. Redrawn from Shapiro (1976) p. 904.

frontogenesis (Hoskins *et al.*, 1985), and which also produces tropopause folding. As discussed previously, many studies have shown that tropopause folding allows ozone-rich air, of stratospheric origin, to move ageostrophically from the cyclonic lower stratosphere into the troposphere. The process is irreversible (Danielsen, 1968) due to mixing by small-scale turbulent motions (Browell *et al.*, 1987) with a substantial amount of stratospheric air remaining in the troposphere, although some air may return into the fold (Danielsen *et al.*, 1987) and to the stratosphere as the tropopause re-establishes itself (Price and Vaughan, 1993).

Vaughan and Price (1991) describe a theoretical relationship between total ozone and absolute vorticity with the aid of the potential vorticity theorem. The relationship is based on the conservation of PV in adiabatic flow on an isentropic surface in the lower stratosphere. Essentially, a cyclonic vorticity anomaly near the tropopause, such as a trough or COL, will generate high total ozone values since air parcels entering the trough converge and stretch, producing more ozone in the vertical column and lowering the tropopause. Conversely, a ridge in the flow will generate low total ozone values due to compression and divergence. As a result, COL systems show up as regions of high vorticity and high total ozone on their respective maps. The magnitude of the ozone anomaly is expressed as a function of the amplitude of the vorticity anomaly and its depth.

Having established that COL systems are an important mechanism for STE in the Northern Hemisphere, their role in STE and consequent association with high total ozone will be examined over southern Africa in the next chapter.

CHAPTER 6

CUT OFF LOWS AND OZONE MAXIMA OVER SOUTHERN AFRICA

6.1 INTRODUCTION

Thus far, a number of factors which contribute to the production of ozone maxima over southern Africa have been identified. The roles of horizontal and vertical transport and *in situ* photochemical formation of ozone are recognised. The aim of this chapter is to investigate the contribution of STE during the passage of deep westerly trough systems. COL pressure systems represent a particularly deep form of the westerly trough and produce efficient mixing of stratospheric and tropospheric air, as outlined in Chapter 5. STE associated with COL systems is well documented in the literature for individual cases in the northern hemisphere. In this chapter the relationship between COLs and total ozone maxima and the vertical distribution of ozone over the southern African region will be explored.

Southern Africa is located in the Southern Hemisphere subtropical latitudes and consequently, the region comes under the influence of tropical, subtropical and temperate systems as described by Preston-Whyte and Tyson (1988). Subtropical influences are effected through the South Indian and South Atlantic anticyclones and the continental high pressure system; and tropical influences through easterly flow and the occurrence of easterly waves and lows. The temperate control is manifest in travelling perturbations in the westerlies that take the form of westerly waves and troughs. An intense form of the westerly trough is the COL.

COLs are recognized as important synoptic systems in South Africa, often dominant for three days at a time and as a result, these features may account for more than 10% of the rainfall south of 27°S (Taljaard, 1985). They are responsible for many of the flood-producing rains over South Africa (Taljaard, 1982).

The COL is an intense form of a cold-cored cyclone. In the upper air, this feature is located equatorward of the mid-latitude westerly winds and described essentially as a system of the subtropical zone (Taljaard, 1985). COLs are unstable, baroclinic systems associated with strong convergence and vertical motion which is illustrated schematically in Figure 6.1. Divergence in the upper air is steered by surface convergence and is usually strongest in the upper troposphere, i.e. from 500 to 200 hPa, over South Africa. The

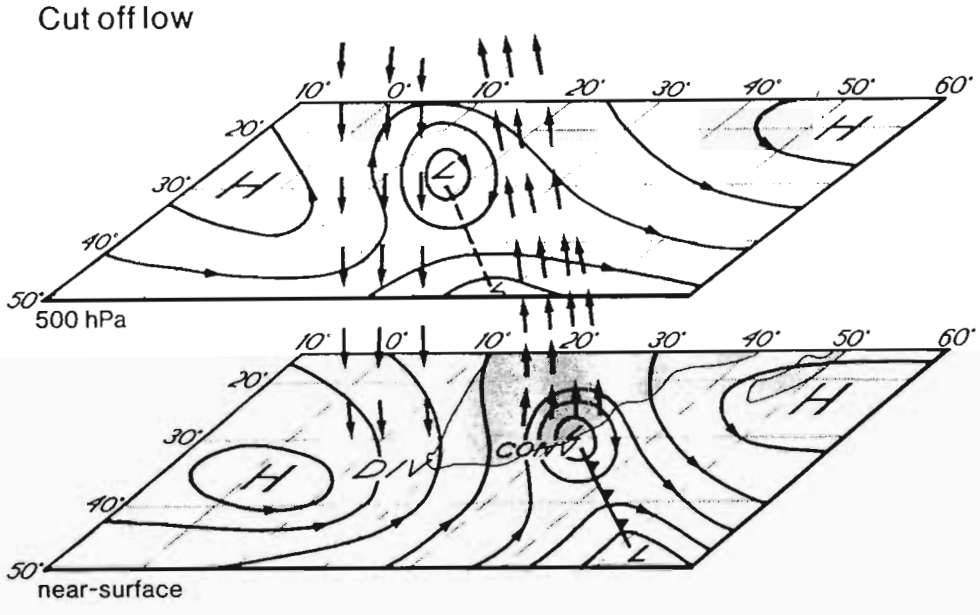

Figure 6.1 Schematic representation of the near-surface and 500 hPa circulation associated with a cut off low. Redrawn from Preston-Whyte and Tyson (1988) p. 227.

frequency of occurrence of these systems is approximately 11 per year (excluding those with a lifespan of less than two days) over and immediately around South Africa (Taljaard, 1985). COLs which produce heavy rains occur most frequently in autumn (March to May) and spring (August to October). Although this is true for COLs lasting for two or more days over South Africa, severe rains associated with COLS have been recorded throughout the year, for example the Laingsburg flood of 25 January 1981, the exceptionally severe COLs of June 1964 (Taljaard, 1985) and September 1987 (Triegaardt *et al.*, 1987).

Besides a superficial examination of total column ozone variation during the passage of a COL (Stranz and Taljaard, 1965), their role as agents of STE and their influence on ozone levels has not been researched in the southern African region. This topic will be addressed in this chapter.

6.2 COMPOSITE ANALYSIS OF COLS AND TOTAL OZONE DISTRIBUTION

6.2.1 Methodology

In order to obtain a general picture of the relationship between COLs and ozone distribution over southern Africa, six case studies of COLs were selected for composite analysis. Full details of the selection criteria for case studies and the construction of the composites are provided in Chapter 2. For each case study, the day exhibiting the deepest COL on the 300 hPa surface was labelled day 0. Conditions two days prior to, and two days following this event are referred to as days -2, -1 and +1 and +2 respectively.

Composite vertical cross sections, through the centre of each COL system, were constructed for atmospheric parameters including PV, RH, the vertical motion field (ω) and wind speed. In addition, composite spatial distributions for an area extending 15° latitude x 15° longitude, of PV, TOMS total ozone and wind speed were produced by normalising the COL systems with respect to their centre points estimated from the 300 hPa upper air chart.

6.2.2 Composite total ozone distribution

The horizontal distribution of ozone is presented in the form of composite plots of total ozone (Fig. 6.2). There is a general zonal pattern, with an increase in total ozone from north to south, and a buildup of ozone near the centre of the domain, caused by equatorward extensions from the relatively

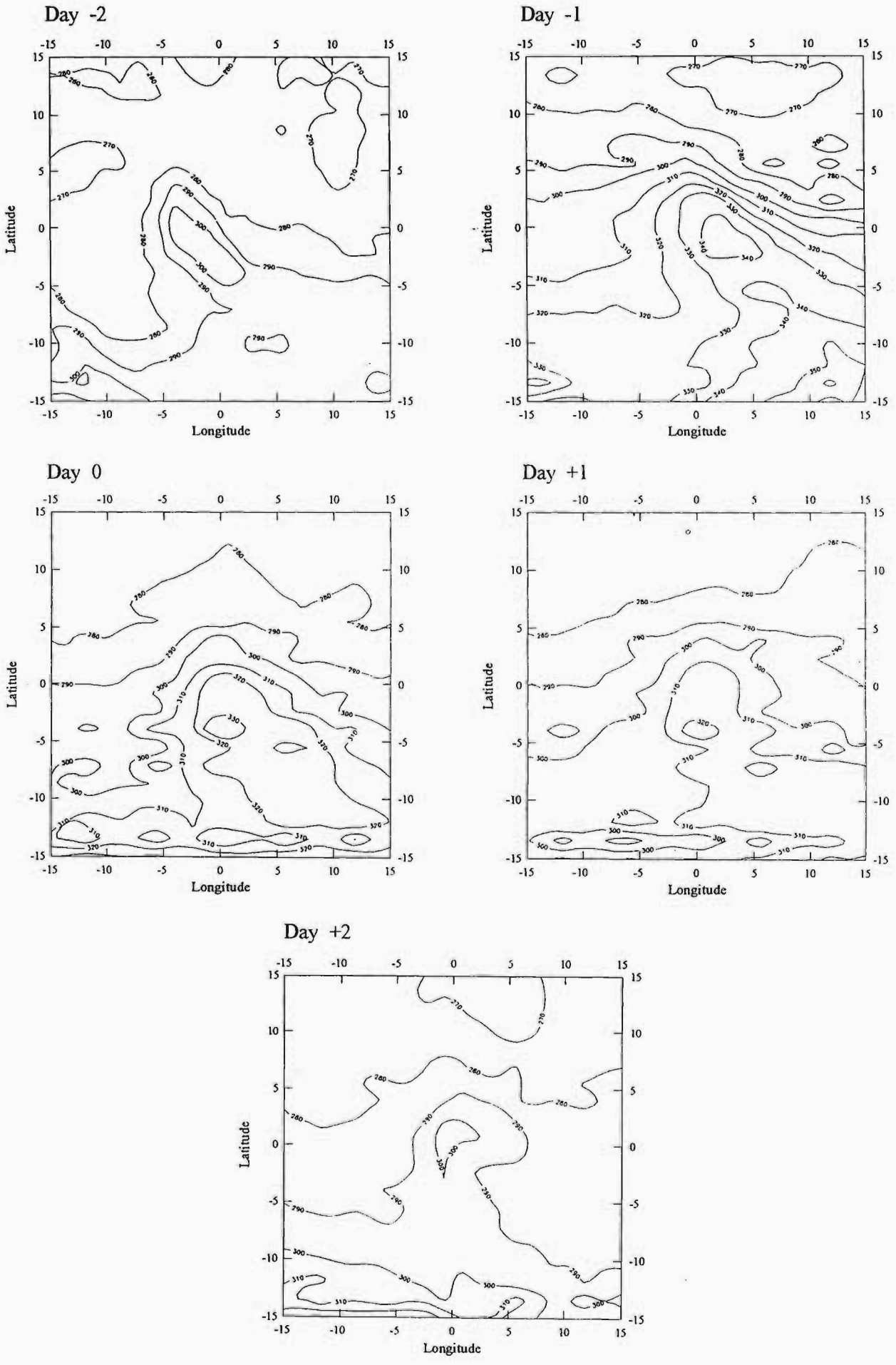

Figure 6.2 Composite spatial distribution of TOMS total ozone (DU), for an area 15° latitude and 15° longitude on either side of the COL centre, for day -2 to day +2.

higher ozone region in the south. On day -2 and -1, a northwest-south east axis in total ozone is clearly evident and which is not present on subsequent days. Highest values (330 to 340 DU) are located in the region of the COL centre, on days -1 and 0 and gradients are also strongest on these days. On day +1, total ozone declines to 320 DU in the region of the COL and by day +2 values in the region of the COL system have fallen to 300 DU. Throughout the five-day period, highest ozone values are always present at the centre of the COL, although clearly by day +2 there is little spatial variation in ozone.

Composite ozone mass, calculated in a 5° x 5° grid surrounding the COL centres (details are provided in Chapter 2), confirms the ozone enhancement associated with well developed COL systems. On day -1 and day 0 ozone mass reaches a maximum (approximately 1.8 x 10^9 kg on both days) (Fig. 6.3), and declines steadily on subsequent days.

6.2.3 Composite dynamic characteristics

An explanation for the total ozone maxima associated with COL events, was sought in the atmospheric dynamics of upper air COL systems. A suitable atmospheric tracer for this purpose is isentropic PV.

COL systems are easily identified as isolated regions of high PV on isentropic surfaces. The composite spatial distribution of PV (Fig. 6.4) on the 340 K isentropic surface, which corresponds roughly to the height of the 300 hPa surface, shows a closed vortex centred around the upper air COL on all five days. The region of concentrated PV extends over approximately 1200 km (estimated from the latitudinal extent of the outermost closed contour). Particularly high values (400-450 x 10^{-7}K hPa^{-1} s^{-1}) at the COL centre, and steep PV gradients are noticeable on day -1 and day 0. Such high PV values are characteristic of stratospheric air, but which may extend to tropospheric altitudes during processes which facilitate STE. This suggests that air of stratospheric origin entered the upper troposphere (approximately 300 hPa) in the vicinity of the COL centre.

The orientation, position and shape of the region of high PV corresponds well with the total ozone maxima shown in Figure 6.2. These observations confirm the well known positive relationship between ozone and PV. It is expected, then, that the total ozone maxima, associated with upper air COLs, are products of the transport of ozone-rich stratospheric air into the troposphere.

In order to investigate the role of STE further, a series of composite vertical cross sections of PV, through the pressure minimum at 300 hPa (taken

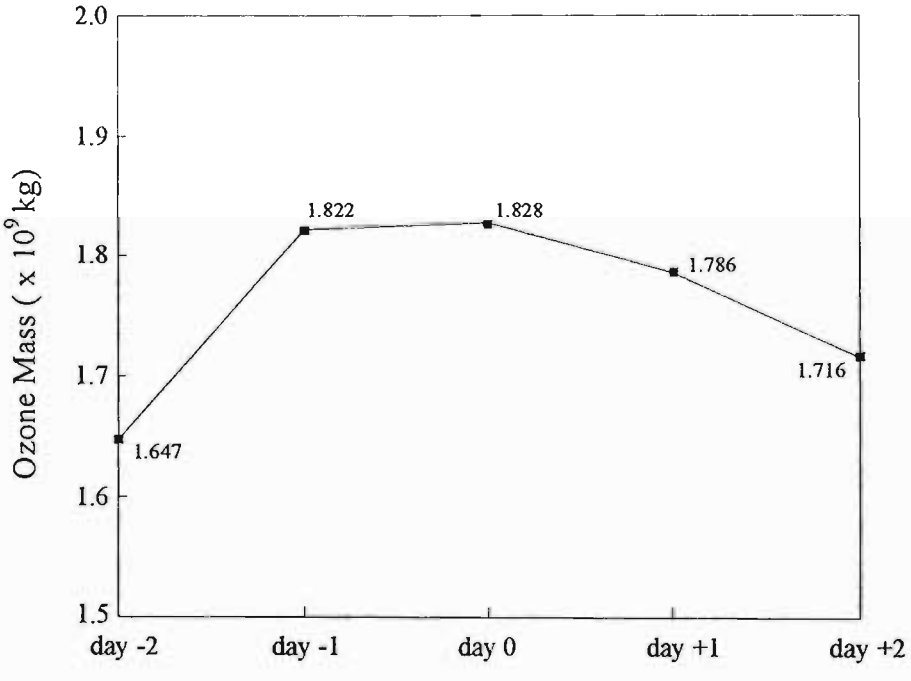

Figure 6.3 Composite ozone mass (kg), calculated for a grid of 5° latitude x 5° longitude over centre of the COL, for day -2 to day +2. Derived from TOMS data supplied by NSSDC.

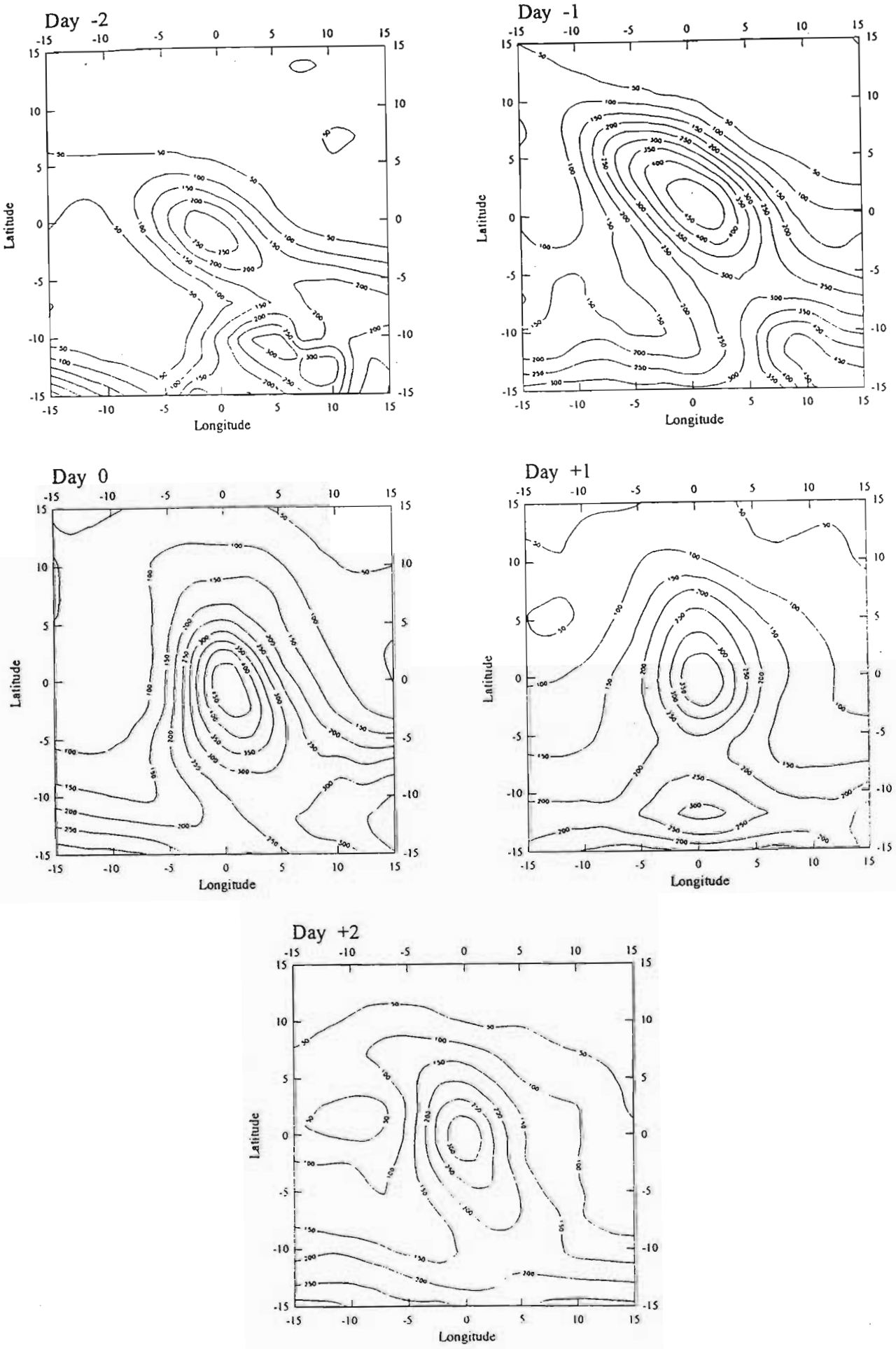

Figure 6.4 Composite spatial distribution of PV (x 10^{-7} $KhPa^{-1}s^{-1}$) on the 340 K isentropic surface, for 15° latitude and 15° longitude either side of the composite COL centre, for day -2 to day + 2. Prepared from ECMWF data. The centre of the upper-air (300 hPa) COL was fixed at 0° latitude x 0° longitude

as the centre of the upper air COL), were constructed (Fig. 6.5). COL systems are characteristically associated with lower tropopause heights relative to the surrounding atmosphere. If 100 x 10^{-7}K hPa^{-1} s^{-1} is taken as the PV tropopause (Shapiro, 1980; 1978), marking the boundary between relatively higher PV levels in the stratosphere and lower levels in the troposphere, tropopause heights can be easily estimated. The PV field shows a downward extension of stratospheric air into the troposphere centred around the upper air COL and is best illustrated on days -1 and 0 (Fig. 6.5). The downward extension of, or undulation in the PV tropopause, reaches well into the troposphere to approximately 5 km on days -1 and 0. On days -2, +1 and +2, the high PV values associated with the centre of the COL are located at approximately 7 km above the surface. The well defined PV maximum and relatively less complex pattern in the upper troposphere on day -2 is explained by the fact that day -2 represents data for one day only (refer to Table 2.1). On day 0, a core of high PV values (550-600 x 10^{-7} $KhPa^{-1}s^{-1}$) is situated roughly at the centre of the composite COL and is located within the vicinity of the downward extension of the PV tropopause on that day. The gradient of the PV isolines is particularly steep in the region of this core. On preceding and subsequent days, the PV isolines are more laminar, although the 100 x 10^{-7} $KhPa^{-1}s^{-1}$ PV isoline still extends downward into the upper troposphere. It is recognised that the composite described here represents a variable statistical sample and as such, should be regarded with caution. Nevertheless, despite the limitations of the sample, the association between the presence of a COL and possible tropopause folding is illustrated.

In the absence of vertical ozone profiles to verify the intrusion of stratospheric air into the troposphere, further evidence was sought in other meteorological parameters. Since stratospheric air is characteristically dry, compared to tropospheric air, composite RH profiles were constructed for the five-day period. A region of relatively dry air (RH=10 to 20%) extends downward into the troposphere, in the region of the centre of the COL, on day -1 and day 0 (Fig. 6.6). An elongated tongue of very dry air reaches downward to approximately 6 km on both days. Thereafter, the RH isolines show a more horizontal pattern. More moist air (RH > 30%) is located in the upper air ahead of the COL system. This is particularly noticeable on day +1 and +2 when RH reaches between 60 and 90%. The dry air intrusion into the upper troposphere on days -1 and 0 correspond to the region of the PV intrusions on those days and provides additional evidence of the intrusion of stratospheric air into the troposphere.

The composite pattern of vertical motion associated with COL systems is presented in vertical cross sections of ω, through the centre of the upper air (300 hPa) COL (Fig. 6.7). On all days a boundary, situated roughly at the centre of the composite COL, between upward and downward motion extends from

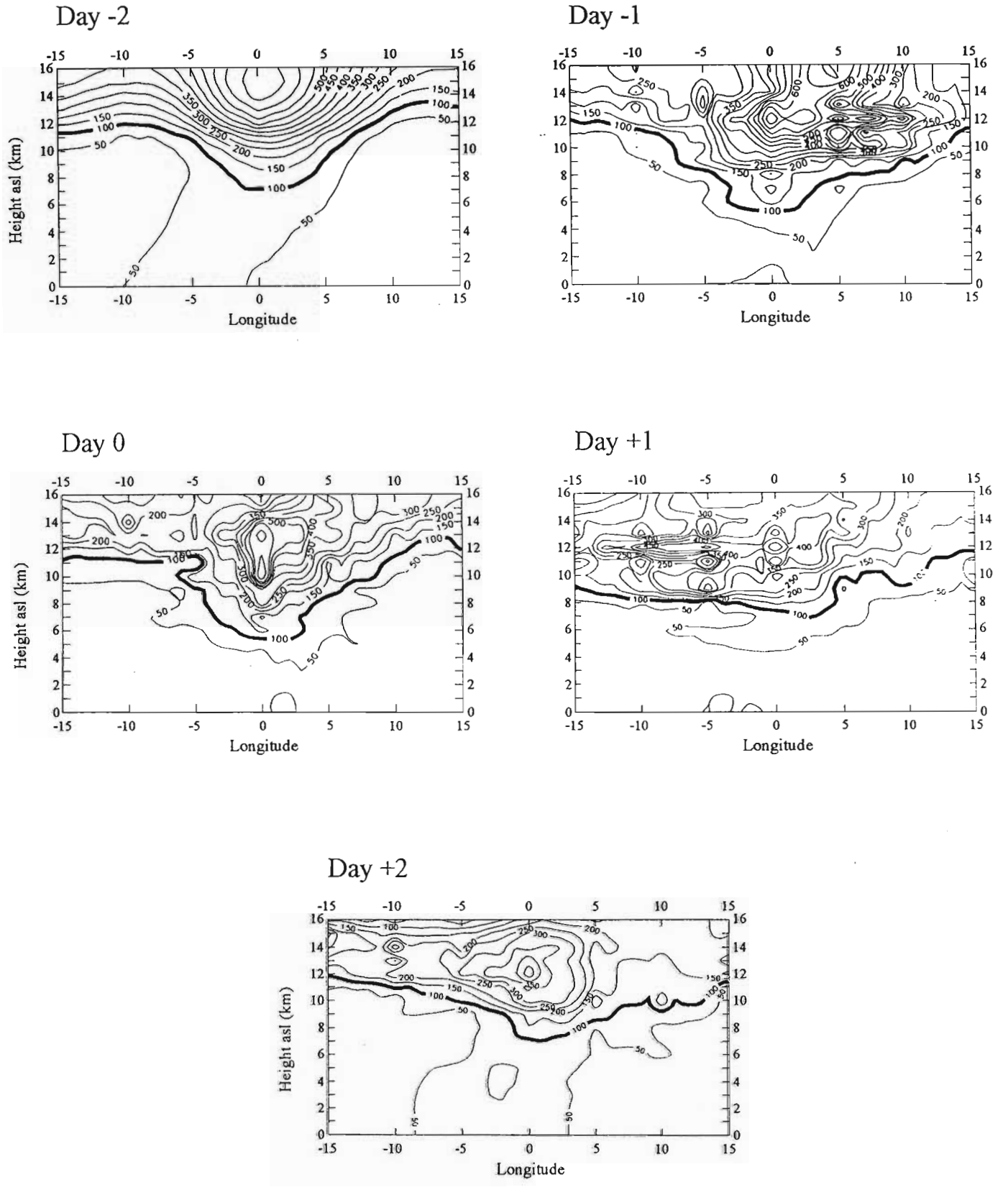

Figure 6.5 Composite vertical cross sections of PV (x 10^{-7} $KhPa^{-1}s^{-1}$), through 0° latitude and 15° latitude either side of the COL centre, for day -2 to day +2. Prepared from ECMWF data.

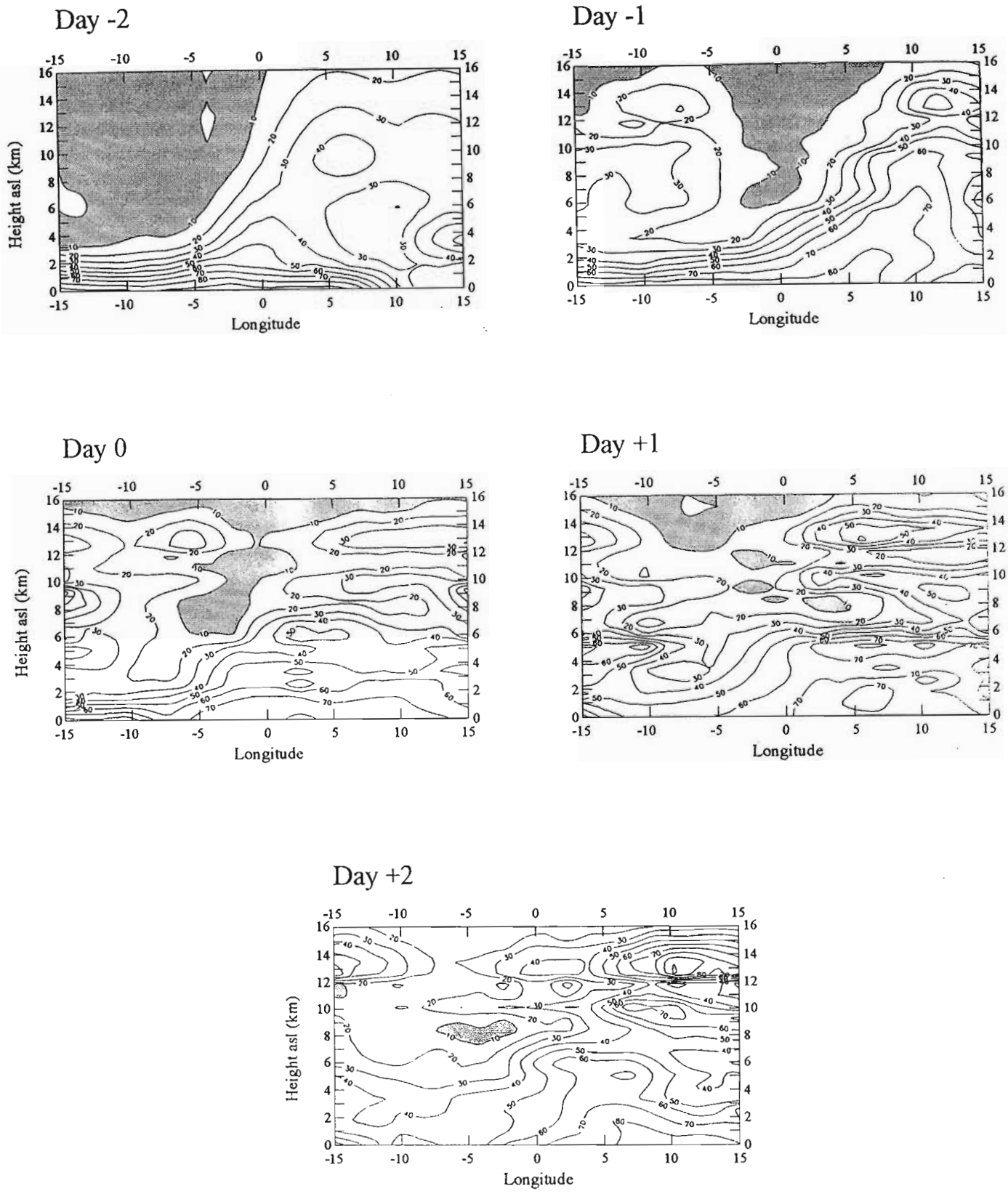

Figure 6.6 Composite vertical cross sections of RH (%), through 0° latitude, for day -2 to day +2. Prepared from ECMWF data. Shading indicates RH ≤ 10%.

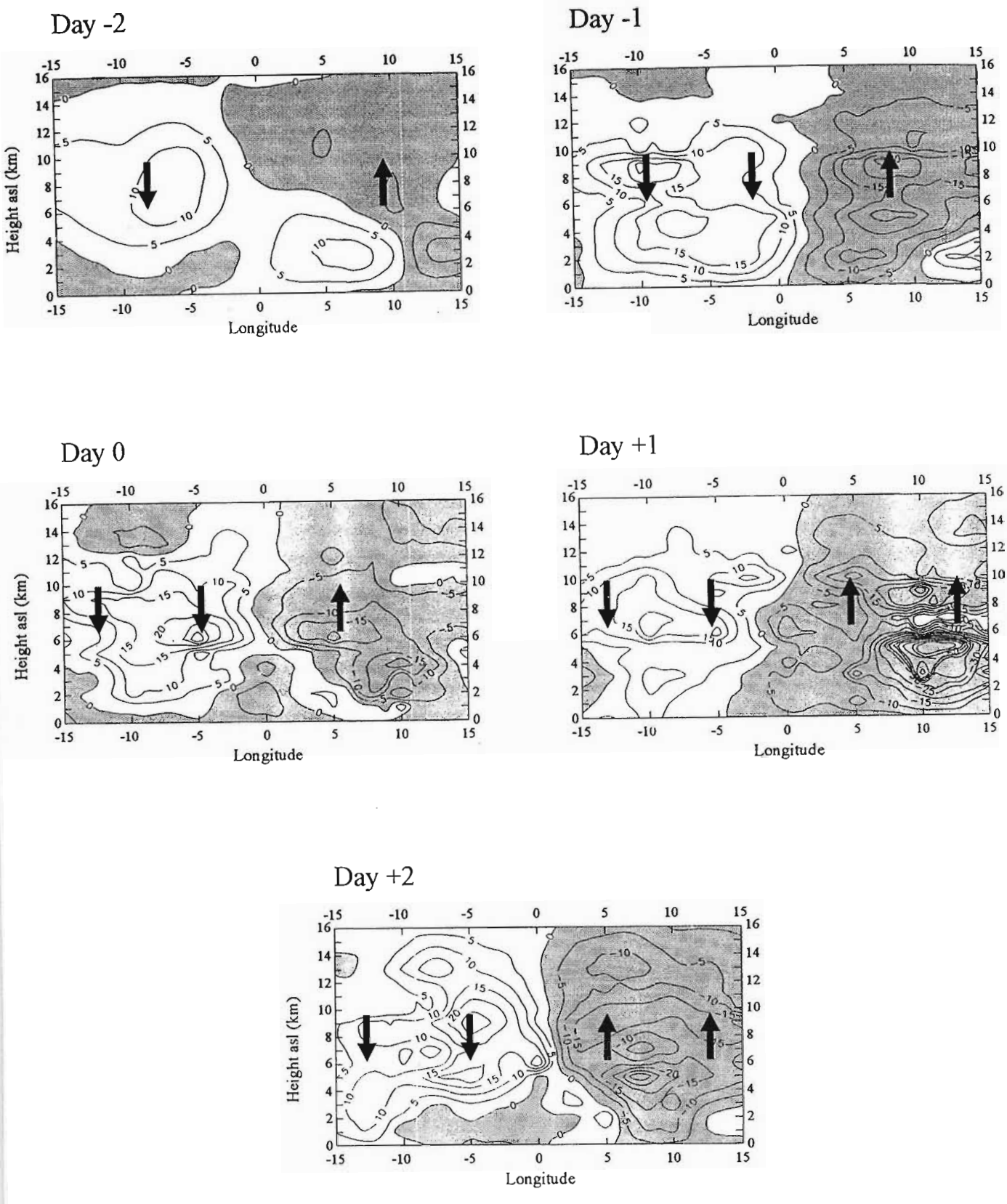

Figure 6.7 Composite vertical cross sections of the ω (Pa s^{-1}) component of the wind, through 0° latitude, for day -2 to day +2. Prepared from ECMWF data. Arrows indicate upward and downward motion. Regions of upward motion (ω < 0) are shaded.

the surface to the lower stratosphere. The boundary is best defined in the middle and upper troposphere. On all days, with the exception of day -2, cores of increased vertical motion are observed between altitudes of approximately 5 and 10 km, located on the east and west sides of the discontinuity. Upward motion occurs on the eastern side, while downward motion is concentrated on the west side of the boundary. Well developed cores of upward (20 Pa s^{-1}) and downward (30 Pa s^{-1}) motion occurred on day 0. The circulation pattern exhibited resembles that accompanying Danielsen's (1968) two-cell model described in Chapter 5. Upward motion in the direct cell occurs in the upper troposphere, ahead of the COL centre, while strong downward motion is concentrated on the west of, but in close proximity to the COL centre. Weaker upward motion, of the indirect cell, is observed on the far western side of the boundary.

Composite vertical cross sections of wind speed (Fig. 6.8) indicate strong vertical wind shear and the presence of jets on either side of the region of the COL centre reflecting the cyclonic circulation. Particularly strong jets (> 40 m s^{-1}) are evident in the upper troposphere (between 8 and 12 km) to the east (ahead) of the COL centre on days -1 and 0. The pattern is reversed on day +1 with strongest wind speeds occurring to the west (rear) of the COL centre, while no prominent jet is observed on day +2. A region of relatively calm air is situated within and beneath the centre of the COL system and is positioned to the west of the upper tropospheric jet stream on days -1 and 0. The two cores of high wind speed shown here present a different picture to that of Danielsen (1968). Rather, Danielsen's (1968) model showed a single core of high wind speed in the vicinity of the tropopause break.

6.2.4 Summary

In summary, it appears from the composite analysis that the total ozone maximum associated with COL systems over southern Africa may be explained by the injection of ozone-rich stratospheric air into the troposphere. The ozone maximum corresponds well with the PV maximum in the region of the COL centre on days when the composite COL is deepest. As the COL system weakens, the total ozone and PV maxima also weaken. Composite vertical cross sections of PV and RH, through the COL centre, provide evidence for the intrusion of dry, ozone-rich stratospheric air into the troposphere. In addition, the composite vertical motion field resembles that described by Danielsen's (1968) two-cell model. Strong downward motion behind the COL centre in the upper air would facilitate the downward transport of stratospheric air in association with a fold or undulation in the tropopause.

Composite analysis as described above, although providing evidence of STE,

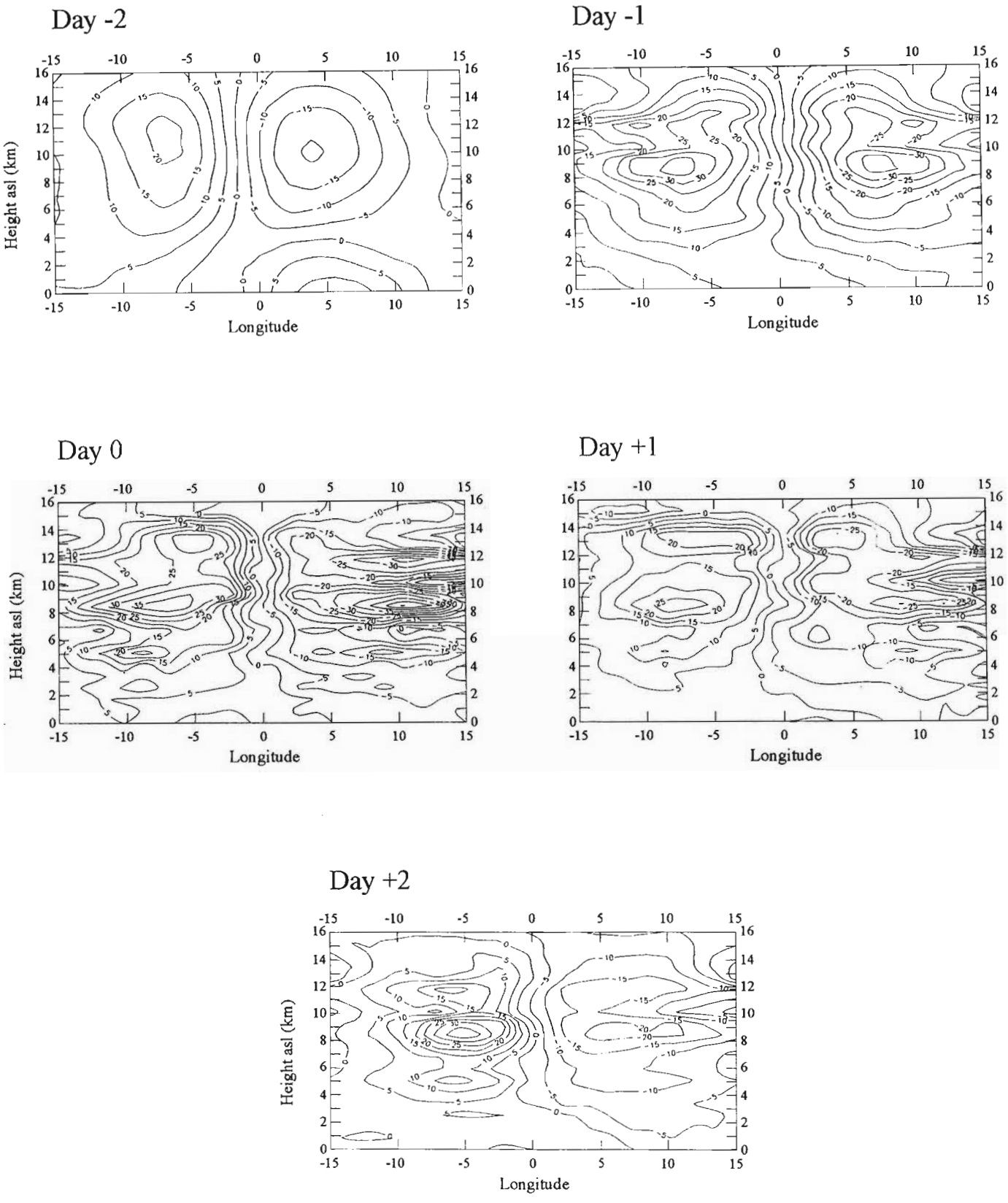

Figure 6.8 Composite vertical cross sections of the v component of the wind (m s^{-1}), through 0° latitude, for day -2 to day +2. Prepared from ECMWF data.

masks the intensity of the tropopause undulations/folds which may contribute to STE. For this reason, an individual case study is presented next.

6.3 CASE STUDY OF A COL AND TOTAL OZONE DISTRIBUTION

6.3.1 Description of the COL event

The period of 26 to 29 September 1987 was selected for case study analysis, as it is representative of a particularly deep COL system, which was responsible for severe floods over KwaZulu-Natal, situated on the eastern seaboard of South Africa. Surface synoptic charts for this period (not shown here) revealed an intense, slow-moving high pressure system situated to the southeast of the country. It was responsible for the advection of cold, moist air into the surface trough and deep low pressure system located over the interior of South Africa. The system moved steadily eastward. A deep trough, aligned in a northwest/southeast direction over the western half of South Africa, was evident at the 300 hPa level on 26 September (Fig. 6.9). As the upper air system moved eastwards over the country, an upper air COL developed and was present on 28 and 29 September (Fig. 6.9). By 30 September, the substantially weakened low pressure system had moved off the east coast.

The passage of the COL over South Africa is reflected in the time series of tropopause heights derived from radiosonde ascents at Cape Town, Port Elizabeth and Durban over the period 26 to 29 September 1987 (Fig. 6.10). On 26 September, when the COL system was situated over Cape Town, the tropopause height was approximately 10 km (asl). As the COL system moved eastwards the tropopause height increased, at Cape Town, to approximately 13 km (asl). Tropopause heights remain fairly stable (~ 10500 gpm (asl)) over Port Elizabeth, but a slight decrease in height was observed on 27 September. As the COL moved north-eastwards towards the east coast the tropopause height decreased significantly at Durban on 28 and 29 September.

6.3.2 Total ozone distribution

Figure 6.11 shows the spatial distribution of total ozone in the region bounded by latitudes 0° to 50°S and longitudes 10°W to 50°E for 26 to 29 September 1987. Enhanced total ozone values are evident in the region of the 300 hPa trough. The ozone maximum is aligned in a northwest/southeast direction as is the trough. The ozone maximum is best expressed on 26 and 27 September when values exceed 350 DU in the vicinity of the COL. In contrast

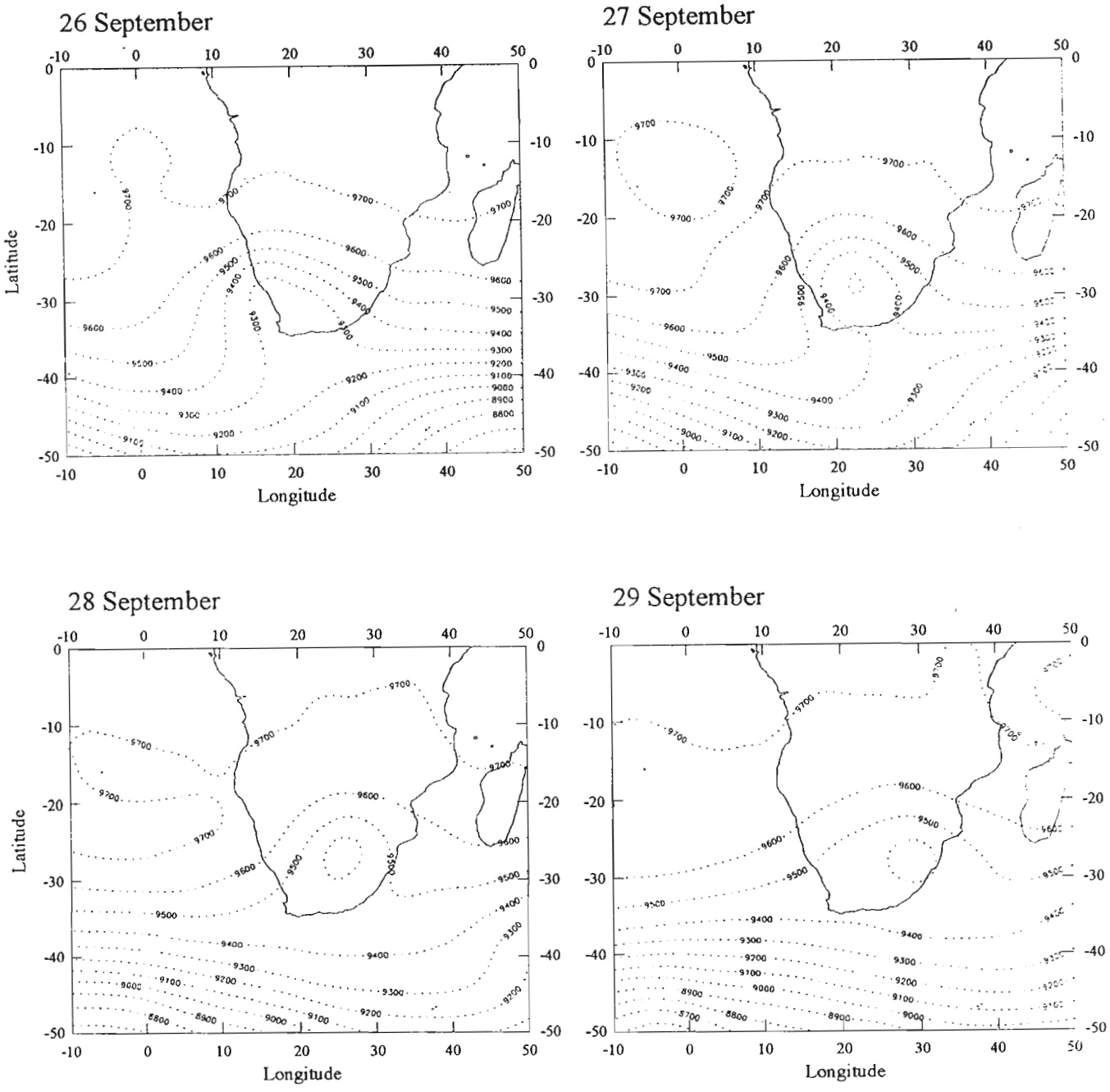

Figure 6.9 Heights of the 300 hPa (gpm) isobaric surface, over southern Africa for a region bounded by latitudes 0° to 50°S and longitudes 10°W to 50°E, for 26 to 29 September. Prepared from ECMWF data.

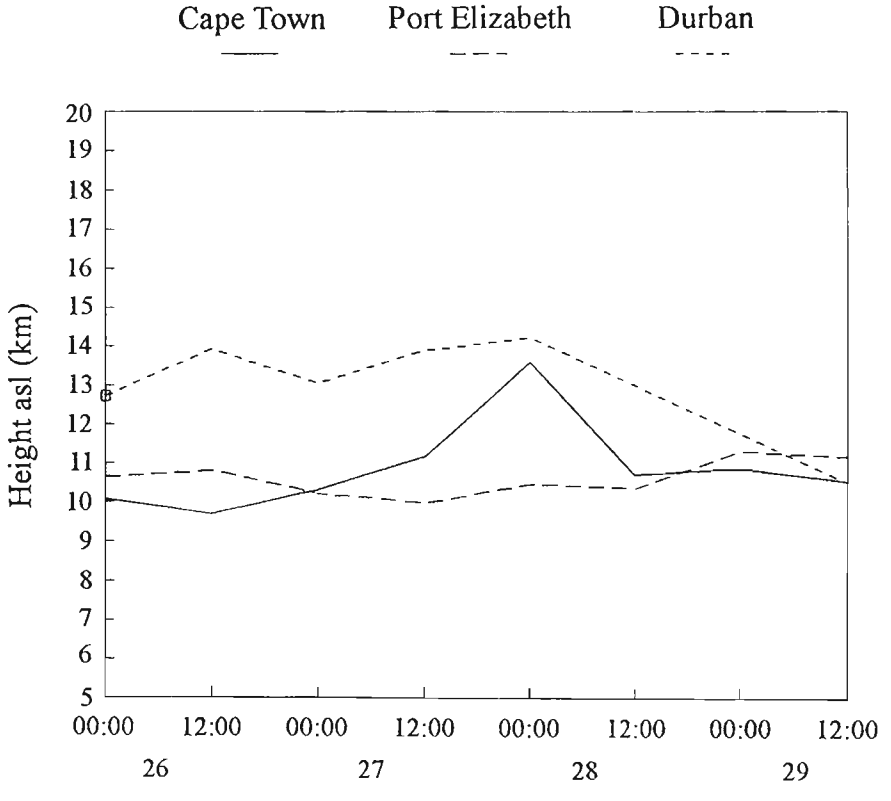

Figure 6.10 Time series of tropopause heights (gpkm) above sea level, at Cape Town, Port Elizabeth and Durban for 26 to 29 September 1987. Derived from midday and midnight radiosonde data (SAWB).

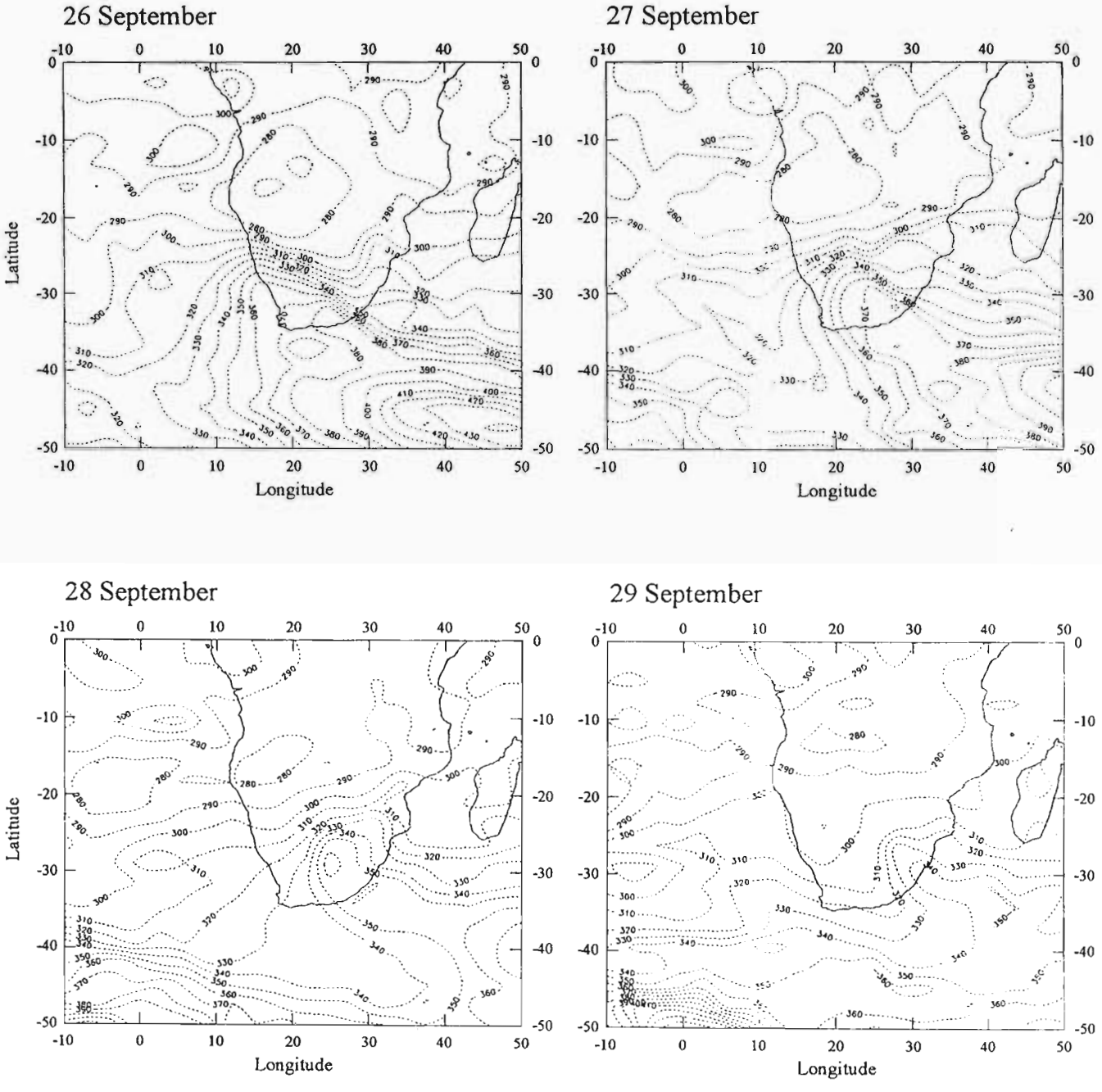

Figure 6.11 Spatial distribution of TOMS total ozone (DU) in the area bounded by latitudes 0° to 50°S and longitudes 10°W to 50°E for 26 to 29 September 1987. Prepared from data supplied by NSSDC.

to areas removed from the sphere of influence of the westerly disturbance, the strong gradient of the isolines reflects the rapid change in ozone over the subcontinent during the passage of the COL system. Thereafter, the region of enhanced ozone moved eastwards and weakened (340 DU) following the COL system.

6.3.3 Dynamic characteristics of the COL event

The spatial distribution of PV on the 340 K isentropic surface (Fig. 6.12), which corresponds roughly to the height of the 300 hPa isobaric surface and is located between approximately 8900 to 12000 gpm (asl) during the period 26 to 29 September 1987, exhibits maximum values (350 - 700 x 10^{-7}K hPa^{-1} s^{-1}) in the vicinity of the upper air COL system. On 26 and 27 September, cores of high PV values occur in the region of the deep trough and COL centre. Particularly steep gradients of the PV isolines are evident on those days. The PV maxima correspond well to the regions of maximum total ozone (ranging between 370 and 430 DU) present on 26 to 29 September, in the vicinity of the COL system, and which extends from the west coast across the continent, south-eastward into the Indian Ocean (Fig. 6.12).

A sequence of vertical cross sections of PV, through the COL at 30°S are shown in Figure 6.13. The cross sections cut through the region of maximum wind speed on the 320 to 360 K isentropic surfaces. Figure 6.13 reveals an intrusion of high PV extending downward into the troposphere between 10° and 30°E in the vicinity of the COL system. The intensity of the stratospheric intrusion is greatest on 26 and 27 September. A core of high PV (700 - 850 x 10^{-7} $KhPa^{-1}s^{-1}$) is located within the tropopause undulation and coincides with the centre of the upper air COL. On 28 September the core of high PV weakened and shifted slightly to the east which reflects the position of the upper air COL on that day. On 29 September the high PV core has shifted to a higher altitude above the COL. PV values in the mid- and upper troposphere are more uniform in the horizontal dimension in response to the weakening low pressure system.

The intrusion of stratospheric air into the troposphere is supported by RH (%) cross sections which reveal very dry air (10-30%) in the vicinity of the upper air COL, particularly on 26 and 27 September, when the intrusion extends toward the surface (Fig. 6.14). This region of dry air moves eastward and dissipates as the COL system weakens. Coupled with this intrusion are well developed jet streams, occurring roughly on either side of the tropopause undulation (Fig. 6.15). The jet is particularly well developed (> 40 ms^{-1}) on 26 and 27 September to the east (ahead) of the tropospheric intrusion, while a weaker (30 ms^{-1}), but prominent jet, is located to the rear of the COL centre on 29 September. A similar observation was noted for the composite COL.

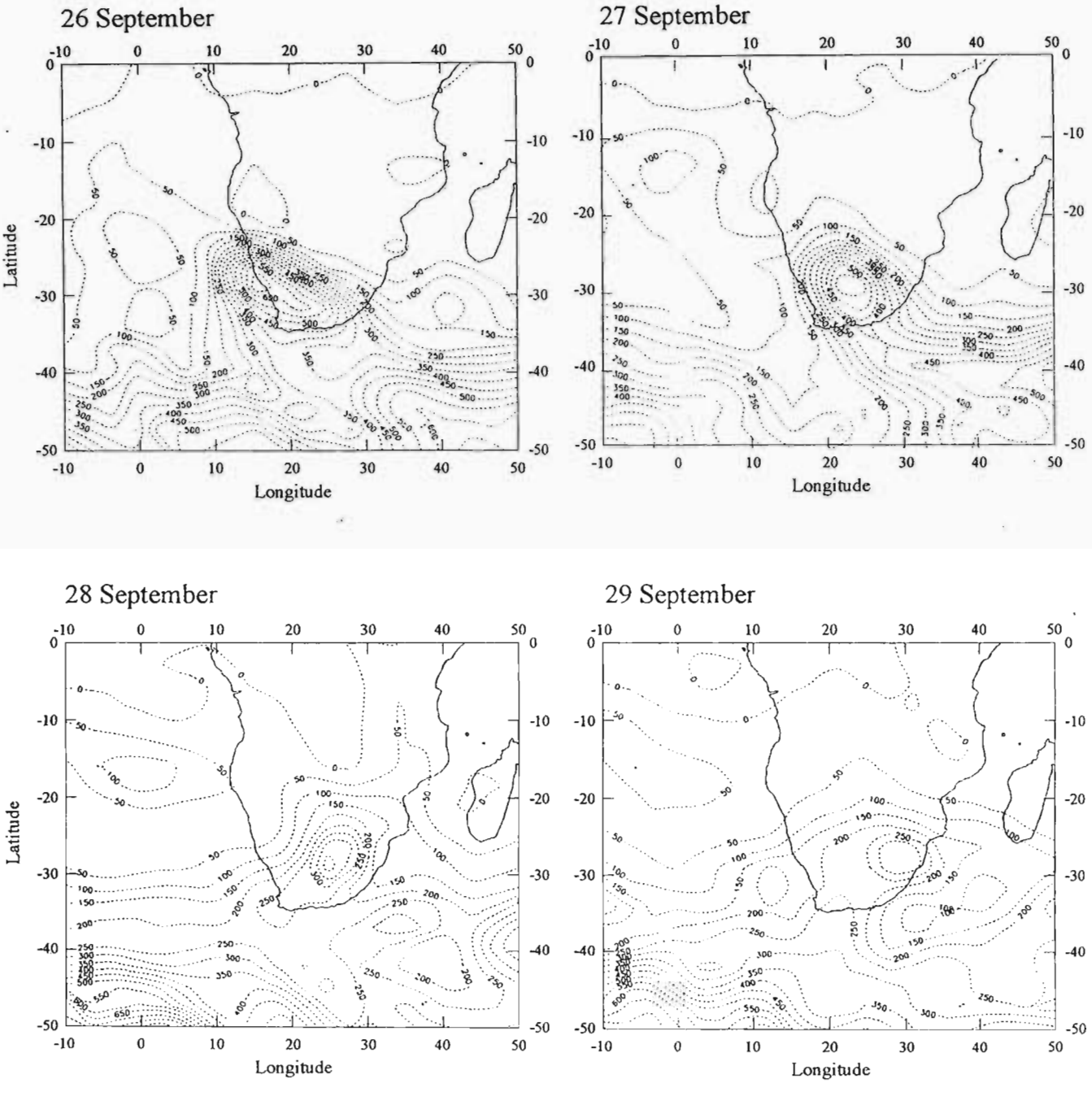

Figure 6.12 Spatial distribution of PV (x 10^{-7} $KhPa^{-1}s^{-1}$) on the 340 K isentropic surface, in the area bounded by latitudes 0° to 50°S and longitudes 10°W to 50°E, for 26 to 29 September 1987. Prepared from ECMWF data.

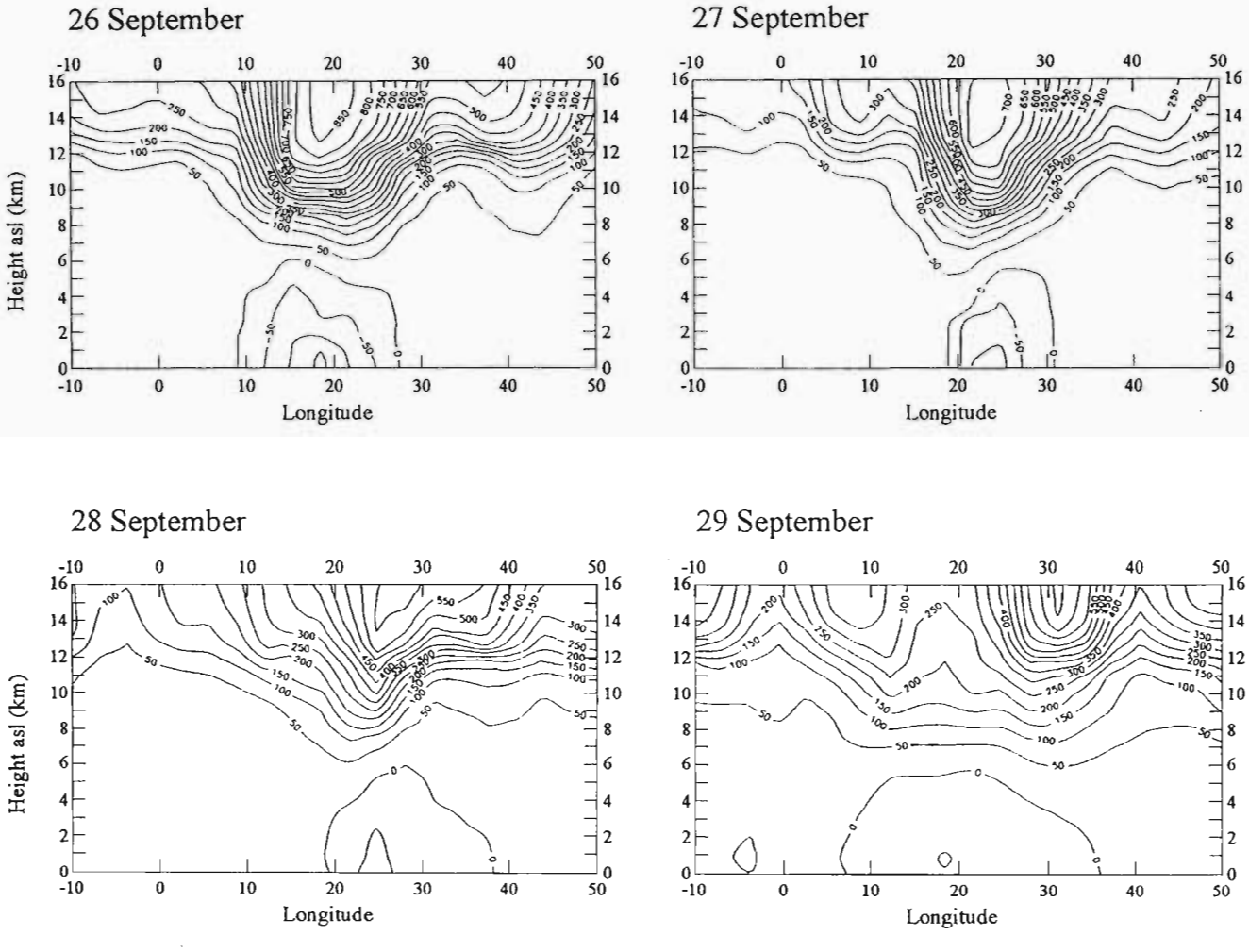

Figure 6.13 Vertical cross sections of PV (x 10^{-7} $KhPa^{-1}s^{-1}$), through 30°S, for 26 to 29 September 1987. Prepared from ECMWF data.

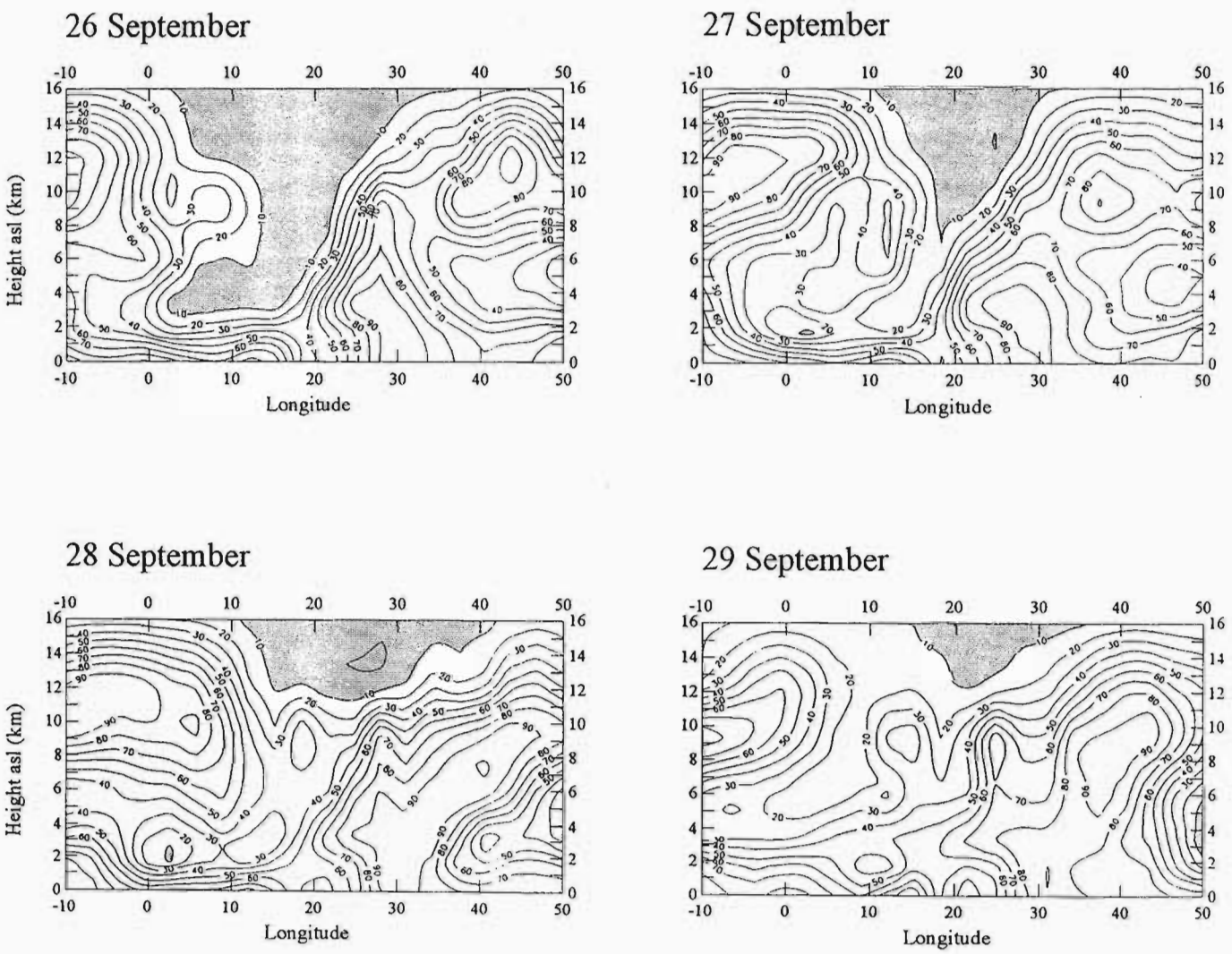

Figure 6.14 Vertical cross sections of RH (%), through 30°S, for 26 to 29 September 1987. Prepared from ECMWF data. RH ≤ 10% is shaded.

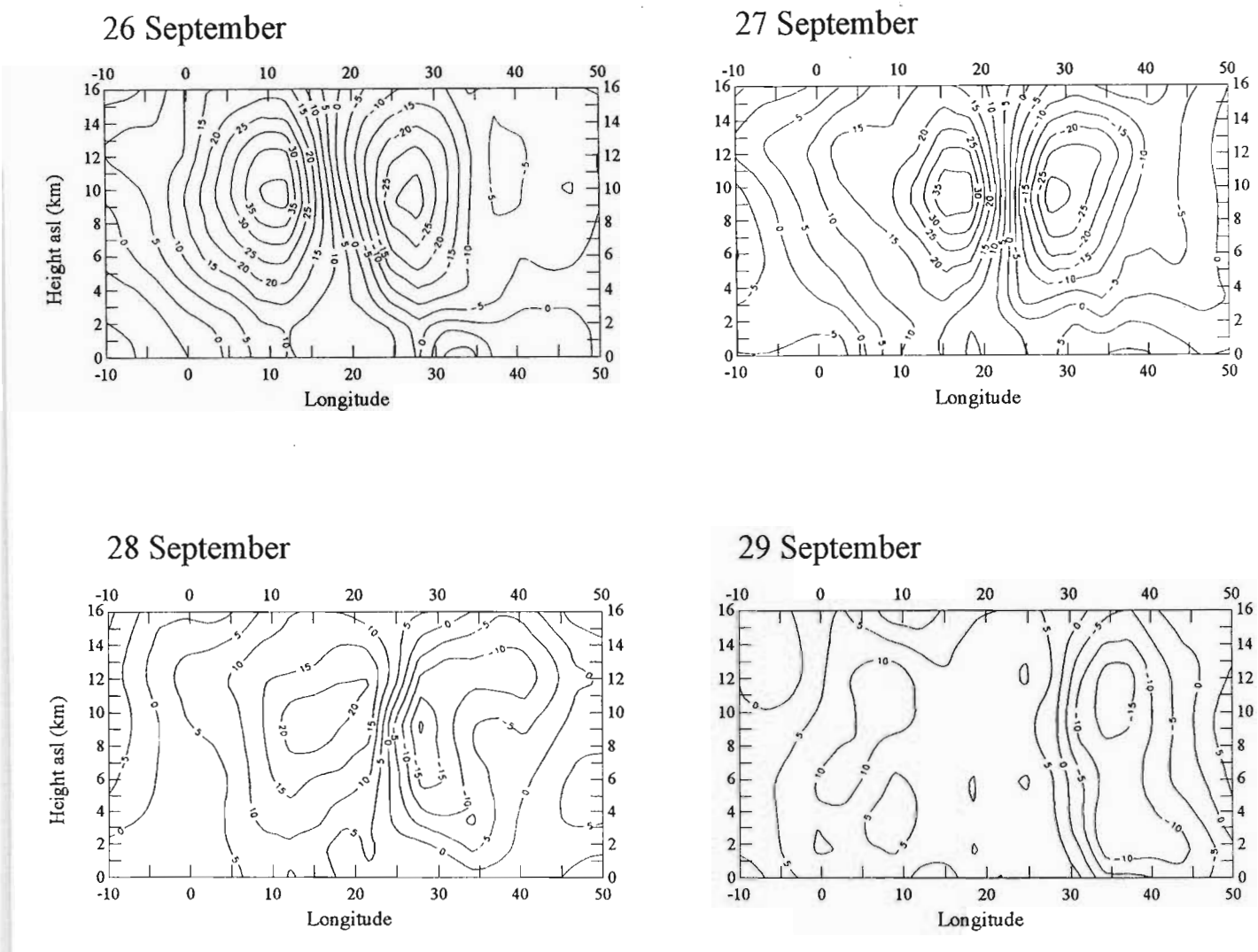

Figure 6.15 Vertical cross sections of the v component of the wind (m s^{-1}), through 30°S, for 26 to 29 September 1987. Prepared from ECMWF data.

A series of vertical cross sections, through the centre of the COL (30°S), of ω, reveal vertical motion which is compatible with the model proposed by Danielsen (1968) (Fig. 6.16). On all four days a clear discontinuity, coincident with the centre of the COL, is observed in the vertical cross sections (Fig. 6.16). Much of the vertical motion is confined within the 2 to 10 km layer. Upward motion occurs to the east of the boundary and downward motion is concentrated on the west side of the boundary. Upward flow consistent with the upward motion in the direct cell, relative to a tropopause fold in Danielsen's model, is evident in the data. On 26, 27 and 28 September, strong upward motion (-10 to -80 Pa s^{-1}) is present ahead of the upper tropospheric high PV intrusion. This pattern is present on 29 September but with weakened vertical flow. Downward flow occurs in the vicinity of, but slightly to the west of, the PV intrusion (approximately located between 10 and 20°E) on 26 to 28 September. A closed core of descending motion, located at approximately 6 km above the surface, is present on these three days but is greatest (40 Pa s^{-1}) on 26 and 27 September. The region of descending motion is located to the west of the region of maximum wind speed in the upper troposphere which is evident on 26 and 27 September (Figure 6.15). The vertical motion field reflects a similar pattern as presented by Danielsen (1968). Ascending motion occurs ahead (east) of the PV and dry air intrusion (Figures 6.13 and 6.14 respectively), within the direct cell, while descending motion is maximised in the region of the PV maximum, to the rear (west) of the discontinuity in the vertical motion field.

Vertical cross sections of temperature through 30°S for this period show no significant variation in the region ahead of, or behind the COL (Fig. 6.17). However, a region of warm air, relative to the surrounding atmosphere, is present between 10° and 28°E above 11 km on 26 and 27 September. The warm air anomaly is located within the PV, dry air intrusion and situated to the west of the upper air jet. This feature is consistent with the warm pool located above the circulation centre of a cut off cyclone as described by Bell and Bosart (1993) and others. The warm air anomaly is absent on 28 and 29 September when the COL system is less well developed.

6.3.4 Summary

It is acknowledged that this case study is an example of a particularly intense COL system which is associated with conditions most likely to produce an intrusion of stratospheric air into the troposphere. The intrusion of very dry air into the troposphere, in the vicinity of the upper air COL, and the accompanying downward motion from the stratosphere provides support for STE in the study area. From the evidence presented thus far, it is contended that subtropical COLs, of which the case study presented here is an example, play

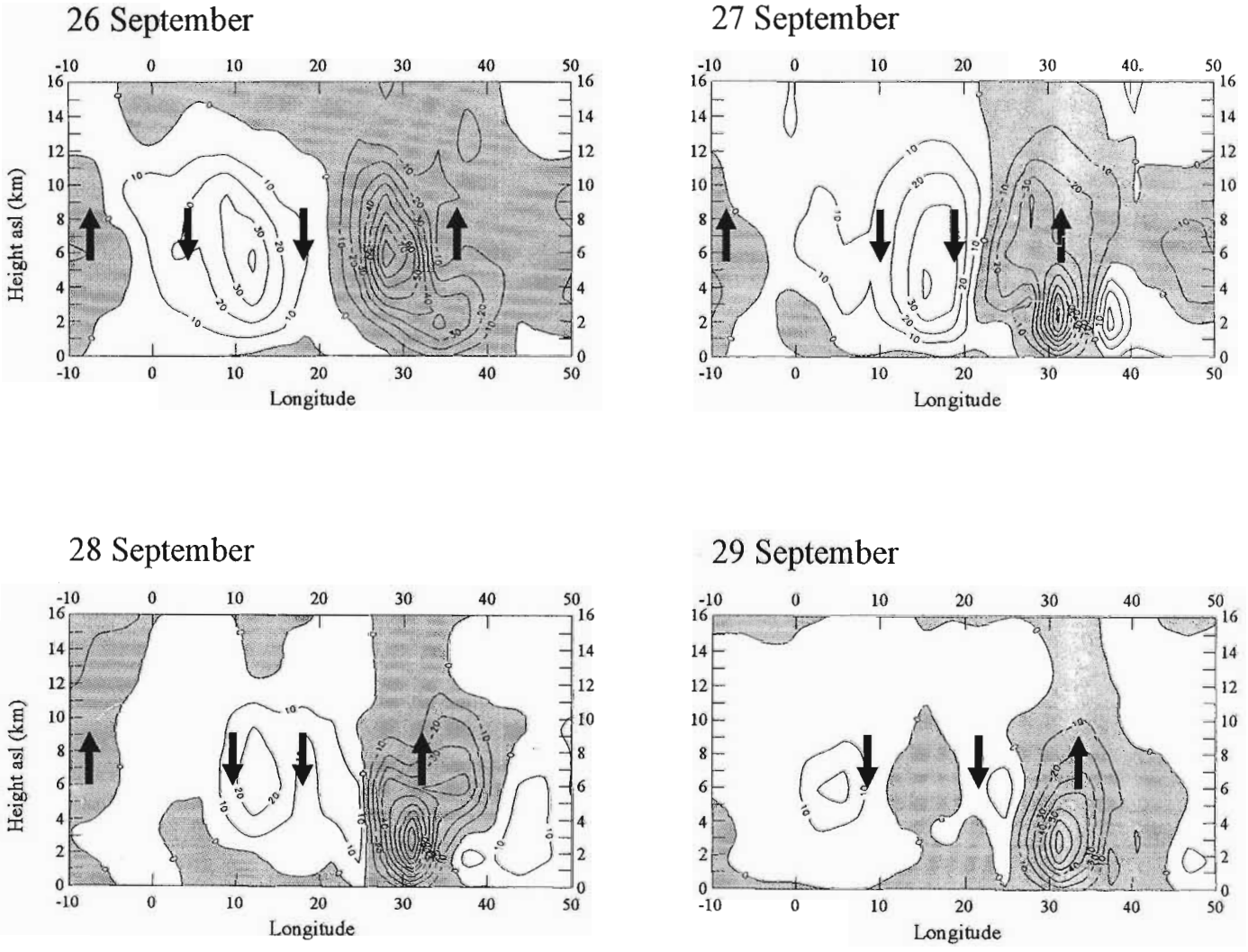

Figure 6.16 Vertical cross sections of ω (Pa s^{-1}), through 30°S, for 26 to 29 September 1987. Prepared from ECMWF data. Arrows indicate upward and downward motion. Regions of upward motion (ω < 0) are shaded.

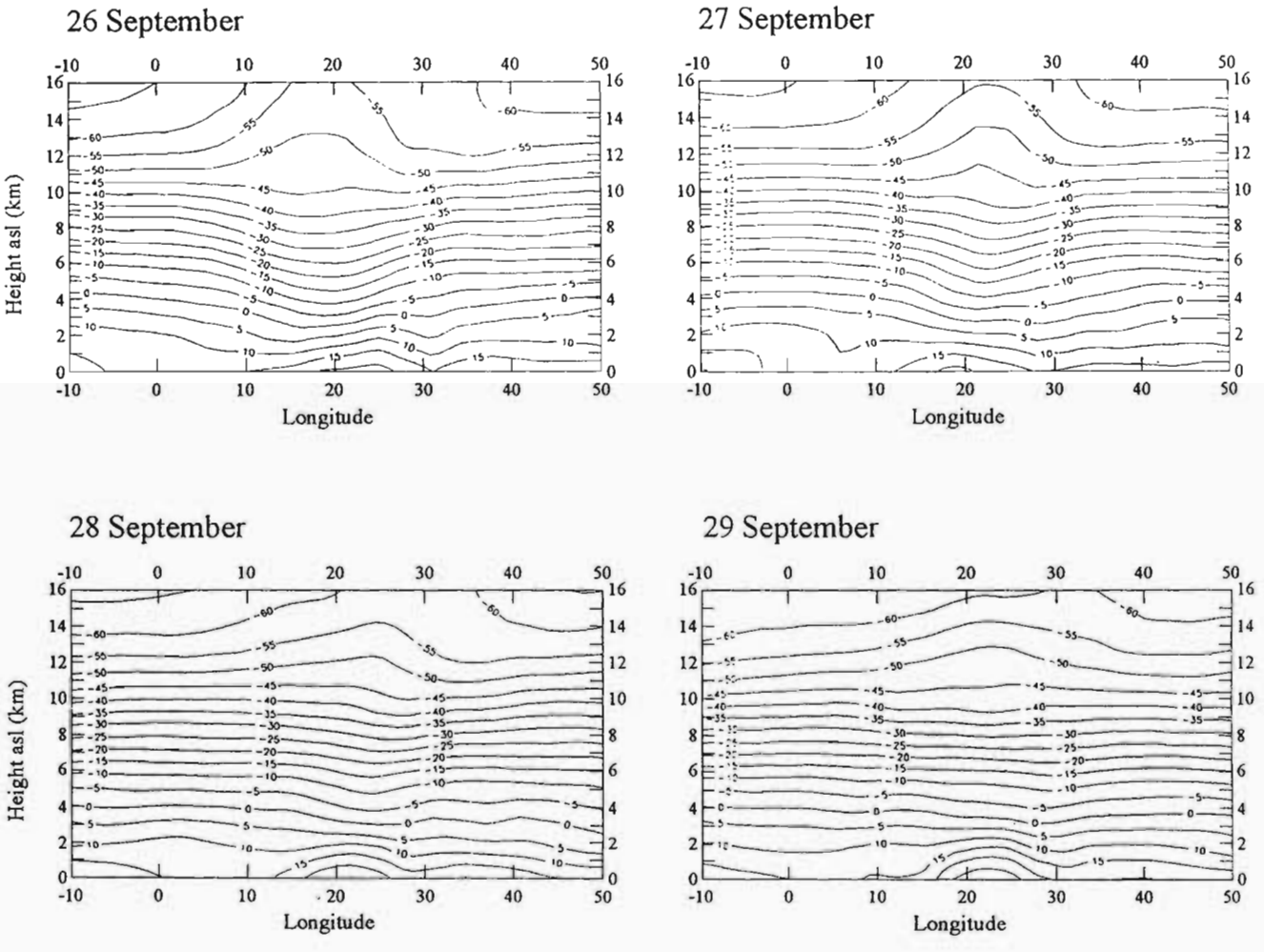

Figure 6.17 Vertical cross sections of temperature (°C), through 30°S, for 26 to 29 September 1987. Prepared from ECMWF data.

a significant role in the generation of total ozone maxima over southern Africa. This evidence suggests that subtropical COL systems, common over South Africa, may play a more significant role in STE than anticipated from the work of Price and Vaughan (1992).

The investigation of the vertical distribution of ozone during the passage of a COL system is the subject of the following section.

6.4 CASE STUDY OF A COL AND HORIZONTAL AND VERTICAL OZONE DISTRIBUTION

6.4.1 Introduction

Evidence providing strong support for STE during the passage of COL pressure systems over southern Africa has been provided above. It is recognised, however, that PV cross sections revealing stratospheric properties at tropospheric altitudes and accompanying increases in total ozone, do not provide conclusive proof that STE has taken place. An attempt is made in this section to investigate STE further by examining ozone profile characteristics. Ozonesonde data are particularly sparse over southern Africa so the analysis is restricted by the data set available. For this reason, STE is investigated for one case only, *viz* Irene (Pretoria), South Africa, when suitable data were collected during SA'ARI-94.

Irene is situated at 25°53'S and 28°13'E and periodically comes under the influence of well developed deep low pressure troughs and COL pressure systems, which occur most frequently between April and September (Taljaard, 1985). These synoptic features usually extend vertically into the stratosphere, thus disturbing the tropopause and create conduits for momentum and air mass transfer between the troposphere and stratosphere and *vice versa*, as discussed in Chapter 5.

Some investigations of vertical ozone distribution and the role of COLs have been documented in the literature. Bamber *et al* (1984) found evidence of STE in a stationary low by examining aircraft measurements of ozone mixing ratios and other chemical species over the north-east Atlantic. The observations revealed evidence of stratospheric air in the upper troposphere and increased variability in ozone mixing ratios above 6.1 km near the centre of the cold pool. The presence of a convectively stable layer at 5.2 km (530 hPa) confirmed the presence of a tropopause fold. Ebel *et al* (1991) provided further evidence of stratospheric intrusion, from ozone soundings and model

simulations of ozone injection, caused by a tropopause fold and COL. Simulations of ozone transport in a tropopause fold and COL revealed a decrease in stratospheric ozone while high levels of ozone occurred in the troposphere.

6.4.2 Description of case study

A case study, 27 to 30 May 1994, has been selected to examine the horizontal and vertical distribution of ozone and the dynamics of the atmosphere at Irene during the passage of a COL over South Africa. The centre of the COL was situated way to the south of the country, however, the effects of the cyclonic circulation were still observed over the continent.

Surface synoptic charts (Fig. 6.18) for this period show the passage of a deep trough moving north-eastwards over the country, producing rain along the southern and eastern coasts and adjacent interior and Mpumalanga (formerly Eastern Transvaal) on 28 and 29 May 1994. The cold front moved over Pretoria on 28 May. The passage of the deep trough over the country is reflected in the 12 Z radiosonde tropopause heights at Irene which steadily drop in height from approximately 17 gpkm on 27 May to approximately 12 gpkm on 29 May and which recover thereafter (Table 6.1). The extensive cloud band associated with this frontal system is depicted by visual satellite imagery for 12:00 (local time) for 27 to 30 May (Fig. 6.19). The upper air (300 hPa) synoptic charts are depicted in Figure 6.20. They show the development of the trough from 27 to 28 May and the subsequent eastwards movement. The charts also reveal that the centre of the system was located to the south of Irene.

Table 6.1 Radiosonde tropopause heights (asl) at Irene (12 Z), 27 to 30 May 1994

DATE	27	28	29	30
Altitude (gpm)	16675	15700	12540	13639

Horizontal windflow, as depicted by wind vectors from the ECMWF database, are indicated in Figures 6.21 and 6.22, in the lower troposphere (700 hPa) and upper troposphere (300 hPa) respectively. Wind flow near the surface, over the subcontinent, is weak and is dominated by anticyclonic circulation (Fig. 6.21). Stronger flow is evident in the westerly wave which is situated to the south-west of the subcontinent and which exerts considerable influence on wind flow. On 27 May, the amplitude of the wave increased significantly and

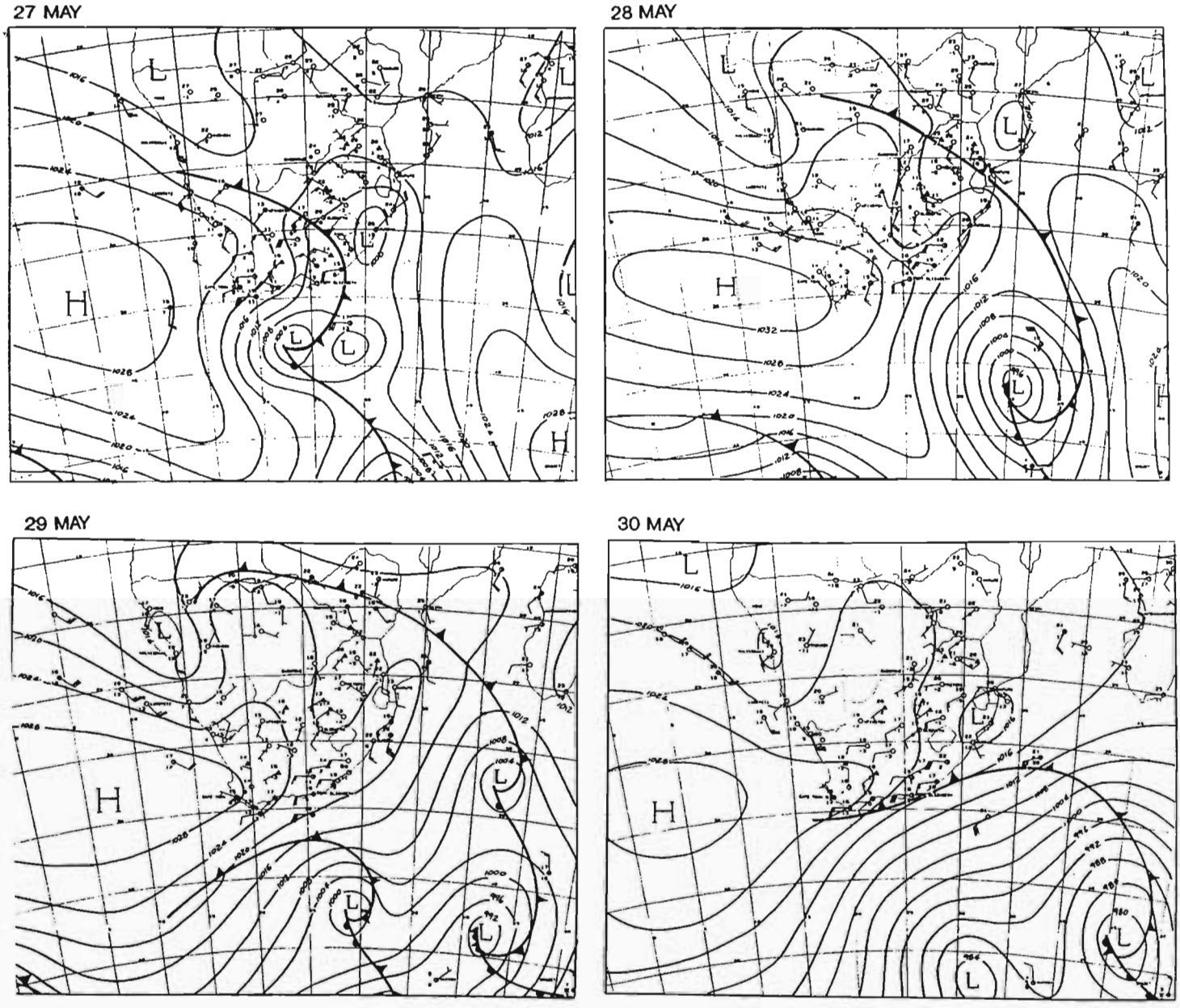

Figure 6.18 Surface synoptic charts over southern Africa for 27 to 30 May 1994. Surface pressure expressed as isobars (hPa) over the sea and heights of the 850 hPa surface (gpm) over the land. From Daily Weather Bulletin, SAWB.

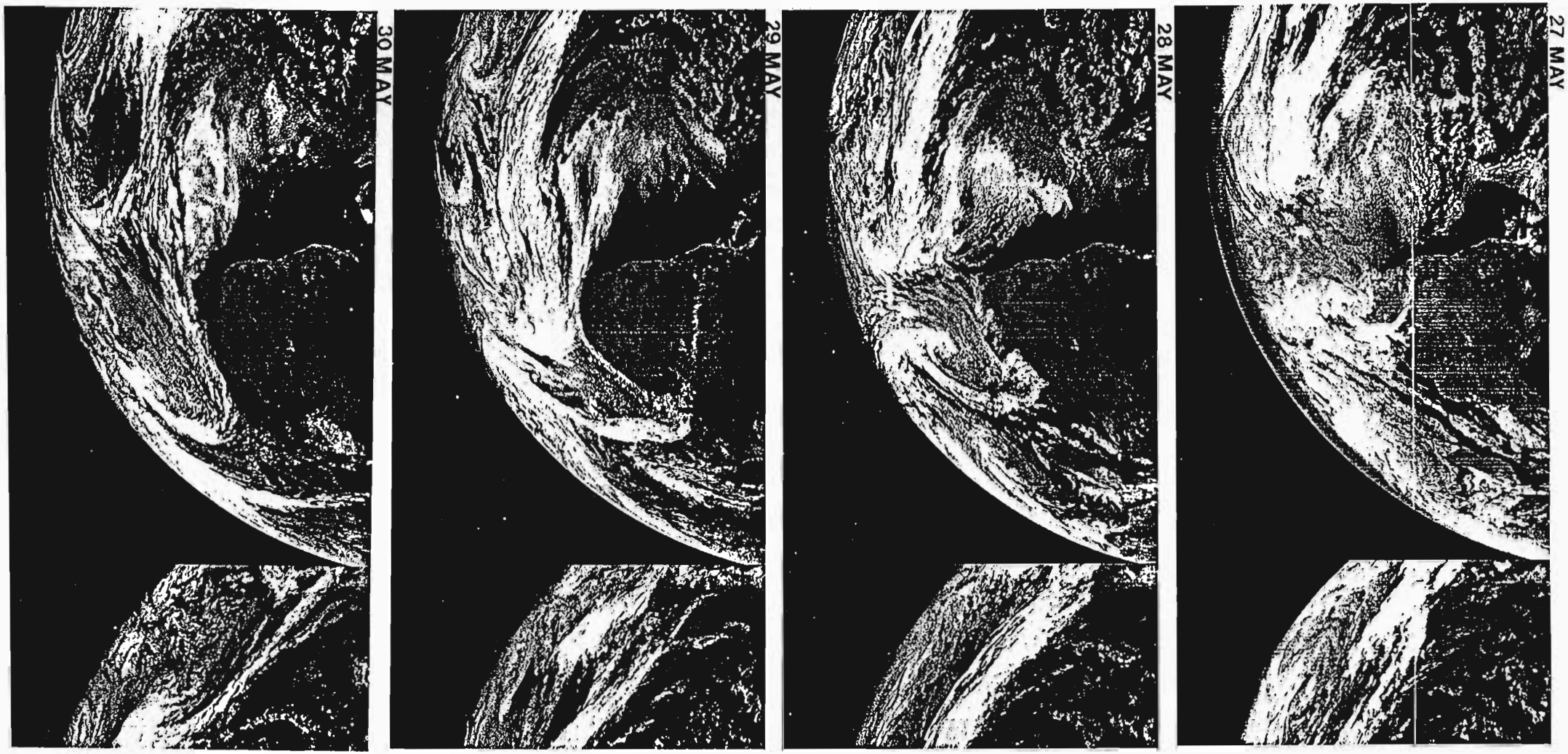

Figure 6.19 Meteosat visual satellite images (12:00 local time) for 27 to 30 May 1994, supplied by SAWB.

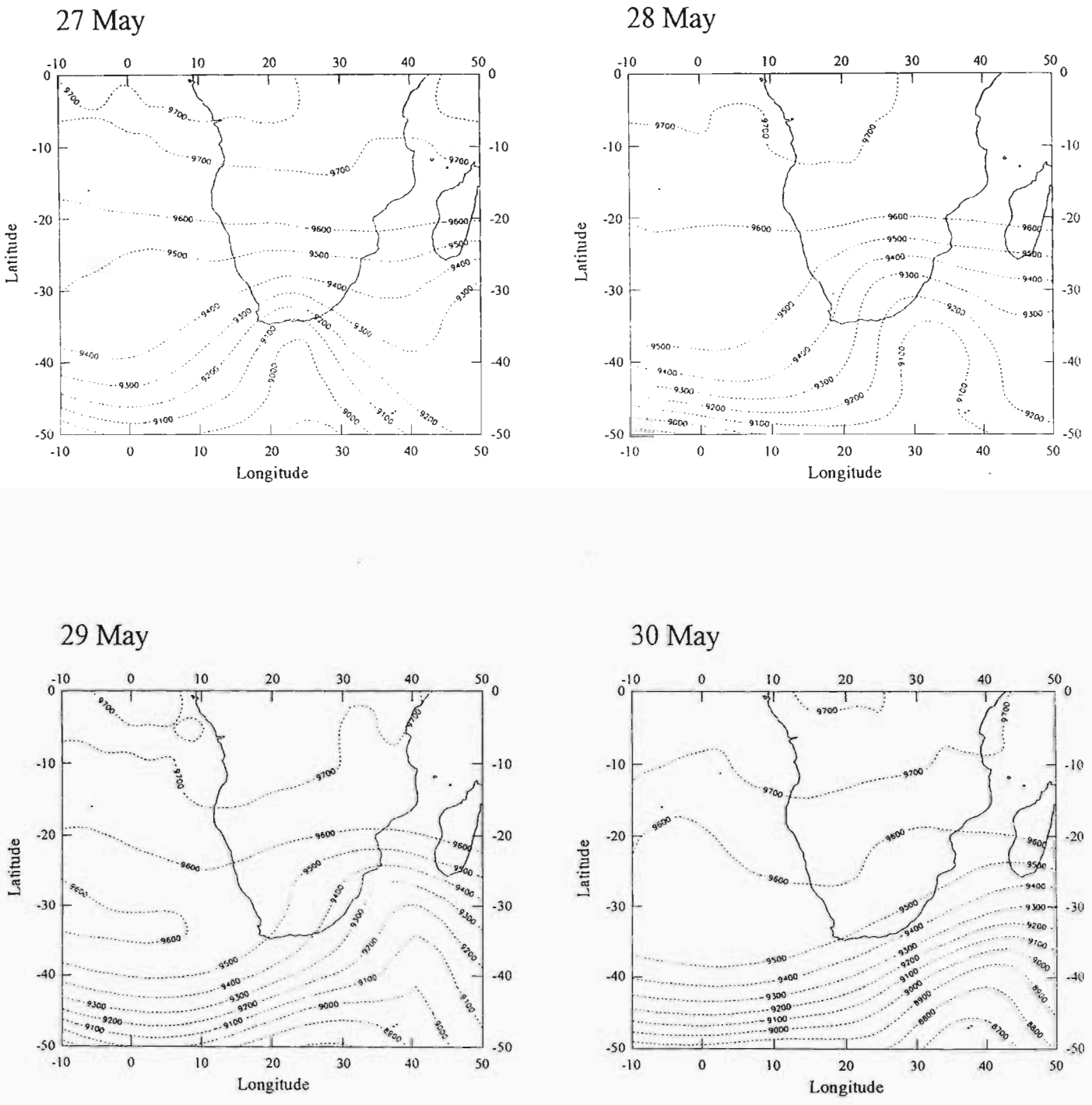

Figure 6.20 300 hPa synoptic charts for an area bounded by latitudes 0° to 50°S and longitudes 10°W to 50°E for 27 to 30 May 1994. Prepared from ECMWF data.

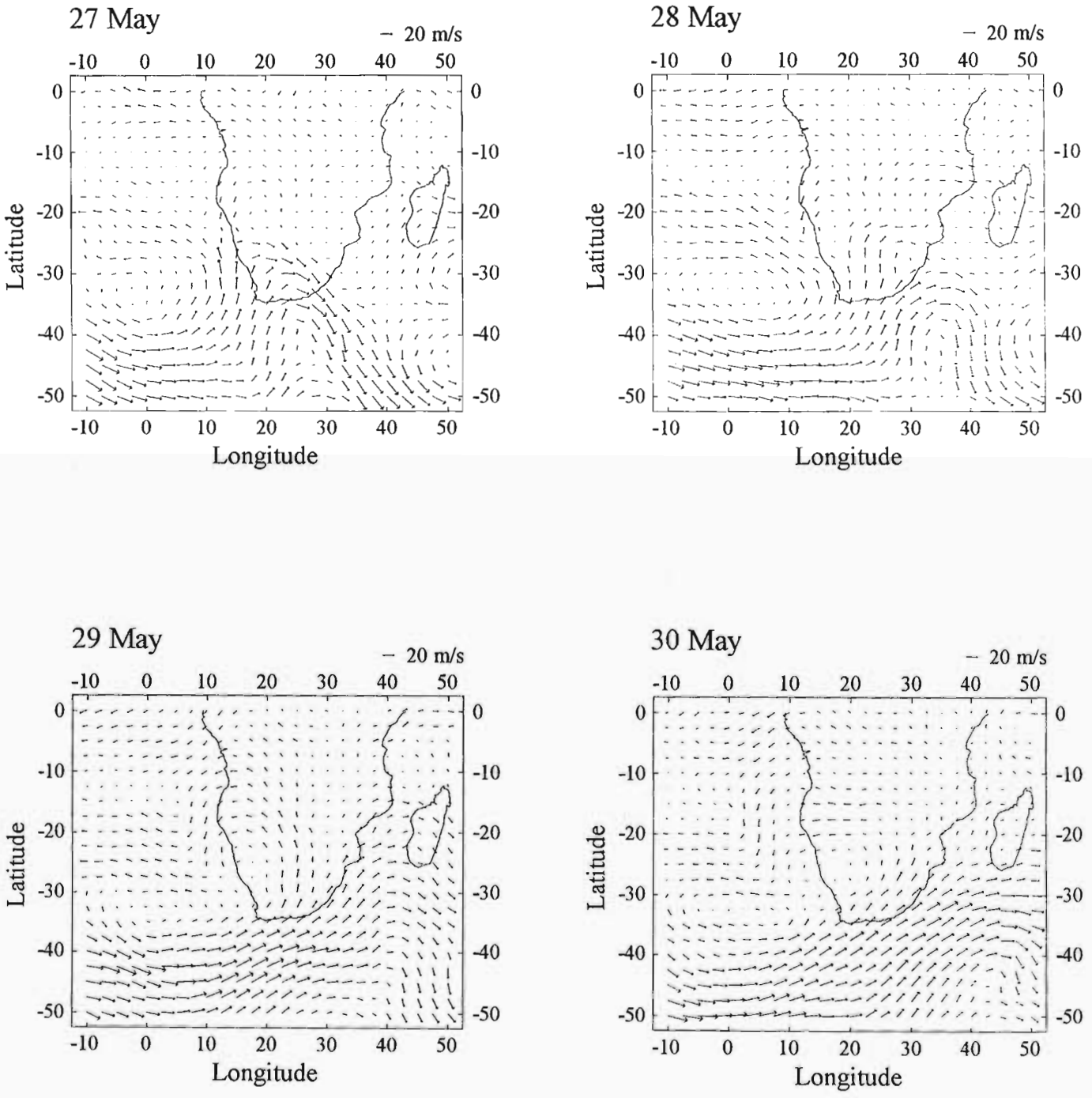

Figure 6.21 700 hPa wind vectors for 26 to 30 May 1994 for the area bounded by latitudes 0° to 50°S and longitudes 10°W to 50°E. Prepared from ECMWF data.

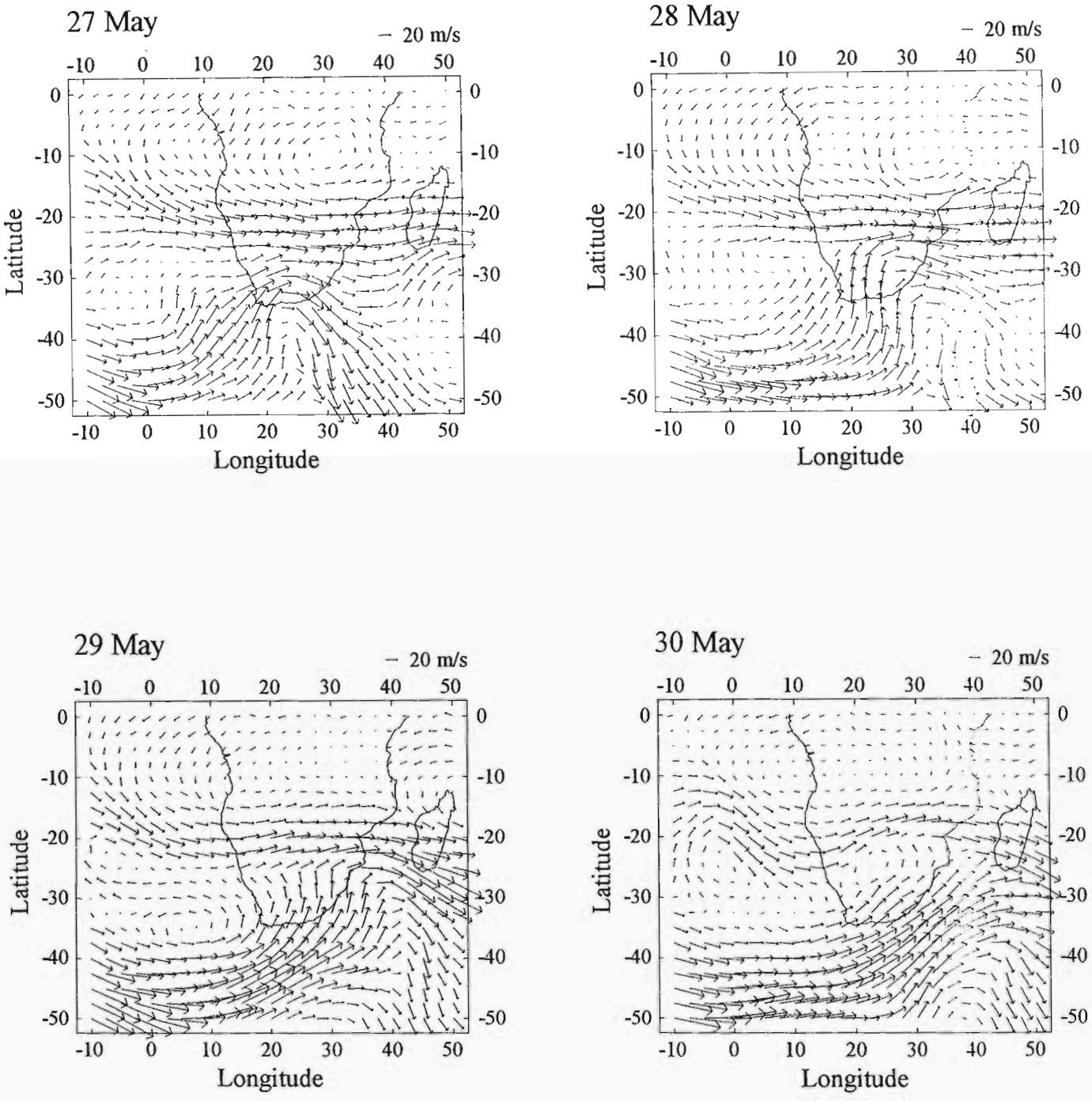

Figure 6.22 300 hPa wind vectors for 26 to 30 May 1994 for the area bounded by latitudes 0° to 50°S and longitudes 10°W to 50°E. Prepared from ECMWF data.

had moved further eastwards by 28 May. By 29 May the wave had significantly disrupted the anticyclonic flow and southerly flow was dominant over much of South Africa.

The pattern is different in the upper troposphere (300 hPa) (Fig. 6.22). Initially, strong westerly flow is evident over the subcontinent, while the presence of the westerly trough is evident on the southern coast of South Africa. Wind speeds remain strong over Irene between 26 to 29 May. On 28 May westerly flow over the country is strengthened as the trough system merges with the dominant upper air westerly flow (Fig. 6.22). The upper air flow remains disturbed in this fashion until 30 May when the trough moved off the east coast into the Mozambique Channel. Weak anticyclonic flow was re-established over the interior, which served to separate two bands of strong wind flow, one to the north and the other to the south of the country. This pattern is evident on 30 May 1994.

6.4.3 Horizontal and vertical distribution of ozone

The spatial distribution of TOMS total ozone (DU) in the area bounded by latitudes 0° to 50°S and longitudes 10°W to 50°E for 27 to 30 May 1994 is depicted in Figure 6.23. A region of enhanced ozone coincides with the centre of the upper tropospheric COL system. Maximum values are evident just south and to the east of the country in the ocean. Total ozone values at Irene increased from 246 DU on 26 May to 264 DU on 29 May and decreased to 255 DU on 30 May.

Daily ozonesondes were launched at Irene between 27 to 30 May 1994, coinciding with the passage of a deep trough and COL pressure system in the upper air (300 hPa). Ozone levels are expressed in partial pressure (mPa), in preference to mixing ratio (ppbv), for ease of graphical representation as the range in values is far smaller. On 27 May, data capture was incomplete and unreliable. However, on 29 May an ozone enhancement, compared to the previous day, is evident in the upper troposphere between 10 to 15 km reaching a maximum of approximately 2.5 mPa (Fig. 6.24). On 30 May the enhanced ozone layer in the upper troposphere (10-12 km) is depleted with maximum values occurring at 14 to 15 km above the surface. This depletion reflects the shorter life time of ozone and the greater efficiency of ozone sinks at lower altitudes.

The upper tropospheric ozone enhancement, on 29 May, is reflected in the changes in integrated column ozone amounts below 16 km (agl) (Table 6.2). There is little change in tropospheric ozone from 27 to 28 May, followed by a 28% increase on 29 May. A breakdown of the troposphere into three layers (1-2, 2-8, and 8-16 km) reveals that there was little change in the lowest layer

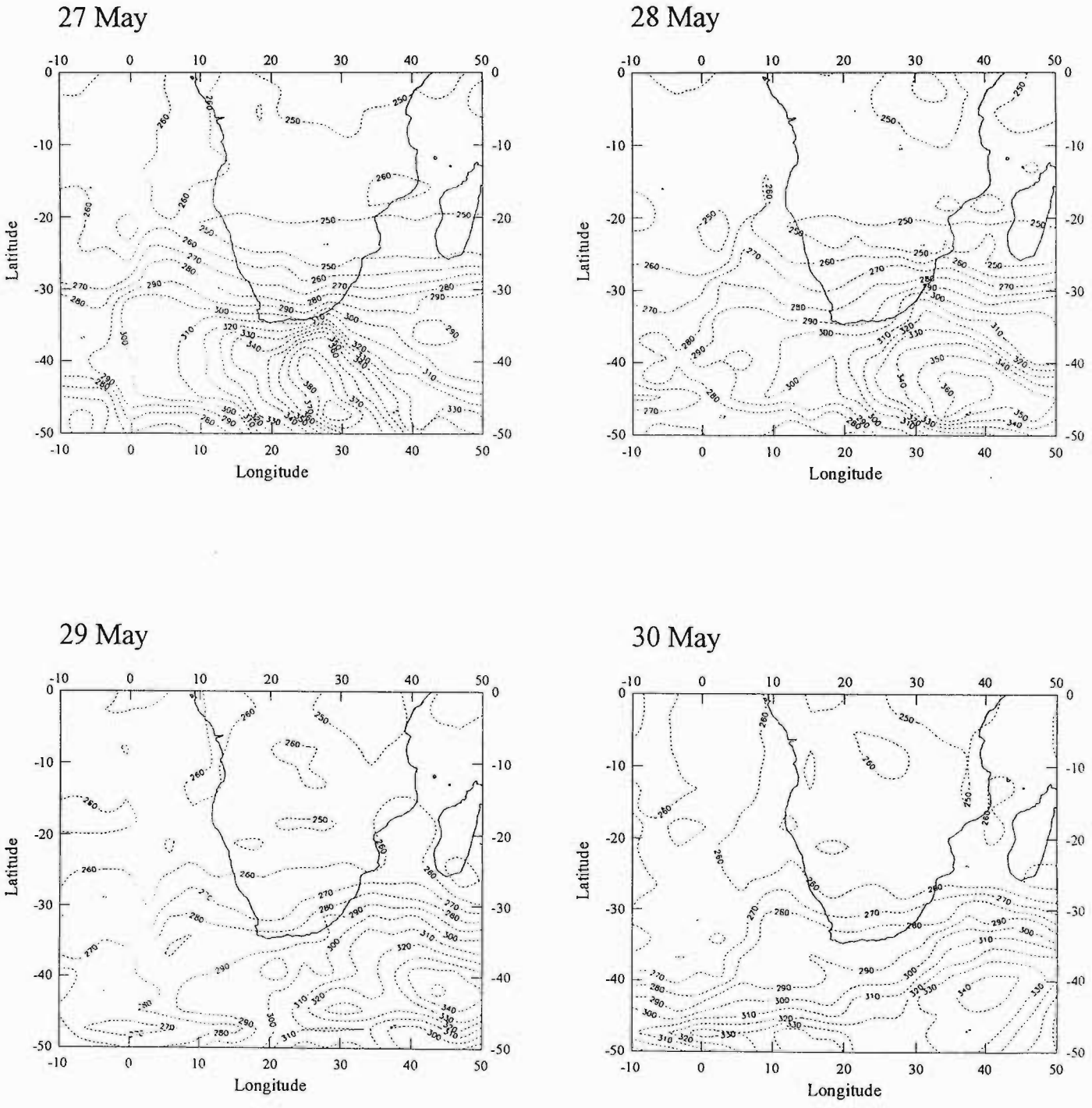

Figure 6.23 Spatial distribution of TOMS total ozone (DU) for an area bounded by latitudes 0° to 50°S and longitudes 10°W to 50°E for 27 to 30 May 1994. Data supplied by NSSDC.

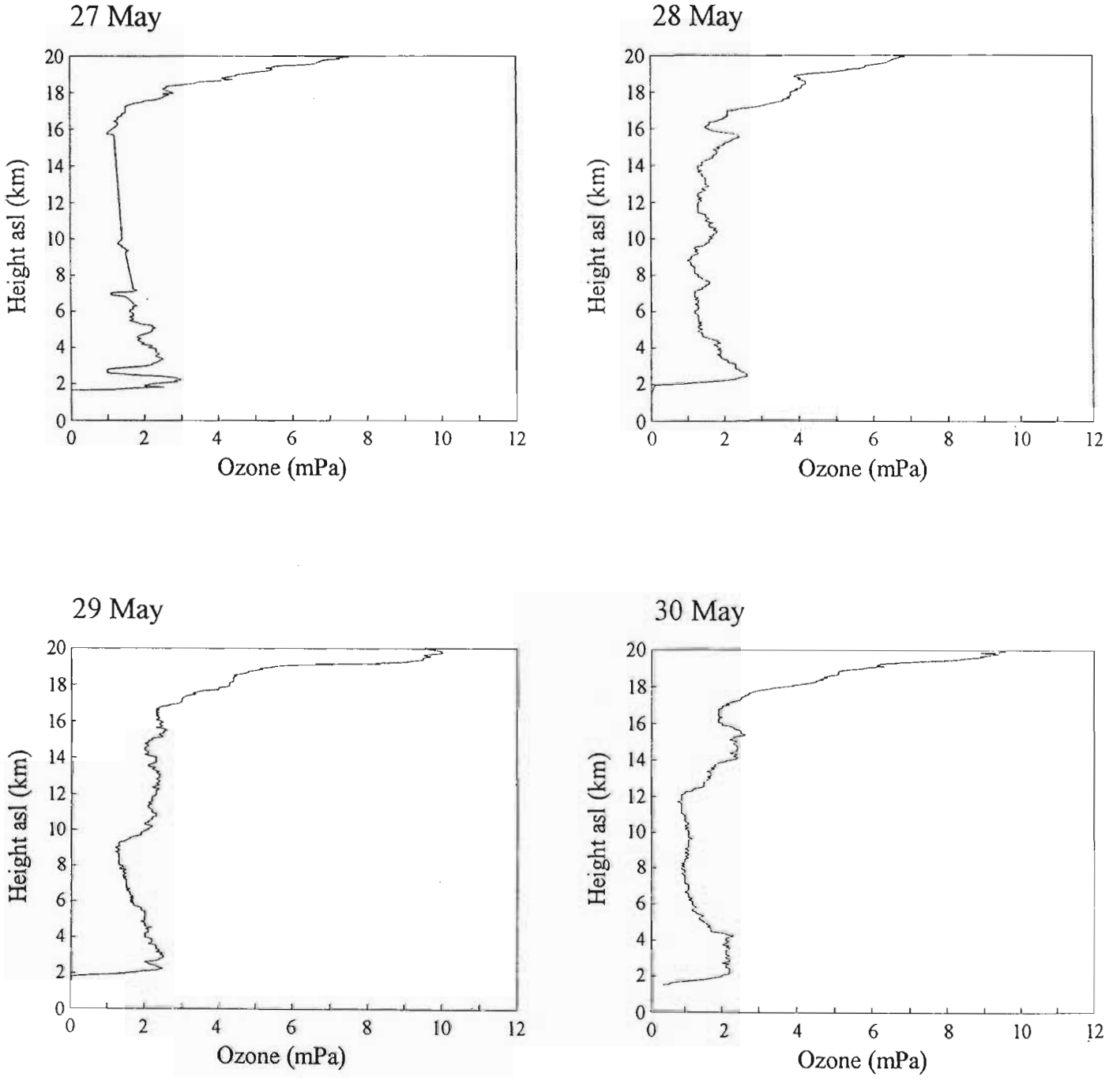

Figure 6.24 Vertical profiles of ozone partial pressure (mPa) at Irene for the period 27 to 30 May 1994. Ozonesonde data supplied by SAWB.

and that the greatest proportion of tropospheric enhancement was observed in the 8 to 16 km layer.

The integrated tropospheric ozone enhancement on 29 May (~ 37 DU) is considerably greater than the mean May integrated tropospheric ozone (~ 28 DU) for Irene calculated by Thompson *et al.* (1995b), for the period 1991 to 1993. Further, it is comparable with the tropospheric maximum in October which has been attributed to biomass burning and STE. Biomass burning occurs in the dry season, during the months of August to October, and thus is not an influencing factor in May.

Table 6.2 Integrated ozone (DU), below 16 km (agl), at Irene from four ozonesonde profiles 27 to 30 May 1994.

DATE	27	28	29	30
< 16 km	28.0	29.0	37.1	29.0
0-2 km layer	3.7	3.0	3.5	3.6
2-8 km layer	11.1	8.8	10.6	8.3
8-16 km layer	13.2	17.2	23.0	17.1

A time-height cross section of ozone mixing ratios (expressed in ppbv) was constructed from the four ozonesonde profiles described above and is presented in Figure 6.25. The upper tropospheric ozone enhancement (between approximately 10 and 15 km) depicted in the vertical profiles of ozone partial pressure (Fig. 6.24) is clearly evident on 29 May. In contrast, ozone mixing ratios are constant at approximately 100 ppbv in the upper troposphere (14 km) on previous days and on 30 May. The ozone enhancement in the upper troposphere on 29 May coincides with the lowering of the tropopause on that day (see Table 6.1). This evidence suggests that ozone was transported downward from the stratosphere on 29 May during the passage of the COL system.

6.4.4 Dynamic characteristics

Spatial PV measurements for the 340 K isentropic surface (Fig. 6.26), which corresponds roughly to the height of the 300 hPa isobaric surface and which fluctuates between approximately 8800 and 12800 gpm (asl), reflect the extent of the low pressure system over the country between 27 and 30 May 1994. An increase in PV levels (up to 200 - 300 x 10^{-7} $KhPa^{-1}s^{-1}$) is evident in the vicinity of Irene on 28 and 29 May when the upper air COL moved northwards and

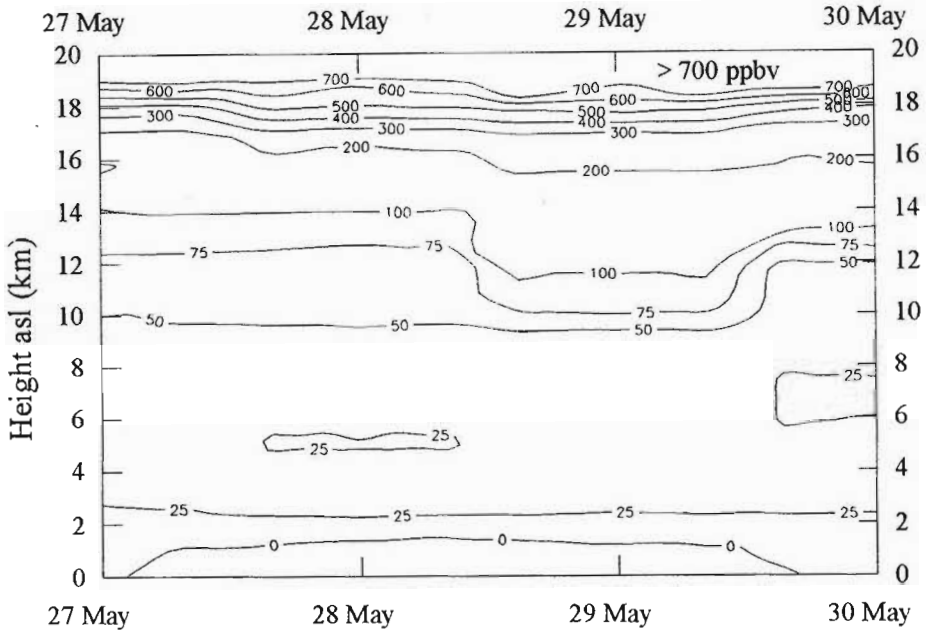

Figure 6.25 Time-height cross section of ozone mixing ratio (ppbv) derived from 4 ozonesonde ascents at Irene for the period 27 to 30 May 1994. Data supplied by SAWB. Values greater than 700 ppbv are excluded.

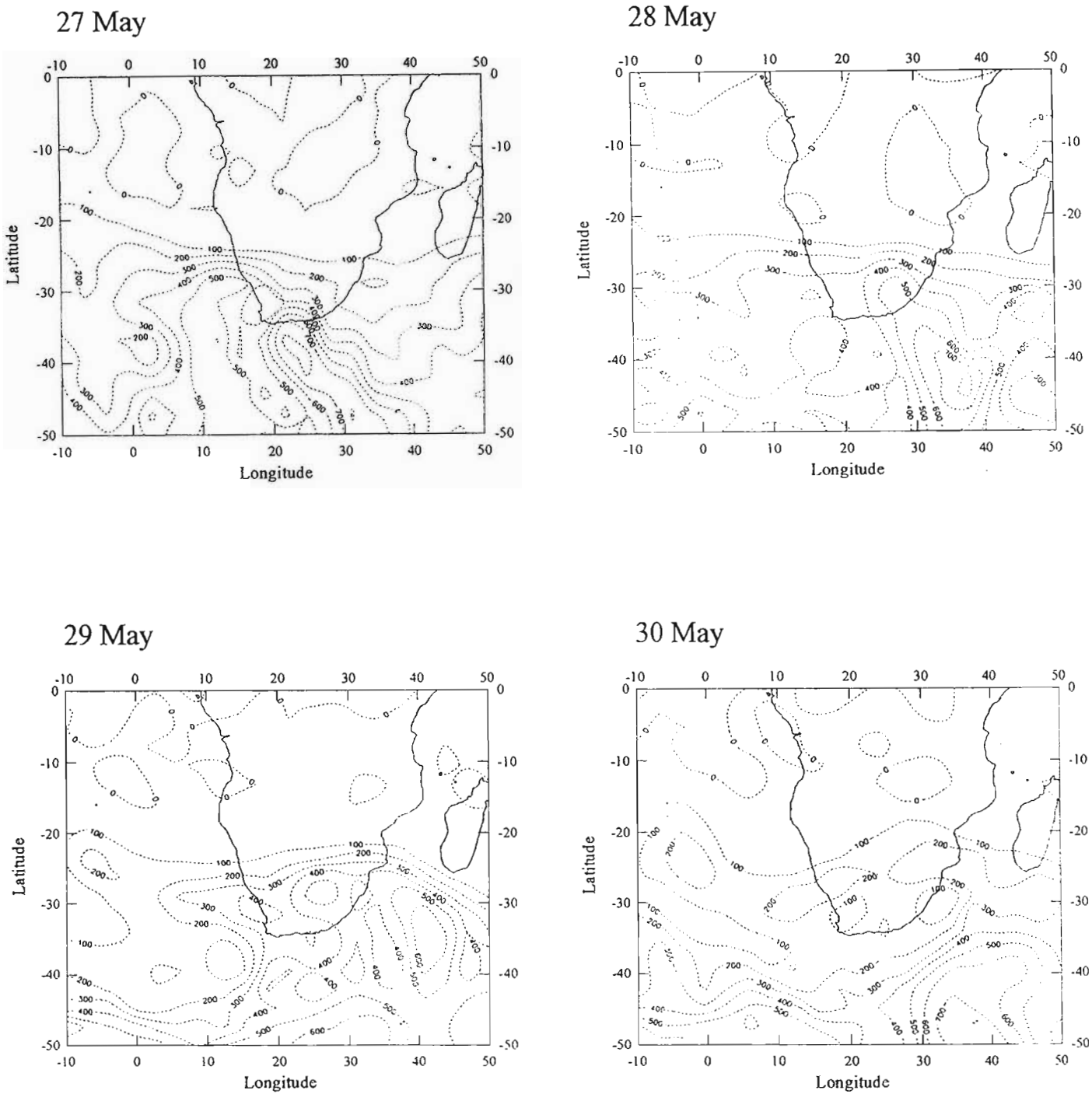

Figure 6.26 Spatial distribution of PV (x 10^{-7} $KhPa^{-1}s^{-1}$) on 340 K isentropic surface for 27 to 30 May 1994 in the region bounded by latitudes 0° to 50°S and longitudes 10°W to 50°E. Derived from ECMWF data.

eastwards, but which remained some distance south of the station. A sequence of vertical cross sections of PV which cut through 25°S, corresponding to the latitude of Irene, are shown in Figure 6.27. An intrusion of high PV, indicative of stratospheric air, is evident in the upper troposphere at approximately 38°E on 29 May. A more significant downward extension of the 100 x 10^{-7} $KhPa^{-1}s^{-1}$ PV line would have been expected had the COL formed closer to Irene. This intrusion of the PV tropopause into the troposphere corresponds to the lowered radiosonde tropopause heights measured at Irene on those days (Table 6.1).

Radiosonde RH (%) profiles at Irene (Fig. 6.28) reveal fairly constant levels (5 to 10 %) above 15 km, while significant differences in the lower layers (<15 km) are evident during this period. It is recognised that radiosonde RH values above 300 hPa (~ 9300-9600 gpm) are not accurate due to the extreme dryness of the atmosphere and the lack of sensitivity of the instruments at these altitudes (Coetzee, pers. comm., 1995). However, the RH signal provides approximate values in this region. On 27 May, RH maxima of approximately 30% are evident at 4 and 7 km. Surface levels exceed 30% on all four days. The two maxima are, however, absent on 28 and 29 May when the air in the upper troposphere is considerably drier. On these days, RH between 6 and approximately 15 km resembles that of higher altitudes. Increased RH levels below 15 km on 30 May are consistent with the increased altitude of the tropopause following the passage of the COL. The apparent drying of the upper troposphere on 28 and 29 May supports the premise that ozone-rich air from the stratosphere is injected into the mid- and upper troposphere when airflow is disturbed by the presence of a COL system.

Figure 6.29 shows vertical cross sections of wind speed for 27 to 30 May 1994. The double jet structure evident in section 6.3.3 is absent on 27 to 29 May. However, a single strong jet (> 50 ms^{-1}) is evident in the upper troposphere (10-14 km) on all days, but moves progressively eastwards during the four day period. A weak second jet is evident in the upper troposphere on 30 May. The prominent jet of the 28 and 29 May is centred in the region of the PV intrusion in the upper troposphere. On 29 May, the jet core is located just east (ahead) of the intrusion. Likewise, Danielsen's (1968) model places the jet core on the south side (ahead) of the PV intrusion.

Cross sections of the ECMWF vertical wind (ω) component through Irene (25°S) are given in Figure 6.30 for 27 to 30 May. A discontinuity between upward and downward motion is evident in the upper troposphere and is located in the vicinity of the COL centre. On 27 May, the discontinuity is situated well to the west of Irene and is marked by a core of strong downward movement (10 to 50 Pa s^{-1}) situated between 15 to 20°E, and which is located to the rear of the upper air trough depicted in Figure 6.20. On 28 May, the discontinuity

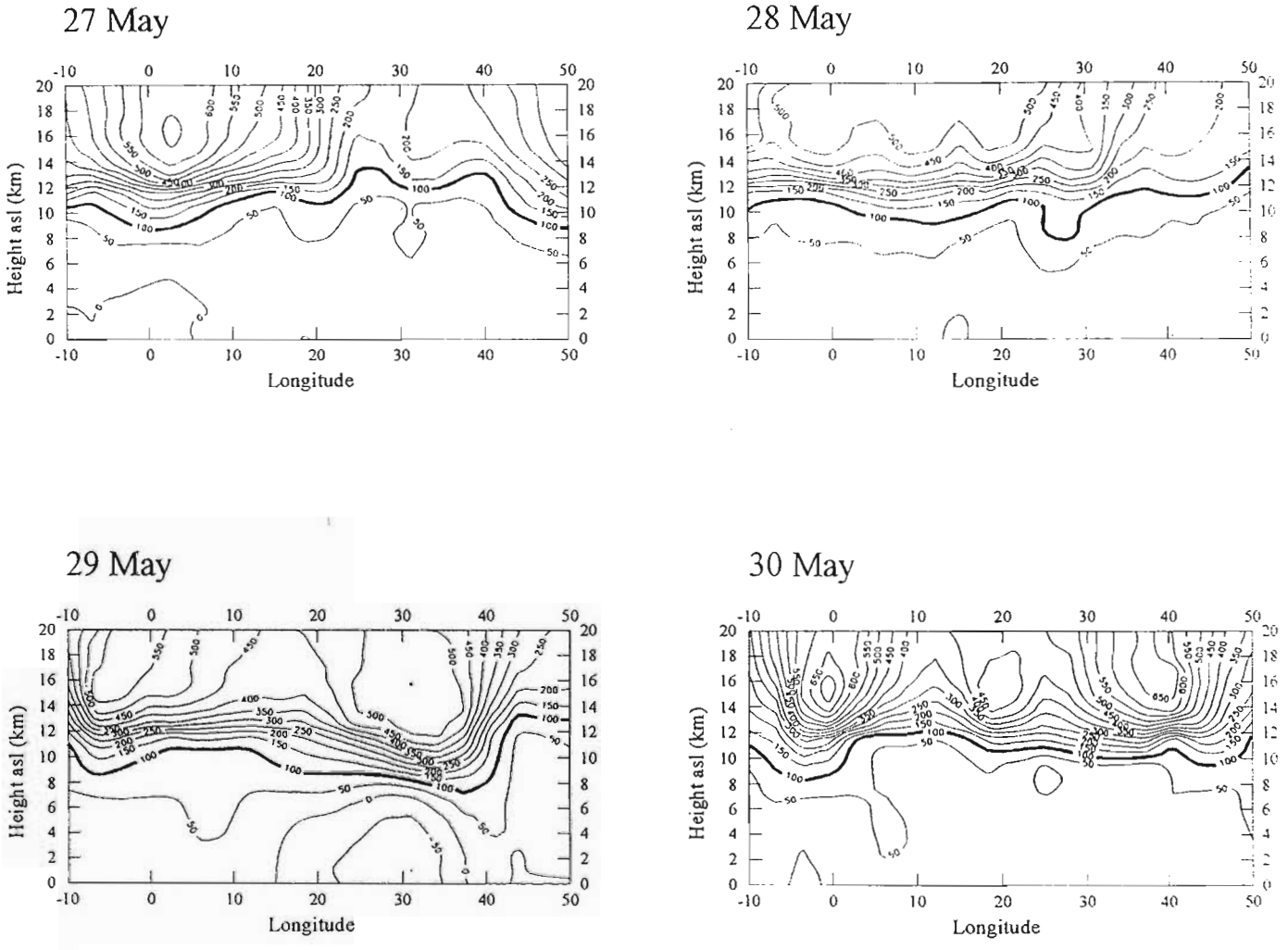

Figure 6.27 Vertical cross sections of PV (x 10^{-7} $KhPa^{-1}s^{-1}$) through 25°S for 26 to 30 May 1994. Derived from ECMWF data.

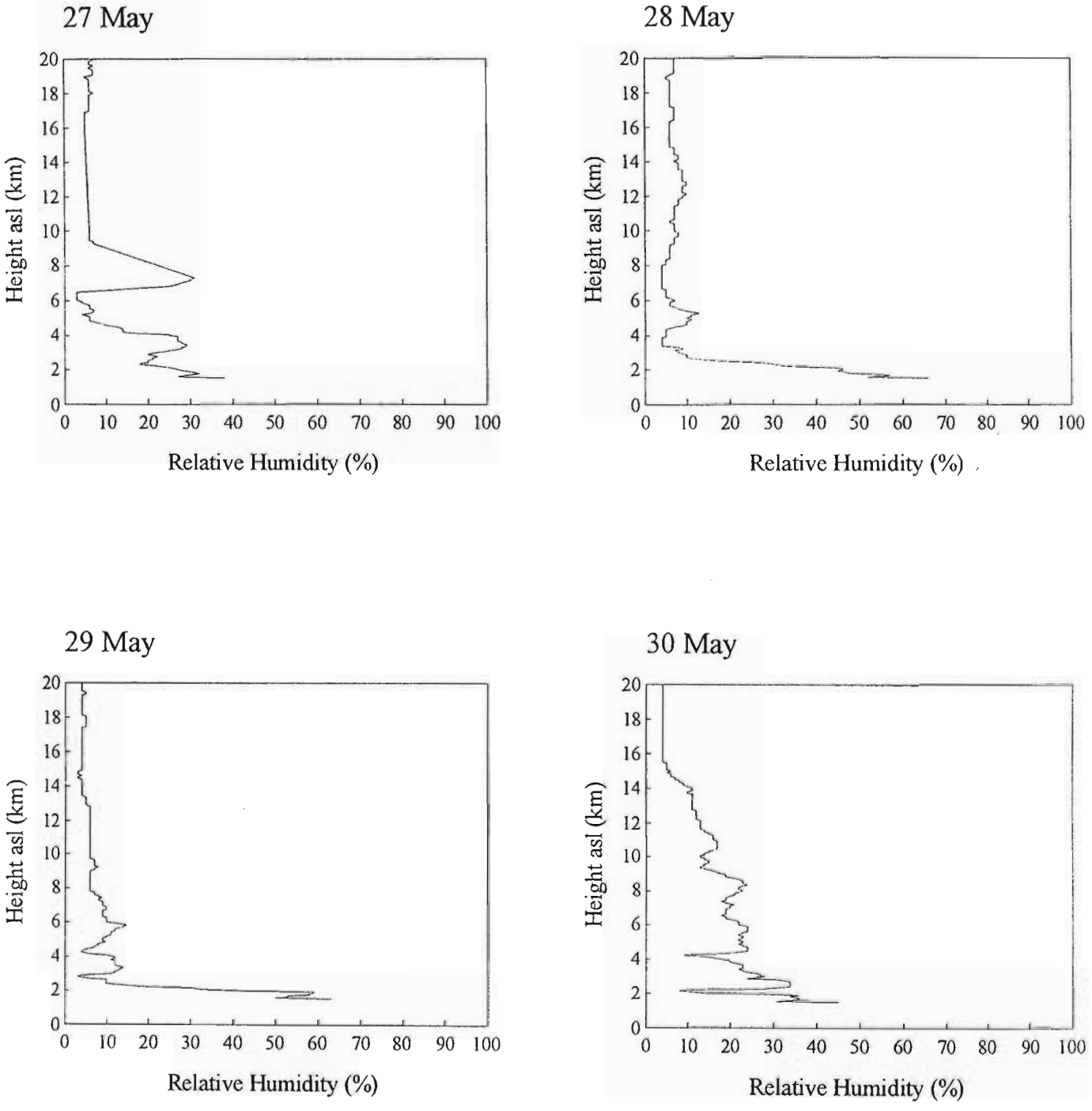

Figure 6.28 RH (%) profiles at Irene for 27 to 30 May 1994. Prepared from radiosonde data supplied by SAWB.

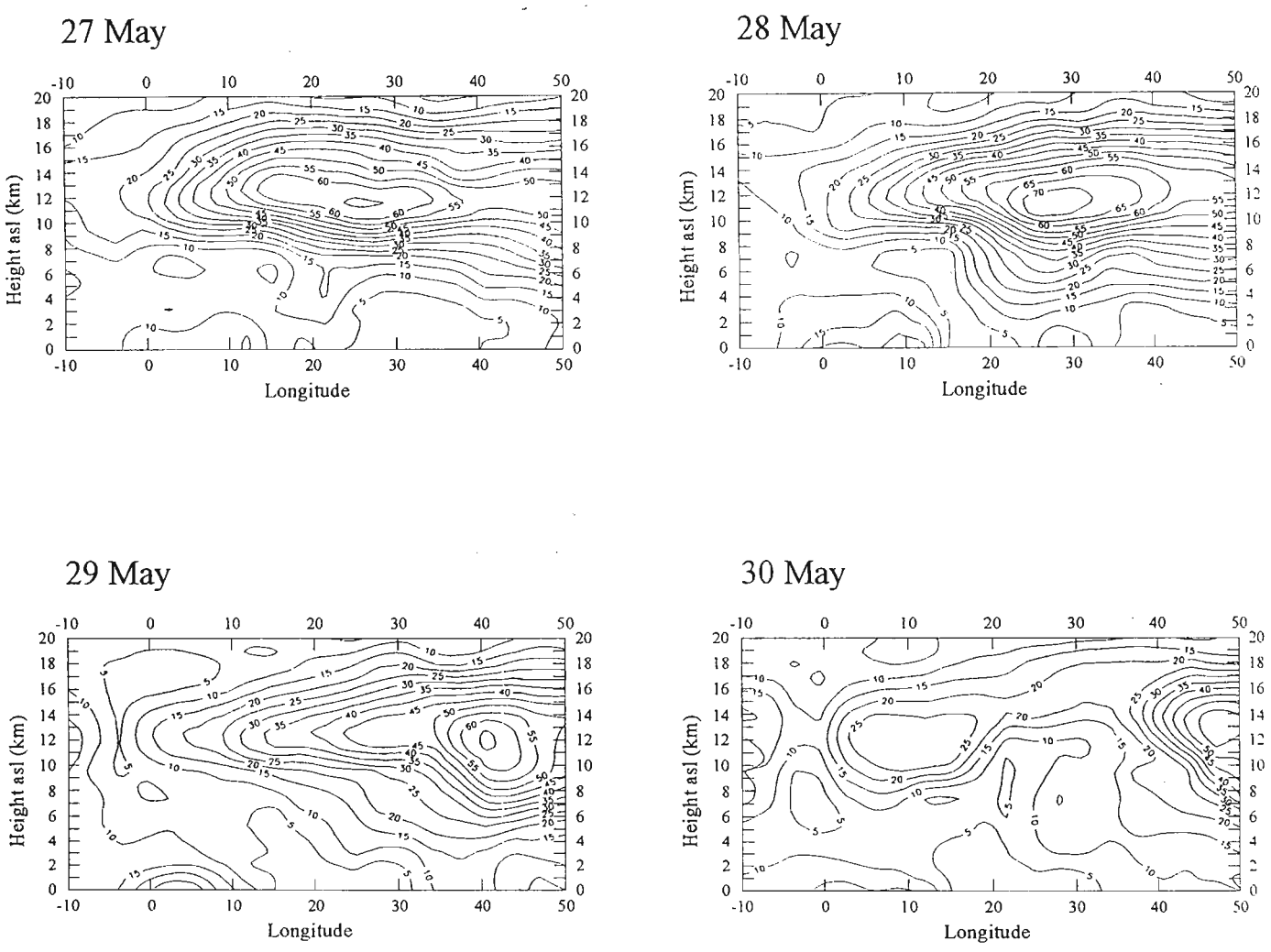

Figure 6.29 Vertical cross sections of wind speed (m s^{-1}), through 25°S, for 27 to 30 May 1994. Derived from ECMWF data.

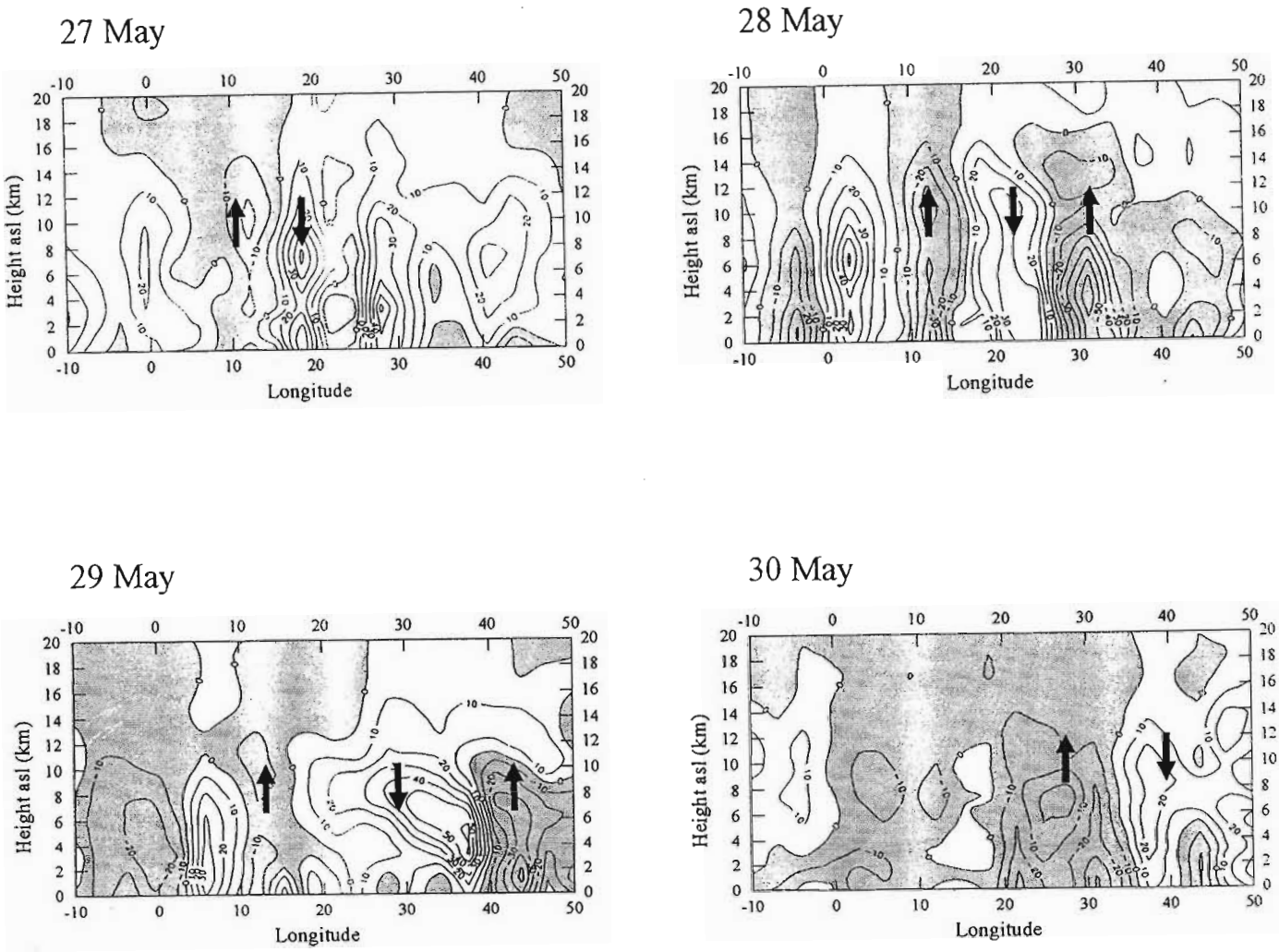

Figure 6.30 Vertical cross section of the ω component of the wind, through Irene (25°S), for 27 to 30 May 1994, derived from ECMWF, 12 Z data. Arrows indicate upward and downward motion. Regions of upward motion (ω < 0) are shaded.

is situated in the vicinity of Irene at approximately 27°E. A region of strong upward (-30 to -60 Pa s^{-1}) motion coincides roughly with the central axis of the upper air trough while downward motion prevails to the rear of the upper air trough. On 29 May, the discontinuity has moved further eastwards following the upper air COL and downward flow (30 to 60 Pa s^{-1}) dominates the region between 25° to 40°E to the rear of the weakening trough. Downward flow is strongest over Irene (~ 28°E) between approximately 7 and 9 km (asl) which corresponds to the height of the 100 x 10^{-7} $KhPa^{-1}s^{-1}$ PV line. Considerably weakened vertical motion occurs throughout the atmosphere on 30 May. However, weak descending motion (10 to 20 Pa s^{-1}) persists to the rear of the eastward moving and dissipating westerly wave which is located east of the subcontinent. A less confused vertical section of the ω field may have emerged had the COL formed closer to Irene. Following the COL, it was expected that a clear discontinuity in ω would occur at approximately 25°, 35° and 40° on 27 to 30 May respectively.

The vertical motion field is compatible with Danielsen's (1968) model and is best illustrated on 29 May when the stratospheric intrusion was most significant. Strong downward flow (40-50 Pa s^{-1}) occurs to the west (rear) of the discontinuity in the vertical motion field and is maximised over Irene (~ 28°E) at the height of the tropopause. This corresponds well to the lowering of the PV tropopause (Fig. 6.27) and upper tropospheric ozone enhancement (Fig. 6.24) on that day. A core of strong upward flow (20-30 Pa s^{-1}) occurs to the east (ahead) of the discontinuity which corresponds to upward arm of the direct cell of Danielsen's (1968) model while the weak upward flow in the upper troposphere, situated to the west of the region dominated by downward motion, completes the indirect circulation cell.

6.4.5 SUMMARY

In this section, data collected during SA'ARI-94 are used to examine the vertical distribution of ozone at Irene during the passage of an upper air COL system over the period 27 to 30 May 1994. The lowering of the radiosonde and PV tropopause at Irene, and the intrusion of high PV and dry stratospheric air to tropospheric altitudes, coupled with downward flow near the tropopause, provides dynamic evidence of the coupling of tropospheric and stratospheric air in the upper troposphere. The PV data do not provide conclusive evidence that tropopause folding took place in this case study, but rather exhibits a lowering of the 100 x 10^{-7} $KhPa^{-1}s^{-1}$ PV line and a disturbance or undulation at the tropopause which leads to enhanced ozone levels in the upper troposphere at Irene.

Turbulent mixing between upper and lower tropospheric air is facilitated by up and downdraughts within the COL system. Vertical mixing and strong downward motion, in the vicinity of the upper tropospheric disturbance, promotes downward transport of ozone-rich stratospheric air producing a fairly well mixed upper tropospheric layer on 29 May. The layer of enhanced ozone in the upper troposphere is reflected in integrated ozone (DU) below 16 km (agl), with maximum enhancement occurring between 8 and 16 km (agl), and is comparable to enhanced levels noted during spring which has been attributed to biomass burning and STE at that time of the year (Thompson, *et al.*, 1996a). As the COL system weakens and moves away from the country, the tropopause is restored at a higher altitude. On 30 May ozone concentration levels off at lower altitudes due to natural sinks which dictate the shorter lifetime of ozone in this region while elevated levels persist in the region 12-16 km.

CHAPTER 7

CONCLUSION

It is recognised that tropospheric ozone maxima are functions of both ozone-related chemistry and atmospheric transport. However, the central hypothesis of this thesis is that tropospheric ozone maxima over sub-tropical southern Africa are functions of atmospheric dynamics. Indeed, the evidence presented in this study has shown that atmospheric circulation and its associated dynamics plays a major role in the generation of enhanced tropospheric ozone amounts. The inter-related nature of the atmosphere and ozone-associated chemistry was highlighted in Chapter 3, and provided a base for the examination of day-to-day weather patterns and high ozone amounts over the southern African region. Chapter 4 began with a general statistical examination of the relationship between total ozone and synoptic weather patterns at nine stations throughout southern Africa and adjacent oceans, and in a region bounded by latitudes 0° to 50°S and longitudes 10°W to 50°E. The study showed important characteristics which provided guidance for the entire study *viz.*:

- A generally weak but negative relationship between total ozone and the synoptic weather, expressed as a function of the height of the 500, 300 and 100 hPa geopotential surfaces.

- Circulation patterns on all days on which the relationship was considered to be good (expressed as r^2 values > 80%), occurred in association with the passage of a mid-latitude cyclone. Conversely, a poor relationship (r^2 values < 20%) was found for days characterized by anticyclonic circulation.

- Subtropical anticyclones showed no dynamical connection, between the stratosphere and troposphere, which substantiated the weak statistical relationship found. On the other hand, the good correspondence between PV and total ozone, during the passage of deep westerly troughs, prompted a more thorough investigation of this subject, which was presented in Chapter 6.

Further inquiry into the relationship between ozone distribution and synoptic weather was conducted using data collected during SAFARI-92. An examination of the vertical ozone distribution associated with composite anticyclonic and composite westerly trough characteristics at Okaukuejo revealed:

- A steady increase in ozone mixing ratio throughout the lower and middle troposphere and the presence of an elevated enriched ozone layer under anticyclonic circulation conditions. This observation was supported by the dominant stable conditions, associated with anticyclonic flow, observed during the SAFARI experiment.

- In contrast, the ozone profile characteristic of the westerly trough synoptic type, has double ozone maxima separated by a mid-tropospheric layer in which ozone values are 20 ppbv lower. The mid-tropospheric minimum reflects the invasion of a relatively clean, ozone-poor maritime air mass from the southwest.

Case studies, for the SAFARI period, characteristic of anticyclonic and westerly trough synoptic flow at Okaukuejo provided:

- Support for the findings of the composite analysis at Okaukuejo.

- Further evidence of the elevated enhanced ozone layer at Okaukuejo, regardless of the change in synoptic flow.

Similar case studies at Irene showed:

- The vertical ozone profile associated with anticyclonic flow resembled the mean as described in Diab *et al.* (1996a). A lower to mid-tropospheric ozone minimum co-incident with the passage of a westerly trough, of similar magnitude to that which is described for Okaukuejo. In contrast to the mean ozone profile for Irene (Diab *et al.*, 1996a), evidence of an elevated ozone layer was found in these isolated case studies.

In the case of the tropical station at Brazzaville, the examination of the vertical distribution of ozone during the SAFARI period, revealed:

- That isolated convective events are capable of supporting short-lived, upper tropospheric ozone maxima. Such enhancements are supported by the transport of pollutants out of the PBL and into the free troposphere, where along with complex photochemical reactions, the generation of ozone is assisted.

The overall message from these findings supports the contention that both vertical and horizontal transport mechanisms play significant roles in the ultimate distribution of ozone and in the generation of ozone maxima over the southern African region.

In order to examine the dynamic link between the stratosphere and the troposphere further, as implied by the statistical analysis presented earlier, the influence of the passage of particularly deep westerly troughs, or COL systems, over southern Africa and ozone distribution was investigated. Firstly, a general picture of the relationship between COLs and total ozone distribution over southern Africa was gained by creating a composite of six case studies. The results exhibited:

- A general zonal pattern in composite spatial plots of total ozone, with an increase from north to south, and a buildup of ozone near the centre caused by the equatorward extensions from the relatively higher ozone region in the south. A maximum in composite ozone mass confirmed the ozone enhancement associated with well developed COL systems.

- A good correspondence between high ozone and high PV, as expressed in spatial plots.

- Evidence of STE defined by dry air and high PV, in the vicinity of the centre of the composite COL.

- A vertical motion field, as expressed by ω, similar to that accompanying Danielsen's (1968) two-cell model of tropopause folding. Upward motion, of the direct cell, occurs ahead (east) of the COL centre and represents the upward limb of the direct cell, while downward motion occurs just to the rear (west) of the COL centre in the region of the confluence of the downward limbs of both the direct and indirect cells described by Danielsen (1968).

The composite analysis provided strong support for a further case study examination of the relationship between total ozone distribution and the passage of subtropical COL systems over southern Africa. A particularly deep system was selected for investigation. The exercise revealed:

- The intrusion of high PV and very dry air, indicative of stratospheric air, into the troposphere, in the vicinity of the upper air COL. This confirmed the dynamic link between the troposphere and stratosphere during the passage of a subtropical COL system. The PV intrusion was accompanied by strong downward motion, when the COL was deepest (26 and 27 September 1987), which is compatible with the tropopause folding model proposed by Danielsen (1968).

- The need for vertical ozone data, coinciding with the passage of a COL, in order to gain more substantive evidence of tropopause folding and the injection of ozone into the troposphere.

An opportunity to measure vertical ozone distribution, at Irene, arose in conjunction with the SA'ARI-94 project. A case study of a deep westerly trough and COL system which passed over southern Africa, between 27 and 30 May 1994, was selected for analysis. Vertical ozone profiles exhibited an upper tropospheric ozone enhancement at Irene and meteorological parameters provided strong support for a dynamic link between the stratosphere and upper troposphere. Meteorological support for STE was found in:

- The lowering of the radiosonde derived thermal and PV tropopause at Irene, and the intrusion of high PV and dry stratospheric air into the upper troposphere, coupled with downward flow near the tropopause.

- The evidence presented in the vertical motion field, ω, is inconclusive due largely to the southerly position of the COL centre. Strong vertical motion is confined largely to the mid-troposphere

Upper tropospheric ozone enhancement associated with the passage of deep westerly troughs, over southern Africa, is undoubtedly a product of STE. An attempt has been made to understand, and to explain the mechanism which gives rise to the observed ozone maxima in the light of the current theory. The evidence suggests that subtropical COL systems, which are common over South Africa, play a more significant role in STE than anticipated from work presented in the literature. However, further development of this assertion is required. The study was limited by the fact that vertical ozone-sounding data was available for Irene only. More suitable data, for example from a more southerly located station such as at Cape Town which frequently experiences the effects of the passage of westerly troughs, and which displayed a particularly good statistical relationship between total ozone and mid- to upper tropospheric weather as expressed by the heights of the 100, 300 and 500 hPa geopotential surfaces, may have provided more conclusive evidence of tropopause folding.

There were some limitations experienced in completing this thesis. Firstly, better use of trajectory analysis could have been made in Chapter 4 in order to emphasise the good relationship between ozone distribution and atmospheric dynamics. However, the limited number of trajectory runs possible for this project, rendered this exercise less flexible to alteration during its development. It is recommended that comparisons with other work, concerning trajectory analysis during SAFARI, be made to strengthen the conclusions presented for the Okaukuejo and Irene case studies. Further, it is recognised that the case study analysis was restricted to the SAFARI period and as such, the findings are representative of a short period only. A temporal (seasonal) component, which governs the dynamics operating in tropical and extra tropical latitudes, may conceivably affect the relationships described here.

Nevertheless, the relationships reported in this thesis, undoubtedly contribute to an expanding body of knowledge concerning the southern African region.

Finally, the value of the vertical ozone data used in this study should be emphasised. This study has demonstrated the worth of daily ozone sounding data, even for very short periods (as little as four days). On the strength of this conclusion, it is contended that a few vertical ozone profiles are worth more than continuous daily total ozone data.

The study of changes in atmospheric ozone has acquired an urgency in recent years particularly with respect to stratospheric ozone depletion. The buildup of tropospheric ozone contributes significantly to the atmospheric load of greenhouse gases over the southern African region. The need to understand both natural sources and those produced through anthropogenic activities is fundamental in order to prevent adverse long-term consequences.

REFERENCES

Andreae, A. (1991). Biomass burning: Its history, use, and distribution and is impact on environmental quality and global climate. In *Global Biomass Burning*, (ed.) Levine, J.S., MIT Press, Cambridge, 3-21, 569pp.

Andreae, M.O., Fishman, J., Garstang, M., Goldammer, J.G., Justice, C.O., Levine, J.S., Scholes, R.J., Stocks, B.J., Thompson, A.M., van Wilgen, B. and STARE/TRACE-A/SAFARI-92 Science Team (1993). Biomass burning in the global environment: First results from the IGAC/BIBEX field campaign STARE/TRACE-A/SAFARI-92. In the Annual Report to the National Science Foundation Division of Atmospheric Sciences, Atmospheric Chemistry, 1-22.

Angell, J.K. and Korshover, J. (1978). Global ozone variations: An update into 1976. *Monthly Weather Review*, 106, 725-737.

Bamber, D.J., Healey, P.G., Jones, B.M.R., Penkett, S.A., Tuck, A.F., and Vaughan, G. (1984). Vertical profiles of tropospheric gases: chemical consequences of stratospheric intrusions. *Atmospheric Environment*, 18 (9), 1759-1766.

Barsby, J. and Diab, R.D. (1994). Ozone maxima over southern Africa: a mid-latitude link. *Ozone in the Troposphere and Stratosphere*, Proceedings of the Quadrennial Ozone Symposium 1992, (ed.) Hudson, R., Deepak, A., Hampton, Virginia, 382-385, 965pp.

Barsby, J. and Diab, R.D. (1995). Total ozone and synoptic weather relationships over southern Africa and surrounding oceans. *Journal of Geophysical Research*, 100 (D2), 3023-3032.

Bell, G.D. and Bosart, L.F. (1993). A case study diagnosis of the formation of an upper-level cutoff cyclonic circulation over the Eastern United States. *Monthly Weather Review*, 121, 1635-1655.

Berggren, R. (1952). The distribution of temperature and wind connected with active tropical air in the higher troposphere and some remarks concerning clear air turbulence at high altitude. *Tellus*, 4, 43-54.

Bodeker, G. (1994). Planetary Waves and the Global Ozone Distribution. Unpublished Phd thesis, Department of Physics, University of Natal, Durban, South Africa, 317 pp.

Bodeker, G., Scourfield, M. and Barker, M. (1992). Total column ozone above South Africa. *South African Journal of Science*, 88, 222-224.

Bojkov, R.D. (1995). *The Changing Ozone Layer*. World Meteorological Organization and the United Nations Environment Programme, 1-24.

Bojkov, R.D. (1988). Ozone changes at the surface and in the free troposphere. In *Tropospheric Ozone*, (ed.) Isakasen, I.S.A., D. Reidel Publishing Co., Dordrecht, 83-96, 425pp.

Bojkov, R.D. and Fioletov, V.E. (1995). Estimating the global characteristics during the last 30 years. *Journal of Geophysical Research.*, 100 (D8), 16537-16551.

Bowman, K.P. (1988). Global trends in total ozone. *Science*, 239, 48-50.

Briggs, J. and Roach, W.T. (1963). Aircraft observations near jet streams. *Quarterly Journal of the Royal Meteorological Society*, 89, 225-247.

Browell, E.V., Danielsen, E.F., Ismail, S., Gregory, G.L. and Beck, S.M. (1987). Tropopause fold structure determined from the airborne Lidar and in situ measurements. *Journal of Geophysical Research*, 92 (D2), 2112-2120.

Carlson, T.N. (1991). *Mid-Latitude Weather Systems*. Chapter 15, 404-447, Harper Collins Academic, Hammersmith, London, 507pp.

Chameides, W. and Walker, J.C.G. (1973). A photochemical theory of tropospheric ozone. *Journal of Geophysical Research*, 78 (36), 8751-8760.

Chatfield, R.B. and Delany, A.C. (1990). Convection links biomass burning to increased tropical ozone: However, models will tend to overpredict ozone. *Journal of Geophysical Research*, 95 (D11), 18473-18488.

Chatfield, R. and Harrison, H. (1977). Tropospheric ozone 2. Variations along a meridional band. *Journal of Geophysical Research*, 82 (37), 5969-5976.

Combrink, J. (1994). The role of cut off lows in ozone distribution. Eleventh Annual Conference of the South Africa Society of Atmospheric Sciences, 12-13 October, 1994.

Combrink, J. (1995). Stratospheric-tropospheric exchange of ozone in southern Africa. Twelfth Annual Conference of the South African Society for Atmospheric Sciences, University of Pretoria, Pretoria, 26-27 October, 1995.

Combrink, J., Diab, R.D., Sokolic, F. (1995). Ozone profile comparisons in southern Africa. WMO-IGAC Conference on the Measurement and Assessment of Atmospheric Composition Change, Beijing, China, 9-14 October 1995.

Combrink, J., Diab, R.D. and Brunke, E-G. (1993). Surface and total column ozone measurements at Cape Point and the Eastern Transvaal Highveld. National Association of Clean Air Conference, Brits, South Africa, 11-12 November, 1993.

Combrink, J., Diab, R.D., Sokolic, F. and Brunke, E.G. (1995). Relationship between surface, free tropospheric and total column ozone in two contrasting areas in South Africa. *Atmospheric Environment*, 29 (6), 685-691.

Combrink, J., Diab, R.D., Sokolic, F. and Brunke, E-G. (1994). Surface and free tropospheric ozone measurements over South Africa. Eighth CACGP Symposium and Second IGAC Conference, Fuji-Yoshida, Japan, 5-9 September, 1994.

Connors, V.S., Cahoon, D.R.Jr., Reichle, H.G.Jr., Brunke, E-G., Garstang, M., Seiler, W. and Scheel, H.E. (1991). Savanna burning and convective mixing in southern Africa: Implications for CO emissions and transport. In *Global Biomass Burning, Atmospheric, Climatic and Biospheric Implications*, (ed.) Levine, J.S., 147-154, MIT, Cambridge, 569pp.

Cros, B., Delmas, R., Clairac, B. and Loemba-Ndembi, J. (1987). Survey of ozone concentrations in an equatorial region during the rainy season. *Journal of Geophysical Research*, 92 (D8), 9772-9778.

Cros, B., Nganga, D., Delmas, R.A., Fontan, J. (1991). Tropospheric ozone and biomass burning in intertropical Africa. In *Global Biomass Burning*, (ed.) Levine, J.S., The MIT Press, Cambridge, 143-146, 569pp.

Crutzen, P.J. (1988). Tropospheric ozone: an overview. In *Tropospheric Ozone*, (ed.) Isaksen, I.S.A., 3-32, D. Reidel Publishing Company, Dordrecht, 425pp.

Crutzen, P. (1973). A discussion of the chemistry of some minor constituents in the stratosphere and troposphere. *Pure and Applied Geophysics*, 106-108, V-VII, 1385-1399.

Crutzen, P.J., Delany, A.C., Greenberg, J., Haagenson, P., Heidt, L., Lueb, R., Pollock, W., Seiler, W., Wartburg, A. and Zimmerman, P. (1985). Tropospheric chemical composition measurements in Brazil during the dry season. *Journal of Atmospheric Chemistry*, 2, 233-256.

Danielsen, E.F. (1961). Trajectories: isobaric, isentropic and actual. *Journal of Meteorology*, 18, 479-486.

Danielsen, E.F. (1968). Stratospheric-tropospheric exchange based on radioactivity, ozone and potential vorticity. *Journal of the Atmospheric Sciences*, 25, 502-518.

Danielsen, E.F. (1974). Review of trajectory methods. In: *Advances in Geophysics*, (ed.) Landsberg, H.E. and Van Mieghem, J., Vol. 18 B, 73-94, 389pp.

Danielsen, E.F., Bleck, R., Shedlovsky, J., Wartburg, A., Haagenson, P. and Pollock, W. (1970). Observed distribution of radioactivity, ozone and potential vorticity associated with tropopause folding. *Journal of Geophysical Research*, 75 (12), 2353-2361.

Danielsen, E.F. (1993). In situ evidence of rapid, vertical, irreversible transport of the lower tropospheric air into the lower tropical stratosphere by convective cloud turrets and by larger-scale upwelling in tropical cyclones. *Journal of Geophysical Research*, 98 (D5), 8665-8682.

Danielsen, E.F. and Hipskind, R.S. (1980). Stratospheric-tropospheric exchange at polar latitudes in summer. *Journal of Geophysical Research*

Danielsen, E.F., Hipskind, R.S., Gaines, S.E., Sachse, G.W., Gregory, G.L. and Hill, G.F. (1987). Three-dimensional analysis of potential vorticity associated with tropopause folds and observed variations of ozone and carbon monoxide. *Journal of Geophysical Research*, 92 (D2), 2103-2111.

Danielsen, E.F. and Mohnen, V.A. (1977). Project Duststorm Report: ozone transport, *in situ* measurements, and meteorological analyses of tropopause folding. *Journal of Geophysical Research*, 82 (37), 5867-5877.

Department of the Environment and the Meteorological Office (1991). *Stratospheric Ozone 1991*. United Kingdom Stratospheric Ozone Review Group, London, HMSO, 18pp.

Diab, R.D. (1992). Unpublished Review of the Ozone Group at the University of Natal. Department of Geographical and Environmental Sciences, University of Natal, Durban.

Diab, R.D., Barsby, J., Bodeker, G.E., Scourfield, M. and Salter, L. (1992). *South African Geographical Journal*, 74, 13-18.

Diab, R.D., Thompson, A.M., Zunckel, M., Coetzee, G.J.R., Combrink, J., Bodeker, G.E., Fishman, J., Sokolic, F., McNamara, D., Archer, C.B. and Nganga, D. (1996a). Vertical ozone distribution over southern Africa and adjacent oceans during SAFARI-92. *Journal of Geophysical Research* (SAFARI special issue).

Diab, R.D., Jury, M.R., Combrink, J. and Sokolic, F. (1996b). A comparison of anticyclonic and trough influences on the vertical distribution of ozone and meteorological conditions during SAFARI-92. *Journal of Geophysical Research* (SAFARI special issue).

Diab, R.D., Combrink, J., Sokolic, F. and Zunckel, M. (1993). Ozone and synoptic weather relationships at Okaukuejo during SAFARI-92. Tenth Annual Conference of the South African Society of Atmospheric Sciences, Pretoria, 13-14 October, 1993.

Dickerson, R.R., Huffman, G.J., Luke, W.T., Nunnermacker, L.J., Pickering, K.E., Leslie, C.D., Lindsey, C.F., Slinn, W.G.N., Kelly, T.J., Daum, P.H., Delany, A.C., Greenberg, J.P., Zimmerman, P.R., Boatman, J.F. (1987). Thunderstorms: An important mechanism in the transport of air pollutants. *Science*, 235, 460-465.

Dobson, G.M.B., Brewer, A.W. and Cwilong, B.M. (1946). *Meteorology of the Lower Stratosphere*. Proceedings of the Royal Society, A, 185, 144-175.

Dobson, G.M.B., Harrison, D.N. and Lawrence, J. (1929). Measurements of the amount of ozone in the earth's atmosphere and its relation to other geophysical conditions, Part III. *Ozone in the Earth's Atmosphere.* Proceedings of the Royal Meteorological Society of London, 456-486.

Ebel, A., Hass, H., Jakobs, H.J., Laube, M., Memmesheimer, M., Oberreuter, A., Geiss, H. and Kuo, Y.-H. (1991). Simulation of ozone intrusion caused by a tropopause fold and cut-off low. *Atmospheric Environment*, 25A (10), 2131-2144.

Elsworth, C.M., Galbally, I.E. and Paterson, R. (1988). Ozone in near surface air. In *Baseline 86,* (ed.) Forgan, B.W. and Fraser, P.J., Department of Science and Technology, CSIRO.

European Centre for Medium-Range Weather Forecasts (ECMWF) (1994). The description of the ECMWF/WCRP level III-A global atmospheric data archive. Technical Attachment, ECMWF, Shinfield Park, Reading, England, 72pp.

European Centre for Medium-Range Weather Forecasts (ECMWF) (1993). The description of the ECMWF/WCRP level III-A global atmospheric data archive. Technical Attachment, ECMWF, Shinfield Park, Reading, England, 49pp.

Farman, J.C., Gardiner, B.G. and Shanklin, J.D. (1985). Large losses of total ozone in Antarctica reveal seasonal ClO_x/NO_x interaction, *Nature*, 315, 207-210.

Farrara, J.D. and Mechoso, C.R. (1986). An observational study of the final warming in the Southern Hemisphere stratosphere. *Geophysical Research Letters*, 13 (12), 1232-1235.

Fehsenfeld, F.C., Parrish, D.D. and Fahey, D.W. (1988). The measurement of NO_x in the non-urban troposphere. In *Tropospheric Ozone*, (ed.) Isaksen, I.S.A., D. Reidel Publishing Co., Dordrecht, 185-215, 425pp.

Fishman, J., Fakhruzzanan, K., Cros, B. and Nganga, D. (1991). Identification of widespread pollution in the southern hemisphere deduced from satellite analyses. *Science*, 252, 1693-1696.

Fishman, J. and Larsen, J.C. (1987). Distribution of total ozone and stratospheric ozone in the tropics: Implications for the distribution of tropospheric ozone. *Journal of Geophysical Research*, 92 (D6), 6627-6634.

Fishman, J. (1988). Tropospheric ozone from satellite total ozone measurements. In *Tropospheric Ozone*, (ed.) Isaksen, I.S.A., D. Reidel Publishing Company, 111-123.

Fishman, J., Watson, C.E., Larsen, J.C. and Logan, J.A. (1990). Distribution of tropospheric ozone determined from satellite data. *Journal of Geophysical Research*, 95 (D4), 3599-3617.

Fishman, J., Minnis, P. and Reichle, H.G.Jr. (1986). Use of satellite data to study tropospheric ozone in the tropics. *Journal of Geophysical Research*, 91 (D13), 14451-14465.

Fishman, J., Watson, C.E. and Larsen, J.C. (1988). The distribution of total ozone, stratospheric ozone, and tropospheric ozone at low latitudes deduced from satellite data sets. Workshop on tropospheric ozone, Quadrennial Ozone Symposium, August 1988, University of Gottingen, Federal Republic of Germany.

Fishman, J., Brackett, V.G. and Fakhruzzaman, K. (1992). Distribution of tropospheric ozone in the tropics from satellite and ozonesonde measurements. *Journal of Atmospheric and Terrestrial Physics*, 54 (5), 589-597.

Fishman, J. (1991). Probing planetary pollution from space. *Environmental Science Technology*, 25 (4), 612-621.

Fishman, J. (1994). Experiment probes elevated ozone levels over the tropical south Atlantic Ocean. *EOS*, 75, 380.

Fleig, A.J., Bhartia, P.K., Wellemayer, C.G. and Silberstein, D.S. (1986). Seven years of total ozone from the TOMS instrument - a report on data quality. *Geophysical Research Letters*, 13 (12), 1355-1358.

Frederick, J.E. and Serafino, G.N. (1985) The detection of long-term changes in stratospheric ozone scientific requirements and current results from satellite-based measurement systems. *Journal of Climate and Applied Meteorology*, 24, 904-914.

Garstang, M. and Macko, S. (1993). Biomass burning in the global environment: First results from the IGAC/BIBEX field campaign STARE/TRACE-A/SAFARI-92. In Annual Report to the National Science Foundation Division of Atmospheric Sciences, Atmos Chemistry, Grant #: ATM92-07924, University of Virginia, Department of Environmental Sciences, Charlottesville.

Garstang, M., Scala, J., Grego, S., Harriss, R., Beck, S., Browell, E., Sachse, G., Gregory, G., Hill, G., Simpson, J., Tao, W-K, and Torres, A. (1988). Trace gas exchanges and convective transports over the Amazonian Rain Forest. *Journal of Geophysical Research*, 93 (D2), 1528-1550.

Garstang, M., Tyson, P.D., Swap, R., Edwards, M., Kållberg, P. and Lindesay, J.A. (1996). Horizontal and vertical transport of air over southern Africa. *Journal of Geophysical Research* (SAFARI special issue).

Gleason, J.F., Bhartia, P.K., Herman, J.R., McPeters, R.P. Newman, P., Stolarski, R.S., Flynn, L., Labow, G., Larko, D., Seftor, C., Wellemeyer, C., Komhyr, W.D., Miller, A.J. and Planet, W. (1993). Record low global ozone in 1992. *Science*, 260, 523-526.

Gray, L.J. and Pyle, J.A. (1989). A two-dimensional model of the QBO of ozone. *Journal of the Atmospheric Sciences*, 46 (2), 203-220.

Gribbin, J. (1988). *The Hole in The Sky*. Transworld Publishers Ltd., London, 160pp.

Guicherit, R. (1988). Ozone on an urban and regional scale. In *Tropospheric Ozone*, (ed.) Isaksen, I.S.A., D. Reidel Publishing Co., Dordrecht, 49-62, 425pp.

Haagenson, P. and Shapiro, M.A. (1979). Isentropic trajectories for derivation of objectively analyzed meteorological parameters, Atmospheric Quality Division, National Center for Atmospheric Research Technical Note (NCAR), NCAR/TN-149+STR, Dec. 1979, Boulder, Colorado.

Haynes, P. (1993). NATO Advanced Research Workshop on "Stratosphere-Troposphere Exchange". SPARC Newsletter, 1993, Number 2, 4-5.

Heath, D.F., Krueger, A.J., Roeder, H.A. and Henderson, B.D. (1975). The solar backscatter ultraviolet and Total Ozone Mapping Spectrometer (SBUV/TOMS) for NIMBUS G. *Optical Engineering*, 14 (4), 323-331.

Held, G. and Lindesay, J.A. (1993). On SAFARI in the Kruger National Park - An exciting breakthrough for South African environmental Science. *ECO Focus*, 2 (1), 6-8.

Herman, J. (1995). Electronic-mail FTP file, Code 916, NASA/Goddard Space light Center, Green belt, MD 20771, USA, January 1995.

Herman, J.R., Hudson, R.D. and Serafino, G. (1990). Analysis of the eight-year trend in ozone depletion from empirical models of solar backscattered ultraviolet instrument degradation. *Journal of Geophysical Research*, 95 (D6), 7403-7416.

Herman, J.R. Krueger, A., Cote, C., Ahmad, Z., Forman, M., Wellemeyer, C., Byerly, W., Pan, L., Jaross, G., Hudson, R., Doscov, V., Salichov,, R., Borisov, Y., Kondratiev, A. Kugaenko, B. and Samvelyn, H. (1994). Global ozone data from the Meteor-3/TOMS ultraviolet spectrometer. In *Ozone in the Atmosphere*, Proceedings of the Quadrennial Ozone Symposium 1992, (ed.) Hudson, R., Deepak, A., Hampton, Virginia, 877-882, 965pp.

Herman, J.R., Hudson, R.D., McPeters, R., Stolarski, R., Ahmad, Z., Gu, X.-Y., Taylor, S. and Wellemeyer, C. (1991). A new self-calibration method applied to TOMS and SBUV backscattered ultraviolet radiation data to determine long-term global ozone change. *Journal of Geophysical Research*, 96 (D4), 7531-7545.

Hill, F.F. and Browning, K.A. (1987). Case study of a persistent mesoscale cold pool. *The Meteorological Magazine*, 116, 297-309.

Hipskind, R.S., Gregory, G.L., Sachse, G.W., Hill, G.F. and Danielsen, E.F. (1987). Correlations between ozone and CO in the lower stratosphere, folded tropopause and maritime troposphere. *Journal of Geophysical Research*, 92 (D2), 2121-2130.

Hoell, J.M., Fishman, J., Kirchhoff, V.W.J.H. and Krishnamurti, T.N. (1991). Proposal for a study of transport and atmospheric chemistry near the equator-Atlantic (TRACE-A). Submitted to Tropospheric Chemistry Program, Earth Science and Applications Division, NASA, Washington, DC, 20546, 90pp.

Holton, J.R. (1992). *An Introduction to Dynamic Meteorology*. Third edition, Academic Press, San Diego, Chapters 6, 11-12, 511pp.

Holton, J.R. (1979). *An Introduction to Dynamic Meteorology*, Second edition, Chapter 11, New York Academic Press.

Hoskins, B.J. and Bretherton, F.P. (1972). Atmospheric frontogenesis models: mathematical formulation and solution. *Journal of the Atmospheric Sciences*, 29, 11-37.

Hoskins, B.J., McIntyre, M.E. and Robertson, A.W. (1985). On the use and significance of isentropic potential vorticity maps. *Quarterly Journal of the Royal Meteorological Society*, 111 (470), 877-946.

Hudson, R.D. and Kim, J-H. (1994). Direct measurements of tropospheric ozone using TOMS data. In *Ozone in the Troposphere and Stratosphere: Proceedings of the Quadrennial Ozone Symposium 1992*, (ed.) Hudson, R., Deepak, A., Hampton, Virginia, 119-121, 965pp.

Hunt, B.G. (1989). Middle atmosphere response to solar and tropospheric forcing. *Solar-Terrestrial Energy Program: Major Scientific Problems*. Proceedings of Scientific Committee on Solar-Terrestrial Physics (SCOSTEP) symposium, Helsinki, 1988. SCOSTEP Secretariat, Illinois, 111-165, 185pp.

Illari, L. (1989). The quality of satellite precipitable water content data and their impact on analysed moisture fields, *Tellus*, 41A, 319-337.

Institute for Environmental Studies, Toronto, (IES) (1977). Atmospheric exchange processes and the ozone problem. In *The Ozone Layer*, (ed.) Biswas, A.K., Environmental Sciences and Applications, Volume 4, Paper 13, 245-300, Oxford, England, Pergamon Press, 381pp.

Jury, M.R. (1993). A peliminary study of climatological associations and characteristics of tropical cyclones in the SW Indian Ocean. *Meteorology and Atmospheric Physics*, 51, 101-115.

Jury, M.R., Brunke, E. And Schormann, M. (1996). Aircraft section measurements of meteorology and ozone in northern Namibia during SAFARI'92. *Journal of Geophysical Research* (SAFARI special issue).

Jury, M.R. and Lutjeharms, R.R.E. (1993). Die struktuur en moontlike aandrywingskragte van die 1991-1992-droogte in suidelike Afrika. *Suid Afrikaanse Tydskrif vir Natuurwetenskap en Tegnologie*, no. 1, 8-16.

Keyser, D., Pecnick, M.J. and Shapiro,M.A. (1986). Diagnosis of the role of vertical deformation in a two-dimensional primitive equation model of upper-level frontogenesis. *Journal of the Atmospheric Sciences*, 43 (8), 839-850.

Keyser, D. and Pecnick, M.J. (1985). A two-dimensional primitive equation model of frontogenesis forced by confluence and horizontal shear. *Journal of the Atmospheric Sciences*, 42 (12), 1259-1282.

Kirchhoff, V.W.J.H., Setzer, A.W. and Pereira, M.C. (1989). Biomass burning in Amazonia: Seasonal effects on atmospheric O_3 and CO. *Geophysical Research Letters*, 16 (5), 469-472.

Levey, K.M. (1993). Intra-Seasonal Oscillations of Convection Over Southern Africa. Unpublished MSc. thesis, Department of Oceanography, University of Cape Town, South Africa, 203pp.

Levine, J.S. (1990). Global biomass burning: Atmospheric, Climatic and biospheric implications. *EOS*, 71 (37), 1075-1077.

Lindesay, J.A. (1996). African Savanna Fires, Global Atmospheric Chemistry and the Southern Tropical Atlantic Regional Experiment: An Introduction. SAFARI Book Chapter, 1-15.

Lindesay, J.A. (1992). Biomass burning as a factor in atmospheric chemistry and terrestrial ecology. *South African Journal of Science*, 88, 143-144.

Liu, S.C., Trainer, M., Fehsenfeld, F.C., Parrish, D.D., Williams, E.J., Fahey, D.W., Hubber, G. and Murphy, P.C. (1987). Ozone production in the rural troposphere and the implications for regional and global ozone distributions. *Journal of Geophysical Research*, 92 (D4), 4191-4207.

Lobart, J.M. and Warnatz, J. (1993) Emissions from the combustion process in vegetation. In *Fire In The Environment : The Ecological, Atmospheric, and Climatic Importance of Vegetation Fires*, (ed.) Crutzen, P.J. and Goldammer, J.G., John Wiley and Sons, Chichester, 15-37, 400pp.

Logan, J.A. (1985). Tropospheric ozone: Seasonal behaviour, trends and anthropogenic influence. *Journal of Geophysical Research*, 90 (D6), 10463-10482.

Matsumoto, S., Ninomiya, K., Haseghawa, R. and Miki, Y. (1982). The Structure and the role of a subsynoptic-scale cold vortex on the heavy precipitation. *Journal of the Meteorological Society of Japan*, 60 (1), 339-353.

McPeters, R.D. and Komhyr, W.D. (1991). Long-term changes in the Total Ozone Mapping Spectrometer relative to world primary standard Dobson Spectrometer 83. *Journal of Geophysical Research*, 96(D2), 2987-2993.

National Research Council (NRC) (1991). *Rethinking The Ozone Problem In Urban And Regional Pollution*. National Academy Press, Washington, D.C., 19-65, 500pp.

Newell, R.E. and Gould-Stewart, S. (1981). A stratospheric fountain? *Journal of the Atmospheric Sciences*, 38, 2789-2796.

Newman, P. (1986). The final warming and polar vortex disappearance during the Southern Hemisphere spring. *Geophysical Research Letters*, 13 (12), 1228-1231.

Normand, C. (1953). Atmospheric ozone and the upper-air conditions. *Quarterly Journal of the Royal Meterological Society*, 79, 39-50.

Ohring, G. and Muench, H.S. (1960). Relationships between ozone and meteorological parameters in the lower stratosphere. *Journal of Meteorology*, 17, 195-206.

Oltmans, S.J. and London, J. (1982). The quasi-biennial oscillation in atmospheric ozone. *Journal of Geophysical Research*, 87 (11), 8981-8989.

Orlanski, I., Marino, M., Menendez, C. and Katzfey, J. (1989). The role of cyclones in the daily variability of Antarctic ozone. Third International Conference on Southern Hemisphere Meteorology and Oceanography. Buenos Aires, 13-17 November, 1989.

Palmén, E. (1958). Vertical circulation and release of kinetic energy during the development of Hurricane Hazel into an extratropical storm. *Tellus*, 10 (1), 1-23.

Palmén, E. (1949). Origin and structure of high-level cyclones south of the maximum westerlies. *Tellus*, 1, 22-31.

Pickering, K.E., Thompson, A.M., McNamara, D.P., Schoeberl, M.R., Lait, L.R., Newman, P.A., Justice, C.O. and Kendall, J.D. (1994a). A trajectory modelling investigation of the biomass burning - tropical ozone relationship. In *Ozone in the Troposphere and Stratosphere*, Proceedings of the Quadrennial Ozone Symposium 1992, (ed.) Hudson, R., Deepak, A., Hampton, Virginia, 101-104, 965pp.

Pickering, K.E., Scala, J.R., Thompson, A.M., Tao, W-K., Simpson, J. (1992a). A regional estimate of convective transport of CO from biomass burning. *Geophysical Research Letters*, 19 (3), 289-292.

Pickering, K.E., Thompson, A.M., Dickerson, R.R., Luke, W.T., McNamara, D.P., Greenberg, J.P. and Zimmerman, P.R. (1990). Model calculations of tropospheric ozone production potential following observed convective events. *Journal of Geophysical Research*, 95 (D9), 14049-14062.

Pickering, K.E., Thompson, A.M., Tao, W-K. and Kucsera, T.L. (1993b). Upper tropospheric ozone production following mesoscale convection during STEP/EMEX. *Journal of Geophysical Research*, 98 (D5), 8737-8749.

Pickering, K.E., Thompson, A.m., Scala, J.R., Tao, W-K., Dickerson, R.R. and Simpson, J. (1992b). Free tropospheric ozone production following entrainment of urban plumes into deep convection. *Journal of Geophysical Research*, 97 (D16), 17985-18000.

Pickering, K.E., Thompson, A.M., Scala, J.R., Tao, W-K., Simpson, J. and Garstang, M. (1991). Photochemical ozone production in tropical squall line convection during NASA Global Tropospheric Experiment. Amazon Boundary Layer Experiment 2A. *Journal of Geophysical Research*, 96 (D2), 3099-3114.

Pickering, K.E., Thompson, A.M., Scala, J.R., Tao, W-K. and Simpson, J. (1992c). Ozone production potential following convective redistribution of biomass burning emissions. *Journal of Geophysical Research*, 14, 297-313.

Pickering, K.E., Thompson, A.M., Scala, J.R., Tao, W-K., Simpson, J. (1994b). Enhancement of free tropospheric ozone production by deep convection. *Ozone in the Troposphere and Stratosphere*, Proceedings of Quadrennial Ozone Symposium. 1992, (ed.) Hudson, R., Deepak, A., Hampton, Virginia, 105-108, 965pp.

Pickering, K.E., Thompson, A.M., McNamara, D.P. and Schoeberl, M.R. (1993a). An intercomparison of isentropic trajectories over the South Atlantic. *Monthly Weather Review*, 121, 387-401.

Preston-Whyte, R.A. and Tyson, P.D. (1988). *The Atmosphere and weather of Southern Africa*. Oxford University Press, Cape Town, 374pp.

Price, J.D. and Vaughan, G. (1994). Detection of STE in cut-off-low systems. *Ozone in the Troposphere and Stratosphere*, Proceedings of Quadrennial Ozone Symposium. 1992, (ed.) Hudson, R., Deepak, A., Hampton, Virginia, 727-730, 965pp.

Price, J.D. and Vaughan, G. (1993). The potential for stratosphere-troposphere exchange in cut-off low systems. *Quarterly Journal of the Royal Meteorological Society*, 119, 343-365.

Price, J.D. and Vaughan, G. (1992). Statistical studies of cut-off-low systems. *Annales Geophysicae*, 10, 96-102.

Ramanathan, V., Callis, L., Cess, R., Hansen, J., Isaksen, I., Kuhn, W., Lacis, A., Luther, F., Mahlman, J., Reck, R. and Schlesinger, M. (1987). Climate-chemical interactions and effects of changing atmospheric trace gases. *Reviews of Geophysics*, 25 (7), 1441-1482.

Randel, W.J. (1992). Atmospheric Circulation Statistics 1000-1mb, NCAR technical note, NCAR/TN-366+STR, 1992.

Reed, R.J. (1950). The role of vertical motions in ozone-weather relationships. *Journal of Meteorology*, 7, 263-267.

Reed, R. and Danielsen, E.F. (1959). Frontis in the vicinity of the tropopause. *Archiv für Meteorologie, Geophysik, Bioklimatologie.*, A11, 1-17.

Reed, R. (1955). A study of a characteristic type of upper-level frontogenesis. *Journal of Meteorology*, 12, 226-237.

Reiter, E.R. (1975). Stratospheric-tropospheric exchange processes. *Reviews of Geophysics and Space Physics*, 13 (4), 459-474.

Riehl, H. and Malkus, J.S. (1958). On the heat balance in the equatorial trough zone. *Geophysica*, 6, 503-538.

Robinson, J.M. (1991). Fire from space: Global fire evaluation using infrared remote sensing. *International Journal of Remote Sensing*, 12 (1), 3-24.

Russel, P.B., Pfister, L., Selkirk, H.B. (1993). The Tropical Experiment of the Stratosphere-Troposphere Exchange Project (STEP): science objectives, operations and summary findings. *Journal of Geophysical Research*, 98 (D5), 8563-8589.

Rycroft, M.J. (1990). The Antarctic atmosphere: a hot topic in a cold cauldron. *The Geographical Journal*, 156, Part 1, 1-11.

Salby, M.L. and Garcia, R.R. (1990). Dynamical perturbations to the ozone layer. *Physics Today*, March 1990, 38-46.

Salby, M.L. and Callaghan, P.F. (1993). Fluctuations of total ozone and their relationship to stratospheric air motions. *Journal of Geophysical Research*, 98 (D2), 2715-2727.

Schoeberl, M.R. and Hartmann, D.L. (1991). The dynamics of the stratospheric polar vortex and its relation to springtime ozone depletions. *Science*, 251, 46-52.

Schoeberl, M.R., Lait, L.R., Newman, P.A. and Rosenfield, J.E. (1992). The structure of the polar vortex. *Journal of Geophysical Research*, 97, 7859-7882.

Shanklin, J. (1994). British Antarctic Survey Preliminary values on ozone hole. BAS ozone bulletin 12/94 issued 11 November 1994.

Shapiro, M.A. (1978). Further evidence of the mesoscale and turbulent structure of upper level jet stream-frontal zone systems. *Monthly Weather Review*, 106, 1100-1111.

Shapiro, M.A., Krueger, A.J. and Kennedy, P.J. (1982). Nowcasting the position and intensity of jet streams using satellite-borne Total Ozone Mapping Spectrometer. In *Nowcasting*, (ed.) Browning, K.A., Academic Press, New York, 137-145.

Shapiro, M.A. (1981). Frontogenesis and geostrophically forced secondary circulations in the vicinity of jet stream-frontal zone systems. *Journal of the Atmospheric Sciences*, 38, 954-973.

Shapiro, M.A. (1976). The role of turbulent heat flux in the generation of potential vorticity in the vicinity of upper-level jet stream systems. *Monthly Weather Review*, 104, 892-906.

Shapiro, M.A. (1980). Turbulent mixing within tropopause folds as a mechanism for the exchange of chemical constituents between the stratosphere and troposphere. *Journal of the Atmospheric Sciences*, 37, 994-1004.

Singh, H.B., Viezee, W., Johnson, W.B. and Ludwig, F.L. (1980). *Journal of Air Pollution Control Association*, 30 (9), 1009-1017.

Spaete, P., Johnson, D.R. and Schaack, T.K. (1994). Stratospheric-tropospheric mass exchange during the Presidents' Day Storm. *Monthly Weather Review*, 122, 424-439.

Staley, D.O. (1960). Evaluation of potential-vorticity changes near the tropopause and the related vertical motions, vertical advection of vorticity, and transfer of radioactive debris. *Journal of Meteorology*, 17, 591-620.

Staley, D.O. (1962). On the mechanism of mass and radioactivity transport from stratosphere to troposphere. *Journal of the Atmospheric Sciences*, 19, 450-467.

Stallard, R.F., Edmond, J.M. and Newell, R.E. (1975). Surface ozone in the south east atlantic between Dakar and Walvis Bay. *Geophysical Research Letters*, 2 (7), 289-292.

Stolarski, R.S. (1988). The Antarctic ozone hole. *Scientific American*, 258, 20-26.

Stolarski, R.S., Bloomfield, P., McPeters, R.D. and Herman, J.R. (1991). Total ozone trends deduced from Nimbus 7 TOMS data. *Geophysical Research Letters*, 18 (6), 1015-1018.

Stolarski, R.S., Krueger, A.J., Schoeberl, M.R., McPeters, R.D., Newman, P.A. and Alpert, J.C. (1986). Nimbus 7 satellite measurements of the springtime Antarctic ozone decrease. *Nature*, 322, 808-811.

Strantz, D. and Taljaard, J.J. (1965). Analysis of an abnormal winter situation in South Africa during June 1964. *Notos*, Atmospheric Project, Southern Hemisphere, South African Weather Bureau, Department of Transport, 17-32, 474pp.

Sumner, E.J. (1953). Cold pools: a statistical and synoptic study. *Meteorological Magazine*, 291-301.

Swap, R., Garstang, M., Macko, S.A., Tyson, P.D., Maenhaut, W., Artaxo, P., Kållberg, P. and Talbot, R. (1996). The long-range transport of southern African aerosols to the tropical south Atlantic. *Journal of Geophysical Research* (SAFARI special issue).

Taljaard, J.J. (1985). *Cut-off lows in the South African Region*. Technical Paper, Number 14, South African Weather Bureau, Department of Transport, 153pp.

Taljaard, J.J. (1982). Cut-off lows and heavy rain over the Republic. News Letter, Number 403, South African Weather Bureau, Department of Transport, 155-156.

Tessier, R. (1989). The Meteosat Programme. *European Space Agency (ESA) Bulletin*, no. 58, 45-57.

Thompson, A.M., Pickering, K.E, McNamara, D.P, Schoeberl, M.R., Hudson, R.D., Kim, J.-H., Browell, E.V., Fishman, J., Kirchhoff, V.W.J.H. and Nganga, D. (1996a). Where did tropospheric ozone over southern Africa and the tropical Atlantic come from in October 1992? Insights from TOMS, GTE/TRACE-A and SAFARI-92. Draft paper for *Journal of Geophysical Research* (TRACE-A special issue).

Thompson, A.M., Diab, R.D., Bodeker, G.E., Zunckel, M., Coetzee, G.J.R., Archer, C.B., McNamara, D.P., Pickering, K.E., Combrink, J., Sokolic, F., Fishman, J. and Nganga, D. (1996b). Total ozone over southern Africa during SAFARI-92/TRACE-A. *Journal of Geophysical Research* (SAFARI special issue).

Thompson, A.M., Zenker, T., Bodeker, G.E. and McNamara, D.P. Ozone Over Southern Africa: Patterns and Influences. (1996c). In *Fire in Southern African Savanna: Ecological and Atmospheric Perspectives*, (ed.) Tyson, P.D., Lindesay, J.A., van Wilgen, B., and Andreae, M.O., University of Witwatersrand Press, Johannesburg.

Thompson, A.M., McNamara, D.P., Pickering, K.E. and McPeters, R.D. (1993). Effect of marine stratocumulus on TOMS ozone. *Journal of Geophysical Research*, 98 (D12), 23051-23057.

Trenberth, K.E. and Olson, J.G. (1988). An evaluation and intercomparison of global analyses from the National Meteorological Center and the European Centre for Medium-Range Weather Forecasts. *Bulletin of the American Meteorological Society*, 69 (9), 1047-1057.

Triegaardt D.O., Terblanche, D.E., van Heerden, J. And Laing, M.V. (1987). The Natal flood of September 1987. *South African Weather Bureau Technical Paper*, no. 19, 62pp.

Tung, K.K., Ko, M.K.W, Rodriguez, J.M., and Size, N.D. (1986). Are Antarctic ozone variations a manifestation of dynamics or chemistry? *Nature*, 321, 755-758.

Tyson, P.D., Garstang, M., Swap, R.J., Browell, E.V., Diab, R.D. and Thompson, A.M. (1995). Transport and vertical structure of ozone and aerosol distributions over southern africa. In *Biomass Burning and Global Change*, (ed.) Levine, J.S. (in press).

Uccellini, L.W., Kocin, P.J., Petersen, R.A., Wash, C.H. and Brill, K.F. (1984). The Presidents' Day Cyclone of 18-19 February 1979: Synoptic overview and analysis of the subtropical jet streak influencing the pre-cyclogenetic period. *Monthly Weather Review*, 112, 31-55.

Uccellini, L.W., Keyser, D., Brill, K.F. and Wash, C.H. (1985). The Presidents' Day Cyclone of 18-19 February 1979: influence of upstream trough amplification and associated tropopause folding on rapid cyclogenesis. *Monthly Weather Review*, 113, 962-988.

United Nations Environment Programme (UNEP) (1994). *Montreal Protocol on Substances that Deplete the Ozone Layer*, Scientific Assessment of Ozone Depletion: 1994. World Meteorological Organization - Global Ozone Research and Monitoring Project, Report No. 37, Geneva, Switzerland, 369pp.

Urone, P. (1986). The pollutants. In *Air Pollution*, (ed) Stern, A.C. Volume VI, Chapter 1, 1-53 Academic Press, 483pp.

Vaughan, G. and Price, J.D. (1991). On the relation between total ozone and meteorology. *Quarterly Journal of the Royal Meteorological Society*, 117, 1281-1298.

Vaughan, G. (1988). Stratosphere-troposphere exchange of ozone. In *Tropospheric Ozone*, (ed.) Isaksen, I.S.A., 125-135, 425pp.

Vaughan, G., Price, J.D. and Howells, A. (1994). Transport into the troposphere in a tropopause fold/cut-off low system. *Ozone in the Troposphere and Stratosphere*, Part 1. Proceedings of the Quadrennial Ozone Symposium, Charlottesville, Virginia, USA, June 4-13, 1992, 154-157, 436pp.

Wakamatsu, S., Uno, I., Ueda, H. and Uehara, K. (1989). Observational study of stratospheric ozone intrusions into the lower troposphere. *Atmospheric Environment*, 23 (8), 1815-1826.

Wang, P.H., McCormick, M.P. and Chu, W.P. (1983). A study on the planetary wave transport of ozone during the late February 1979 stratospheric warming. *American Meteorological Society*, 40, 2419-2431.

Warneck, P. (1988). *Chemistry of the Natural Atmosphere*. Chapter 5, 176-222, Academic Press, New York, 757pp.

Whitaker, J.S., Uccellini, L.W. and Brill, K.F. (1988). A model-based diagnostic study of the rapid development phase of the Presidents' Day Cyclone. *Monthly Weather Review*, 116, 2337-2365.

Zenker, T., Thompson, A,M., McNamara, D.P., Kucesera, T.L., Wienhold, G., Harris, G.W., LeCanut, P., Andreae, M.O. and Koppmann, R. (1995). Regional trace gas distribution and airmass characteristics in the haze layer over southern Africa during the biomass burning season (September/October 1992): observations and modeling from the STARE/SAFARI-92/DC-3. In *Biomass Burning and Global Change*, (ed.) Levine, J.S. (in press).

Zunckel, M. (1992a). Ozone profile changes above Pretoria: 1965 to 1991. Unpublished MSc. thesis, Department of Physics, University of Natal, Durban, 194pp.

Zunckel, M., M.W.J. Scourfield and Diab, R.D. (1992b). Vertical distribution of ozone above Pretoria from 1965 to 1968. *South African Journal of Science*, 88, 217-220.

PERSONAL COMMUNICATION

Bracket, V. (1995). NASA, Flight Facility Wallops Island.

Coetzee, G. (1993; 1995). SAWB, Pretoria.

Fielding, K. (1995). Data Services, ECMWF, Shinfield Park, Reading RG29AX, UK.

Kendall, J. (1993). NASA Science, Systems, and Applications inc.

McNamara, D. (1993). NASA/GSFC, Applied Research Corporation.

Sokolic, F. (1995). Department of Geographical and Environmental Sciences, University of Natal, Durban.